Université de Montréal

Immune Mechanisms Controlling Angioimmunoblastic T cell Lymphoma Progression

par

Mariko Witalis

Département de biologie moléculaire

Faculté de médecine

Thèse présentée en vue de l'obtention du grade de Philosophiae Doctor (Ph.D.) en biologie moléculaire, option médecine cellulaire et moléculaire

Août 2020

Abstract

Angioimmunoblastic T cell lymphoma (AITL) is an aggressive peripheral T cell lymphoma manifesting with symptoms such as generalized lymphadenopathy and hypergammaglobulinemia. Currently, AITL patients have limited treatment options and poor clinical outcomes with a 5-year survival rate around 30%. AITL tumor cells derive from a subset of $CD4^+$ T cell, the T follicular helper (Tfh) cell. Tfh cells are essential in germinal centers (GC), where they facilitate B cell expansion and differentiation into plasma cells. This helper function is supported by numerous Tfh cell-derived proteins and transcriptional programs which may still be operational in AITL tumor cells. Therefore, disrupting key signaling mechanisms sustaining Tfh cell identity and their ability to interact with B cells could inhibit AITL tumor growth.

Studies have demonstrated that these hyperactive Tfh-like cells lead to the accumulation of immune cell subsets such as B cells, plasma cells, and macrophages within tumor lymph nodes. Nevertheless, the AITL tumor microenvironment itself has not been well-studied and whether some immune cells could be harnessed to impede tumor growth has not been tested. In human AITL, although circulating Tfh cells have been reported, the rate of tumor spreading can vary between patients. As such, one possibility is the presence of immune surveillance mechanisms opposing tumor progression. In line with this idea, SLAMF7, a positive signal for macrophage-mediated phagocytosis (counterbalanced by the inhibitory CD47-SIRPα pathway), is expressed in a subset of AITL patients. Despite this, whether differing levels of SLAMF7 expression correlates with improved patient outcomes has not been investigated.

Using *Roquin*$^{san/+}$ mice, a spontaneous AITL-like mouse model, we addressed the role of immune signaling mechanisms within Tfh-like tumor cells and the surrounding tumor microenvironment that would promote tumor regression. First, we aimed to inhibit signature Tfh cell proteins and downstream signaling pathways in developed AITL-like tumors to evaluate potential therapeutic value. Second, we investigated the role of macrophage-mediated phagocytosis in the context of SLAMF7 and how modulating CD47-SIRPα signaling may enhance the efficiency of AITL tumor cell engulfment. Our central hypothesis is that by removing fundamental Tfh cell supporting programs from tumor cells or by promoting the

phagocytic removal of Tfh-like tumor cells we can favour tumor regression and impair future growth.

Through this work, we demonstrated that AITL-like tumors continuously require critical Tfh cell identity proteins such as transcription factor Bcl6 and adaptor protein SAP, as well as T cell-B cell (T-B) crosstalk. Importantly, despite the absence of conventional GCs, Tfh-like tumor cells provided functional support to B cells as evidenced by elevated IgG titers and accumulation of plasma cell precursors in tumors. We also found evidence of opposition between immune surveillance and evasion within AITL-like tumors as Tfh-like cells upregulated inhibitory CD47 levels while macrophages increased expression of prophagocytic SLAMF7. Moreover, AITL-like tumor cells were more efficiently phagocytosed *in vitro* when CD47 signaling was blocked. Taken together, we demonstrate that pathways important for Tfh cell identity and T-B communication are critical for AITL-like disease progression and suggest that ongoing macrophage-mediated immune surveillance may influence disease outcomes. Future studies may explore combining inhibitors of Tfh cell activity or T-B crosstalk along with drugs which boost antitumor phagocytic activity to further improve the therapeutic efficacy of treatment.

Keywords

Angioimmunoblastic T cell lymphoma, T follicular helper cell, Bcl6, SAP, LFA-1, Germinal center, phagocytosis, immune surveillance, SLAMF7, CD47

Résumé

Le lymphome angioimmunoblastique à cellules T (AITL) est un lymphome périphérique à cellules T agressif dont les symptômes sont la lymphadénopathie et l'hypergammaglobulinémie. Actuellement, les patients atteints du AITL ont des options de thérapeutiques limitées et des résultats cliniques défavorables, avec un taux de survie sur 5 ans d'environ 30%. Les cellules tumorales du AITL proviennent de cellules T $CD4^+$ appelées cellules T auxiliaires folliculaires (Tfh). Les cellules Tfh sont essentielles dans le centre germinatif (GC), où elles facilitent l'expansion et la différentiation des cellules B en plasmocytes. Cette fonction d'aide est soutenue par de nombreuses protéines dérivées des cellules Tfh et des programmes de transcription qui pourraient aussi fonctionner dans les cellules tumorales du AITL. Par conséquent, la perturbation des principaux mécanismes de signalisation soutenant l'identité des cellules Tfh et leurs interactions avec les cellules B pourrait inhiber la croissance du AITL. Des études ont démontré que les cellules hyperactives de type Tfh provoquent une accumulation de cellules immunitaires telles que les cellules B, les plasmocytes et les macrophages dans les tumeurs.

Cependant, le microenvironnement du AITL n'a pas été bien étudié et il n'a pas été vérifié si certaines cellules immunitaires pourraient être utilisées pour arrêter la croissance de la tumeur. Bien que l'on trouve des cellules Tfh circulantes dans l'AITL humain, le taux de propagation peut varier d'un patient à l'autre. Ainsi, une possibilité est la présence de mécanismes de surveillance immunitaire s'opposant à la progression de la tumeur. En accord avec cette hypothèse, un signal positif pour la phagocytose nommé SLAMF7 (contrebalancé par la voie inhibitrice CD47-SIRPα) est exprimé dans un sous-ensemble de patients atteints du AITL. Toutefois, la corrélation entre les différents niveaux d'expression du SLAMF7 et l'amélioration des résultats pour les patients n'a pas été étudiée.

En utilisant des souris *Roquin*$^{san/+}$, qui développent spontanément l'AITL, nous avons étudié le rôle des mécanismes de signalisation immunitaire dans les cellules tumorales de type Tfh et du microenvironnement tumoral. Nous avons cherché à inhiber les protéines et les voies de signalisation typiques des cellules Tfh dans les tumeurs afin d'évaluer la valeur thérapeutique potentielle. Nous avons aussi étudié le rôle de la phagocytose dépendante des macrophages dans le contexte SLAMF7 et comment la modulation de la signalisation de CD47-SIRPα peut

améliorer l'efficacité de la phagocytose des cellules tumorales. Notre hypothèse centrale est qu'en supprimant les programmes fondamentaux des cellules Tfh ou en favorisant l'élimination phagocytaire des cellules tumorales de type Tfh, nous pouvons favoriser la régression de la tumeur.

Nous avons démontré que les tumeurs AITL nécessitent des protéines d'identité des cellules Tfh essentielles telles que le facteur de transcription Bcl6 et la protéine adaptatrice SAP, ainsi que la communication entre les cellules T et B (T-B). Même en l'absence de GC classiques, les cellules tumorales de type Tfh ont apporté un soutien aux cellules B. Cela est démontré par des titres élevés d'IgG et l'accumulation de cellules précurseurs des plasmocytes dans les tumeurs. Nous avons trouvé des preuves de l'opposition entre la surveillance immunitaire et l'évasion au sein des tumeurs de type AITL, car les cellules Tfh augmentent l'expression de la molécule inhibitrice CD47 tandis que les macrophages stimulent le niveau de SLAMF7. Les cellules de type AITL ont été phagocytées plus efficacement *in vitro* quand la signalisation du CD47 était bloquée. En résumé, nous démontrons que les voies de signalisation importantes pour l'identité des cellules Tfh et la communication entre les cellules T et B sont essentielles pour la progression de l'AITL et suggèrent qu'une surveillance immunitaire continue par les macrophages peut influencer l'évolution de la maladie. Des études futures pourraient explorer la possibilité de combiner des inhibiteurs de l'activité des cellules Tfh ou T-B avec des médicaments qui stimulent l'activité phagocytaire antitumorale pour améliorer l'efficacité thérapeutique du traitement.

Les mots-clés

Lymphome angioimmunoblastique à cellules T, cellule T auxiliaire folliculaire, Bcl6, SAP, LFA-1, centre germinatif, phagocytose, surveillance immunitaire, SLAMF7, CD47

List of Figures

List of Tables

Chapter 1

List of Acronyms and Abbreviations

Abbreviation	Full Name
2-HG	2-hydroxyglutarate
Ago2	Argonaute 2
AID	Activation-induced deaminase
AITL	Angioimmunoblastic T cell lymphoma
ALCL	Anaplastic large cell lymphoma
AML	Acute myeloid leukemia
ATAC	Assay for Transposase-Accessible Chromatin
ATLL	Adult T cell leukemia/lymphoma
APC	Antigen-presenting cell
APRIL	A proliferation inducing ligand
Ascl2	Achaete-scute homolog 2
BAFF	B cell activating factor
Bcl6	B cell lymphoma 6
BCOR	Bcl6 corepressor
BCR	B cell receptor
Blimp1	B lymphocyte-induced maturation protein 1
BMDM	Bone marrow-derived macrophage
BTB/POZ	Broad complex, tramtrack and bric-a-brac/poxvirus and zinc-finger
Card11	Caspase recruitment domain family member 11
CBX8	Chromobox protein homolog 8
CCR7	C-C chemokine receptor type 7
ChIP	Chromatin immunoprecipitation
CHOP	Cyclophosphamide Hydroxyldaunorubicin Oncovin Prednisone
CSR	Class-switch recombination
CtBP	C-terminal binding protein 1
CTLA-4	Cytotoxic T-lymphocyte-associated protein-4
CTNNB1	Catenin Beta 1

CXCL13	C-X-C motif chemokine ligand 13
CXCR5	C-X-C chemokine receptor type 5
DC	Dendritic cell
DLBCL	Diffuse large B-cell lymphoma
DNMT3A	DNA methyltransferase 3A
DTR	Diphtheria toxin receptor
DZ	Dark zone
EAE	Experimental autoimmune encephalomyelitis
EAT-2	Ewing's sarcoma-associated transcript 2
EBV	Epstein-Barr virus
Edc4	Enhancer of mRNA decapping 4
EFNB1	Ephrin B1
ELISA	Enzyme-linked immunosorbent assay
ENU	Ethylnitrosourea
ERT	EAT-2 related transducer
EZH2	Enhancer of zeste homolog 2
FBXO11	F-box only protein 11
FDC	Follicular dendritic cell
Foxo1	Forkhead box protein O1
FTCL	Follicular T cell lymphoma
GC	Germinal center
GTF2I	General transcription factor Iii
HDAC	Histone deacetylase
ICAM-1	Intercellular adhesion molecule-1
ICOS	Inducible costimulator
IDH2	Isocitrate dehydrogenase 2
ILC	Innate lymphoid cell
Ig	Immunoglobulin
i.p.	Intraperitoneal
IRF4	Interferon regulatory factor 4

ITIM	Immunoreceptor tyrosine-based inhibitory motif
ITSM	Immunoreceptor tyrosine-based switch motif
Klf2	Krüppel-like factor 2
LFA-1	Lymphocyte function-associated antigen-1
LZ	Light zone
Mac-1	Macrophage antigen-1
MAPK	Mitogen activated protein kinase
Mb	Megabase
MHC	Major histocompatibility complex
Miz-1	Myc interacting zinc-finger protein-1
MTA3	Metastasis associated protein 3
mTORC1	Mammalian target of rapamycin complex 1
NCOR	Nuclear receptor corepressor
NF-κB	Nuclear factor kappa-light-chain-enhancer of activated B cells
NIK	NF-kappa-B-inducing kinase
NK	Natural killer
NOS	Not otherwise specified
NuRD	Nucleosome remodeling and deacetylase complex
OPN-i	Osteopontin
PD-1	Programmed cell death protein-1
PDK1	Phosphoinositide-dependent kinase 1
PD-L1	Programmed cell death ligand 1
PDX	Patient-derived xenograft
PEST	Proline (P), Glutamic acid (E), Serine (S), Threonine (T)
PI3K	Phosphoinositide 3-kinase
PLCG1	Phospholipase C, gamma 1
PRC	Polycomb repressive complex
Prkd2	Serine/Threonine protein kinase D2
PRMT5	Protein arginine methyltransferase 5
PTCL	Peripheral T cell lymphoma

Rap1	Ras-related protein 1
RD2	Repression domain 2
RHOA	Ras homolog family member A
RIAM	Rap1-interacting adapter molecule
RING	Really Interesting New Gene
SAP	SLAM-associated protein
Seq	Sequencing
SHM	Somatic hypermutation
SIRPα	Signal regulatory protein alpha
SH2	Src homology 2
SHP-1	Src homology region 2 domain-containing phosphatase-1
SLAM	Signaling lymphocytic activation molecule
STAT	Signal transducer and activator of transcription
T-ALL	T cell acute lymphoblastic leukemia
TAM	Tumor-associated macrophage
TBM	Tingible body macrophage
T-B	T cell-B cell
TCF-1	Transcription factor T cell factor-1
TCR	T cell receptor
TET2	Ten-Eleven Translocation 2
Tfh	T follicular helper
TGF-β	Transforming growth factor beta
TIL	Tumor-infiltrating lymphocyte
TLR9	Toll-like receptor 9
TNF	Tumor necrosis factor
TSP-1	Thrombospondin-1
UTR	Untranslated region
VEGF-A	Vascular endothelial growth factor-A
VEGFR1	Vascular endothelial growth factor receptor 1
VLA-4	Very late antigen-4

Zap70	Zeta chain of T cell receptor-associated protein kinase 70

Contribution of Authors

All chapters in this thesis have been proofread by **Dr. Woong-Kyung Suh**, who gave insightful comments and feedback.

Chapter 2

A version of Chapter 2 has been published in *Blood Advances*: **Witalis M**, Chang J, Zhong MC, Bouklouch Y, Panneton V, Li J, et al. Progression of AITL-like tumors in mice is driven by Tfh signature proteins and T-B cross talk. Blood Adv. 2020;4(5):868-79.

Mariko Witalis performed the majority of experiments such as flow cytometry, ICAM-1 binding assays, ultrasound imaging, enzyme-linked immunosorbant assays (ELISA) and genotyping. Tumor-bearing mice were monitored by **Mariko Witalis** as well as animal technicians at the IRCM animal facilities. Oral gavage and intraperitoneal (i.p.) injections were performed by animal technicians in CPA. **Mariko Witalis** and **Dr. Woong-Kyung Suh** designed the experiments and analyzed the data. The figures were prepared by **Mariko Witalis** with input from **Dr. Woong-Kyung Suh**. **Dr. Woong-Kyung Suh** conceptualized and supervised this study, and the original manuscript was written and edited by **Mariko Witalis** and **Dr. Woong-Kyung Suh**. **Jinsam Chang** performed genotyping and experiments with *Roquin*$^{san/+}$ mice that did not appear in this manuscript or thesis. **Dr. Ming-Chao Zhong** and **Dr. André Veillette** provided *Sh2d1a*$^{f/y}$ and *Sh2d1a*$^{R78A/y}$ mice, SAP antibodies and insightful advice. **Yasser Bouklouch** performed genotyping and designed primers to identify the Cre-excised *Bcl6* allele. **Vincent Panneton** and **Joanna Li** performed genotyping and proofread the original manuscipt prior to publication. **Dr. Thorsten Buch** provided *Cd4-Cre*^{ERT2} mice. **Dr. Seok Jin Kim**, **Dr. Won Seog Kim** and **Dr. Young Hyeh Ko** provided immunohistochemistry and immunoflurescence on human samples.

Chapter 3

The results presented in Chapter 3 have been used for a grant proposal and will be used for a future publication. **Mariko Witalis** completed all flow cytometry experiments and captured micropscopy images for immunohistochemistry. **Jiaxin Li** prepared bone marrow-derived

macrophages (BMDMs), performed phagocytosis assays, collected micropscopy images of phagocyotsis assays and analyzed data from phagocytosis assays. Tumor-bearing mice were monitored by **Mariko Witalis** and animal technicians in the IRCM animal facilities. Immunohistochemistry was done by the core facility at the Institut de recherche en immunologie et en cancérologie (IRIC). The study was conceptualized and supervised by **Dr. Woong-Kyung Suh**. **Mariko Witalis** and **Dr. Woong-Kyung Suh** designed the experiments and analyzed the data. The figures were prepared by **Mariko Witalis** with input from **Dr. Woong-Kyung Suh**. The manuscript was written by **Mariko Witalis** and also proofread and edited by **Dr. Woong-Kyung Suh**. **Mariko Witalis**, **Jiaxin Li**, **Vincent Panneton**, **Jinsam Chang** and **Joanna Li** participated in genotyping. **Dr. André Veillette** provided experimental advice.

Acknowledgements

This thesis and Ph.D. degree finally comes to fruition through the combined effort and support of countless individuals in my personal and professional lives. I would not have made it this far without all of you. There are not enough words to fully express my gratitude and appreciation, so I will simply say this – **thank you**. Reflecting on this Ph.D. journey, I retrospectively appreciate how the challenges I faced have helped me grow to become a wiser, stronger and more confident scientist. In this section, I would like to sincerely thank and acknowledge all the wonderful individuals who were instrumental in supporting me throughout my research.

First and foremost, I would like to thank my lab supervisor, **Dr. Woong-Kyung Suh** for accepting me into his lab as both a Master's and Ph.D. student. This journey would not have been possible if it were not for you taking a chance on me as a Master's student. Thank you for your patience at the beginning of my journey, as I slowly began learning new lab techniques. I am grateful to have you as a supervisor and mentor, and I appreciate your endless dedication to your students' success both inside and outside the lab. Inevitably, attempting experiments for the first time or creating new protocols can lead to instances of disappointment and "failure". Thank you for always fostering a lab environment where obtaining unexpected or negative experimental results were not framed through the lens of personal failure and instead, promoting these as learning opportunities to critically think and trouble-shoot. My deepest thanks and gratitude for your supervision, guidance and mentorship.

I would also like to express my sincere gratefulness and appreciation for having the privilege of working with members of the Suh lab – both present and current, those with brief stays and those who have worked alongside me since the beginning of my Ph.D. I am immensely proud to say that I belong to this amazing team of "SUHper Hippos" and I cannot wait to see the success of future lab members. To the two latest graduates of the Suh lab: **Dr. Joanne Leung** and **Dr. Sahar Yazdchi Bagherzadeh** – thank you for your advice, guidance and training. To me, you were my upper-level Ph.D. student-mentors, and I am grateful that you promoted a friendly and kind lab environment. I would also like to acknowledge **Philippe St-Onge**, who for a short time as a Ph.D. student worked in parallel with me on a *Roquin*$^{san/+}$ AITL project in the Suh lab. **Yasser Bouklouch**, while we worked together for only a brief time, your passion,

expertise and advice regarding genomic-related topics was appreciated and extremely helpful. I also would like to thank **Jiaxin Li**, who was a Master's rotation student in our lab, for whom I was responsible for mentoring. As much as I was responsible for teaching you flow cytometry, ultrasound imaging and tumor palpation, you also brought your knowledge and enthusiasm for immunology and particularly, phagocytosis assays, for which I am grateful. Thank you for your contribution to this project. To my current colleagues: **Vincent Panneton, Jinsam Chang**, **Joanna Li** and **Antoine Bouchard** – my deepest thanks. **Vincent Panneton**, thank you for your help editing my abstract into French on numerous occasions, including this thesis. Thank you to everyone for the stimulating conversations both related and unrelated to science. I would like to express my deepest appreciation for all the help, support, advice and friendship – this experience would not have been the same without all of you.

I also need to take this opportunity to sincerely thank the dedicated individuals involved in leading and supporting the IRCM core facilities, particularly CPA (**Manon Laprise, Valerie Darisse-Lafrance, Marie-Anne Riquelme Jacob, Caroline Dubé** and **Marie-Claude Lavallée**), histology (**Simone Terouz)**, microscopy (**Dominic Filion**) and flow cytometry (**Eric Massicotte, Julie Lord** and **Philippe St-Onge)**. I am also very grateful to the dedicated and hard-working animal technicians in SPF (**Viviane Beaulieu**) and SPF+ (**Stephanie Lemay**) for assistance with animal care and monitoring. I would also like to thank the specialized equipment service team: **Richard Cimon**, **Sami Sukkar** and **Jean-François Lauzon** for always diligently taking care of and fixing scientific equipment.

I also would like to express my appreciation to my committee members over the years: **Dr. Michel Cayouette**, **Dr. Javier Di Noia** and **Dr. Jörg Fritz** who diligently followed up on my progress each year. Thank you for your advice, suggestions and positive words of encouragement. Additionally, I would like to thank the Academic Affairs Advisors at the IRCM, **Virginie Leduc** and **Myrna Khuon** as well as **Lucie Yan Liu** from the Molecular biology department at the Université de Montréal for their assistance with regards to degree and graduate requirements.

I would also like to take this opportunity to acknowledge the support of my parents - thank you, *for everything*. Lastly, to **Vitalijs Arkulinskis, my husband,** thank you for being my number one cheerleader throughout this journey with your continuous words of encouragement.

Table of Contents

Chapter 1 General Introduction

1.1 Characteristics of AITL disease

1.1.1 Clinical features of AITL

Angioimmunoblastic T cell lymphoma (AITL) is an aggressive type of non-Hodgkin lymphoma with a median age of onset around 62-65 years of age, although cases have been reported in younger patients closer to 20 years old (1, 2). At the time of diagnosis, the majority of AITL patients are at later stages of disease progression such as stage III or IV (1, 3), contributing to poor survival rates (5-year survival rate is ~30%) (1-3). Even so, the rate at which AITL tumors spread to other lymph nodes can vary from months to years (4). The majority of patients present with generalized lymphadenopathy and B-symptoms which include fevers, weight loss, and/or night sweats (1-3). Lymphadenopathy can be observed in cervical, mediastinal, axillary and inguinal lymph nodes (5, 6), but some case studies have also reported swollen mesenteric lymph nodes (7, 8). AITL patients may also experience extranodal involvement in the liver, spleen, skin and bone marrow as well as hypergammaglobulinemia and hemolytic anemia (1-3, 9). Patients with bone marrow involvement are more likely to also have B-symptoms, hepatosplenomegaly and circulating tumor cells (3, 10, 11).

Due to the gross immune dysregulation driven by AITL, patients may also suffer from infections such as tuberculosis, cryptococcus and lymphotropic viruses, most notably Epstein-Barr virus (EBV) (12-14). EBV infected B cells are also detected in a majority of AITL cases (~80%) (3), and approximately 10% of AITL patients also develop secondary B cell lymphomas, a large proportion of which are linked to EBV positivity (15). Detection of EBV^+ B cells in young patients (less than 60 years) has been reported to correlate with improved prognosis, although, no such relation was found in older patient groups, which better represent the majority of AITL patients (16). Additionally, detection of higher viral loads of EBV in AITL has been associated with B cell monoclonality as well as more advanced histological AITL patterns (17).

1.1.2 Histological features of AITL

Within AITL tumor lymph nodes, there is an inflammatory immune cell environment that contains not only abnormal neoplastic T cells, but also reactive T and B cells, plasma cells, histocytes, and eosinophils (3, 14, 18). Other key features of AITL histology include branching of high endothelial venules (feature of angiogenesis) and atypical expansion of follicular

dendritic cell (FDC) meshworks (11, 18). Neoplastic AITL tumor cells express CD4, T cell receptor (TCR) α/β, B cell lymphoma 6 (Bcl6), inducible costimulator (ICOS), SLAM-associated protein (SAP), programmed cell death protein-1 (PD-1), C-X-C chemokine receptor type 5 (CXCR5), and C-X-C chemokine ligand 13 (CXCL13), all of which are signature molecules for the T follicular helper (Tfh) cell lineage (3, 11, 19-23). More details regarding the Tfh cell origin of AITL tumor cells will be discussed in the next section 1.1.3. CD10 is heterogeneously expressed in 70-90% of AITL but is also present on other types of mature T cell lymphomas, and as such, compared to Tfh cell-specific proteins, is not as commonly used as an AITL diagnostic marker (6, 18, 24, 25). CD30 is also expressed in approximately 40-60% of AITL patients, and recent phase III clinical trial data suggests that these CD30-positive patients may benefit from additional CD30-directed antibody-drug conjugate therapy (3, 26). In line with the neoangiogenic features observed in AITL, vascular endothelial growth factor-A (VEGF-A) and receptor VEGFR-1 are found overexpressed in both lymphoma and endothelial cells and are linked with poorer disease outcomes (27, 28).

AITL lymph nodes have three different histological presentation patterns: I, II and III, which appears to relate to disease progression (4, 14, 18). In type I, which represents ~20% of patients, the normal lymph node structure is still intact but hyperplasic B cell follicles with an ill-developed mantle zone and enlarged paracortical region are present (3, 4, 14, 18). In pattern II (~30% of patients) there is a loss of normal lymph node architecture and an expansion of FDC meshworks that surrounds developing blood vessels (3, 11, 14, 18). Pattern III is the most common histological pattern observed amongst AITL patients, seen in ~50% of cases (14). In this pattern, there is an effacement of lymph node architecture, as well as extensive FDC and vascular proliferation (3, 4, 11, 14, 18). Additionally, it is usually around these branched vascular networks that AITL tumor cells are clustered (11). Intriguingly, the neoplastic T cell population is only a minor proportion of the AITL tumor mass and consequently, the distinct histological features as aforementioned are mostly related to the abnormal growth of FDCs and B cell populations (3, 14).

1.1.3 Origin of AITL tumor cells

Numerous gene expression and immunohistochemical studies have determined that AITL tumor cells derive from a specialized subset of $CD4^+$ T cells, more specifically, the T follicular

helper (Tfh) cell (1, 19, 21, 23, 27, 29-32). Signature Tfh cell proteins such as Bcl6, CXCR5, PD-1, CXCL13, SAP, ICOS and CD40L are overexpressed in patient samples suggesting the Tfh cell origin of neoplastic cells in AITL (19-24, 33). Moreover, serial transplantation of splenocytes from immunodeficient NOD/Shi-*scid*/IL-2Rγ^{null} mice originally xenografted with human AITL cells demonstrated preferential survival and expansion of a $CD4^+$ T cell compartment enriched for Bcl6 and Tfh cell markers, further supporting their Tfh cell origin (32). Tfh cells play an essential role within the context of humoral immunity by providing help to B cells in germinal centers (GC), and this interaction relies on critical signaling pathways that support B cell proliferation, differentiation and crosstalk with Tfh cells (34, 35). Further details regarding the role of Tfh cells within the context of GCs and specific signaling molecules will be discussed within section 1.2. The functional consequence of neoplastic Tfh cell-derived tumor cells is further reinforced in the various clinical pathologies experienced by AITL patients, such as B-symptoms, hypergammaglobulinemia, autoimmune hemolytic anemia and increased risk for developing secondary B cell lymphomas (3, 15).

1.1.4 Genetic mutations involved in AITL disease onset

1.1.4.1 *RHOA*

Approximately 50-70% of AITL patients have a somatic point mutation in the small GTPase *RHOA*, which results in the conversion of a glycine residue to a valine residue at amino acid 17 ($RHOA^{G17V}$) (3, 36-38). While this $RHOA^{G17V}$ mutation is very characteristic to AITL, it has also been identified in ~20-25% of peripheral T cell lymphomas (PTCL) with a Tfh cell phenotype (3, 38), follicular T cell lymphoma (FTCL) (39, 40) and adult T cell leukemia-lymphoma (ATLL) (41). Importantly, FTCL patients with *RHOA* mutations share characteristics with AITL disease such as presence of B-immunoblasts and high expression levels of BCL6 or CXCL13 (39). *RHOA* mutations are often observed along with loss-of-function *TET2* mutations (will be described in more detail in section 1.1.4.2) (36, 38). Due to the fact that *TET2* mutations are also found in non-tumor hematopoietic cells such as B cells in AITL patients, whereas *RHOA* mutations are exclusive to tumor cells, a multistep process for AITL disease initiation has been hypothesized (36, 38, 42).

The $RHOA^{G17V}$ mutation leads to a loss of GTP binding activity and inhibition of wildtype RHOA (36, 37). Additionally, it appears that RHOA-G17V can specifically interact

with VAV1 and in so doing, activates VAV1 adaptor protein functionality and promotes T cell receptor signaling (43). A more recently described novel K18N mutation in RHOA has been reported in three AITL patients, but extensive studies characterizing its altered function have not been conducted (44). *In vivo* mouse models studying $Rhoa^{G17V}$ demonstrates that this mutation leads to abnormal $CD4^+$ T cell proliferation and polarization into the Tfh cell lineage, consistent with the Tfh cell nature of AITL (45, 46). Importantly, only mice with combined loss of TET2 and expression of mutant RHOA-G17V developed AITL-like disease (45-47). Critical signaling pathways that support AITL-like disease in this context include ICOS, PI3K and MAPK signaling as well as alterations in forkhead box protein O1 (FOXO1) expression, phosphorylation and localization, all of which are reported to play roles in Tfh cell biology (38, 47, 48).

1.1.4.2 Epigenetic modifiers – *TET2*, *DNMT3A*, *IDH2*

Mutations in epigenetic modifiers such as *TET2*, *DNMT3A* and *IDH2* have been identified in AITL as well as PTCLs with a Tfh cell phenotype (36, 38, 42, 49, 50). TET2 is an enzyme that converts 5-methylcytosine into 5-hydroxymethylcytosine, an intermediate in the DNA demethylation process (51, 52). Loss-of-function mutations in *TET2*, such as frameshift indels and nonsense mutations (36, 38, 53) have been reported in 30-80% of AITL patients (54, 55) but can also be observed in myeloid cancers (56, 57) and B cell lymphomas (58). Interestingly, approximately 57% of AITL and PTCL patients are reported to have multiple (2 or 3) *TET2* mutations (36, 53).

DNMT3A is a DNA methyltransferase mutated in approximately 10-48% of AITL patients, which catalyzes 5-methylcytosine methylation and as such, also plays an essential role in regulating gene expression (36, 38, 59-61). Approximately 60% of *DNMT3A* mutations occur in its methyltransferase domain and ~25% of these are missense mutations at the R882 position (36, 38, 53). The result of this R882 mutation has been reported to generate a hypomorphic variant that inhibits wildtype methyltransferase activity to deregulate DNA methylation patterns (59, 62).

IDH2 mutations, specifically at position R172 (20-45% of AITL patients), leads to altered enzymatic function that results in the conversion of isocitrate into the oncometabolite 2-hydroxyglutarate (2-HG) instead of the normally produced alpha-ketoglutarate (49, 61, 63). The accumulation of 2-HG can be oncogenic since it disrupts the activity of enzymes that depend on

alpha-ketoglutarate, such as TET2 (3, 49, 63, 64). Comparison of AITL patient samples with or without $IDH2^{R172}$ mutations found that patients with $IDH2^{R172}$ mutations had stronger expression of CD10 and CXCL13 (61) and also carried a unique gene signature (63), thereby identifying patients with $IDH2^{R172}$ mutations as a unique subgroup amongst AITL (61, 63).

In a majority of patients (70-97%), loss of TET2 function coincides with mutations in either $RHOA^{G17V}$ and/or $IDH2^{R172}$ (36, 61, 63, 65, 66). Additionally, approximately 70-80% of AITL patients with *DNMT3A* mutations also have *TET2* mutations (60, 63). Studies using mice with these combined mutations demonstrated synergistic effects on the development of AITL-like lymphomas with predominant features of Tfh-like cells (55, 62, 67). Additional descriptions of mouse phenotype for each model, as well as others not mentioned here will be discussed at length in section 1.4. Furthermore, it has been reported that the allelic frequencies of *TET2* and *DNMT3A* mutations are higher than those of $IDH2^{R172}$ or $RHOA^{G17V}$, suggesting that these mutations are acquired beforehand (53, 61). In line with this, mutations in *TET2* and *DNMT3A* have been observed in non-neoplastic cells of the B cell lineage (36, 42, 60, 68), further signifying that these mutations occur at earlier stages of hematopoiesis.

1.1.4.3 Activating mutations in T cell receptor signaling

Approximately half of AITL patients have activating mutations relating to T cell receptor or costimulatory signaling genes (44). Point mutations in costimulatory molecule CD28 have been identified in approximately 10-20% of AITL patients (44, 65, 69, 70). These mutations augment downstream signaling through increased ligand or adaptor protein binding affinity (44, 69). Additionally, in one cohort of AITL patients studied, approximately 60% had a *CTLA4-CD28* fusion gene, encoding the extracellular domain of cytotoxic T-lymphocyte-associated protein-4 (CTLA-4) with the cytoplasmic portion of CD28, likely transforming inhibitory signaling inputs downstream as activating signals (71). Additionally, recurrent *FYN* kinase mutations (~5-10% of patients), an important player downstream of TCR signaling, have also been reported in AITL (3, 38, 44). These *FYN* mutations interrupt intramolecular inhibitory Src homology 2 (SH2)-mediated interactions, resulting in increased kinase activity (3, 38). Other activating mutations in AITL patients related to elevated TCR signaling are found in genes such as *PLCG1* (14%), *PI3K* elements (7%), *CTNNB1* (6%), *GTF2I* (6%), *PDK1* (6%), *VAV1* (5%) and *CARD11* (3.5%) (44). Except for patients with the *CTLA4-CD28* fusion, other patients with

activating mutations in TCR signaling components were found to be mutually exclusive or more specifically, these mutations did not co-occur with *RHOA* mutations (44, 71).

Thus, it seems that AITL lymphomagenesis can occur through at least two different routes. In the first model, mutations in epigenetic modifier genes such as *TET2* or *DNMT3A* in early hematopoietic precursor cells initiate primary oncogenic events, which when coupled with secondary mutations such as $RHOA^{G17V}$ within the $CD4^+$ T cell compartment leads to AITL disease (72). However, since there are also AITL patients with mutations only in components related to TCR signaling, in the second model, acquiring certain activating mutations in TCR signaling without *TET2* or *RHOA* mutations can be sufficient to cause AITL.

1.1.5 Epigenetic modifications in AITL

Although mutations in epigenetic modifiers are well-characterized in AITL, less is known about the outcome of these mutations on DNA methylation patterns. It has been reported that in most AITL patients with *TET2* mutations, hypermethylation occurs at intron 1, a silencer region of *BCL6*, which importantly, is also linked to increased protein expression of Bcl6 (54, 55). As Bcl6 is a critical transcription factor defining the Tfh cell lineage, this alteration in Bcl6 expression as a result of loss-of-function TET2 in AITL tumors may promote $CD4^+$ T cell differentiation into Tfh-like cells (3). $IDH2^{R172}$ mutations have been associated with global DNA hypermethylation and higher levels of H3K27me3 (63). Genes involved in the negative regulation of TCR signaling and Th1 differentiation were downregulated as a result of this altered hypermethylation induced by $IDH2^{R172}$ mutations (63). Importantly, these *IDH2* mutations do not appear to have an additional impact with *TET2* mutations on *BCL6* methylation status (54). Since the accumulation of 2-HG as a result of mutant IDH2 inhibits TET2 functionality, in patients where both *TET2* and *IDH2* mutations occur, this may provide an additive effect that supports Tfh cell identity (63). To further add to this, as *TET2* mutations are hypothesized to occur before $IDH2^{R172}$ mutations (53, 61), one possibility is that TET2-mediated alterations in *BCL6* promote Tfh cell differentiation and predispose individuals to AITL development, whereas these secondary *IDH2* mutations work to reinforce DNA methylation patterns to further reduce TET2 function.

1.1.6 Prognostic markers for AITL patients

Since survival rates for AITL patients are rather low (1, 73), finding prognostic markers can be incredibly useful to help predict which patients may experience more severe cases. Patients with the $RHOA^{G17V}$ mutation are reported to more likely experience B-symptoms, splenomegaly and increased microvessel density (74, 75). Additionally, patients with mutant RHOA also had greater FDC expansion and expression of Tfh cell-related proteins (75, 76). In one AITL cohort, presence of $RHOA^{G17V}$ was linked to poorer progression-free survival rates, possibly related to a higher association with B-symptoms and later stage disease (75, 76). On the other hand, presence of *IDH2* mutations in AITL patients does not appear to impact survival rates (49). Elevated levels of serum soluble IL-2 receptor, IL-10 and β2 microglobulin in AITL patients have also been associated with poorer patient outcome (77-79). Furthermore, AITL tumors with high levels of TLR9 and PD-L1 were reported to be predictors of more advanced stage disease and lower survival rates (80). Additionally, increased infiltration of M2-macrophages in AITL also correlated with poorer survival (78, 81). Higher levels of enhancer of zeste homolog 2 (EZH2) or histone deacetylase (HDAC) in PTCL patients, including AITL is also associated with worsened overall survival rates (82). Lastly, AITL patients with reduced cytoplasmic FOXO1 levels are also more likely to have advanced disease stage, bone marrow involvement and poorer survival rates as compared to patients with FOXO1 levels distributed in both the cytoplasm and nucleus (83). Since it has been reported that enforcing FOXO1 nuclear localization in mouse models can suppress Tfh cell differentiation (84), AITL patients with increased cytoplasmic FOXO1 may have poor prognosis due to stronger facilitation of a FOXO1-mediated Tfh cell phenotype.

1.1.7 Current treatment options for AITL patients

The front line treatment for most AITL patients generally aims to be curative and is based on addition(s) to CHOP (cyclophosphamide, hydroxyldaunorubicin, Oncovin/vincristine, prednisone) therapy (3, 5, 85). This is also the main type of therapy for PTCLs (3, 5, 85). Combining CHOP therapy with autologous stem cell transplant after first remission in AITL has shown promising outcomes (3, 5). In younger patients less than 60 years of age, etoposide in addition to CHOP is prescribed as front line therapy, since it appears to improve patient outlook (3, 5, 86, 87). For elderly patients, CHOP is still recommended as the standard first line therapy

(86). These therapeutic regimens for patients > 60 years of age tend to be milder and focus on suppressing symptoms associated with AITL rather than being curative (5). Although the response rate to these initial CHOP therapies is high, AITL patients are also extremely prone to relapse, and as such, the 5-year survival rate remains quite low at around 30% (3, 5, 88, 89).

For relapsed and refractory cases of AITL, studies observing cohorts of AITL patients that received allogenic stem cell transplantation yielded positive results, with high 5-year overall survival rates of 80% (3, 90). However, this type of therapy is not always feasible for patients as a result of their age, presence of comorbidities, or inability to locate an appropriate donor (3). Due to the Tfh cell-derived nature of AITL, and the natural ability of Tfh cells to support B cell proliferation and survival, the majority of the tumor mass can be attributed to B cells (3, 11, 14). Consequently, one intriguing idea to treat AITL would be to use a B cell depleting therapy such as anti-CD20 (rituximab) in addition to standard CHOP regimen. However, studies reported that although rituximab plus CHOP had a high overall response rate, the progression-free survival rates were not better than CHOP therapy alone (91). One possible explanation for why B cell depletion in AITL tumors does not lead to durable responses is that although B cells contribute to AITL-associated pathologies, they are not the primary drivers of disease (91).

Bearing in mind the T cell hyperactivity associated with AITL, therapies designed to either inhibit T cell-B cell (T-B) crosstalk or TCR activation may be more effective. On this note, treating a small cohort of AITL patients with dasatinib, an inhibitor of multiple Src family kinases, many of which are involved in TCR downstream activation, showed partial effectiveness in relapsed/refractory AITL patients (92). In murine models, PI3Kδ signaling has been shown to be a critical regulator of Tfh cell differentiation (93). Moreover, in a group of relapsed/refractory PTCL patients, including 3 AITL patients, the use of duvelisib, a PI3Kδ/γ inhibitor, showed an overall response rate of 50% (5, 94). Due to the Tfh cell nature of AITL, inhibitors of Bcl6, which have shown efficacy in certain B cell lymphomas, may also be an attractive candidate for future AITL therapies (95).

As aforementioned, a majority of AITL patients carry mutations in epigenetic modifiers such as *TET2*, *DNMT3A* or *IDH2*, which also impacts DNA methylation patterns and gene expression (54, 63). In myeloid malignancies associated with *TET2* mutations, use of hypomethylating agent 5-azacytidine has shown encouraging results (96, 97). Administering 5-azacytidine to AITL patients demonstrated higher overall and complete response rates, even

when compared to other PTCLs (98). Moreover, all AITL patients who experienced a response after 5-azacytidine treatment also carried *TET2* mutations (98), potentially indicating that *TET2* loss-of-function mutations continually help maintain AITL disease. Although much research has been done and is underway to improve AITL therapies and patient outcomes, currently, there is no effective therapy for AITL patients. Therefore, understanding the molecular pathways and cellular interactions which support the expansion of neoplastic Tfh-like cells may help develop novel therapeutic options.

1.2 T follicular helper cells and the germinal center

1.2.1 Overview of germinal centers

Germinal centers are microanatomical structures which develop within B cell follicles of secondary lymphoid organs such as the spleen or lymph nodes, typically after immunization or infection (34, 99-102). In gut mucosal areas such as Peyer's patches, spontaneous GCs also develop due to constant exposure to foreign dietary antigens as well as commensal bacteria (103). A general overview of important steps within the GC reaction will be discussed in sections 1.2.1.1-1.2.1.3 and is also depicted in Figure 1.1. Germinal centers are the site of B cell clonal expansion and differentiation into high affinity antibody-secreting plasma cells or memory B cells (101, 102). GCs are further segregated into two distinct compartments, the dark zone (DZ) and light zone (LZ) (100-102, 104). It is within the DZ that B cells rapidly divide and undergo somatic hypermutation (SHM) to produce high affinity B cell receptors (BCR) (100-102, 104). In the LZ, follicular dendritic cells capture and retain intact antigen such that B cells with suitable BCR signaling capacity are protected from apoptosis (104-106). From here B cells will compete based on the affinity of their BCR for Tfh cell help, and if successful, Tfh cells will support the survival and differentiation of these high affinity B cell clones (100-102, 104, 106). In addition to promoting B cell selection, and survival, Tfh cells also facilitate cyclic re-entry into the DZ for further rounds of SHM (104). Tfh cells provide help through a variety of signaling pathways including TCR-peptide/major histocompatibility complex II (MHCII) interactions, costimulatory molecules, adhesion molecules, cytokines and chemokines (34, 35, 48, 107). There are also numerous regulatory molecular elements involved in the GC reaction

which, if not properly balanced, can lead to the onset of autoimmune disease or lymphomas derived from either T or B cell lineages (35).

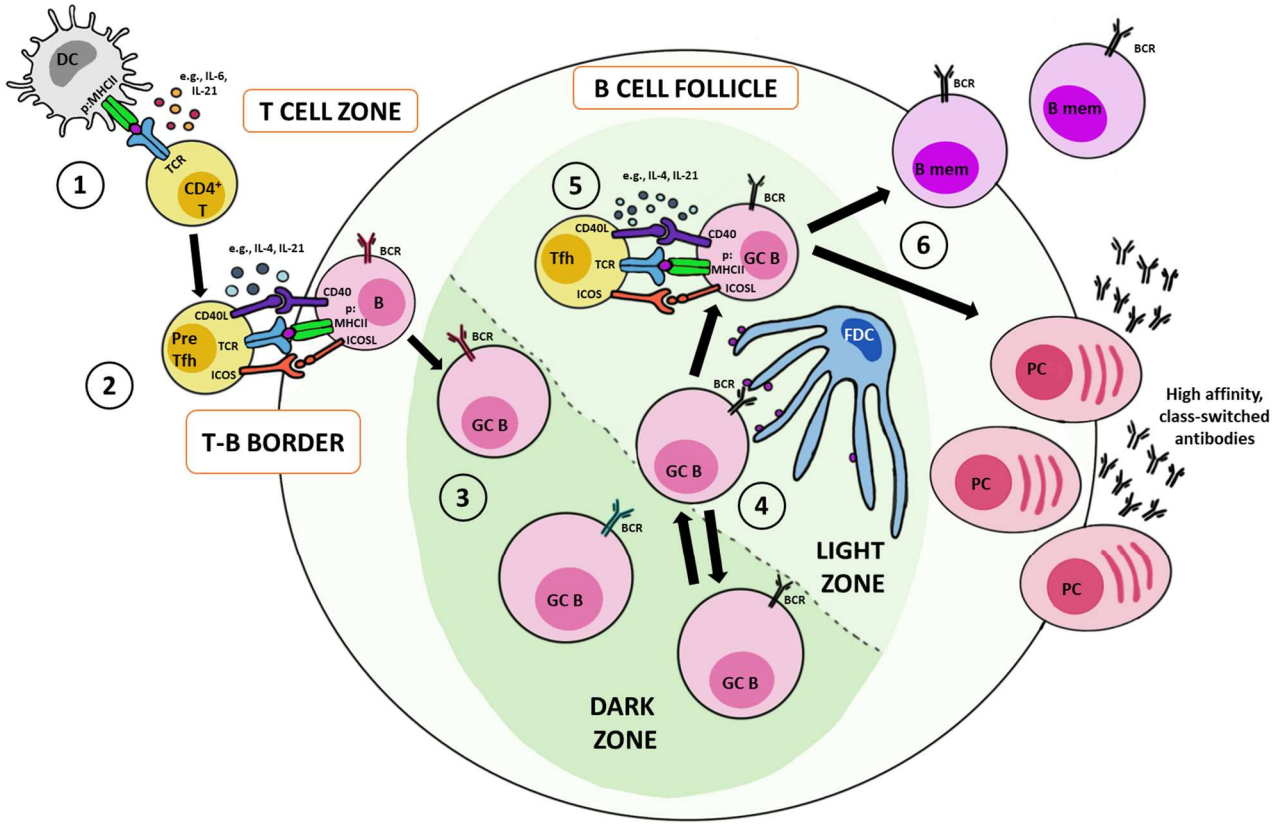

Figure 1.1 Overview of the germinal center reaction

(1) In the T cell zone, dendritic cells (DC) prime naïve $CD4^+$ T cells and support initial Tfh cell generation by providing costimulatory signals and an optimal cytokine environment. (2) At the T-B border, pre-Tfh cells will interact with bystander B cells until they find their cognate B cell and then form stable T-B conjugates. (3) GC B cells in the GC dark zone rapidly proliferate and mutate their immunoglobulin genes. (4) GC B cells migrate into the light zone where they are exposed to antigen captured by FDCs. These GC B cells can also re-enter the dark zone to go through more rounds of somatic hypermutation. (5) GC B cells in the light zone compete for Tfh cell help. (6) GC B cells with antigen-specific B cell receptors (BCRs) can differentiate into memory B cells (B mem) or plasma cells (PCs).

1.2.1.1 GC Initiation

GC formation initiates when B cells bind to either soluble antigen or antigen presented on the surface of FDCs, dendritic cells (DCs) or macrophages, which leads to activated B cell migration towards the T cell zone (101). In order for naïve $CD4^+$ T cells to differentiate into the Tfh cell lineage, they first must undergo priming with antigen-presenting DCs and receive antigen-specific TCR stimulation, where T cells with stronger peptide/MHCII binding are more

likely to become Tfh cells (34, 107-109). Additionally, proper Tfh cell differentiation depends on costimulatory molecules, such as CD28 and ICOS, adhesion molecules as well as cytokines IL-6 and IL-21 (35, 107) and will be further discussed in sections 1.2.2 and 1.2.3, respectively. Importantly, naïve $CD4^+$ T cells induce a short-lived primary wave of Bcl6 expression when primed by DCs, whereas interaction with cognate B cells augment Bcl6 expression levels and establish the Tfh cell program (110). Moreover, upregulation of Bcl6 is also associated with increased expression of other signature Tfh cell proteins such as CXCR5, PD-1 and ICOS (110-113). More details regarding Bcl6 function in the context of both T and B cells in GCs will be reviewed in section 1.2.4. In particular, increased expression of CXCR5 is a critical event to allow pre-Tfh cells to migrate towards the B cell follicle through its attraction to ligand CXCL13 (35, 107). Importantly, expression of CXCR5 is insufficient to mediate migration into the follicle and rather must be synchronized with the reduction of C-C chemokine receptor type 7 (CCR7) levels, important for T cell zone retention (34, 35, 108, 114). At the T-B border, primed pre-Tfh cells will interact with both bystander and cognate B cells which serve as primary antigen-presenting cells (APCs) to further reinforce the Tfh cell program (34, 107, 110). Here, ICOS signaling plays an important role to facilitate both T cell migration and costimulation at the T-B border until pre-Tfh cells locate their cognate B cells (115). Generally, PD-1 is believed to negatively regulate Tfh cells by inhibiting T cell activation, however, at the T-B border, independent of TCR signaling, PD-1 can also inhibit T cell recruitment into B cell follicles by limiting CXCR3 expression (116, 117). Importantly, once pre-Tfh cells receive antigen-specific signals from cognate B cells, they will form conjugates stabilized by signaling lymphocytic activation molecule (SLAM) family receptors and their adaptor protein SAP as well as lymphocyte function-associated antigen-1 (LFA-1), which maintains the Tfh cell phenotype and allows for GC formation (35, 107, 110, 118-120).

1.2.1.2 Intimate T-B communication at the height of the GC response

Generally, Tfh cells are key in supporting GC B cell differentiation through the production of IL-4 and IL-21 as well as expression of CD40L (102, 121-125) (Fig. 1.2A-C). Further details on how these cytokines and molecules support the GC response will be discussed in sections 1.2.2 and 1.2.3. It is largely within the LZ where T-B communication serves an essential role in the selection of GC B cells with high affinity BCRs to promote their proliferation and differentiation (104). Tfh cells interacting with antigen-specific B cells respond

by increasing contact surface area (also described as entanglement between T and B cells) and contact duration time (119, 124, 126). Generally, these entangled T-B contacts are transient, lasting less than 5 minutes, however, higher amounts of cognate peptide/MHCII presentation from B cells can increase this contact time, leading to stable T-B conjugates (104, 124, 126, 127). The formation of these stable conjugates is essential for proper GC development as well as antibody production and in addition to this, stronger T-B communication preferentially facilitates GC B cell differentiation into plasma cells (125). In line with this idea, reduced humoral immunity is observed in SAP-deficient mice, since durable T-B conjugates cannot be properly formed in the absence of SAP-expressing $CD4^+$ T cells (128).

1.2.1.3 Mechanisms and outcomes of GC response

Tfh cells are fundamental in determining the final fate of GC B cells to differentiate into memory B cells or antibody-secreting plasma cells (35, 107, 129). Plasma cell lineage commitment is heavily dependent on the stable formation of T-B contacts supported by CD40/CD40L, LFA-1/ICAM-1 and SLAM/SLAM interactions (125, 130) (Fig. 1.2B). Although transcription factor Bcl6 plays a critical role in supporting GC B cell differentiation and function, its downregulation is necessary for commitment into memory B cells or plasma cells (125, 131-134). Plasma cell differentiation is initiated by high expression levels of transcription factor interferon regulatory factor 4 (IRF4), which then induces expression of B lymphocyte-induced maturation protein 1 (Blimp1) in an IL-21 dependent manner, reinforcing the plasma cell program (129, 135-139). Interestingly, B cell-specific loss of IRF4 leads not only to failed plasma cell generation, but a reduction in differentiated GC B cells (139). This has been linked to the relative dose of IRF4 within a given B cell. While lower amounts of IRF4 stimulate activation-induced cytidine deaminase (AID) and Bcl6 expression, which promotes class-switch recombination (CSR) and early GC B cell differentiation, higher IRF4 levels drive Blimp1 expression and thus, terminal plasma cell differentiation (129, 138-140) (Fig. 1.2D). Blimp1 facilitates global changes in gene expression to maintain the plasma cell phenotype as well as to support efficient immunoglobulin (Ig) secretion (132, 136, 141). However, Blimp1 is not essential to initiate plasma cell formation, and instead, it maintains mature plasma cell differentiation and supports the main purpose of plasma cells as antibody-secreting cells (137). Lastly, once formed, plasma cells migrate to bone marrow niches where they receive survival signals such as CXCL12, APRIL and BAFF from the stromal environment (142, 143).

Memory B cell formation is also an important part of long-lived immunological memory and another potential fate of the GC reaction (144). Memory B cells are able to rapidly re-activate and produce class-switched high affinity antibodies in response to a previously experienced pathogen (144). Generally, high affinity GC B cells are more likely to differentiate into plasma cells, possibly due to their ability to elicit more help from Tfh cells and form stronger T-B contacts (145). In contrast, it has been reported that low affinity GC B cells are predetermined to become part of the memory B cell lineage (146-148). Although specific lineage-defining transcription factors such as Blimp1 in plasma cell biology have not been clearly identified for memory B cells, high levels of transcription factor Bach2 has been suggested to preferentially promote memory B cell differentiation (144, 148).

Once Tfh cells have completed their B cell helper activities they can either migrate into a different GC or follicle or can downregulate Bcl6 to become a memory Tfh cell (34, 149-151). Memory Tfh cells still express CXCR5, but have lower amounts of PD-1 and Bcl6, although, levels of Bcl6 can be rapidly upregulated upon interaction with cognate memory B cells (152, 153). In both humans and mice, it appears that memory Tfh cells can also develop in the absence of proper GCs, since SAP-deficient mice and humans do not have fully differentiated Tfh cells, yet circulating memory Tfh cells have been identified (35). In both humans and mice, although memory or long-lived Tfh cells have been reported, and functional studies demonstrate their ability to support memory B cell responses, the manner in which they originate, either as memory $CD4^+$ T cells with Tfh-like features or Tfh cells with acquired memory properties, has yet to be clearly elucidated (35, 108, 153).

1.2.2 Critical cytokines supporting Tfh cell differentiation and GC dynamics

Numerous cytokines play critical roles in the GC and impact both T and B cell differentiation and function (Fig. 1.2C). Initiation of the Tfh cell program in mice depends heavily on a specific cytokine milieu which contains IL-6 and IL-21 (34, 48). In contrast, for humans, Tfh cell generation appears to be influenced by a different cytokine milieu involving TGF-β, IL-12 and IL-23 (35). Nevertheless, in murine models, IL-6 is essential for supporting early stages of Tfh cell differentiation by transiently elevating Bcl6 levels (112, 154-156). In contrast, loss of IL-6 signaling does not impact GC B cell development, although the generation of antigen-specific class-switched antibodies is affected (156, 157). IL-6 signaling can also

promote IL-21 production (155, 158, 159), through c-Maf mediated association with IL-21 gene regulatory elements, which may reinforce Tfh cell differentiation and provide help to B cells (160).

With regards to the role of IL-21 signaling in Tfh cells, three different outcomes have been reported. In some instances, IL-21 signaling deficiency alone had no impact on Tfh cell generation (156, 157, 161, 162), which may be explained by the compensatory nature between IL-6 and IL-21 through shared STAT1 and STAT3 signaling pathways (35, 154, 156-158). In other studies, lack of IL-21 signaling impaired Tfh cell formation (163, 164), while it has also been suggested that the absence of IL-21 signaling does not impact early Tfh cell generation but only later stages of Tfh cell maintenance (165). Nonetheless, overall, IL-6 and IL-21 are essential to support GC reactions but may have different functions depending on the type of immune challenge (protein immunization versus viral infection).

Tfh-produced cytokines IL-4 and IL-21 are also key components for supporting GC B cell proliferation, affinity maturation and selection (35). Both IL-4 and IL-21 have been reported to regulate Bcl6 expression in GC B cells (123, 165). Loss of IL-21 signaling negatively impacts GCs by reducing GC B cell proliferation and plasma cell generation (161, 165). IL-4-producing Tfh cells have also been shown to express high levels of CD40L (166), which enhances plasma cell production (125, 167). IL-4 also regulates AID gene expression in GC B cells, and thus supports the production of high affinity class-switched antibodies (168). The process of affinity maturation and CSR is reliant on both IL-4 and IL-21, as deficiency in either cytokine has been linked to impaired IgG1 affinity maturation (161, 165, 169, 170). Interestingly, mice lacking the IL-21 receptor have increased IL-4 dependent production of IgE, potentially linked to sequential class-switching, a model unique to the IgE subtype (169, 171). Importantly, it has been reported that during the GC response, Tfh cells gradually differentiate into IL-21- and then IL-4-producing cells which are differentially localized and also have distinct transcriptional profiles (166). These differences also impact their B cell helper functions as IL-21-producing Tfh cells are reported to be superior in supporting high affinity maturation whereas IL-4-producing Tfh cells are better at promoting plasma cell differentiation and CSR (108, 166).

For Th1, Th2 and regulatory T cell lineages, IL-2 plays an important role in supporting their differentiation and growth (172), however, in contrast, IL-2 signaling through STAT5 has an inhibitory role in Tfh cell development, as it suppresses Bcl6 expression (173, 174). $CD4^+$ T

cells with stronger TCR signaling upregulate Bcl6 and become IL-2-producing Tfh precursor cells which can then deliver IL-2 in a paracrine way to reinforce a Blimp1-mediated differentiation program in non-Tfh effector cells (175). In line with this, it has also been observed that Tfh cells produce large amounts of IL-2 during the GC response and yet remain unresponsive to this Tfh cell suppressing cytokine (176). Within this context, intrinsic IL-6 signaling prevents STAT5 binding to the *Il2rb* locus, thereby downregulating a component of the IL-2 receptor, IL-2Rβ (176).

1.2.3 Costimulatory and adhesion molecules at the T-B interface

The intimate T-B crosstalk that initiates at the T-B border and continues inside the GC is central to successful humoral immunity. There are numerous molecules which support and finetune this interaction to ensure its success. While cognate T and B cell interactions heavily depend on antigen-specific TCR signaling strength, the expression and upregulation of costimulatory, coinhibitory as well as adhesion molecules also guides the differentiation and maintenance of Tfh and GC B cells (35) (Fig. 1.2B). CD28, CTLA-4 and ICOS are part of the immunoglobulin superfamily, sharing a common evolutionary origin as a result of tandem duplication of an ancestral gene with different, albeit important roles in Tfh cell biology (121, 177, 178). Both CD28 and ICOS positively regulate T cell activation and Tfh cell formation (121, 179-181). Loss of CD28 or ICOS signaling in mice leads to deficiencies in Tfh cell development and GC formation, whereas ICOS overexpression caused by the *sanroque* mutation in Roquin-1 leads to spontaneous GCs and increased frequency and activity of Tfh cells (35, 179, 182-185). In contrast, CTLA-4 inhibits Tfh cell differentiation, as CTLA-4 deficiency in mice causes increased Tfh cell numbers and B cell responses (186, 187).

CD28 is expressed on the surface of both naïve and activated $CD4^+$ T cells whereas ICOS is upregulated after TCR activation and/or CD28 costimulation (121, 181). Although initial studies reported that CD28 is only important during early Tfh cell generation, specifically during T cell priming, recent research suggests it may also be critical for Tfh cell survival and maintenance (183, 184, 188). CD28-mediated signaling also induces the expression of other costimulatory molecules essential for Tfh cell generation, such as ICOS which is involved in Bcl6 upregulation and production of key GC cytokines, IL-4 and IL-21 (180, 185, 187). ICOS is reported to impact Bcl6 expression through its ability to inactivate transcription factor FOXO1,

an inhibitory pathway to Tfh cell differentiation (84). However, ICOS signaling subunit p85α has also been observed to aid in the stabilization of Bcl6 expression (189). ICOS signaling initiated by engagement with ICOSL-expressing bystander B cells at the T-B border also facilitates T cell motility in a PI3K-dependent manner (115). Additionally, within the GC itself, ICOS-ICOSL signaling is implicated in the formation of entangled T and B cell contacts that promotes a feedforward loop involving ICOS-mediated calcium signaling and the CD40/CD40L pathway, which supports B cell differentiation (124). Moreover, ICOS is also important in maintaining Tfh cell homing molecules such as CXCR5 by downregulating transcriptional repressor Krüppel-like factor 2 (Klf2) (188).

The SLAM family of receptors and adaptor protein, SAP through their role as adhesion molecules also stabilize T-B contacts in the GC (119, 120). More details regarding the types of SLAM family receptors involved in the GC response and signaling transduction pathways through SAP will be discussed at length in section 1.2.5. Additionally, integrins and adhesion molecules also facilitate the humoral immune response (190). Integrin LFA-1 and intercellular adhesion molecule-1 (ICAM-1) are important in T-B interactions and the GC response and will be examined in section 1.2.6. Other than that, integrin α_v also supports GC formation but is not key in the formation T-B conjugates (191). Instead, it is important in facilitating interactions between Tfh cells and the extracellular matrix to properly localize Tfh cells within the B cell follicle and generate long-lived plasma cells (191). Additionally, other proteins normally involved in different biological processes have also been recently associated with Tfh cell interactions with GC B cells (190). For instance, the interaction between Plexin B2 and Semaphorin 4C, molecules normally involved in synapse formation and axon guidance in the nervous system can support T-B adhesion and GC recruitment (190, 192). Lastly, ephrin B1 (EFNB1), usually associated with cell migration and axon guidance during development is also expressed on GC B cells and can prevent proper Tfh cell localization and T-B adhesion (190, 193).

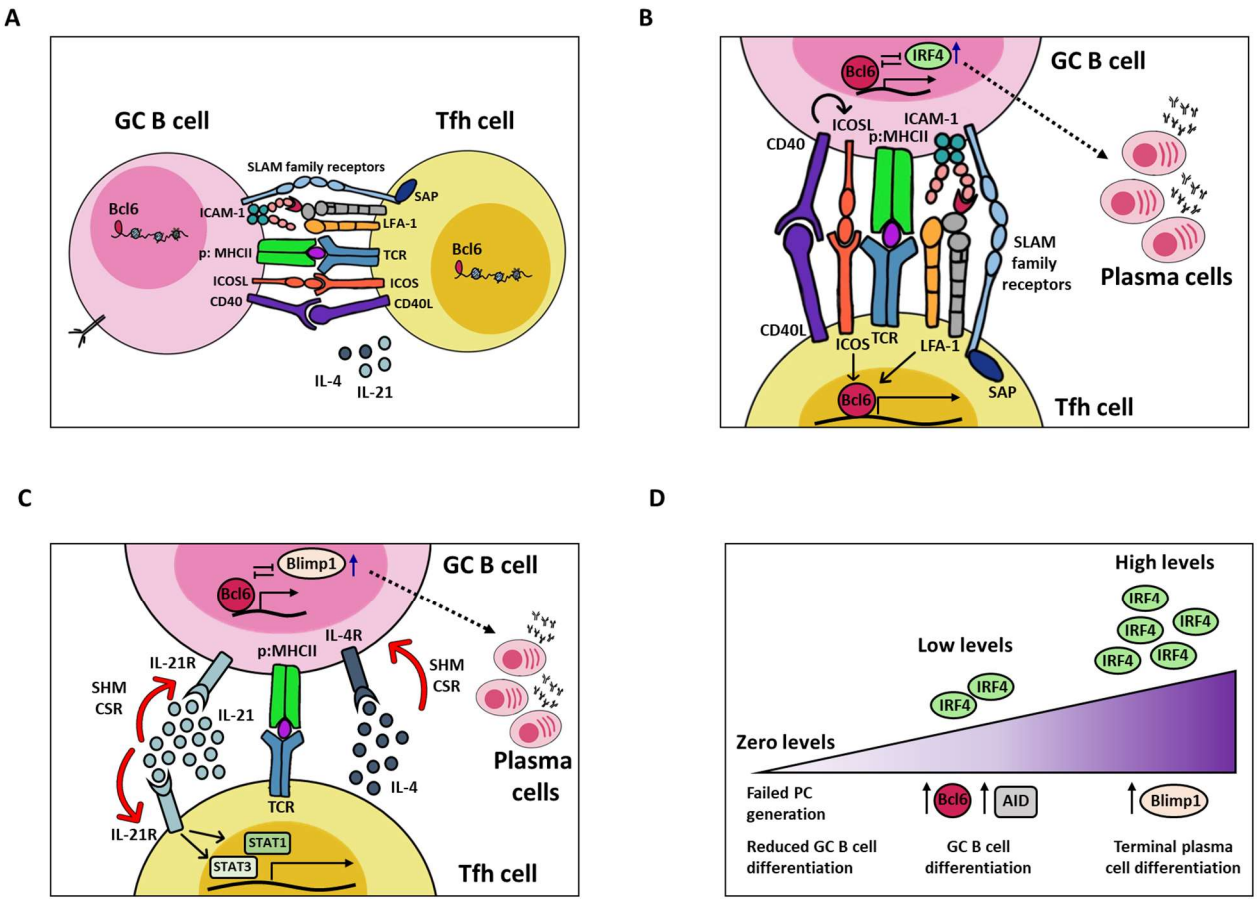

Figure 1.2 Overview and potential outcomes of intimate T-B communication

(A) In the germinal center, communication between Tfh and GC B cells occurs in an antigen-specific manner and is supported by adhesion molecules, costimulatory molecules and cytokines. (B) T-B crosstalk in GCs is maintained by costimulatory molecules such as ICOS and CD40L as well as adhesion molecules such as integrin LFA-1 and SLAM family receptors. The adaptor protein SAP, downstream of SLAM family receptors is also a critical mediator of T-B interactions. These stable T-B contacts are important for promoting GC B cell differentiation into plasma cells. This occurs through a process where GC B cells downregulate Bcl6 expression and upregulate IRF4, thereby initiating their transition into the plasma cell lineage. (C) IL-4 and IL-21 are key cytokines produced by Tfh cells within the context of the GC response and support T-B communication. Both IL-4 and IL-21 can regulate Bcl6 expression in GC B cells and have been implicated in promoting somatic hypermutation (SHM) and class switch recombination (CSR). IL-21 is also important for inducing expression of Blimp1, another signature plasma cell transcription factor. In Tfh cells, IL-21 can support STAT1 and STAT3 signaling pathways which further promote Tfh cell maintenance. (D) In B cells, the relative level of IRF4 impacts B cell differentiation. Low IRF4 levels lead to increased Bcl6 and AID expression, promoting early GC B cell differentiation. High levels of IRF4 supported by stable T-B conjugate formation leads to Blimp1 expression and terminal plasma cell differentiation.

1.2.4 B cell lymphoma 6 (Bcl6): Central transcription factor of the GC reaction

Bcl6 was first identified as a proto-oncogene involved in the pathogenesis of diffuse large B-cell lymphoma (DLBCL) (194). Bcl6 is part of the BTB/POZ (bric-a-bric, tramtrack, broad complex-poxvirus zinc-finger) family of zinc-finger containing transcription factors (35, 195). Overall, Bcl6 is a transcriptional repressor whose most well-studied functions surround GC dynamics for both B and T cells (112, 149, 162, 195-199). However, outside of the GC, Bcl6 has also been reported to impact macrophage activity (199, 200). Bcl6 deficiency in mice leads to the inability to form GCs and mount proper antibody responses, owing to its fundamental role in GC B and Tfh cell programs (201, 202). *Bcl6*$^{-/-}$ mice also experience lethal Th2-mediated immune infiltration in many organs including the lungs and heart as a result of increased inflammatory chemokine production by Bcl6-deficient macrophages (203). Importantly, this observation is specific to the DNA-binding ability of Bcl6 (202, 204, 205). Bcl6 has three conserved domains: a N-terminal BTB/POZ domain, a central domain containing a second repression domain (RD2) and a C-terminal zinc-finger domain (195, 206, 207). The N-terminal domain is important for transcriptional repression, dimerization and interaction with corepressors such as Bcl6 corepressor (BCOR) (195, 207).

Bcl6 interaction with corepressors is important for its ability to support Tfh cell identity, as Bcl6 BTB domain mutant mice show defects in Tfh cell differentiation and antigen-specific antibody responses (204, 208). The middle portion of Bcl6 is critical for transcriptional repression through its interactions with HDAC2, Nucleosome remodeling and deacetylase complex (NuRD) and Metastasis associated protein 3 (MTA3) and is also involved in Bcl6 protein stability (195, 207, 209). Mice lacking this middle domain or mice with an acetylated middle domain that prevents MTA3 binding have impaired GC B cell differentiation and Tfh cell function (205, 210). The middle domain also contains PEST motifs which regulates Bcl6 protein stability (195). Downstream of antigen-specific BCR activation, phosphorylation of this middle domain via MAPK facilitates Bcl6 degradation, thereby encouraging post-GC fates such as plasma cell differentiation (211). Interestingly, corepressor C-terminal binding protein 1 (CtBP) can interact with the POZ and middle domains of Bcl6 and together, their recruitment to the Bcl6 promoter region suppresses its own transcription (212). In DLBCL, point mutations found in the first non-coding exon of *BCL6* have been linked to loss of this negative autoregulatory loop (213,

214). In Tfh cells, however, it has been reported that this negative autoregulation involves interactions between Bcl6 and nuclear receptor corepressor1 (NCOR1) (215).

The C-terminal domain contains six C2H2 zinc-fingers that facilitate the DNA-binding ability of Bcl6 to specific DNA sequences (195, 207). Importantly, only the latter zinc-fingers 3 to 6 are required to mediate repressive Bcl6 binding activity and accordingly, genetic ablation of this DNA-binding region leads to reduced Tfh and GC B cell responses (197, 202, 216, 217). While these zinc-finger mutants still produce a truncated form of Bcl6, they are considered functionally null as they match the phenotype of Bcl6 protein null mice (202). Certain zinc-fingers are also associated with nuclear localization, as mutating zinc-finger 4 or 6 promotes the cytoplasmic localization of Bcl6 (216). Further, experiments that compare Bcl6 zinc-finger deficient mice in parallel with BTB/corepressor binding or middle RD2 domain mutants demonstrate that although there are substantial deficits in GC formation and Tfh cell development, their phenotypes do not perfectly match Bcl6 mutant mice without zinc-fingers (204, 205). This strongly suggests that the DNA-binding ability of Bcl6 is essential in mediating its action in both T and B cell lineages.

Although Bcl6 was first reported to exert its repressive function by binding to promoter regions, genome-wide sequencing approaches reveal that in T cells, B cells and macrophages, Bcl6 can also bind to intergenic, intron and exon regions (198, 199, 218). Among these three cell types, though Bcl6 does have shared gene targets, a majority of Bcl6 bound genes were unique between T cells, B cells and macrophages and in addition to this, Bcl6 binding motifs differed between Tfh and non-Tfh cells (199). Moreover, Bcl6 is differentially expressed in GC B cells as compared to Tfh cells (149). Throughout most of the GC response, Bcl6 levels continue to be maintained in GC B cells whereas Tfh cells gradually reduce levels of Bcl6 towards the end of the GC reaction, which is reported to correspond with increased expression of markers associated with a quiescent, memory-like state (149). Specifically in GC B cells, it appears that Bcl6 through its interaction with a non-canonical polycomb repressive complex 1 (PRC1) that includes BCOR can cooperate with EZH2 to repress activation of genes involved in cell cycle arrest or plasma cell differentiation (206, 219). While this particular mechanism has not been identified in Tfh cells, CD4-specific BCOR deficiency, loss of Bcl6-corepressor interactions as well as CD4-specific EZH2 deficiency leads to impaired Tfh cell responses and

thus, it is plausible that Tfh cells and GC B cells may share this Bcl6-BCOR-EZH2 pathway (Fig. 1.3) (208, 220, 221).

Post-translational modifications to Bcl6 also modulate its function in both B and T cell lineages (206). Within the context of DLBCL, it has been shown that F-box only protein 11 (FBXO11) containing ubiquitin ligase complex plays a role in the ubiquitylation of Bcl6, which leads to its degradation (222). In line with this, GC B cell-specific loss of FBXO11 causes increased GC B cell formation and Bcl6 expression (223). Additionally, in Tfh cells, Bcl6 is protected from ubiquitin-mediated degradation as a result of interactions between PI3K subunit p85α and osteopontin (OPN-i) (189). Moreover, p300-mediated acetylation or protein arginine methyltransferase 5 (PRMT5)-mediated methylation of Bcl6 also modulates its ability to repress GC B cell target genes (224, 225). Lastly, localization of Bcl6 in the cytoplasm or nucleus in Tfh cells is influenced by serine/threonine protein kinase D2 (Prkd2)-dependent phosphorylation, which inhibits its function (226).

Thus, the multiple layers of regulatory mechanisms controlling Bcl6 expression and localization reflects its pivotal role in regulating GC responses and humoral immunity. To exert its function in GC B or Tfh cells, Bcl6 must be able to localize into the nucleus and bind its target genes in order to introduce epigenetic changes and alter gene expression patterns.

1.2.4.1 B cell-specific functions of Bcl6

Even before proper GC formation, Bcl6 protein levels are upregulated in B cells, which has been associated with promoting GC entry and stabilizing T-B interactions (149). Bcl6 is also involved in the suppression of genes that govern GC exit such as those encoding IRF4 and Blimp1 proteins and consequently, Bcl6 downregulation is important for commitment into plasma cell or memory B cell lineages (207, 227, 228). More specifically, in order for plasma cell lineage commitment to occur, GC B cells must not only downregulate levels of Bcl6 protein, but also upregulate levels of IRF4, a biological process dependent on stable T-B conjugates and CD40 signaling (125). Importantly, it has been shown that CD40-mediated activation of NF-κB in B cells activates *Irf4* expression, which in turn is able to repress *Bcl6* transcription by binding to its promoter region (229). Additionally, in GC B cells, Bcl6 can suppress apoptotic and cell cycle arrest through direct repression of tumor-suppressor p53 or indirectly by repressing the activation of p21, a cell cycle arrest gene, through interactions between Bcl6 and Miz-1 (230-232). This is key during the GC response when GC B cells must rapidly proliferate and undergo

DNA breaks and recombination for SHM as well as CSR without triggering apoptosis or cell cycle arrest (230).

1.2.4.2 T cell-specific functions of Bcl6

Early in the GC response, during DC priming, Bcl6 is transiently upregulated in pre-Tfh cells, however, in order to fully acquire GC Tfh cell features, a second stronger and continuous wave of Bcl6 expression is needed (110). Induction of Bcl6 in $CD4^+$ T cells has been reported to occur through multiple pathways. Initial Bcl6 upregulation is likely a result of STAT1 and STAT3 activation downstream of IL-6 receptor signaling (154). It has also been shown that type I interferons (IFN) through STAT1 activation can induce certain aspects of the Tfh cell phenotype such as Bcl6, CXCR5 and PD-1 (233). Additionally, in *Roquin*$^{san/san}$ mice, which experience lupus-like symptoms, excessive interferon-γ signaling has been linked to Tfh cell accumulation and Bcl6 overexpression (234). Moreover, transcription factor T cell factor 1 (TCF1) is also important in promoting Bcl6 expression through its ability to recruit histone methyltransferase EZH2 in its phosphorylated form to the Bcl6 promoter and thus, loss of either TCF1 or EZH2 leads to an impairment in Tfh cell differentiation (Fig. 1.3) (221, 235).

Bcl6 maintains Tfh cell identity and function largely through the repression of genes relating to other T helper cell phenotypes (35). Studies of *Bcl6*$^{-/-}$ mice show increased skewing to Th1, Th2 and Th17 cell lineages, attributed to the ability of Bcl6 to bind to the promoter of genes associated with Th1, Th2 and Th17 cell differentiation (112, 113, 198, 236). Bcl6 in Tfh cells mostly binds to motifs at promoter or enhancer sites also associated with STAT or AP-1 transcription factors, suggesting that Bcl6 works in concert with other factors to enforce the Tfh cell program (35, 198, 199). On this note, IL-2- or IL-7-mediated activation of STAT5, which represses *Bcl6* and Tfh cell differentiation may be due to competition between STAT5 and Bcl6 as a result of their shared binding sequences (173, 199). Analogous to GC B cells, Bcl6 also limits Blimp1 expression in Tfh cells by binding to its promoter region in order to maintain Tfh cell identity (111, 198). In one study, overexpression of Bcl6 in non-Tfh cells from human tonsils demonstrated its ability to increase protein levels of CXCR5, PD-1, SAP, CD40L, and ICOS, although, whether this occurs in a direct or indirect manner is unclear in some cases (237). For instance, although CXCR5 is associated with Bcl6-expressing $CD4^+$ T cells during the GC, numerous reports suggest that Bcl6 does not directly induce CXCR5 expression and instead,

CXCR5 expression may be regulated by other transcription factors which also regulate Tfh cell activities such as Ascl2, Maf and Klf2 (188, 196, 215, 237, 238).

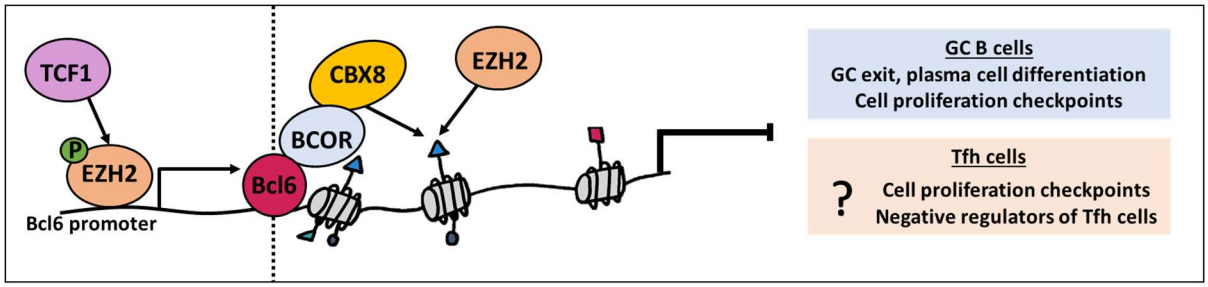

Figure 1.3 Example of GC regulation mediated by Bcl6 and EZH2 and potential implications for AITL disease

Left panel: In Tfh cells, transcription factor TCF1 can facilitate the recruitment of EZH2 in its phosphorylated form to the Bcl6 promoter, which leads to Bcl6 induction. Right panel: In GC B cells, Bcl6 and its corepressor BCOR cooperates with methyl transferase EZH2 to add repressive H3K27me3 marks to genes involved in GC exit, plasma cell differentiation and checkpoints of cell proliferation. This mechanism has been implicated in the onset of certain B cell lymphomas of germinal center origin such as DLBCL. Although such a mechanism has not been validated in Tfh cell biology, considering the important role both BCOR and EZH2 independently play in Tfh cell function, it is highly plausible that a parallel Bcl6-BCOR-EZH2 pathway operates in Tfh cells and in AITL disease.

1.2.5 Signaling lymphocytic activation molecule (SLAM) family receptors and SLAM-associated protein (SAP)

SLAM family receptors are type I transmembrane receptors with six members: SLAMF1 (SLAM; CD150), SLAMF3 (CD229; Ly-9), SLAMF4 (2B4; CD244), SLAMF5 (CD84), SLAMF6 (Ly108) and SLAMF7 (CRACC; CD319) (239, 240). SLAM family receptors are generally involved in homotypic interactions, although other methods of engagement are reported for SLAMF4 and SLAMF7 (239, 241). SLAM family receptors are broadly expressed on immune cells; however, only SLAMF1, SLAMF5 and SLAMF6 have been implicated in humoral immunity and will be discussed in more detail within this section (120, 128, 242). SLAM family receptors contain immunoreceptor tyrosine-based switch motifs (ITSM) through which they interact with the SH2 domain found in proteins part of the SAP family of adaptor proteins (239, 243). There are three adaptor proteins: SAP, Ewing's sarcoma-associated transcript-2 (EAT-2) and EAT-2 related transducer (ERT), of which only SAP is reported to directly impact GC responses and Tfh cell activity (119, 120, 128, 244, 245). With the exception

of SLAMF7 which interacts only with EAT-2, all SLAM family receptors can interact with SAP (239). Moreover, through the arginine 78-containing motif of SAP, it can uniquely interact with the SH3 domain of Fyn kinase, leading to receptor tyrosine phosphorylation and activation of downstream signaling pathways (240, 243). SLAM family receptor association with SAP or EAT-2 inhibits binding of other SH2 domain-containing phosphatases such as Src homology 2 domain-containing protein tyrosine phosphatase-1 (SHP-1) and consequently, in the absence of adaptor protein binding, SLAM family receptors become inhibitory receptors (239, 240, 243).

SAP deficiency is strongly associated with defects in T cell-dependent GC formation and antibody responses, as result of a reduced ability for GC B and Tfh cells to form stable conjugates (119, 120, 128). Moreover, SLAMF5 and SLAMF6 are reported to promote and stabilize these T-B conjugates in the presence of SAP adaptor protein (120). Nevertheless, the result of mouse models of SLAMF5 or SLAMF6 deficiency and how they impact GC responses yield conflicting results. Although one group has shown that *Slamf5*$^{-/-}$ mice have partial defects in humoral immunity (120), other groups demonstrated that loss of either SLAMF5 or SLAMF6 did not significantly inhibit GC development (246, 247). SLAMF1 has also been implicated in regulating the helper function of Tfh cells through IL-4 production, although, loss of SLAMF1 alone does not impact Tfh cell differentiation (242). Moreover, triple deficiency in *Slamf1*, *Slamf5* and *Slamf6* does not hinder GC B or Tfh cell development after acute viral infection or protein immunization, however, enhanced antigen-specific plasma cell expansion in these triple knockout mice was only observed after protein immunization (247, 248). Importantly, most groups report that deficiency in all or select SLAM family receptors can restore the humoral immune defects associated with loss of SAP, strengthening the idea that SLAM family receptors are by default inhibitory receptors that exert even stronger negative effects on T-B crosstalk in the absence of SAP (246, 248, 249). A summary of SLAM family receptor ligands, expression profile and role in the GC response is highlighted in Table 1.1.

SLAM family receptor	Physiological ligand	Adaptor protein interaction		General immune cell expression profile					Role in GC reaction
		SAP	EAT-2	T cell	B cell	NK cell	DC	Macro-phage	
SLAMF1 (SLAM; CD150)	SLAMF1	✓	✓	✓	✓	-	✓	✓	**IL-4 production by GC Tfh cells**
SLAMF3 (Ly-9; CD229)	SLAMF3	✓	✓	✓	✓	✓	✓	✓	Not described in literature
SLAMF4 (2B4; CD244)	CD48	✓	✓	✓ **($CD8^+$)**	-	✓	✓	✓	Not applicable
SLAMF5 (CD84)	SLAMF5	✓	✓	✓	✓	✓	✓	✓	**Support stable T-B interactions**
SLAMF6 (Ly108)	SLAMF6	✓	✓	✓	✓	✓	✓	-	**Support stable T-B interactions**
SLAMF7 (CRACC; CD319)	SLAMF7	-	✓	✓ **(activated)**	✓	✓	✓	✓	Not described in literature

References for information found within Table 1.1: (120, 239, 242, 243, 250)

EAT-2, Ewing's sarcoma-associated transcript-2; ERT, EAT-2 related transducer; DC, dendritic cell; NK cell, natural killer cell; GC, germinal center; SAP, SLAM-associated protein; SLAM, signaling lymphocytic activation molecule; Tfh, T follicular helper; ✓, positive; -, negative

Table 1.1 Summary of similarities and differences between SLAM family receptors

1.2.6 Lymphocyte function-associated antigen-1 (LFA-1)

LFA-1 (CD11a/CD18) is a β_2 integrin which binds ligand ICAM-1 and plays an important role in T cell migration and activation (251, 252). LFA-1 is expressed not only on T cells but also B cells, DCs, neutrophils and monocytes (252). While ICAM-1 is also expressed on these immune cells, it is also found on endothelial cells, and in this context facilitates tissue migration of immune cells (252, 253). LFA-1 can exist in three different conformations which impacts the affinity of binding to ICAM-1 (251). Antigen-specific TCR activation leads to inside-out signaling by initiating a series of phosphorylation events that changes the conformation and

clustering of LFA-1 and thus, increases its affinity for ICAM-1 (251, 252). In particular, activation of the small GTPase Rap1 and the recruitment of RAPL, Rap1-interacting adaptor protein (RIAM) as well as talin, a cytoplasmic scaffolding protein, to LFA-1 is important for its activation (252, 254-257). Interactions between LFA-1 and ICAM-1 can also initiate numerous outside-in signaling pathways such as enzyme activation or deactivation, cytoskeletal remodeling and changes in gene expression (256). For instance, in T cells, LFA-1 activation can lead to phosphorylation of Lck and Zap70, which then further amplifies downstream TCR signaling pathways (256, 258). Additionally, LFA-1 engagement can lower TCR signaling threshold and appears to be needed for IL-2 and IFN-γ cytokine production as well as antigen-specific responses, which may be related to its role in supporting humoral immunity (259, 260).

Upon immune challenge, levels of LFA-1 on Tfh cells as well as ICAM-1 on GC B cells increase (118, 261). It has been reported that B cell-specific expression of ICAM-1/2 supports long-lasting antigen-specific Tfh-B cell interactions and promotes plasmablast formation (125, 261). Moreover, LFA-1 is also important for Tfh cell survival and differentiation as well as GC maintenance (118). It has also been observed that in the context of TCR activation, LFA-1/ICAM-1 interactions are involved in Bcl6 protein induction in $CD4^+$ T cells (118). In particular, Tfh cells express more high affinity LFA-1, and in line with this, mice with CD4-specific loss of talin, essential in supporting the high affinity conformational change of LFA-1, could not induce Bcl6 levels or support Tfh cell differentiation (118). Thus, it is evident that LFA-1 interactions are pivotal in supporting T-B crosstalk not only through its adhesive properties, but also as a signaling molecule that can support TCR activation pathways, T cell survival and Tfh cell identity via Bcl6 expression.

1.3 Immune surveillance in AITL

1.3.1 Cell subsets involved in immune surveillance

Tumor immune surveillance is an ongoing battle within the tumor microenvironment between developing cancer cells and immune cells (262). T cells, B cells, natural killer (NK) cells, innate lymphoid cells (ILCs), dendritic cells and macrophages have been implicated in the regulation of cancer growth (262, 263). As a result of this immune pressure, tumor cells that have not been removed adapt and gain survival advantages, allowing them to be resistant to

further elimination (262). Tumor cells can do this by using numerous mechanisms which includes but is not limited to upregulation of inhibitory molecules such as PD-L1/PD-L2 and CD47 or downregulation of proteins involved in mediating apoptosis (264).

Since only a minor portion of the AITL tumor mass is represented by the neoplastic Tfh-like cell population, expansion of other immune cell types such as B cells, plasma cells and macrophages contribute to the dense tumor microenvironment and are likely to be important to augment AITL disease pathogenesis (3) (Table 1.2). Moreover, in AITL, circulating tumor Tfh cells are detected in patient blood samples and yet, tumor dissemination from one lymph node to the next can occur very rapidly over a few months or slowly over a span of many years (4, 10, 91, 265). One possible explanation is that AITL tumor cells require a unique niche provided by either an extensive FDC network or other types of stromal cells in order to establish themselves successfully in other lymph nodes. However, another possibility is that the strength of opposing immune surveillance mechanisms may play a critical role in the rate of disease progression. On that note, there is some evidence in literature which may allude to the possibility of breached immune surveillance in AITL. AITL patients are reported to have higher levels of serum IL-10, an immunosuppressive cytokine as compared to PTCL-NOS and ALCL patients, which is also associated with worsened patient survival (78). Moreover, production of proangiogenic factor VEGF-A from both tumor and endothelial cells in human AITL can also impact the tumor microenvironment beyond the hallmark neovascularization common to AITL (27, 28). VEGF-A can have numerous immunosuppressive roles, and could possibly be involved in macrophage recruitment, protumor Treg cell activation or promoting exhaustion in antitumor $CD8^+$ T cells within the AITL tumor microenvironment (266, 267). Lastly, since poor prognosis in AITL patients is associated with a higher proportion of M2-like macrophages (78, 81), one plausible interpretation is that these M2-like macrophages are poorly phagocytic and overall less effective in controlling disease. The subsequent sections will delve into different immune cell subsets reported to be involved in tumor immunity in relation to T cell lymphomas and AITL.

Tfh-like tumor cells promote a unique tumor microenvironment in AITL				
B cell	**Follicular dendritic cell (FDC)**	**T cell (non Tfh cell)**	**Macrophage**	**Cytokines and Chemokines**
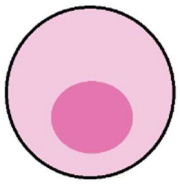	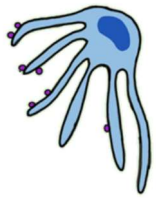	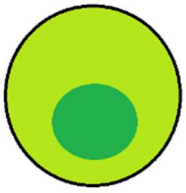		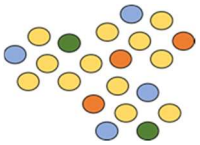
B cell expansion can be due to hyperactive tumor Tfh-like cells, EBV infection, and/or genetic mutations in genes such as *TET2* (3, 42, 47, 58, 268, 269)	**FDC meshworks are highly expanded, which may be a result of EBV infection (3, 270, 271)** **FDCs and tumor cells are typically localized near blood vessels (11)**	**Cytotoxic T cell gene signature correlates with poor prognosis (272)** **Treg cells are present but their role is unknown (273, 274)**	**Presence of both M1-like and M2-like macrophages (78, 81)** **Increased ratio of M2-like macrophages is associated with poor patient outcome (78, 81)**	**Angiogenic factors: IL-8, VEGF-A (28, 30, 272)** **Immunosuppressive cytokines: IL-10 (272)** **Tfh cell-promoting signals: IL-4, IL-6, IL-21, CXCL13 (272)**

AITL, angioimmunoblastic T cell lymphoma; EBV, Epstein-Barr virus; FDC, follicular dendritic cell; Tfh, T follicular helper; Treg, T regulatory; VEGF-A, vascular endothelial growth factor-A

Table 1.2 Immunological features linked to the AITL tumor microenvironment

1.3.1.1 Tumor-infiltrating lymphocytes

Tumor-infiltrating lymphocytes (TILs) are generally classified as $CD4^+$ helper and $CD8^+$ cytotoxic T cells, however, $CD4^+$ regulatory T cells (Treg) also play a protumor immunosuppressive role in the tumor microenvironment (275-277). Importantly, TILs tend to have a higher specificity and reactivity against tumor cells compared to non-TIL lymphocytes (276). Genetic mutations, epigenetic modifications or inappropriate signaling pathway activation are all important factors driving oncogenic transformation, which in turn can lead to the production of tumor-specific or tumor-associated proteins (278). These tumor antigens can be presented in the context of MHCI on the tumor's cell surface, potentially eliciting a TIL-mediated antitumor response (277, 278). By increasing perforin-mediated delivery of intracellular granzyme or expression of apoptotic molecules such as Fas ligand, $CD8^+$ cytotoxic T cells can facilitate their antitumor activity (279). $CD8^+$ TILs preferentially remove tumor cells

that highly express MHCI and as such, over time, this leads to the survival of tumor cells with lower MHCI levels and reduced tumor antigen presentation, which can then evade TIL-mediated removal (277, 280). Finally, due to chronic antigen stimulation in the tumor microenvironment, TILs can also express exhaustion markers such as PD-1, which makes it difficult to mount an efficient antitumor response (281).

The role of $CD4^+$ T cell subsets within the tumor microenvironment is more intricate as various subpopulations in different contexts show helper, cytotoxic as well as immunosuppressive functions (282). Certain subsets such as Th1 cells have antitumor functions by producing IFN-γ and promoting the recruitment of other antitumor cells such as $CD8^+$ T cells or NK cells (282). Moreover, other $CD4^+$ T cell subsets such as Th2 or Th17 cells have been associated with both antitumor and protumor roles (282). Lastly, Treg cells are reported to provide an immunosuppressive environment through their ability to produce TGF-β and thus oppose antitumor immune cell activities (275, 282).

In many types of solid cancers such as breast cancer, the increased presence of $CD8^+$ TILs within the tumor is often associated with improved clinical prognosis (262, 277, 283). However, in AITL as well as DLBCL, patients with more cytotoxic T cells or a cytotoxic T cell gene signature are associated with poor prognosis and clinical outcomes (272, 284). This may reflect immune pressure by these TILs such that only the tumor cells which have evolved to become resistant to TIL-mediated killing mechanisms can continue to survive and support tumor growth (284). To also support this, gene expression studies of AITL samples show enrichment of genes associated with cell division, cell cycle progression and anti-apoptosis (285).

Although increased tumor mutational burden is expected to positively correlate with the presence of neo-antigens, in the context of cancer immunotherapy, elevated neo-antigen formation is not always associated with improved antitumor responses (278). Tumor mutational burden can vary greatly depending on the cancer type from as low as 0.001 mutations per Megabase (Mb) to more than 400 mutations/Mb (286). In one cohort of AITL patients tested for tumor mutational burden, the majority of patients (8/10) had a low tumor mutational burden of less than 6 mutations/Mb while a minority (2/10) had an intermediate burden (6-19 mutations/Mb) (287). Nonetheless, whether a comparatively higher mutational burden in AITL patients correlates with poorer patient outcomes or response to therapy has not been investigated.

In general, T cell-mediated immune surveillance in AITL is under-studied, likely because it is challenging to differentiate between T cell-derived neoplastic cells and tumor-infiltrating T cells using surface markers alone. Additionally, because AITL tumor cells can share expression of molecules such as PD-1 with exhausted TILs, understanding the impact of checkpoint inhibitors such as anti-PD-1 on both counterparts is vital. This has been exemplified through a phase II clinical trial testing the efficacy of nivolumab, an anti-PD-1 antibody in relapsed/refractory PTCLs, which included AITL patients (288). In this context, and also in another clinical trial for adult T-cell leukemia-lymphoma patients, anti-PD-1 therapy lead to adverse effects as well as disease hyperprogression in many patients (288, 289), presumably due to the inhibitory role PD-1 has not only in tumor-infiltrating T cells but also on neoplastic tumor cells of T cell origin. As a result of the large proportion of patients that developed hyperprogressive disease, the clinical trial was stopped and not completed (288). Nonetheless, identifying ways to harness specific signaling pathways to boost immune surveillance involving other types of immune cell subsets such as NK cells or macrophages is also a less studied avenue in AITL, and yet has great potential as effective therapies to improve AITL disease outcomes.

1.3.1.2 Natural killer cells

Natural killer (NK) cells are a heterogenous group of cytotoxic innate lymphoid cells (ILC) also involved in tumor immune surveillance (290-292). Recently, other ILC subsets have been implicated in tumor immunity, but their contribution to tumor progression as antitumor or protumor cells is still unclear and is cancer-type dependent (293). Having the appropriate balance between activating and inhibitory receptors on the surface of NK cells is important to properly mount a successful antitumor response (292). NK cells mediate their cytotoxic activity through the perforin/granzyme pathway, and also assist in immune surveillance by secreting large amounts of antitumor cytokines such as IFN-γ (292). In general, under physiological conditions, cells express MHCI, as a marker of self and in addition, do not express ligands that would engage activating NK receptors (292). In contrast, tumor cells expressing lower levels of MHCI and elevated levels of activating NK ligands are more susceptible to NK cell-mediated tumor surveillance (290-292). However, many cancers evade NK cell recognition by shedding these ligands (294). There is not much studied regarding NK cells in the context of T cell lymphomas, including AITL, however, transgenic T cell receptor-expressing mice with NK cell depletion are

reported to have an increased rate of lymphoma development, suggesting that NK cells may play a role in the immune surveillance of T cell lymphomas (295).

1.3.1.3 Macrophages

Macrophages are a diverse population of phagocytes that are important for engulfment of cell debris, foreign pathogens, and dying cells (296-298). Importantly, macrophages also recognize and eliminate tumor cells and thus are critical mediators of immune surveillance (299, 300). However, in many cases, tumor cells successfully escape this process, selecting for tumor cell variants that have evasive properties which favour tumor growth (300). Depending on the type of stimulating signals received, macrophages can polarize into several different subsets (298, 301). The two subsets most differently polarized and commonly described are classically activated (M1) and alternatively activated (M2) macrophages (298, 301, 302). However, due to macrophage plasticity, different environmental stimuli allows activated macrophages to continually change functional characteristics (298). On the one hand, M1 macrophages are an important defense against invading pathogens and tumor growth (303, 304). M1 macrophages are produced in response to IFN-γ and microbial triggers and mediate their activity by secreting proinflammatory cytokines such as IL-6, IL-12 and TNF-α (298, 299, 301, 302). M2 macrophages, in contrast, produce anti-inflammatory cytokines such as IL-10 and TGF-β and are involved in numerous processes including tissue repair, angiogenesis as well as parasite clearance (298, 299, 301, 302). Nonetheless, even amongst the M2 classification, four different subsets of M2 macrophages have been described (M2a-M2d), which respond to different stimuli, secrete different effector molecules and have diverse functions (302, 303, 305).

Tumor-associated macrophages (TAM) support tumor growth in numerous ways by enhancing cancer survival, proliferation, invasiveness and angiogenesis (302, 306). The phenotype of TAMs is shaped by the tumor microenvironment, however, they are more commonly associated with M2-like characteristics (299, 302, 304). TAMs are not only inefficient at phagocytosing tumor cells but also express inhibitory receptors, ligands and cytokines to suppress the antitumor response (297, 299, 302, 307). Importantly, TAM reprogramming from an M2-like phenotype into M1-like macrophages has been reported to boost antitumor responses (303, 304, 307). In human AITL, TAM reprogramming may also be a useful therapeutic approach, as it has been reported that patients with an increased ratio of M2:M1 macrophages have poorer disease prognosis and survival (78, 81). However, clinical

examination of M1 or M2 macrophages is done using immunohistochemical staining of CD68 (M1) and CD163 (M2) and therefore, may not fully reflect their functionality (78, 81).

Tissue-resident macrophages can also have varying functions based on their anatomical location (301). For instance, lymph nodes have three unique subsets: subcapsular sinus, medullary sinus and medullary cord macrophages, which capture and present antigens to support humoral immune responses (301, 308). Furthermore, tingible body macrophages (TBM) are also regulators of the GC reaction, and are involved in the clearance of apoptotic GC B cells that arise as a result of negative selection, although whether they phagocytose Tfh cells under physiological conditions is unclear (309). Moreover, the unique cytokine milieu that is associated with GCs as well as the AITL tumor microenvironment makes it challenging to predict the dynamic roles macrophages may play during tumor initiation, maintenance and spreading. For instance, while GC cytokine IL-4 is strongly associated with the M2 phenotype, IL-21 in different experimental conditions appears to be able to polarize macrophages towards both M1 and M2 phenotypes (303, 310, 311). Additionally, VEGF-A is overexpressed in human AITL by both lymphoma and endothelial cells, which contributes not only to the unique angiogenic features associated with AITL, but may also serve as a monocyte chemoattractant into lymph node tumors (27, 28, 312). Although the understanding of macrophage biology in AITL is rather superficial, phagocytic macrophages are by default, localized within lymph nodes (308, 313). In addition to this, while AITL tumor cells are commonly reported in patients' blood, the rate of tumor spreading to distal lymph nodes can vary, raising an intriguing possibility that differing macrophage activities between patients may control the rate of AITL disease progression (4, 10, 91, 265).

1.3.2 Mechanisms of macrophage-mediated phagocytosis

The process of macrophage-mediated phagocytosis is regulated through the expression of both activating and inhibitory receptors, allowing appropriate phagocytic responses against tumor cells, aged cells, dying cells or foreign pathogens while preventing the engulfment of healthy cells (296, 314). Examples of activating or prophagocytic receptors include SLAMF7, integrin macrophage antigen-1 (Mac-1; CD11b), Fc receptors and phosphatidylserine receptors (296, 315). Moreover, triggering an inhibitory signaling pathway in macrophages via signal regulatory protein α (SIRPα) engagement with CD47 prevents phagocytosis of target cells,

which is useful under homeostatic conditions to prevent removal of healthy cells (296, 300, 316). However, in many types of cancer including acute myeloid leukemia (AML) and B cell lymphomas, tumor cells are reported to evade phagocytosis by increasing levels of CD47, which is also associated with worsened disease outcomes (317, 318).

Importantly, in non-Hodgkin lymphoma, inhibiting CD47 signaling along with anti-CD20 (rituximab) treatment greatly enhanced macrophage-mediated engulfment of tumor cells and lead to objective clinical responses in 50% of patients (318-320). In human AITL samples, both CD47 and SLAMF7 are expressed, however, there appears to be no correlation between higher CD47 levels and disease outlook (321-323). Nevertheless, using AITL patient-derived xenograft (PDX) models, it has been reported that AITL tumor cells are more efficiently phagocytosed when CD47 signaling is blocked *in vitro*, strongly suggesting that this may be a beneficial avenue for AITL disease treatment (323). The enhanced phagocytosis of hematopoietic-derived tumors after CD47 blockade is reported to be dependent on the presence of prophagocytic SLAMF7 and Mac-1 signaling (241). Thus, the following sections will describe in more detail (1) inhibitory CD47-SIRPα and (2) prophagocytic SLAMF7 signaling pathways.

1.3.2.1 Inhibitory CD47-SIRPα signaling

CD47 is considered to be an inhibitory "don't eat me" membrane protein that is ubiquitously expressed on both non-immune and immune cells (296, 300, 316). CD47 contains five transmembrane regions along with a single Ig-like domain and can interact not only with SIRPα but also thrombospondin-1 (TSP-1) and certain integrins (300, 316). In contrast, expression of SIRPα is restricted to immune cells such as monocytes, macrophages, neutrophils and dendritic cells (296, 300, 316). SIRPα has three Ig-like domains as well as a cytoplasmic tail that contains immunoreceptor tyrosine inhibitory motifs (ITIM) whose phosphorylation is important to propagate inhibitory functions (300, 316). SIRPα binding to CD47 prevents target cell phagocytosis by initiating ITIM phosphorylation, which in turn leads to SHP-1/2 phosphatase recruitment, followed by the inhibition of myosin IIA accumulation (296, 300, 324). Physiologically, decreases in CD47 levels are important to promote the removal of aging red blood cells whereas increased CD47 expression on $CD4^+$ T cell effector cells can promote the survival of long-lived $CD4^+$ memory T cells (316, 325, 326).

CD47 signaling blockade, by targeting either CD47 or SIRPα has been reported to enhance phagocytosis of target tumor cells (241, 296, 300, 327). However, blocking CD47

signaling does not only increase the phagocytic efficiency of both M1 and M2 macrophages but can also promote macrophage polarization into an antitumor M1-like phenotype (328). Furthermore, mere removal of inhibitory CD47 signaling is not always adequate to promote target cell engulfment, which has been demonstrated in T cell leukemia or colon cancer cell lines (241, 296). On this note, if target tumor cells downregulate positive prophagocytic receptors or express additional antiphagocytic signals, inhibition of CD47 signaling alone can be insufficient to drive tumor cell engulfment (296). To further add to this, it has also been reported that during apoptosis, total CD47 levels do not necessarily increase, but rather, CD47 clustering patterns become more dispersed along the cell membrane, which decreases SIRPα engagement and promotes macrophage-mediated phagocytosis (329). Therefore, it may also be informative in different cancers, including AITL, to investigate CD47 distribution patterns on tumor cells to see whether this may also correlate with patient survival outcomes.

Beyond initiating an inhibitory antiphagocytic pathway in macrophages, it is also plausible that CD47 could be involved in signaling mechanisms that may serve to support tumor cells. In T cells, it has been shown that CD47 can engage in *cis* interactions with β_2 integrins such as LFA-1 or very late antigen-4 (VLA-4) and can also support their high affinity conformation in Th1 cells (330). Furthermore, in a model of experimental autoimmune encephalomyelitis (EAE), it was reported that *Cd47*$^{-/-}$ CD4^{+} T cells had impaired proliferation and survival also due to reduced LFA-1 activation (331). As outlined in section 1.2.6, high affinity LFA-1 is important for Tfh cell identity by supporting Bcl6 induction as well as GC survival (118). In line with this, *Cd47*$^{-/-}$ mice were observed to have reduced frequencies of Tfh cells in the spleen and lymph nodes at both steady-state and after protein immunization, indicating that CD47 may also play a role in supporting Tfh cell formation (332).

1.3.2.2 Prophagocytic SLAMF7 interactions

SLAMF7 is expressed on immune cell subsets such as activated T cells, B cells, NK cells, dendritic cells and macrophages (239, 333). Unlike other SLAM family receptors, it does not associate with the adaptor protein SAP, but another member of the adaptor protein family, EAT-2 (239). EAT-2 is expressed in NK cells, macrophages and dendritic cells but is not reported to be found in T or B cells (334). SLAMF7 has been identified as a critical prophagocytic signal in macrophage-mediated phagocytosis of hematopoietic-derived tumors (241). Importantly, this increased phagocytosis during CD47 signaling blockade is also reliant on SLAMF7 interactions

with integrin Mac-1 (241). In this case, SLAMF7 promotes phagocytosis by regulating actin polarization which occurs independently of its association with EAT-2 (241). In NK cells, SLAMF7 is critical for enhancing NK cell activation and cytotoxicity in an EAT-2 dependent manner (333). In $CD4^+$ T cells, levels of SLAMF7 are shown to increase during activation, and may be involved in an inhibitory feedback loop during antigen-induced T cell proliferation (333). This is because $CD4^+$ T cells are naturally deficient in EAT-2, and SLAMF7 engagement in the absence of SAP family adaptor proteins promotes the inhibitory nature of SLAMF7 (333). Nonetheless, with regards to GC dynamics, GC B cell formation or Tfh cell generation, whether SLAMF7 is a vital signaling molecule has not been reported.

1.4 AITL mouse models

Numerous mouse models have been developed to increase not only our understanding of AITL disease pathogenesis but to also identify novel signaling pathways that may be modified in order to improve AITL patient outcomes. The following section will detail these different AITL mouse models with emphasis on relevance to AITL pathogenesis, features and experimental utility. A summary table is also presented at the end of the section to compile these elements (Table 1.3).

1.4.1 Patient-derived xenograft (PDX)

Patient-derived xenografts (PDX), where human tumors are transplanted into immunosuppressed murine hosts, are a useful translational tool to bridge the gap between fundamental science and clinical application. In AITL, there are several groups that have developed PDX models to gain insight into the tumor cell population (32, 94, 323, 335-337). Transplanting human AITL tumor cells into immunocompromised mice demonstrate successful tumor cell engraftment into the spleen, bone marrow and blood (32, 335, 337). In addition, histological and immunological features as well as T cell clonality from AITL tumor donors were recapitulated in mouse PDX samples (32, 337). Moreover, in one AITL-PDX model, mice also produced human class-switched antibodies, suggesting that the helper function of tumor Tfh-like cells remained intact (32). In this study, serial transplantation of splenocytes from a primary AITL-PDX mouse demonstrated that over time, there was an enrichment of a $CD4^+$ Tfh-like cell population with high levels of Bcl6, but a decrease in the frequency of B cells (32). In

contrast, a similar serial transplantation experiment using a different primary patient sample demonstrated an accumulation of both T and B cells (337). AITL tumor cells from this patient had mutations in *TET2*, $RHOA^{G17V}$ as well as other genes (337). While it was not reported whether *TET2* mutations were also identified in these expanded B cell populations (337), in a separate study, approximately 67% of AITL patients were observed to have *TET2* mutations in B cells as well (42). Consequently, one interpretation for the expansion of T and B cells after serial transplantation of this particular primary tumor could be that a proliferative advantage is conferred to both T and B cell populations as a result of these *TET2* mutations (42, 68, 337). Another possibility is that since T cells with *TET2* mutations are more likely to acquire features of Tfh-like cells (50), such as the ability to support T-B interactions, they may also be more efficient at supporting B cell survival and/or proliferation.

Recent work has been centered around using AITL-PDX models to test the efficacy of duvelisib, a PI3Kδ/γ inhibitor and elotuzumab, a stimulator of SLAMF7 signaling (94, 336, 337). The use of duvelisib in AITL-PDX mice demonstrated alterations in TAM polarization *in vivo* where there was a significant increase in the proportion of M1-like macrophages in the spleen of duvelisib-treated mice (94). Nevertheless, due to the short-term nature of this experimental set up, whether duvelisib treatment lessened AITL disease symptoms in these PDX models was not investigated (94). In addition to this, two different groups have studied the efficacy of elotuzumab in AITL-PDX models in combination with 5-azacytidine or rituximab, and their work demonstrates that the combinatorial use extended survival times for these AITL-engrafted mice (336, 337). In future studies, it would be useful to comprehensively test whether AITL tumors with combined mutations in $RHOA^{G17V}$ and *TET2* or activating mutations in T cell signaling genes manifest differently in PDX models and/or respond differently to therapeutic treatments.

One of the main strengths of PDX models is the ability to test the efficacy of different drugs within an *in vivo* system as compared to *in vitro* cell cultures while still maintaining the original histologic and genomic characteristics of the patient (338). However, recipient mice often come from an immunocompromised background, such as NOD/*scid* /IL2Rγ^{null} (NSG) or NOG mice. NOG mice are similar to NSG mice in that they share a NOD background and the *scid* mutation, but express a truncated IL-2Rγ with no signaling capacity instead of a completely null protein as is found in NSG mice (339). Thus, since both NSG and NOG mice lack a

functional immune system, they may not be ideal for the transplantation of lymphoma cells (340). It has been reported that mice without the common γ chain (*Il2rg*), which both NSG and NOG mice also lack, have defective development of peripheral lymph nodes (340, 341). This has been attributed to reduced lymphoid tissue inducer cells, which relies on the IL-7 receptor (composed of IL-7Rα and the common γ chain) (340, 341). To further support this, lymph nodes could not be easily observed using magnetic resonance imaging or upon dissection from NOG mice (342). Additionally, histological analysis of underdeveloped submandibular or mesenteric lymph nodes from NSG or NOG mice revealed hypocellularity and lack of clearly defined medullar and cortical regions (339). Thus, one limitation is that these mice may lack the proper lymphoid microenvironment to support lymphomagenesis. As such, AITL tumor cells are typically identified in the peripheral blood, spleen or bone marrow of PDX mice (32, 335, 337), but are not described in the lymph nodes of engrafted mice. Consequently, a successful pharmacological response in AITL-PDX mice is not measured by the physical regression of lymph node tumors but rather extended survival rates for engrafted mice treated with certain drugs (336, 337).

Another factor to consider is that since most PDX recipient mice are from the NOD background, they inherit a polymorphism in SIRPα (343, 344). This is reported to enhance binding between human CD47 and mouse SIRPα, thus amplifying an inhibitory "don't eat me" signal which prevents macrophages from effectively removing newly engrafted human tumor cells (343, 344). However, rejection of human red blood cells in NSG mice is observed to be dependent on macrophage-mediated phagocytosis, suggesting that macrophages in NSG mice are capable of target cell engulfment (345). Thus, it is possible that macrophages in NSG mice may preferentially phagocytose a certain subset of AITL tumor cells, such as cells with higher expression of prophagocytic SLAMF7. As a consequence of this, following several serial passages between NSG mice, the original heterogeneity of the primary AITL tumor may be lost (338). Instead, in its place, only tumor cells capable of surviving this immune pressure may remain and additionally, engrafted tumors may become less representative of what occurs in human AITL.

1.4.2 *Tet2* mutation

Although mutations in *TET2* are commonly found in AITL patients (54, 55), they are also observed in myeloid and B cell malignancies (55, 346-348). Moreover, since loss-of-function *TET2* mutations also occur in T, B and myeloid cells, this may explain the presence of co-existing myeloid neoplasms and B cell lymphomas that can develop in a proportion of AITL patients (4, 42, 349). In line with this, approximately 92% of *Tet2*$^{-/-}$ mice develop myeloid malignancies (346, 348, 350), however, after a longer time period, a smaller proportion can also develop B cell (~3%) or T cell (~4%) malignancies (55, 58, 268, 350). Hematopoietic stem cells from TET2-deficient mice have increased self-renewal, proliferative abilities and are also associated with genomic hypermutability (346, 348, 350, 351). Tfh-like lymphomas were reported in >60 week old mice with TET2 deficiency, reminiscent to PTCLs with a Tfh cell phenotype (55). *Tet2*$^{-/-}$ mice do not fully recapitulate AITL disease as they lack the hypergammaglobulinemia, FDC meshwork expansion and increased vascularization typically associated with AITL (55). These mice experience splenomegaly as well as multiple swollen lymph nodes and have an expansion of CD4^{+}PD-1^{+}CXCR5^{+} Tfh-like cells (55). These tumor cells also express high levels of genes associated with Tfh cell biology, such as *Bcl6*, *Icos*, *Pdcd1* and *Cxcr5* (55). Moreover, these mice have increased methylation of a *Bcl6* intronic silencer region, which correlates with higher *Bcl6* mRNA levels and as such, is possibly one way loss of TET2 function promotes the Tfh cell program (55). This is also supported by the observation made in tumors from human PTCL patients, where harbouring *TET2* mutations was highly associated with Tfh-like features (50).

1.4.3 Combined *Rhoa*^{G17V} and *Tet2* mutations

Different mouse models investigating the impact of *Rhoa*^{G17V} and *Tet2* mutations in the development of AITL generally demonstrate that they are synergistic in the acquisition of an AITL-like phenotype. At around 10 weeks of age, transgenic mice expressing RHOA-G17V under the control of CD4 cell regulatory elements develop severe autoimmunity, have an expansion of Tfh cells but do not develop AITL-like disease (46). However, if RHOA-G17V mutant mice also have TET2 deficiency, this manifests into AITL-like disease exemplified by characteristics such as Tfh cell expansion, splenomegaly, lymphadenopathy and increased vascularization (46). NSG mice transplanted with these AITL-like tumor cells and treated with

mammalian target of rapamycin complex 1 (mTORC1) inhibitor everolimus also showed improved overall survival rates, highlighting the potentially clinically relevant outcome of modulating this signaling pathway (46). Another group used a similar AITL-like mouse model with loss of TET2 and expression of RHOA-G17V to demonstrate that use of dasatinib could improve survival of nude mice transplanted with AITL-like lymphomas by dampening TCR signaling via VAV1 and PLCγ1 phosphorylation (92). Importantly, treatment of dasatinib in a small cohort of relapsed or refractory AITL patients also showed partial response in most patients (92).

Overexpression of RHOA-G17V in TET2-deficient $CD4^+$ T cells then transferred into *Tcrα*$^{-/-}$ mice led to the development of enlarged lymph nodes, lymphocyte infiltration, weight loss as well as increased Tfh and GC B cell populations (47). However, AITL-like disease was not observed in these mice, which may be due to their shorter survival time, approximately 21 weeks (47). In a different approach, using mice with tamoxifen-inducible and CD4-specific expression of *Rhoa*^{G17V} led to increased $CD4^+$ T cell proliferation and Tfh cell generation without developing AITL-like disease (45). This is an improved genetic approach as compared to mice which produce RHOA-G17V as soon as CD4 is expressed, as firstly, this is reported to impact early T cell development in the thymus and spleen in younger mice (46). Secondly, this does not accurately reflect what happens in human AITL, where *RHOA*^{G17V} is a secondary driver mutation acquired in mature T cells (9). Moreover, wildtype hosts that received *Tet2*$^{-/-}$ bone marrow cells infected with mutant *Rhoa*^{G17V} developed AITL-like lymphomas with splenomegaly, swollen lymph nodes (~2mm), monoclonal T cell populations, expanded FDC meshworks and increased vascular networks (45). Transplantation of bone marrow cells from mice with CD4-specific, tamoxifen-induced expression of RHOA-G17V in combination with CD4-specific TET2 loss into lethally irradiated wildtype mice also led to AITL-like disease development, with increased Tfh cell frequencies, FDC meshworks and angiogenesis (45). It was also reported that induction of RHOA-G17V mutant expression led to increased ICOS levels and that furthermore, ICOS-PI3K signaling supported tumor cell proliferation in *Tet2*$^{-/-}$; *Rhoa*^{G17V} mice (45).

From these mouse models, the overarching trend is that although expression of mutant RHOA-G17V leads to inappropriate Tfh cell expansion, it is indeed the cooperation between TET2 deficiency and RHOA-G17V that ultimately leads to AITL-like disease development.

Nonetheless, while all mouse models indeed address the impact of combined *RHOA* and *TET2* mutations, none faithfully reproduce the human scenario, where loss of TET2 activity is an early event followed by the acquisition of $RHOA^{G17V}$ in $CD4^+$ T cells (9, 53, 61). Furthermore, another limitation of these mouse models is that they represent only a specific subset of AITL patients and thus, findings made using these mice may not translate clinically into therapeutic responses for AITL patients with different causative genetic mutations.

1.4.4 Combined *Tet2* and *Dnmt3a* mutations

Initial bone marrow transplantation of $Tet2^{-/-}$ cells expressing reduced activity DNMT3A mutant, $DNMT3A^{R882H}$ (352), led to increased myeloid cell expansion in the blood and bone marrow (62). Most of these mice develop disorders reminiscent to AML or T-ALL, although one mouse in this cohort was observed to develop AITL-like disease (62). After secondary and tertiary engraftment of hematopoietic progenitor cells, there was an increase in the proportion of T cells as compared to myeloid or B cell compartments in the blood of recipient mice (62). Moreover, approximately 1 year after secondary or tertiary transplantation, a majority of these mice developed swollen thymus, spleen and lymph nodes which contained $CD4^+$ T cells expressing high levels of *Bcl6*, *Pdcd1*, *Cxcr5* and *Icos*, indicative of a Tfh cell phenotype and AITL-like disease (62). Because AITL-like disease development has a long latency after secondary or tertiary engraftment, this suggests that the accumulation of additional mutations may be necessary for onset of AITL-like symptoms (62).

1.4.5 Swiss Jim Lambert mice

Swiss Jim Lambert (SJL) mice develop B cell lymphomas which have been reported to depend on GC B cell-specific expression of endogenous mouse mammary tumor virus superantigen, which in turn stimulates $CD4^+$ T cells to produce critical signaling molecules, thereby driving B cell lymphomagenesis (353-356). At 3 months of age, SJL mice have increased frequencies of Tfh and GC B cells as well as altered follicular structure in the spleen and lymph node but usually develop tumors closer to 1 year of age (353). SJL mice also have elevated levels of IgG2b and IL-21 in their sera, supporting a functional role for Tfh cells identified in this mouse model (353). Moreover, SJL mice which lack expression of the IL-21 receptor have largely intact spleen and lymph node structures, lower IgG2b levels, as well as

reduced GCs, suggesting the importance of IL-21 in tumor development (353). While SJL mice do share certain features with AITL such as an increased Tfh cell compartment, expanded B cell populations, hypergammaglobulinemia and elevated IL-21 levels, these mice also lack the FDC expansion and vascularization associated with human AITL (353). Furthermore, since monoclonal or oligoclonal cell populations for B cells but not T cells were identified in these mice (353), a more plausible interpretation is that SJL mice develop B cell lymphomas which not only are promoted by intimate Tfh cell interactions but reciprocally produce cytokines and/or signaling molecules that support the activity of Tfh cells.

1.4.6 T cell-specific GAPDH overexpression model

Mice generated to overexpress glyceraldhedye-3-phosphate dehydrogenase (GAPDH) in a T cell-specific manner develop AITL-like disease at around 18 months of age (357). These mice developed enlarged spleens, livers as well as lymph nodes (357). The lymph nodes of these mice exhibited infiltration of both T and B cells, altered structure and increased vascularization (357). Importantly, overexpression of GAPDH in these mice leads to an accumulation of Tfh-like cells, as well as increased GC B and plasma cells (357). In line with this, these mice also had hypergammaglobulinemia and expanded FDC meshworks (357). Specifically, it appears that GAPDH overexpression in T cells promotes AITL-like lymphomagenesis by activating the non-canonical NF-κB pathway via NF-κB-inducing kinase (NIK) and EZH2 (357). Although it has been reported that GAPDH mRNA is increased in human AITL tumor lymph nodes (357), it is unclear whether in human AITL this plays a causal role or is instead a survival mechanism to support neoplastic Tfh cell activity in a hypoxic or stressful environment.

1.4.7 *Roquin*$^{san/+}$ mutation

1.4.7.1 Functional characteristics of Roquin-1

The Roquin family of RNA-binding proteins consists of paralogs Roquin-1 and Roquin-2 (358-360). Roquin-1 and Roquin-2 can be detected in various organs such as the brain, lung and spleen but are most highly expressed in the thymus and lymph nodes (361). Roquin proteins contain a N-terminal Really Interesting New Gene (RING) zinc-finger domain that is associated with E3 ubiquitin ligases, a ROQ domain which is essential for RNA binding, followed by a CCCH-type zinc-finger (358, 360). They are mostly located in cytoplasmic stress granules,

which are sites where mRNA translation and decay are regulated (182, 362). Roquin proteins post-transcriptionally target mRNA species for degradation by recognizing stem-loop structures and linear sequences found in the 3'-untranslated region (UTR) of target genes such as *Icos*, *Ox40*, *Il6* and *Tnf* (361-367). Interactions between Roquin proteins and deadenylating complexes such as Ccr4-Caf1-Not or proteins associated with mRNA decapping such as Edc4 facilitate mRNA decay (363, 364, 367). Additionally, Roquin-1 has also been reported to interfere with expression of *Icos* and *Pten* through interactions with certain microRNAs (368, 369). For instance, interactions between Roquin-1, miR-146a and Ago2 at the 3'-UTR of *Icos* leads to its degradation (368).

Antigen-specific TCR activation is shown to cause downstream cleavage of Roquin-1 by paracaspase MALT1, likely important for the induction of genes that support T cell activation such as ICOS (365). The immunosuppressive cytokine IL-10 is observed to transcriptionally promote Roquin-1 expression (370) but generally, not much else has been studied regarding the regulation of Roquin proteins. In $CD4^+$ T cells, Roquin-1 is expressed 5-fold more than Roquin-2, and this trend is also observed in other tissues where Roquins are expressed (361). Roquin-1 and Roquin-2 have overlapping functions in the negative regulation of Tfh cell generation by targeting *Icos* and *Ox40* mRNA for degradation (361, 366). However, loss of Roquin-1 from $CD4^+$ T cells is insufficient to induce Tfh cell differentiation and increase GC B cell numbers (361, 371). Moreover, it is only the combined loss of Roquin-1 and Roquin-2 from $CD4^+$ T cells which leads to increased Tfh cell generation (361). It has also been found that Roquin-1 and Roquin-2 can induce a Tfh cell gene signature in Treg cells, which further highlights its role in promoting Tfh cell features (369). Importantly, in $CD4^+$ T cells, Roquin-1 also promotes FOXO1 localization into the nucleus, which was reported to be related to its ability to inhibit PI3K-mTOR signaling and Itch, which is a negative regulator of FOXO1 (369). As increased nuclear FOXO1 localization is associated with an inhibition of the Tfh cell phenotype (84), this could explain why loss of Roquin-1 and Roquin-2 promotes Tfh cell differentiation (361).

Roquin-1 deficient pups die within 6 hours of birth with malformed spinal columns and impaired lung function (371). This perinatal lethality experienced by Roquin-1-deficient pups highlights the developmental importance of Roquin-1 activity (371). Although Roquin-2 deficiency does not lead to the same neural defects as Roquin-1 loss, Roquin-2-deficient mice die quickly after birth and experience impaired lung functionality (361). Loss of the RING

domain in Roquin-1 or Roquin-2 prevents its localization into stress granules and as such, leads to minimal or no increase in ICOS levels (366). Interestingly, while mice without the Roquin-1 RING domain experience lethality similar to complete deficiency in the Roquin-1 protein, mice without the RING domain of Roquin-2 remain viable, suggesting that this domain in Roquin-1 is more essential during certain developmental processes (366).

1.4.7.2 *Sanroque* mutation: Autoimmunity

Mice with a point mutation, M199R, termed "sanroque" introduced into the ROQ domain of Roquin-1 were developed using an ethylnitrosourea (ENU) mutagenesis approach, where mice were screened for signs of autoimmunity based on autoantibodies titers (182). *Roquin-1*$^{san/san}$ mice, from around 6 weeks of age develop severe autoimmunity, spontaneous GCs, as well as enlarged spleens and lymph nodes (182). Crossing *Roquin*$^{san/san}$ mice into backgrounds lacking critical Tfh cell signaling proteins such as CD28, ICOS, SAP and Bcl6 highlight the pathogenic influence of the *sanroque* mutation in Tfh cell accumulation and hyperactivity (372-374). It has also been reported that excessive IFN-γ receptor signaling in CD4$^+$ T cells from *Roquin*$^{san/san}$ mice contributes to spontaneous GC development, CD4$^+$ T cell proliferation as well as Bcl6 expression in early Tfh cell precursors (234). Moreover, *Ifng* mRNA in *Roquin*$^{san/san}$ T cells has an increased half-life, suggesting that Roquin-1 can also regulate *Ifng* degradation as another mechanism to prevent the pathogenic accumulation of Tfh cells and autoimmunity (234). The *sanroque* mutation leads to only a minor conformational change in the protein structure of Roquin-1, which does not inhibit its ability to bind target genes such as *Icos* or localize to stress granules (182, 363, 368, 374). In fact, the *sanroque* protein can bind to *Icos* mRNA with 3-times higher affinity to that of wildtype Roquin-1 (362) and also stabilizes target mRNA instead of promoting decay (374).

The stark contrast between the overt autoimmunity observed in *Roquin-1*$^{san/san}$ as compared to mice with CD4-specific loss of Roquin-1 has been attributed to the redundant functions of Roquin-2 which can compensate when Roquin-1 is lost (366). Because the *sanroque* variant of Roquin-1 still binds to target RNA in stress granules, it can prevent the normal compensatory activity of Roquin-2 (366). Nonetheless, the fact that dual loss of Roquin-1 and Roquin-2 from CD4$^+$ T cells promotes spontaneous formation of GC Tfh and B cells but not systemic autoimmunity as seen in *Roquin*$^{san/san}$ mice further suggests that the *sanroque* mutant may have other novel functions or that the *sanroque* mutation also generates myeloid and/or B cell

populations which support autoimmune or inflammatory conditions (361). In support of this, *Rag1*$^{-/-}$*Roquin*$^{san/san}$ mice which are devoid of T and B cells, were observed to have an increased propensity to develop clinical symptoms after induction of rheumatoid arthritic-like disease, suggesting a role for Roquin-1 in preventing myeloid cell-driven inflammation (366). Furthermore, Roquin-1 appears to also impact B cell activity, as B cell-specific loss of Roquin-1 also led to increased spleen cellularity, B cell number and effector-like CD4^{+} T cell expansion (371). In summary, the *sanroque* mutation in Roquin-1 demonstrates that the prevention of Roquin-1-mediated mRNA decay while blocking Roquin-2 compensatory actions promotes the development of pathogenic Tfh cells which support spontaneous GC formation and systemic autoimmunity.

1.4.7.3 *Sanroque* mutation: AITL-like disease

Heterozygosity of the *sanroque* mutation (*Roquin*$^{san/+}$) leads to the development of AITL-like disease at around 4-6 months of age in approximately 50% of mice (270). These mice share several features with human AITL including splenomegaly, asymmetric lymphadenopathy (5-12mm in diameter) and hypergammaglobulinemia (270). AITL-like tumors are reported to have nearly 50 to 150 times increased cellularity as compared to normal lymph nodes (270). Furthermore, AITL-like tumors share histological features with human AITL, such as destroyed lymphoid architecture and expansion of blood vessel networks (270) (Fig. 1.4). Moreover, as with the human disease counterpart, AITL-like tumors contain an increased proportion of B cells and oligoclonal Tfh cell populations (270). Although Tfh cells from non-tumor lymph nodes also demonstrate oligoclonality, whether these are clonally related to tumor Tfh-like cells has not been investigated (270). Furthermore, the potential clonal nature of B cells in tumor-bearing *Roquin*$^{san/+}$ mice has yet to be studied, but as clonal B cell populations have been identified in human AITL patients (2, 11), this may also be the case in this mouse model. Importantly, *Roquin*$^{san/+}$ AITL-like tumors are also derived from Tfh cells (270). This was clearly shown by breeding *Roquin*$^{san/+}$ mice into genetic backgrounds with deficiencies in essential Tfh cell molecules such as ICOS, CD28 or SAP (34, 35, 107), which led to a reduction in initiation rates of AITL-like disease (270).

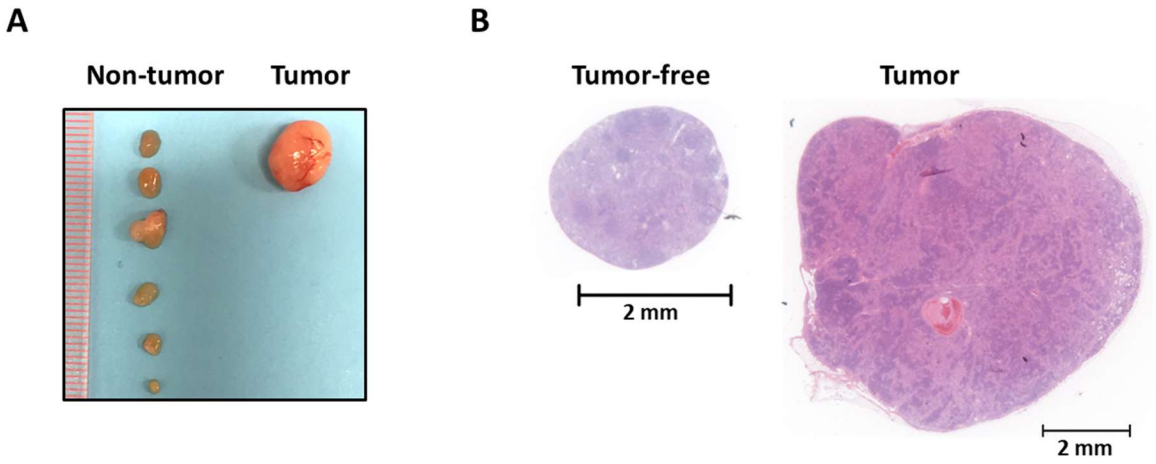

Figure 1.4 AITL-like tumors in *Roquin*$^{san/+}$ mice

(A) Comparison of non-tumor and tumor lymph nodes from the same tumor-bearing mouse. (B) Representative H&E sections from a tumor-free mouse and AITL-like tumor showcasing differences in lymph node architecture as well as blood vessel expansion.

1.4.7.4 Advantages and disadvantages of *Roquin*$^{san/+}$ model

The clearly palpable AITL-like lymph node tumors which develop in *Roquin*$^{san/+}$ mice share numerous features with human AITL such as hyperactive Tfh cells, immune cell infiltration, destroyed lymph node structure, expansion of blood vessel networks, hypergammaglobulinemia and hepatosplenomegaly (270). Because AITL-like tumors in *Roquin*$^{san/+}$ mice can grow between 5-12mm in diameter, this provides an advantage when trying to test the effect of conditional gene deletion or pharmacological intervention on tumor regression without needing to rely on other immune organs such as the spleen. In contrast, wildtype mice transplanted with hematopoietic stem cells manipulated to have combined *Tet2*$^{-/-}$; *Rhoa*^{G17V} expression developed lymph nodes around 2mm in diameter (45), which is within the range of a regular-sized, murine peripheral lymph node, usually between 1-2mm (375). This makes it difficult to accurately follow the impact of certain pharmacological interventions on tumor lymph node regression and thus, instead, the focus is often placed on the spleen (45, 46, 92). Nevertheless, while there are certainly advantages to using *Roquin*$^{san/+}$ mice, there are also some differences between these mice and human AITL. For instance, *Roquin*$^{san/+}$ tumors do not develop expanded FDC meshworks as is characteristic of human AITL (270). Additionally, while ROQUIN1 is expressed in human AITL, its protein levels are not dysregulated as

compared to healthy controls and further, no mutations in *ROQUIN1* have been detected in human AITL patients (376).

However, certain molecular signaling pathways mediated by Roquin-1 have been reported to overlap with other AITL-like mouse models as well as human AITL, beyond that of a hyperactive Tfh-like tumor cell population. It has been shown that tumor-bearing mice with combined *Rhoa* and *Tet2* mutations have elevated levels of ICOS (45), which is also observed in *Roquin*$^{san/+}$ tumors (270). Moreover, ICOS signaling was shown to promote activation of PI3K and MAPK signaling pathways in AITL-like tumor cells with *Rhoa* and *Tet2* mutations (45). Since Roquin-1 has been implicated in regulating not only ICOS (182, 362, 374) but also repressing PI3K-mTOR signaling (369), it is plausible that elevated PI3K signaling in *Roquin*$^{san/+}$ mice may also influence AITL-like disease pathogenesis. Furthermore, Roquin-1 has also been reported to regulate FOXO1 activation and localization, as loss of Roquin-1 in $CD4^+$ T cells led to FOXO1 accumulation in the cytoplasm (369), which likely helps promote Tfh cell differentiation (84). This is a shared finding with combined *Tet2*-deficient and *Rhoa*^{G17V}-expressing mice (47) and importantly, also with human AITL, as patients with no FOXO1 protein levels or restricted cytoplasmic FOXO1 expression are associated with poor prognosis and aggressive clinical course (83). Finally, approximately half of AITL patients have activating mutations in TCR signaling components such as *PI3K* elements, *FYN* or *CD28* (38, 44, 69-71), and as such, tumor-bearing *Roquin*$^{san/+}$ mice may converge with these common hyperactive signaling pathways that can promote Tfh cell-derived lymphomas.

Mouse Models	Human AITL Feature							Ref.
	Spleno-megaly	Lymph-adenopathy	Hyper-gamma-globulinemia	Tfh cell origin	Shared genetic mutation	Branching blood vessels	FDC meshwork expansion	
PDX	✓	**ND**	✓	✓	✓	✓	**ND**	(32, 337)
Tet2	✓	✓	-	✓	✓	**ND**	**ND**	(55)
Rhoa and *Tet2*	✓*	✓	-	✓	✓	✓	✓	(45-47)
Tet2 and *Dnmt3a*	✓*	✓*	**ND**	✓	✓	**ND**	**ND**	(62)
SJL mice	✓*	✓*	✓	✓	-	-	-	(353)
T cell-specific GAPDH over-expression	✓	✓	✓	✓	-	✓	✓	(357)
Roquin$^{san/+}$	✓	✓	✓	✓	-	✓	-	(270)

PDX, patient-derived xenograft; SJL, Swiss Jim Lambert; Tfh, T follicular helper; ✓, positive; -, negative; ND, not described; *, described but data not shown; Ref., References.

Table 1.3 Comparison of different features between AITL-like mouse models

1.5 Rationale

AITL has an aggressive clinical course with ineffective therapeutic options, exemplified by the low 5-year survival rate of ~30%, which unfortunately has not improved for many decades (5, 73, 88, 89). Most patients are treated with a type of CHOP chemotherapy, and while the initial response is usually positive, most AITL patients experience multiple episodes of disease relapse for which currently, there exists no effective pharmacological intervention (5). In fact, the median overall survival time after relapse or progression in PTCL or AITL patients that

responded to initial treatment is only 6 months (377). As such, there is a need to identify better targets to improve AITL treatments, for both initially diagnosed and relapsed/refractory patients.

It is clear that AITL tumor cells are derived from the Tfh cell lineage as they share the expression of numerous signature Tfh cell proteins such as Bcl6, SAP, ICOS, and PD-1 which are also important clinical diagnostic markers (3, 6, 18-21, 23, 30, 265, 378). Nonetheless, it has not been studied whether AITL tumor cells express these key Tfh cell molecules simply as a reflection of their Tfh cell origin or, if they continuously serve a functional purpose to propagate AITL disease. Understanding the importance of these molecules and downstream signaling pathways in the context of AITL tumor cells can be pivotal in the search to find new pharmacological targets for AITL treatment.

Moreover, because of the gross immune dysregulation caused by Tfh-like tumor cells, a large proportion of the AITL tumor mass is filled with activated B cells, plasma cells, FDCs and macrophages (3, 11, 14, 18). The intimate interaction between Tfh and B cells within the GC is a critical part of a successful humoral immune response (34, 35, 107). The B cell expansion in tumors and hypergammaglobulinemia experienced by AITL patients would suggest that Tfh-like cells in AITL tumors are still able to communicate with B cells, however, whether this T-B crosstalk is somehow important for tumor progression has yet to be investigated.

Lastly, it is curious that while AITL tumor cells are commonly found in the peripheral blood of AITL patients (265), the sequential appearance of tumors in other lymph nodes can occur within a wide range of months to years, depending on the patient (4). On the one hand, this may reflect a requirement for a tumor-specific lymphoid niche capable of supporting tumor spreading, but on the other hand, this could also suggest that in AITL patients, there may be antitumor mechanisms that oppose the establishment of tumors in new lymph nodes. Because the AITL tumor microenvironment is filled with numerous types of immune cells, there is the possibility that one or many subsets may work to delay tumor growth. Since the ratio of M2 macrophages in AITL has been associated with poor prognosis, this also demonstrates that macrophage polarization impacts patient outcomes and suggests that macrophages could be involved in AITL disease severity (78, 81). SLAMF7, a prophagocytic molecule is also found expressed in a subset of AITL patients (321, 322), and while no correlational studies with patient prognosis have been conducted yet, this may be one way to enhance antitumor macrophage-mediated phagocytic efficiency in a subset of AITL patients. In summary, the relevance of the

Tfh cell nature of tumor cells as well as interactions between AITL tumor cells and their microenvironment are poorly studied areas which can be vital in understanding the best way to approach AITL disease treatment (Fig. 1.5A-B).

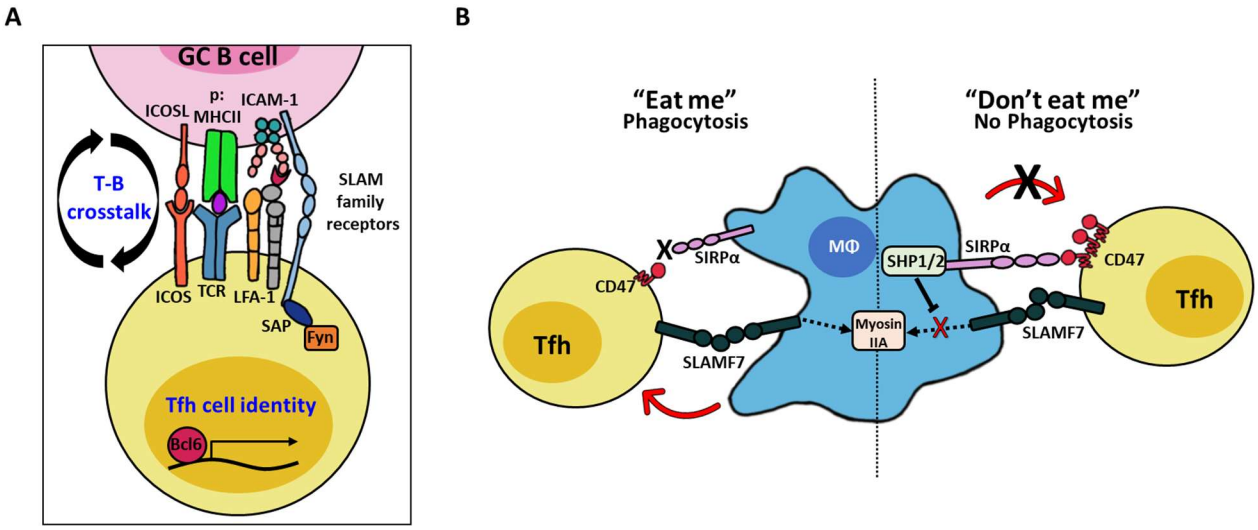

Figure 1.5 Summary of key immune mechanisms explored in Aims 1 and 2

(A) Although the Tfh cell origin of AITL tumor cells is well-established, whether Tfh-like tumor cells continue to rely on signature Tfh cell proteins during disease progression has yet to be determined. In Aim 1, we address the potential role of Tfh cell master regulator transcription factor Bcl6 in AITL-like disease. Additionally, since an important function of Tfh cells is to form stable conjugates with B cells in GCs, this thesis will also address whether certain molecules involved in T-B crosstalk such as ICOS, SAP and LFA-1 may also be involved in supporting AITL-like disease maintenance. (B) In Aim 2, this thesis will explore whether there is evidence of altered macrophage-mediated immune surveillance mechanisms in AITL-like tumors, specifically within the context of prophagocytic molecule SLAMF7 versus the CD47-SIRPα "don't eat me" inhibitory signaling axis.

1.6 Hypothesis

My main hypothesis is that by impairing critical Tfh cell signature signaling pathways and/or by boosting immunosurveillance in AITL, this will favour tumor regression and prevent tumor cell dissemination. Because the process of Tfh cell generation involves several stages where Tfh cells both respond and produce various stimulatory signals that promote its own differentiation and proliferation (35, 107), I hypothesize that Tfh-like AITL tumor cells rely and/or amplify these positive signaling pathways to support their hyperactivity in tumor lymph nodes. Thus, by inhibiting critical Tfh cell signaling pathways such as transcription factor Bcl6 or SAP, an

adaptor protein that supports T-B crosstalk, I theorize that AITL tumors will not be able to successfully maintain themselves and will consequently, regress.

Furthermore, by promoting immune surveillance mechanisms in AITL, I also hypothesize that this can prevent tumor progression and spreading. The AITL microenvironment contains numerous types of immune cells including NK cells and macrophages (3), as well as others which are well-established to be critical in antitumor responses. The ability of macrophages to engulf tumor cells relies on the expression of prophagocytic signals such as SLAMF7, however, tumor cells oppose this by upregulating molecules that engage inhibitory antiphagocytic pathways in macrophages, such as the CD47-SIRPα pathway (241, 296, 300). As has been demonstrated with other types of hematopoietic cancers (241), I believe that inhibition of this negative CD47-SIRPα pathway will boost macrophage-mediated phagocytosis against AITL tumor cells. Thus, to summarize, I hypothesize that blocking critical Tfh cell signaling proteins in AITL tumors and/or promoting the ability of macrophages to engulf AITL tumor cells will ultimately prevent AITL disease progression and spreading.

1.7 Aims and Objectives

1.7.1 Aim 1

The focus of Aim 1 is to study the role of key Tfh cell molecules Bcl6 and SAP on AITL tumor growth. This will be done through the following objectives.

1. Investigate whether critical Tfh cell signaling proteins Bcl6 or SAP are continuously required for AITL-like disease maintenance.
2. Identify signaling molecules downstream of Bcl6 or SAP signaling pathways that support AITL-like tumor growth.
3. Test the impact of different Tfh cell signaling protein inhibitors *in vivo* on AITL-like tumor growth.

1.7.2 Aim 2

Through Aim 2, the goal is to explore the role of macrophage-mediated immune surveillance in AITL and will be approached through the following objectives.

1. Profile expression levels of SLAMF7, CD47 and SIRPα on appropriate immune cell populations such as T cells, B cells and macrophages in *Roquin*$^{san/+}$ mice.
2. Test whether *in vitro* phagocytosis efficiency of AITL-like tumor cells is improved after inhibition of CD47 signaling.
3. Determine the role of SLAMF7 in AITL-like tumor cells by gene ablation of *Slamf7* in developed tumors.

Chapter 2 The role of key Tfh cell proteins Bcl6 and SAP in AITL-like disease progression

Progression of AITL-like tumors in mice is driven by Tfh signature proteins and T-B crosstalk

Mariko Witalis[1,2], Jinsam Chang[1,2], Ming-Chao Zhong[1], Yasser Bouklouch[1,3], Vincent Panneton[1,4], Joanna Li[1,5], Thorsten Buch[6], Seok Jin Kim[7], Won Seog Kim[7], Young Hyeh Ko[7], André Veillette[1], and Woong-Kyung Suh [1,2,3,4,5]

[1]Institut de recherches cliniques de Montréal (IRCM), Montréal, QC, Canada
[2]Molecular Biology Department, University of Montréal, Montréal, QC, Canada
[3]Department of Experimental Medicine, McGill University, Montréal, QC, Canada
[4]Department of Microbiology, Infectious Diseases and Immunology, University of Montréal, Montréal, QC, Canada
[5]Department of Microbiology and Immunology, McGill University, Montréal, QC, Canada
[6]Institute of Laboratory Animal Science, University of Zürich, Zürich, Switzerland
[7]Samsung Medical Center, Sungkyunkwan University, Seoul, Korea

Note: A version of Chapter 2 has been published in *Blood Advances*: Witalis M, Chang J, Zhong MC, Bouklouch Y, Panneton V, Li J, et al. Progression of AITL-like tumors in mice is driven by Tfh signature proteins and T-B cross talk. Blood Adv. 2020;4(5):868-79.

2.1 Summary

Angioimmunoblastic T cell lymphoma (AITL) is an aggressive peripheral T cell lymphoma driven by a pool of neoplastic cells originating from T follicular helper (Tfh) cells and concomitant expansion of B cells. Conventional chemotherapies for AITL have shown limited efficacy, and as such, there is a need for improved therapeutic options. Since AITL originates from Tfh cells, we hypothesized that AITL tumors continue to rely on essential Tfh cell components and intimate T cell-B cell (T-B) interactions. Using a spontaneous AITL mouse model (*Roquin*$^{san/+}$), we found that acute loss of Bcl6 activity in growing tumors drastically reduced tumor size, demonstrating that AITL-like tumors critically depend on Tfh cell lineage-defining transcription factor Bcl6. Since Bcl6 can upregulate expression of signaling lymphocytic activation molecule (SLAM)-associated protein (SAP), which is known to promote T-B conjugation, we next targeted the SAP-encoding *Sh2d1a* gene. We observed that *Sh2d1a* deletion from CD4$^+$ T cells in fully developed tumors also led to tumor regression. Further, we provide evidence that tumor progression depends on T-B crosstalk facilitated by SAP and high affinity LFA-1. Our study shows that AITL-like tumors heavily rely on molecular pathways that support Tfh cell identity and T-B collaboration, revealing potential therapeutic targets for AITL.

2.2 Introduction

AITL is an aggressive non-Hodgkin lymphoma representing 15-20% of peripheral T cell lymphomas (PTCL) (1). Patients suffer from generalized lymphadenopathy, hypergammaglobulinemia, and autoimmune hemolytic anemia with poor prognosis (5-year survival rate ~33%) (6, 73). Typically, tumors display oligoclonal expansion of T cells and an effacement of lymph node architecture with prominent arborization of endothelial venules (1, 4, 379). Gene expression profiling, immunohistochemical studies, and xenograft experiments established that neoplastic cells in AITL are derived from CD4$^+$ Tfh cells (10, 21, 30, 32). However, the actual tumor Tfh cell content in the AITL tumor mass is kept low throughout disease progression with concomitant expansion of bystander B cells and other reactive immune cells (4, 30, 36). Currently, chemotherapy is the most common treatment for AITL, but its limited efficacy demands more effective therapeutic options (73).

The etiology of AITL has not been fully elucidated, however, genome sequencing of AITL tumor samples have uncovered heterogeneous somatic mutations with a few recurrent genes. Most frequently mutated genes include epigenetic modifiers (*IDH2*, *TET2*, *DNMT3A*), genes encoding the small GTPase RHOA, and components of T cell receptor/costimulatory signaling including the Src-related protein tyrosine kinase Fyn (36-38, 44). Importantly, activating mutations in T cell signaling components were found in ~50% of AITL patients, suggesting that hyperactivation of T cells during germinal center (GC) reactions may play an important role in the malignant transformation of Tfh cells and tumor growth (38, 44).

Tfh cells are a subset of $CD4^+$ T cells whose differentiation is driven by the transcription factor Bcl6 (34, 35). Excessive Tfh cell activity can lead to pathologies such as autoimmunity, as well as Tfh cell-driven lymphomas (35, 270). Directly or indirectly, Bcl6 suppresses other lineage-committing transcription factors and promotes the expression of signature Tfh cell genes such as those encoding CXCR5, PD-1, and SAP, as well as key cytokines such as IL-21 (198, 199, 237). Tfh cells have a unique ability to migrate into B cell follicles, forming transient yet stable T-B conjugates during germinal center reactions. These processes are supported by signaling lymphocytic activation molecule (SLAM) family receptors and their adaptor protein SLAM-associated protein (SAP) (119, 120, 124, 244, 246) as well as LFA-1 (118). After repeated interaction with T cells, GC B cells that have received sufficient T cell help and B cell receptor (BCR) signaling downregulate Bcl6 and upregulate IRF4 to differentiate into antibody-secreting plasma cells (125, 380).

Mice possessing one copy of the *sanroque* allele of *Roquin* ($Roquin^{san}$), a dominant negative point mutation, spontaneously develop AITL-like disease (270). The *sanroque* mutation increases the stability of an array of mRNA species, such as those coding for ICOS, OX40, and IFN-γ in CD4 T cells due to the disruption of Roquin-mediated mRNA degradation machinery (359). Mice homozygous for this *sanroque* mutation ($Roquin^{san/san}$) have hyperactive Tfh cells, spontaneous GC reactions, and develop lupus-like autoimmune disease combined with AITL-like disease within 4-months of age (182). Heterozygous $Roquin^{san/+}$ mice do not develop lupus-like disease but still have hyperactive GC reactions and present with AITL-like disease (~50% incidence rates at 6-months of age) (270). Although *ROQUIN1* gene mutations have not been discovered in AITL patients (376), hyperactivation of T cells and Tfh cells are shared features of tumors arising in $Roquin^{san/+}$ mice and AITL patients.

In this study, we found that the AITL-like tumors in *Roquin*$^{san/+}$ mice accumulate B cells with features of early-stage plasma cells. This B cell expansion coincided with highly proliferative CD4^{+}CXCR5^{+}PD-1^{+} Tfh-like cells equipped with Bcl6, SAP, and high affinity LFA-1. Importantly, acute abrogation of Bcl6 or SAP function or inhibition of high affinity LFA-1 led to partial or full tumor regression. Taken together, these data suggest that AITL-like tumors in *Roquin*$^{san/+}$ mice are driven by Tfh-like CD4^{+} cells that continuously interact with B cells in a manner resembling germinal center T-B interactions.

2.3 Materials and Methods

2.3.1 Mice

Mice with the *Roquin*^{san} allele (182, 270) were provided by Dr. C. Vinuesa (Australia National University, Australia) and bred with other lines of mice to make composite mouse lines. UBC-Cre^{ERT2} (Jax 008085) (381) and CD4-Cre^{ERT2} mice (382) were used for tamoxifen-inducible ubiquitous or CD4^{+} cell-specific knockout models. Bcl6 conditional knockout mice were provided by Dr. T. Takemori (RIKEN, Japan) (217). SAP conditional knockout (*Sh2d1a*^{f}) (128) and SAP^{R78A} mice (*Sh2d1a*^{R78A}) (383) were previously described. All mice have been backcrossed into the C57BL/6J background for more than 10 generations before generating composite lines. Mice were maintained in the animal facility at the Institut de recherches cliniques de Montréal (IRCM) in a specific pathogen-free environment and all experiments were performed in compliance with animal use protocols approved by the IRCM Animal Care Committee.

2.3.2 Antibodies and chemicals

All antibodies, streptavidin-conjugates and reagents used for flow cytometry were from ThermoFisher unless otherwise stated: B220 (RA3-6B2), Bcl6 (K112-91, BD Biosciences), CD4 (GK1.5), CD16/CD32 (2.4G2, BioXCell), CD95 (BD Biosciences), CD138 (281-2, Biolegend or BD Biosciences), CXCR5 (SPRCL5), GL7, ICAM-1 (YN1/1.7.4), IRF4 (3E4), Ki-67 (SolA15), PD-1 (J43, BD Biosciences), SAP (1A9, BD Biosciences or produced by André Veillette laboratory), streptavidin-APC, and streptavidin-PE-Cy. Dead cells were stained with 7-AAD (BD Biosciences) or fixable viability dye (ThermoFisher). Fixation/permeabilization kits (BD

Biosciences or ThermoFisher) were used to perform intracellular stainings. Tamoxifen was purchased from Millipore Sigma; isoflurane from CDMV; Lovastatin from Selleck Chem. Anti-LFA1 (CD11a) (M17/A) was purchased from BioXCell.

2.3.3 Flow cytometry

Single cell suspensions of tumors or pooled non-tumor or pooled tumor-free lymph nodes (cervical, axillary, brachial, and inguinal) were prepared from age-matched mice (6-13 months of age) by mechanical dissociation using a 70μM nylon mesh filter (BD Biosciences), in PBS or staining buffer (PBS with 1% bovine serum albumin (BSA) (Wisent)). Cells were first blocked with anti-CD16/CD32 and then stained with primary antibodies followed by streptavidin-conjugates. For intracellular stains, cells were fixed and permeabilized with Cytofix/Cytoperm solution or Fix/Perm Buffer, according to manufacturer's instructions. Samples were acquired using LSR Fortessa (BD Biosciences) and analyzed on Flowjo Version 10 (Treestar).

2.3.4 ICAM-1 binding assay

Single cell suspensions (1×10^7 cells per ml) were resuspended in RPMI (Gibco) supplemented with 0.1% BSA, 1mM EGTA (Sigma) and 5mM Mg^{2+} (Sigma). Cells were incubated with 5-10μg/ml of murine recombinant ICAM-1 Fc Chimera Protein (R&D Systems, Inc). To test the effect of Lovastatin on high affinity LFA-1, 100μM of Lovastatin was added prior to incubation with ICAM-1. Stainings were performed as described in the flow cytometry section.

2.3.5 ELISA

To analyze steady-state titers of IgG1 and IgG2c, MaxiSorp 96-well plates (ThermoFisher) were coated with goat anti-mouse Ig (Southern Biotech). Pre-diluted sera were added in duplicates (1:25 000 for IgG1 or 1:100 000 for IgG2c) and bound immunoglobulins were detected using alkaline phosphatase-conjugated goat anti-mouse IgG1 or IgG2c (Southern Biotech). After incubation with pNPP substrate (Southern Biotech), optical density (at 405 nM) was measured using the VMAX Kinetic ELISA Microplate Reader and data were analyzed using SoftMax Pro 4.7 software.

2.3.6 Genomic DNA preparation and PCR

Total $CD4^+$ T cells were isolated from lymph nodes of tamoxifen-treated *Roquin*$^{san/+}$; *Cd4-Cre*$^{ERT2+/-}$; *Bcl6*$^{+/+}$ or *Roquin*$^{san/+}$; *Cd4-Cre*$^{ERT2+/-}$; *Bcl6*$^{f/f}$ mice according to manufacturer's instructions (EasySEP ™ Mouse CD4+ T cell Isolation Kit, STEM Cell). Genomic DNA was prepared from CD4 cells and non-CD4 cells by Proteinase K digestion (4 hours, 55°C) followed by ethanol precipitation. The extracted DNA samples were quantified using a NanoDrop 2000 and approximately 10ng of DNA from each sample was used for PCR reaction. PCR amplification was performed at 94°C, 20 seconds - 58°C, 30 seconds - 72°C, 60 seconds (33 cycles), using RedTaq® ReadyMix PCR Mix (Millipore Sigma).

Primers for *Bcl6* alleles (a mixture of the following 3 primers; Fig. S2.5A):
primer 1, *5'- CCATTCTCAGAAGATTATGGCAGA-3'*;
primer 2, *5'- CACACTATACATCAGAAAAGAATG-3'*;
primer 3, *5'- GGCCACCTTATGACATAGGCAC-3'*,
Primers for wildtype *Sh2d1a*:
Sh2d1a forward, *5'- TCTGACATACAGTGAGCATC-3'*
Sh2d1a reverse, *5'-CTTGGACTGTCACAGTGGTGTAC-3'*.

2.3.7 Tumor monitoring and treatment

Tumors in cervical, axillary, brachial, and inguinal lymph nodes were palpated and monitored by *in vivo* ultrasound imaging (VEVO 770, Visual Sonics), using the RMV 707B scanhead. A minimum of 5 cross-sectional ultrasound images were taken and the largest diameter and cross-sectional surface area was chosen. Cre recombinase activity was initiated in tumor-bearing mice (6-13 months) when tumors reached ~5-12mm diameter; ~13-77mm^2 cross-sectional surface area. To induce Cre recombinase activity, oral gavage was performed for 5 consecutive days (200μg/gram of body weight per day in corn oil). Lovastatin was administered through intraperitoneal (i.p.) injections (2mg/kg, every other day for two weeks).

2.3.8 Immunohistochemistry and immunofluorescence on human AITL samples

Immunohistochemical staining of AITL patient biopsy samples was performed using antibodies against CD3 (DAKO, polyclonal, 1:500 dilution) and BCL6 (LEIKA, LN22, 1:80

dilution). Five-μm thick sections of formalin-fixed paraffin-embedded tissues were stained using Autostainer instruments (BOND-MAX, Leica Biosystems) according to manufacturer's instructions.

For immunofluorescence staining, paraffin-embedded tissue of human AITL or normal tonsillar samples were cut in 5-μm thick sections and stained with antibodies against CD4 (VENTANA, SP35, ready to use), BCL6 (Abcam, ab172610, 1:200), and DAPI (PerkinElmer, FP1490A, 1:2000). Human samples were obtained with informed consent at the Samsung Medical Center following protocols approved by the Samsung Medical Center Institutional Review Board in accordance with the Helsinki Declaration.

2.3.9 Statistical analysis

Data were analyzed using Prism 7.0 (GraphPad Software). When comparing two groups an unpaired *t* test was performed. When comparing three groups, a one-way ANOVA test was used. For time courses of tumor regression, a two-way ANOVA test was utilized. When comparing tumor incidence rates, a Fisher's exact test was used. A p value of < 0.05 was considered statistically significant. For all experiments p values are as follows: *$p<0.05$, **$p<0.01$, ***$p<0.001$, ****$p<0.0001$.

2.4 Results

2.4.1 Signs of elevated helper T cell activities in *Roquin*$^{san/+}$ tumor-bearing mice

A longitudinal study of AITL patient biopsy samples revealed that B cell follicles in tumor lymph nodes gradually disappear leading to a complete disruption of T-B boundaries (4, 18). This hallmark feature of AITL has been recapitulated in lymph node tumors spontaneously developing in *Roquin*$^{san/+}$ mice, which are 50-150 times increased in their cellularity as compared to normal lymph nodes (270). Similar to human AITL, rather than a disproportionate expansion of T cells, it is an expansion of B cells that contributes to most of the tumor mass (270). While it was presumed that this B cell expansion was driven by the hyperactive helper functions of neoplastic CD4$^+$ cells (270), the different B cell populations in *Roquin*$^{san/+}$ tumor-bearing mice during progression have not been well-characterized. Thus, we phenotyped B cell populations in

tumor-free, non-tumor, and tumor lymph nodes from *Roquin*$^{san/+}$ mice (6-13 months old) (Fig. 2.1A).

Consistent with mild spontaneous GC reactions, there was a greater frequency of GC B cells ($B220^{+}GL7^{hi}Fas^{+}$) in non-tumor compared to tumor-free lymph nodes (Fig. 2.1B-C). Interestingly, in tumors, the frequency of typical GC B cells was reduced as confirmed by flow cytometric analysis of $B220^{+}GL7^{hi}Fas^{+}$ (Fig. 2.1B-C) and $B220^{+}Bcl6^{+}Fas^{+}$ (Fig. S2.1B) populations. We reasoned that this could be due to a rapid transition of GC B cells into the plasma cell lineage, reflecting hyperactive helper T cell activities during tumor growth. Consistent with this, we observed an increase of $CD138^{+}B220^{int}$ plasmablasts in tumors (Fig. 2.1E and F). Furthermore, we found that $B220^{+}GL7^{hi}Fas^{+}$ cells in tumors had an increased subset of cells that express high levels of IRF4 and reduced Bcl6 (Fig. 2.1G-I), a population reported to be the immediate precursor of plasma cells (125, 380). The $B220^{+}GL7^{hi}Fas^{-}$ cells that accumulated in tumor lymph nodes were almost exclusively $IRF4^{hi}Bcl6^{-}$. We also confirmed that tumor-bearing mice have elevated IgG2c and IgG1 titers (Fig. S2.2A-B), consistent with previous data (270). This hypergammaglobulinemia is a shared feature between human AITL and our mouse model (6). Thus, tumor-bearing *Roquin*$^{san/+}$ mice have signs of ongoing T-B crosstalk within tumors despite a lack of conventional germinal centers.

2.4.2 Persistent activity of Bcl6 is required for tumor progression

When heterogeneous human AITL tumor cell populations were xenografted into immunodeficient mice, after repeated rounds of serial transplantation, putative neoplastic $CD4^{+}$ T cells persisted whereas $CD8^{+}$ T cells and B cells gradually disappeared (32). Importantly, the enriched T lineage cells were mostly $Bcl6^{+}$, suggesting that sustained expression of Bcl6 in $CD4^{+}$ tumor cells might be required for AITL tumor progression. Similar to this observation, we found that consecutive sections of AITL patient biopsy samples had comparable staining patterns for CD3 and Bcl6, likely signifying that Bcl6 is expressed in this T cell subset (Fig. 2.2A). To further confirm that Bcl6 is co-expressed within a $CD4^{+}$ T cell subset, we performed multi-color immunofluorescence imaging on human AITL samples. We observed predominant expression of Bcl6 in $CD4^{+}$ cells in AITL, whereas Bcl6 expression was restricted to non-$CD4^{+}$ cells, presumably B cells within the germinal center of human tonsils (Fig. S2.3A-B). In fact, Bcl6 positivity is now considered a reliable diagnostic tool, especially for AITL patients with bone

marrow involvement (19, 54). In *Roquin*$^{san/+}$ tumors, the conventional CD4^{+}CXCR5^{+}PD-1^{+} Tfh cell population was decreased with reduced PD-1 expression (Fig. 2.2B-D) (270). However, this difference was less pronounced when we gated on CD4^{+}CXCR5^{+}Bcl6^{+} cells (Fig. S2.4A-B) and high levels of Bcl6 in CD4^{+}CXCR5^{+}PD-1^{+} cells were maintained regardless of tumor status (Fig. 2.2E-F). Because this CD4^{+}CXCR5^{+}PD-1^{+} population expresses the highest levels of Bcl6 and is also highly proliferative (Fig. 2.2G), we suspect that these cells represent the neoplastic cells driving tumor growth by interacting with B cells. Based on these, we predicted that acute ablation of Bcl6 activity halts AITL-like tumor growth. To test this idea, we generated mice expressing a CD4-driven tamoxifen-inducible Cre recombinase and conditioned *Bcl6* genes in the *Roquin*$^{san/+}$ background (*Roquin*$^{san/+}$; *Cd4-Cre*$^{ERT2+/-}$; *Bcl6*$^{f/f}$) (Fig. 2.2H). Upon exposure to Cre recombinase activity, the conditioned *Bcl6* gene loses exons 7-9 (encoding zinc-finger domains) and thereby its capacity to drive GC B or Tfh cell differentiation (217, 384). We confirmed that our *Cd4-Cre*^{ERT2} system efficiently removed the floxed *Bcl6* DNA segment specifically in CD4-expressing cells (~73% efficiency) (Fig. S2.5A). Under the same conditions, the Bcl6 antibody (clone K112-91) detected intact levels of Bcl6 in Cre-experienced Tfh-like cells (Fig. S2.5B). It has been reported that loss of exons 8-9 from *Bcl6* results in a truncated protein with a mainly cytoplasmic localization pattern that cannot bind DNA (202). This, taken together with our observation, may suggest that in our model, the deleted *Bcl6* allele still produced a non-functional truncated version of Bcl6. Once these mice developed full-size tumors, we followed tumor growth by palpation and ultrasound imaging after tamoxifen administration. Notably, tamoxifen treatment alone in control tumor-bearing mice (*Roquin*$^{san/+}$; *Cd4-Cre*$^{ERT2+/-}$) reduced tumor size within the first week after treatment (Fig. 2.2I). This may be due to a general anti-cancer effect of tamoxifen, possibly mediated through several mechanisms such as induction of mitochondrial apoptosis, angiogenesis inhibition or suppression of cell proliferation (385). However, tumors grew back after the initial shrinkage at 2 weeks post-treatment. In contrast, *Roquin*$^{san/+}$; *Cd4-Cre*$^{ERT2+/-}$; *Bcl6*$^{f/f}$ showed continued tumor regression (Fig. 2.2I and J). Mice that showed tumor regression had no recurrence in primary or distal lymph nodes up to 12 weeks after tamoxifen treatment (Fig. 2.2I). Therefore, we conclude that persistent Bcl6 activity is indispensable for the continued growth of AITL-like tumors in *Roquin*$^{san/+}$ mice.

2.4.3 SAP is critical for tumor progression

Next, we sought to identify key mechanisms downstream of the Bcl6-dependent Tfh cell program that supports AITL-like tumor growth in *Roquin*$^{san/+}$ mice. As a master regulator of Tfh cell differentiation, Bcl6 has many direct or indirect target genes, ~50% of which are distinct from those identified in B cells (198, 199). Relevant to its role in Tfh cell differentiation, Bcl6 overexpression in human CD4$^+$ T cells led to upregulation of SAP, along with CXCR5 and PD-1 (237). SAP has been shown to be crucial for the formation of T-B conjugates during early and late stages of the GC reaction (119, 244). This is likely the reason why SAP deficiency drastically reduced tumor incidence in *Roquin*$^{san/+}$ mice (270). Consequently, we predicted that sustained expression of SAP is critical for AITL-like tumor growth. We found increased frequencies of SAP^{hi} cells among CD4$^+$ T cells (Fig. 2.3A) and Tfh-like cells from tumors in *Roquin*$^{san/+}$ mice, although we observed no differences in SAP MFI amongst Tfh-like cells (Fig 2.3B). Notably, SAP^{hi} CD4$^+$ T cells from tumors had more Ki-67$^+$ cells when compared to SAP^{hi} CD4$^+$ T cells from non-tumor or tumor-free lymph nodes (Fig. 2.3C). Within tumors, SAP^{hi} CD4$^+$ T cells were more proliferative than SAP^{lo} CD4$^+$ T cells (Fig. 2.3D). These results suggest that tumor cells require high levels of SAP expression for their growth. To directly test this idea, we generated *Roquin*$^{san/+}$; *Cd4-Cre*$^{ERT2+/-}$; *Sh2d1a*$^{f/f}$ *or Sh2d1a*$^{f/y}$ mice (the *Sh2d1a* gene is X-linked) (Fig. 2.3E). As expected, abrogation of SAP protein expression in CD4$^+$ T cells by tamoxifen administration (~90% efficiency) (Fig. S2.5E) led to durable tumor regression until 12 weeks post-treatment (Fig. 2.3F-G). Similar results were obtained when the *Sh2d1a* gene was deleted ubiquitously by using a *UBC-Cre*^{ERT2} system in growing tumors (Fig. S2.6). Despite similar tumor regression kinetics caused by abrogation of functional Bcl6 or SAP, the two signature Tfh cell proteins appear to have distinct roles in AITL-like tumor maintenance. First, acute disruption of Bcl6 gene function does not cause immediate loss of SAP protein (Fig. S2.5C). Second, Bcl6 disruption leads to a small but clear reduction of CXCR5 expression levels among Tfh-like cells without grossly affecting their total frequency (Fig. S2.5D). In contrast, abrogation of SAP expression leads to a clear 2-fold reduction in the percentage of Tfh-like cells without affecting CXCR5 levels (Fig. S2.5F).

2.4.4 Selective abrogation of SAP-Fyn signaling pathway does not greatly alter AITL-like disease

SAP promotes the production of cytokines such as IL-4 by activating Src family protein kinase, Fyn (383). When SAP-Fyn interactions were abrogated by the SAP-R78A point mutation, the ability of SAP to activate Fyn was abolished (383). However, this SAP-R78A mutant retained the ability to promote Tfh cell maturation and germinal center reactions (120, 245). Interestingly, a few Fyn mutations with disrupted auto-inhibitory mechanisms have been discovered in human AITL tumors, suggesting a positive role for Fyn kinase in AITL tumorigenesis (38, 44). Although SAP-deficient *Roquin*$^{san/+}$ mice had dramatically reduced tumor incidence – no tumors developed out of 16 mice monitored (270), the contributions of the SAP-Fyn signaling pathway to disease incidence and severity have not been evaluated. To address these questions, we generated cohorts of *Roquin*$^{san/+}$ mice possessing the *Sh2d1a*$^{+/y}$ or *Sh2d1a*$^{R78A/y}$ genotype. Although there was some trend toward reduced tumor incidence, a substantial portion (9/29) of SAP-R78A mutant mice still developed tumors (Fig. 2.4A). Also, there was no difference in the number and size of tumors. Furthermore, the percentages of $CD4^+CXCR5^+PD\text{-}1^+$ Tfh-like cells in tumors with wildtype or mutant SAP were similar (Fig. 2.4B). We observed no differences in Bcl6 levels but increased Ki-67^+ populations in SAP-R78A tumors, as compared to tumors with wildtype SAP (Fig. 2.4C). SAP-R78A tumors also recapitulated the phenotype of B cell populations found in SAP wildtype-containing tumors (Fig. 2.4D-E). Lastly, there was no difference in the adhesive capacities of $CD4^+$ T cells derived from the two groups of tumors as judged by an ICAM-1 binding assay (Fig. S2.7). These results indicate that SAP mostly utilizes Fyn-independent pathways such as T-B conjugation to promote AITL-like disease.

2.4.5 Evidence for LFA-1-dependent T-B crosstalk in AITL-like tumor progression

Since ongoing T-B crosstalk is evident in growing AITL-like tumors, we wanted to test for upregulation of adhesion molecules on $CD4^+$ and $B220^+$ cells in tumors. It has been reported that Tfh cells express high levels of LFA-1 and that disruption of LFA-1 activity severely compromises Tfh cell survival and GC reactions (118). Interestingly, using an ICAM-1 binding assay, we found that $CD4^+$ T cells from tumors had elevated levels of functional or high affinity LFA-1 compared to tumor-free *Roquin*$^{san/+}$ mice, whereas non-tumor $CD4^+$ T cells had

intermediate levels of active LFA-1 (Fig. 2.5A). Additionally, tumor samples contained B cells that expressed relatively higher levels of ICAM-1 compared to their counterparts in tumor-free mice although the differences in absolute MFI was not very strong (Fig 2.5B). This suggests that B cells in tumor-bearing mice have a better capacity to engage with T cells. Among B cell subsets, regardless of tumor progression, ICAM-1 levels were highest in $B220^{+}GL7^{hi}Fas^{+}$ GC B-like cells, the known partner of Tfh cells in germinal centers (Fig. 2.5C). Accordingly, we tested if repeated injection of LFA-1 blocking antibodies could reduce tumor size. However, we could not detect clear regression of AITL-like tumors. We reasoned that macromolecules such as antibodies may not be able to infiltrate tumor lymph nodes due to their highly disorganized lymph node architecture. Therefore, we decided to test small molecule inhibitors for LFA-1. A cholesterol-lowering drug, Lovastatin, has been reported to inhibit LFA-1 allosterically (386, 387). We validated this inhibitory effect of Lovastatin *in vitro* using Tfh cells isolated from Peyer's patches with minimal change to cell viability (Fig. 2.5D). Importantly, when we administered Lovastatin to tumor-bearing *Roquin*$^{san/+}$ mice, we observed a full regression (>60% reduction in area) or partial regression (25-60% reduction in area) in 6/13 tumors (Fig. 2.5E-F). However, the impact of Lovastatin on tumor growth may involve mechanisms other than LFA-1 inhibition such as alteration of cholesterol metabolism, warranting further study. Additionally, a caveat of this experimental design is that because we do not have a vehicle-treated control group, we cannot rule out the potential influence of drug diluent and/or animal handling. Since absence of SAP in murine natural killer (NK) cells diminished high affinity LFA-1 (388), we tested if acute loss of SAP expression could lead to a drastic disappearance of high affinity LFA-1 in $CD4^{+}$ T cells. However, both *in vitro* and *in vivo* tamoxifen-induced abrogation of SAP expression did not affect active LFA-1 levels (Fig. S2.8). Taken together, we showed that high affinity LFA-1 and ICAM-1 are more highly expressed in tumors as compared to tumor-free lymph nodes, suggesting that T-B crosstalk may occur with a higher probability in tumor-bearing mice. However, as inhibition of LFA-1 affinity resulted in an overall partial response, it is more probable that LFA-1-mediated crosstalk works in parallel with other adhesion and/or costimulatory molecules to support T-B interactions within tumor-bearing *Roquin*$^{san/+}$ mice.

Because ICOS is important for Tfh cell generation and function, specifically as a costimulatory signaling molecule involved in T-B crosstalk, it is another attractive candidate to study within the framework of AITL-like disease (35, 389). As such, in a similar manner to Bcl6

and SAP, we asked whether ICOS is also continually required to support AITL-like disease progression. To test this idea, we ubiquitously deleted the *Icos* gene from fully developed AITL-like tumors using the *UBC-Cre*^{ERT2} system. Unlike what we observed for Bcl6 and SAP, we found a heterogenous response where 2/6 mice experienced a full regression and 4/6 mice had overall no response 3 weeks post-gene deletion (Fig. S2.9). From this data, it is evident that ICOS does not have a unanimous impact on AITL-like tumor progression, and accordingly, supplementary experiments will need to be done in order to delineate differences between non-responder and responder *Roquin*$^{san/+}$ mice.

2.5 Discussion

We report evidence that CD4$^+$ and B220$^+$ cells in AITL-like tumors intimately influence each other and resemble Tfh-GC B cell interactions in physiological germinal centers. First, there is an accumulation of B220$^+$GL7^{hi} Fas$^+$ populations with signs of plasma cell commitment (Bcl6^{lo}IRF4^{hi}), a product of successful Tfh-GC B cell collaboration. Second, AITL-like tumor progression heavily relies on continued expression of Tfh cell lineage-defining transcription factor Bcl6, and high levels of SAP, a key element of T-B conjugation. In addition, CD4$^+$ T cells from tumor-bearing mice had increased active LFA-1, an adhesion molecule highly expressed on Tfh cells, as well as elevated levels of its binding partner ICAM-1 on B cells. Lastly, we found that tumor CD4$^+$ T cells can drive tumor growth without Fyn-mediated SAP signaling mechanisms, consistent with previous studies that T-B collaboration during germinal center reactions is SAP-Fyn independent.

It is intriguing that Bcl6 plays critical roles both in GC-derived T and B cell malignancies. Dysregulated Bcl6 expression is important in the development and progression of GC-derived B cell lymphomas (219, 231, 232, 390). In B cell lymphomas, the oncogenic effects of persistent Bcl6 is likely mediated by its ability to suppress cell cycle inhibitor p21 and p53 (232). In contrast, *BCL6* mutations have not been discovered in human AITL, but sustained expression of Bcl6 appears to be critical for maintaining malignant CD4$^+$ T cell populations in xenografted human AITL samples (32) and our mouse model. Considering that ~50% of Bcl6 target genes in Tfh cells are distinct from those regulated in GC B cells (198), Bcl6 may play different roles in T cell lymphoma generation and progression compared to B cell lymphomas.

The association between Bcl6 and SAP has been well-established in Tfh cells. Both in mouse and human Tfh cells, Bcl6 expression levels highly correlate with SAP levels and B cell helper functions (237, 242, 391). High levels of SAP in Tfh cells appear to promote T-B conjugation by inhibiting negative signals provided by SLAMF6 (246). Analogous to this, Bcl6-expressing Tfh-like cells in tumor lymph nodes had higher levels of SAP expression along with an expansion of B cells progressing into the plasma cell lineage. However, we found that acute disruption of Bcl6 activity does not lead to a drastic change in SAP expression level in $CD4^+$ T cells. Since tumor regression becomes evident 2 weeks after tamoxifen treatment, we predict that these differences may be greater at later stages. However, we have not pursued this possibility as newly generated T cells from the thymus may complicate the interpretation. Despite this, our data suggest that SAP is not an immediate downstream component of Bcl6. Further mechanistic studies are required to identify proximal components of Bcl6-regulated genes relevant to AITL tumor progression.

There have been a handful of human AITL patients reported with somatic mutations in the *FYN* gene. These Fyn mutations disrupt auto-inhibitory mechanisms and suggest that hyperactive Fyn could drive AITL tumor initiation and progression. Previous work has shown that *Roquin*$^{san/+}$ mice cannot develop tumors in SAP-deficient mice (270). However, specific roles for SAP-Fyn signaling in AITL-like tumor incidence and progression have not been clarified. In this study, we could not find clear differences in tumor incidence rates, severity, or characteristics, indicating that SAP-Fyn signaling has a very limited role in tumorigenesis and maintenance. Although it remains possible that persistently hyperactive Fyn activity through other upstream signals (such as TCR) may drive tumor progression, it is not the main mechanism of how SAP drives AITL-like disease in our mouse model.

Although we demonstrated that key Tfh cell proteins Bcl6 and SAP are continually important to maintain AITL-like disease in *Roquin*$^{san/+}$ mice, we observed that loss of ICOS in fully developed AITL-like tumors led to a heterogenous response where only one-third of mice experienced full tumor regression (>50% reduction in tumor area). One simple explanation to contextualize the differences observed between Bcl6/SAP and ICOS gene deletion is that certain tumors may depend less on ICOS-related signaling pathways and may instead co-opt other costimulatory pathways to support their growth. However, another explanation could be that loss of ICOS may cause Treg cell populations to be less immunosuppressive as observed in

Roquin$^{san/san}$ mice bred with *Icos*$^{-/-}$ mice, which led to increased splenic cellularity and effector T cell expansion, a phenomenon which did not occur with *Roquin*$^{san/san}$ mice bred with *Sh2d1a*$^{-/-}$ or *Bcl6*$^{+/-}$ mice (234, 373). The different outcomes observed in Bcl6/SAP versus ICOS deletion is interesting because Bcl6, SAP and ICOS are all reported to be critical mediators of Tfh cell generation and function (34, 35). Likewise, Bcl6, SAP and ICOS are also reported to impact Tfr cell formation, however, only ICOS has been strongly implicated in supporting Treg cell identity, suppressive abilities, survival and proliferation (389, 392-395). As such, ICOS may have a greater influence on certain important aspects of Tfr cell functionality that mirrors Treg cells as compared to Bcl6 or SAP. Consequently, when selecting candidates for pharmacological inhibition of T-B communication, it is important to consider the impact of these signaling molecules on other immune cell subsets to avoid selecting agents which may cause an undesired outcome, such as a worsened disease course for AITL patients.

Within solid tumors, Treg cells are considered potent suppressors of antitumor responses, for instance, by preventing proper immunosurveillance mechanisms (396). In GCs, Treg and Tfr cells are also reported to suppress Tfh and GC B cell activities, particularly in the context of autoimmune and allergic responses (397-399). Foxp3^{+} cells have been identified in human AITL, but how they might contribute to tumor progression has not been studied (273, 274). On the one hand they could promote tumor growth by suppressing immune surveillance mechanisms or conversely, counter tumor progression by inhibiting Tfh-like tumor cell activity. Treg/Tfr cells could also contribute to disease symptoms, such as autoantibody production which can be observed in clinical laboratory tests for certain AITL patients (11), especially if Treg/Tfr cells are also abnormal due to mutations in RHOA, epigenetic modifiers or TCR signaling components. The overall impact of combined TET2 and RHOA-G17V mutations on Treg/Tfr cells is also uncertain. Mice with inducible CD4-specific expression of *Rhoa*^{G17V} are reported to have increased Treg and Tfr cells (45), while loss of Tet2/3 from Foxp3^{+} Treg cells has been demonstrated to promote an effector phenotype with an increased gene expression profile relating to Tfh and Th17 cells (400). Taken together, their combined impact could be increased Treg/Tfr cells which have a proinflammatory Tfh-like phenotype that may directly or indirectly be involved in AITL pathogenesis.

There are several mouse models of AITL that have provided insights into the pathogenesis of human AITL. An early study using transplantation of human AITL cells into

immunodeficient mice confirmed that neoplastic $CD4^+$ T cells express high levels of Bcl6 (32). Studies using genetically engineered mouse models confirmed the relevance of the most prevalent somatic mutations discovered in human AITL. Approximately 60-70% of human AITL patients present with a recurrent *RHOA*^{G17V} mutation, often associated with loss-of-function mutations in *TET2* (36, 38, 44, 45). Several recent mouse models support a two-hit model of AITL tumorigenesis which requires both TET2 deficiency and expression of RHOA-G17V. Loss of TET2 in hematopoietic progenitor cells is shown to predispose mice to both lymphoid and myeloid malignancies but an additional *Rhoa*^{G17V} mutation in T cells is required to initiate Tfh cell-driven lymphomas (45-47, 55). These studies also showed that combining TET2 deficiency with the RHOA-G17V mutation synergistically elevates Tfh cell differentiation, as well as PI3K-mTORC1 and TCR signaling pathways, which leads to AITL-like disease. While spleen and swollen lymph nodes (<2mm in diameter) in these mouse models share histological features with human AITL, they do not phenocopy the hypergammaglobulinemia and palpable lymphadenopathy seen in human patients. In contrast, *Roquin*$^{san/+}$ mice give rise to easily detectable tumors with most of the pathological features of human AITL. The gross change in the size of tumor lymph nodes provides a unique opportunity to test the impact of gene deletion or drug treatment in a preclinical setting. Despite these advantages, it should be noted that *ROQUIN1* gene mutations have not been detected in human AITL (376). Also, it remains unclear whether T cells in *Roquin*$^{san/+}$ mice transform into tumor cells due to elevated TCR or cytokine signaling as is often shown in peripheral T cell lymphomas (44, 401). Therefore, our findings made in *Roquin*$^{san/+}$ mice need to be further validated in more relevant disease models. In this context, patient-derived xenograft models using human AITL cell lines with defined causative mutations may provide further insights (94, 335).

In summary, our data suggest that ongoing T-B crosstalk is a driving force for the progression of Tfh cell-derived T cell lymphomas. Importantly, this may apply not only to AITL but other PTCLs with features of Tfh cell origin. Therefore, we propose that future therapies for AITL should focus on T cell signaling components which mediate T-B interactions.

2.6 Acknowledgement

We thank Dr. C. Vinuesa (Australian National University, Australia) for *Roquin*$^{san/+}$ mice; Dr. T. Takemori (RIKEN, Japan) for Bcl6 conditional knockout mice; Dr. I. King (McGill University, Canada) for assistance with ICAM-1 binding assay. We also thank the IRCM Flow Cytometry Core Facility and IRCM Animal Facilities for their service. This work was supported by operating grants from Cancer Research Society (W.-K. S.) and Canadian Institutes of Health Research (MT-14429, MOP-82906, FDN-143338 to A.V.). A.V. holds the Canada Research Chair on Signaling in the Immune System. M.W. and J.L. received CIHR Master's Awards; M.W. and V.P. received FRQS Doctoral Scholarships.

2.7 Author contribution and conflict-of-interest statements

Contributions: W.-K.S. conceptualized the study; M.W., J.C., M.-C.Z., Y.B., V.P., J.L., T.B., A.V. developed experimental tools; M.W. performed all flow cytometric, PCR and ELISA experiments as well as tumor monitoring and ultrasound imaging studies; Y.B. designed primers to detect the Cre-excised floxed *Bcl6* allele; S.J.K., W.S.K., and Y.H.K contributed human AITL immunohistochemistry and immunofluorescence experiments; M.W. and W.-K.S. analyzed the data; M.W. and W.-K.S. prepared the figures; M.W. and W.-K.S. wrote the manuscript with input from J.C., Y.B., V.P., J.L., T.B., M.-C.Z., A.V., S.J.K., W.S.K., and Y.H.K. All authors approved the final version of the manuscript.

Conflict-of-interest disclosure: A.V. receives a contract from Bristol Myers-Squibb to study the mechanism of action of anti-SLAMF7 monoclonal antibody elotuzumab in multiple myeloma. The authors have no additional financial interests.

2.8 Footnote

A modified version of Chapter 2 has been published in *Blood Advances* (402).

2.9 Figures and figure legends

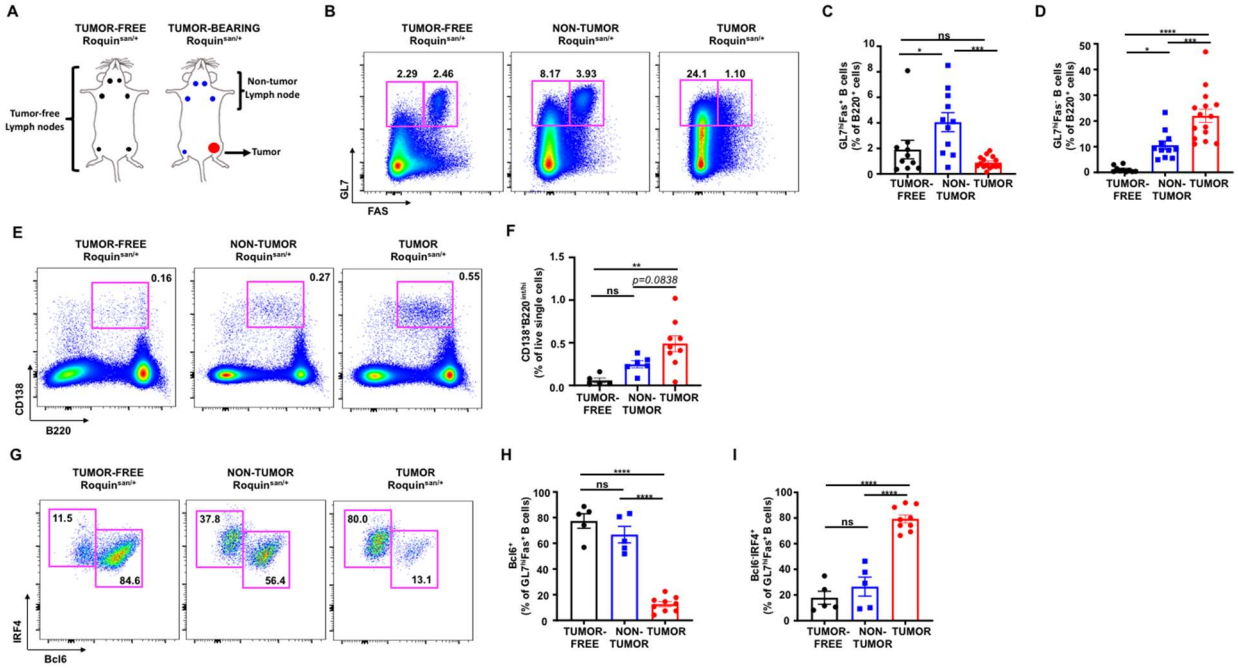

Figure 2.1 An increase of plasmablasts in tumor lymph nodes of *Roquin*$^{san/+}$ mice

(A) Pictogram illustrating differences between tumor-free and tumor-bearing mice as well as pictorial explanation of tumor-free, non-tumor and tumor lymph nodes. (B-D) Representative flow cytometric analyses and frequencies of B cell populations using surface markers Fas and GL7 (n=10 tumor-free; n=11 non-tumor; n=15 tumor samples). (E) Representative flow cytometry plots and histograms comparing frequency of plasmablasts (n=5 tumor-free; n=6 non-tumor; n=9 tumor samples). (G-I) Expression profile of Bcl6 and IRF4 in GL7^{hi}Fas^{+} B cells as depicted through representative flow cytometry plots and frequencies (n=5 tumor-free; n=5 non-tumor; n=9 tumor samples). Error bars in C, D, F, H and I represent SEM. Data are pooled from at least 2 independent experiments.

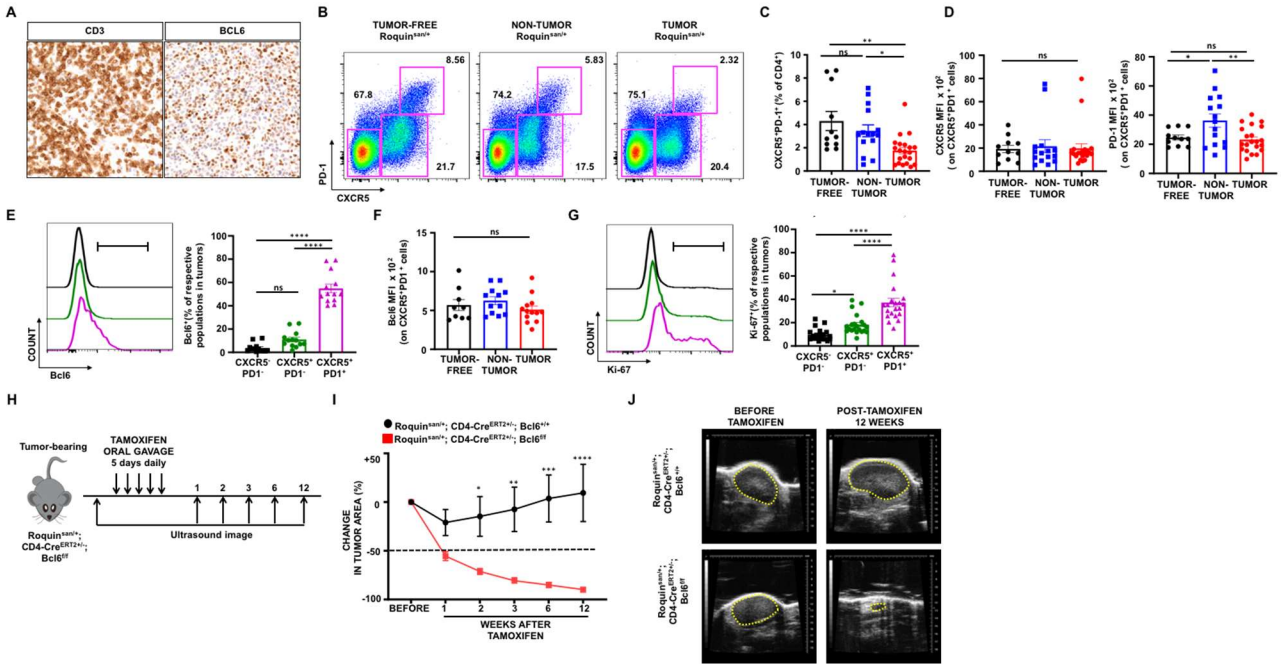

Figure 2.2 Disruption of functional *Bcl6* gene in growing AITL-like tumors leads to tumor regression

(A) Exemplary immunohistochemistry sections of human AITL patient samples depicting CD3 and Bcl6 expression. (B) Representative flow cytometric plots showing subsets of CD4 cells based on expression of PD-1 and CXCR5. (C) Comparing frequencies of $CD4^+CXCR5^+PD\text{-}1^+$ cells between tumor-free, non-tumor and tumor samples (n=11 tumor-free; n=15 non-tumor; n=21 tumor). (D) Median fluorescence intensity (MFI) of CXCR5 and PD-1 on $CD4^+CXCR5^+PD\text{-}1^+$ cells (n=11 tumor-free; n=15 non-tumor; n=21 tumor). (E) Bcl6 expression in $CXCR5^-PD1^-$, $CXCR5^+PD\text{-}1^-$ and $CXCR5^+PD\text{-}1^+$ cells from tumor samples and Bcl6 MFI of $CD4^+CXCR5^+PD\text{-}1^+$ cells (F) (n=9 tumor-free; n=12 non-tumor; n=13 tumor). (G) Representative histogram and frequency of Ki-67 levels in tumor $CD4^+$ subsets (n=21 tumor). (H) *Roquin*$^{san/+}$ mice were bred with a CD4-specific tamoxifen-inducible Cre recombinase to target the *Bcl6* gene (*Roquin*$^{san/+}$; *Cd4-Cre*$^{ERT2+/-}$; *Bcl6*$^{f/f}$). (I-J) Representative ultrasound images and time course demonstrating tumor regression in mice with *Bcl6* gene deletion. (n=5 *Roquin*$^{san/+}$; *Cd4-Cre*$^{ERT2+/-}$; *Bcl6*$^{+/+}$; n=6 *Roquin*$^{san/+}$; *Cd4-Cre*$^{ERT2+/-}$; *Bcl6*$^{f/f}$). Error bars in C, D, E, F, G and I represent SEM. Data are pooled from at least 2 independent experiments.

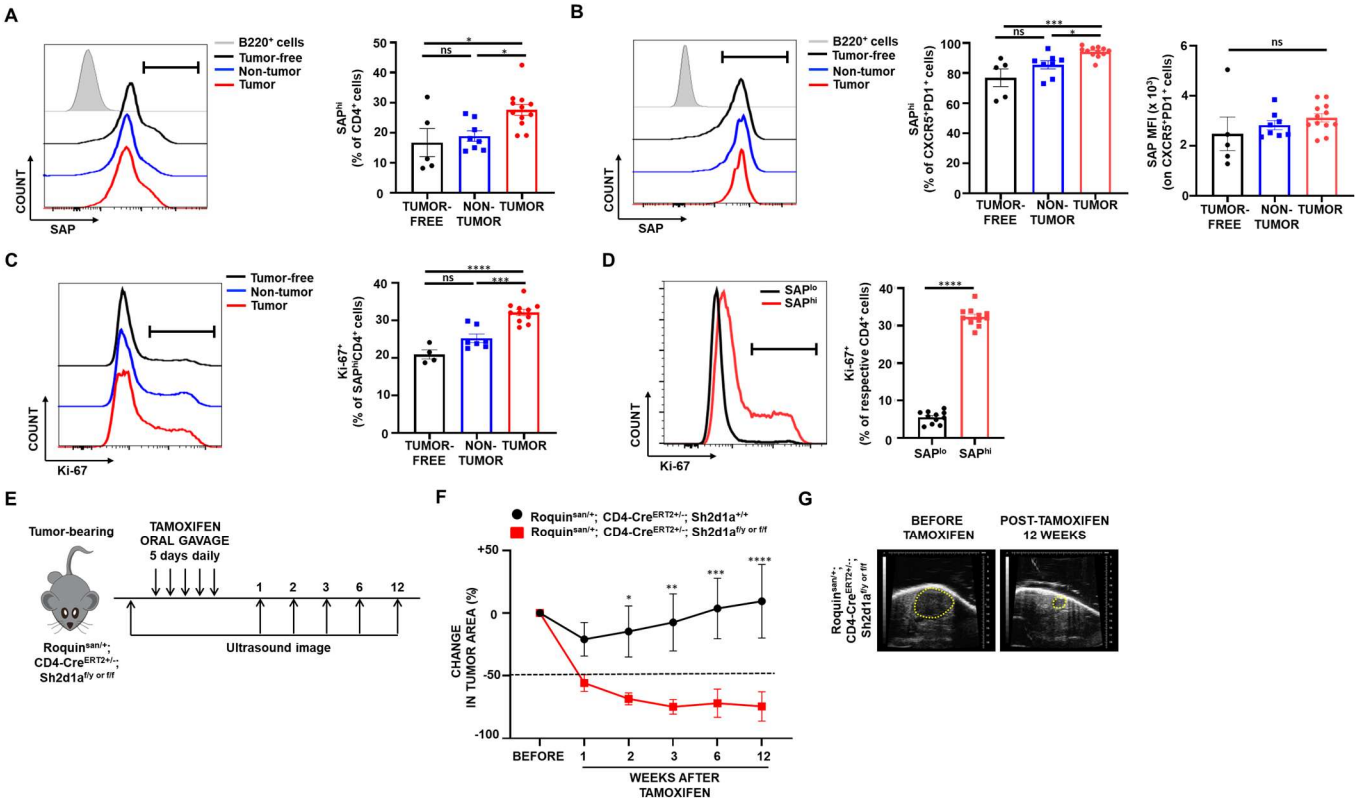

Figure 2.3 Abrogation of SAP expression from AITL-like tumors leads to tumor regression

(A) Increased expression of SLAM adaptor protein, SAP in CD4 cells from AITL-like tumors (n=5 tumor-free; n=8 non-tumor; n=12 tumor samples). (B) Frequency and median fluorescence intensity (MFI) of SAP in $CXCR5^{+}PD\text{-}1^{+}$ cells from tumor-free, non-tumor and tumor samples (n=5 tumor-free; n=8 non-tumor; n=12 tumor). (C) SAP^{hi} CD4 cells from tumors are more proliferative, as depicted through increased frequencies of $Ki\text{-}67^{+}$ cells (n=4 tumor-free; n=7 non-tumor; n=11 tumor samples). (D) SAP^{hi} $CD4^{+}$ tumor cells are more proliferative than SAP^{lo} as shown in representative histogram and frequencies. (E) *Roquin*$^{san/+}$ mice were bred with a CD4-specific tamoxifen-inducible Cre recombinase and conditional *Sh2d1a* allele (*Roquin*$^{san/+}$; *Cd4-Cre*$^{ERT2+/-}$; *Sh2d1a*$^{f/y\ or\ f/f}$). Representative ultrasound images and time course (F, G respectively) demonstrating tumor regression in mice with CD4-specific abrogation of SAP (n=5 *Roquin*$^{san/+}$; *Cd4-Cre*$^{ERT2+/-}$; *Sh2d1a*$^{+/+}$; n=9 *Roquin*$^{san/+}$; *Cd4-Cre*$^{ERT2+/-}$; *Sh2d1a*$^{f/y\ or\ f/f}$). In F, we reused CD4-Cre$^{ERT2+/-}$ control data shown in Figure 2.2I to perform statistical analysis for different time points. Error bars in A, B, C, D, and F represent SEM. Data are pooled from at least 2 independent experiments.

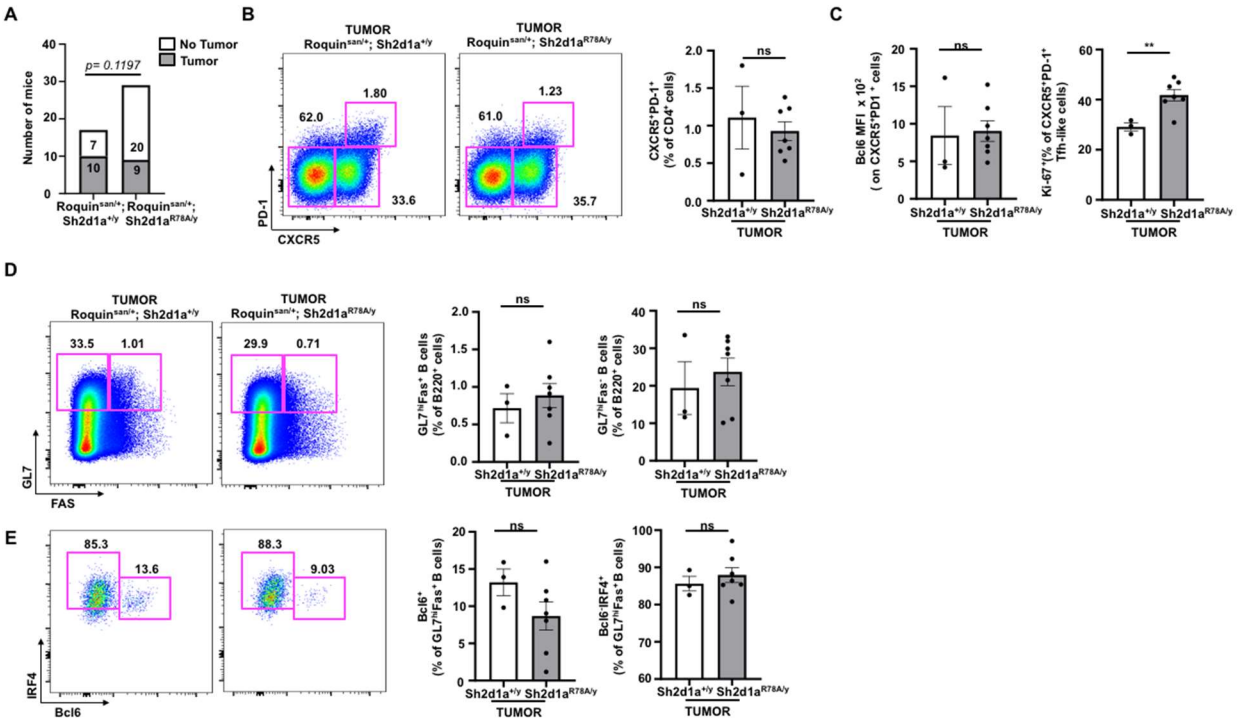

Figure 2.4 Loss of SAP-Fyn signaling pathway does not greatly alter AITL-like disease

(A) Abrogation of downstream signaling between SAP and Fyn kinase does not prevent tumor incidence but may have a partial effect (n=17 *Roquin*$^{san/+}$; *Sh2d1a*$^{+/y}$; n=29 *Roquin*$^{san/+}$; *Sh2d1a*$^{R78A/y}$). (B-E) Tumors from *Roquin*$^{san/+}$; *Sh2d1a*$^{+/y}$ or *Roquin*$^{san/+}$; *Sh2d1a*$^{R78A/y}$ show comparable T and B cell expression patterns and frequencies. (n=3 *Roquin*$^{san/+}$; *Sh2d1a*$^{+/y}$ tumors; n=7 *Roquin*$^{san/+}$; *Sh2d1a*$^{R78A/y}$ tumors). Error bars in B, C, D and E represent SEM. Data are pooled from at least 2 independent experiments.

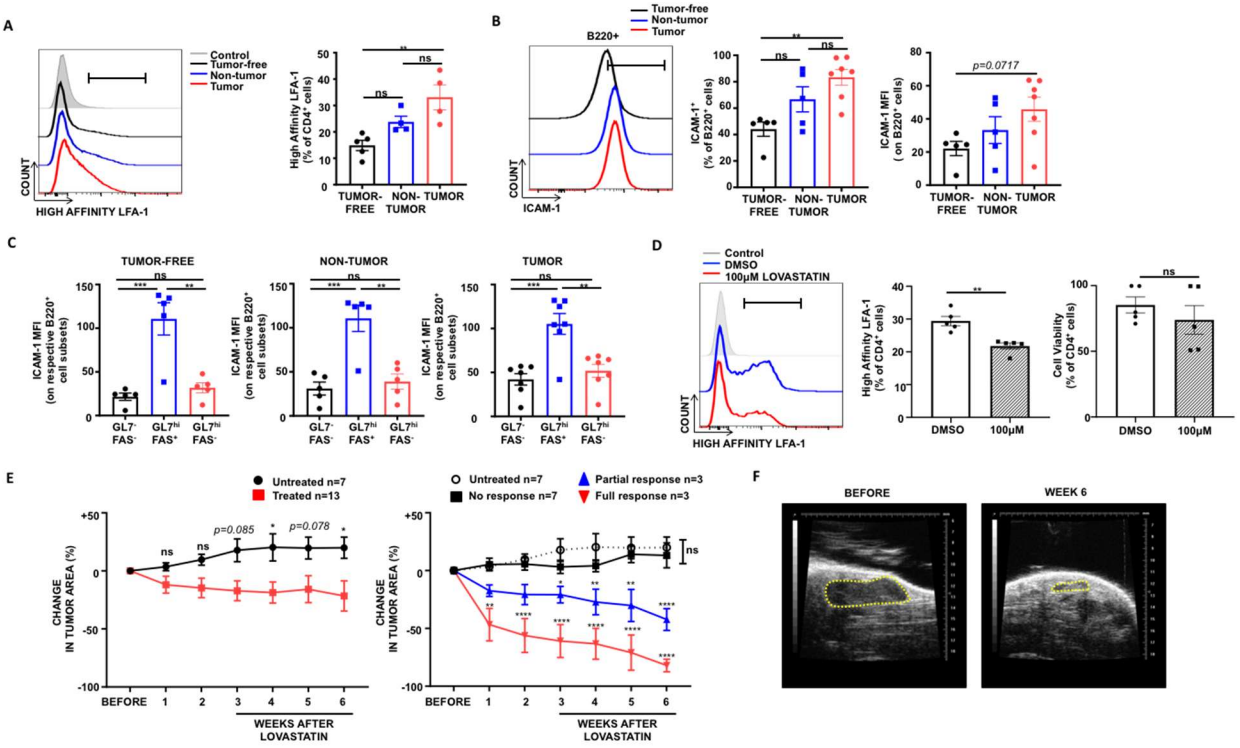

Figure 2.5 Elevated high affinity LFA-1 and ICAM-1 levels in *Roquin*$^{san/+}$ tumors

(A) Tumor samples have increased frequency of high affinity LFA-1. Representative flow cytometric analyses and frequency of high affinity LFA-1 expression on CD4$^+$ cells from recombinant ICAM-1 binding assay (10μg/ml of murine recombinant ICAM-1) (n=5 tumor-free; n=4 non-tumor; n=4 tumor samples). (B) Concomitant increased expression of ICAM-1 on B220$^+$ cells in *Roquin*$^{san/+}$ tumors as shown in representative flow cytometric analyses and frequencies. (B-C) Median fluorescence intensity (MFI) of ICAM-1 on B cell subsets (n=5 tumor-free; n=5 non-tumor; n=7 tumors). (D) Incubating wildtype Peyer's patch cells with Lovastatin during ICAM-1 binding assay verifies reduction in high affinity LFA-1 levels on CD4$^+$ T cells with minimal differences in cell viability (n=5 wildtype). (E) Left graph shows a time course of change in tumor size after treatment with Lovastatin (2mg/kg, i.p., every other day for 2 weeks) compared to the untreated control group (n=7 untreated; n=13 treated). Lovastatin treated mice were further sub-grouped based on the following criteria: no response (<25% reduction in area or growth), partial response (25-60% reduction in area) or full response (>60% reduction in area) at the final time point (week 6). The right graph further compares each response type with the untreated control group (n=7 untreated; n=7 no response; n=3 partial response; n=3 full response). (F) Exemplary regressed tumor is shown through ultrasound imaging. Error bars in A-E represent SEM. Data are pooled from at least 2 independent experiments.

2.10 Supplemental figures and figure legends

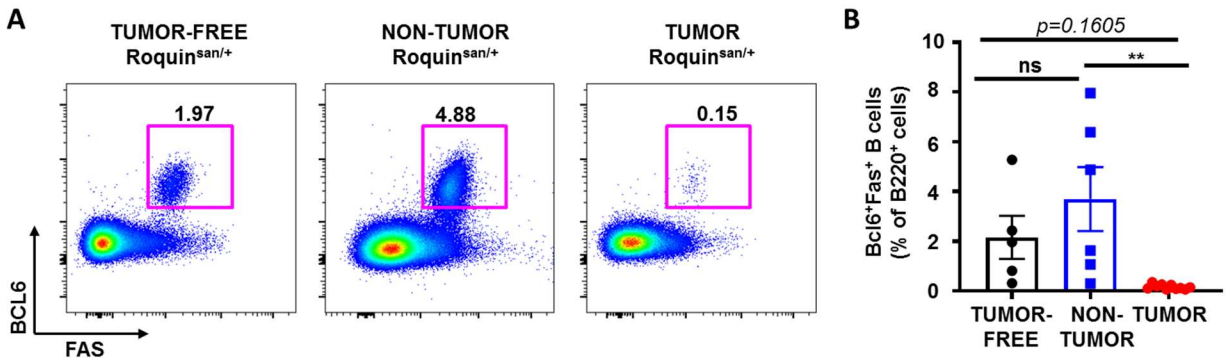

Figure S 2.1 Reduced Bcl6$^+$Fas$^+$ GC B-like cells in tumor samples

Representative flow cytometric plots for tumor-free, non-tumor and tumor lymph node samples of Bcl6$^+$Fas$^+$ B cell populations (A) and their quantification (B). (n=5 tumor-free; n=6 non-tumor; n=10 tumor samples) Errors bars in B are SEM. Data are pooled from at least 2 independent experiments.

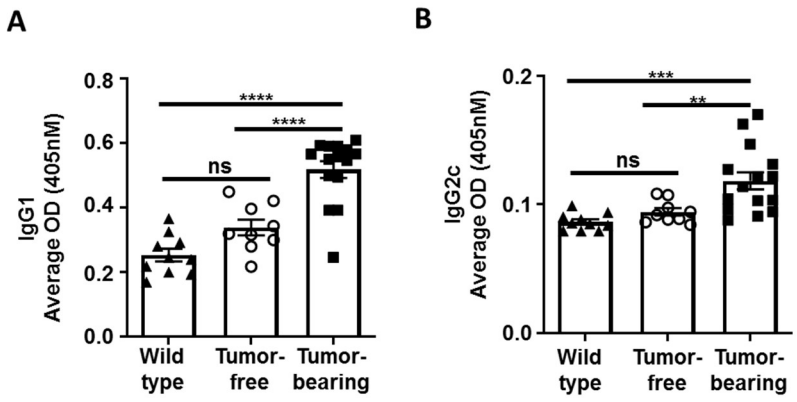

Figure S 2.2 Hypergammaglobulinemia in tumor-bearing mice

Steady-state levels of IgG1 and IgG2c were measured by ELISA using serum samples from wildtype, tumor-free or tumor-bearing mice. Each dot represents one mouse. (n=10 wildtype; n=9 tumor-free; n=15 tumor-bearing mice). Errors bars in A and B are SEM.

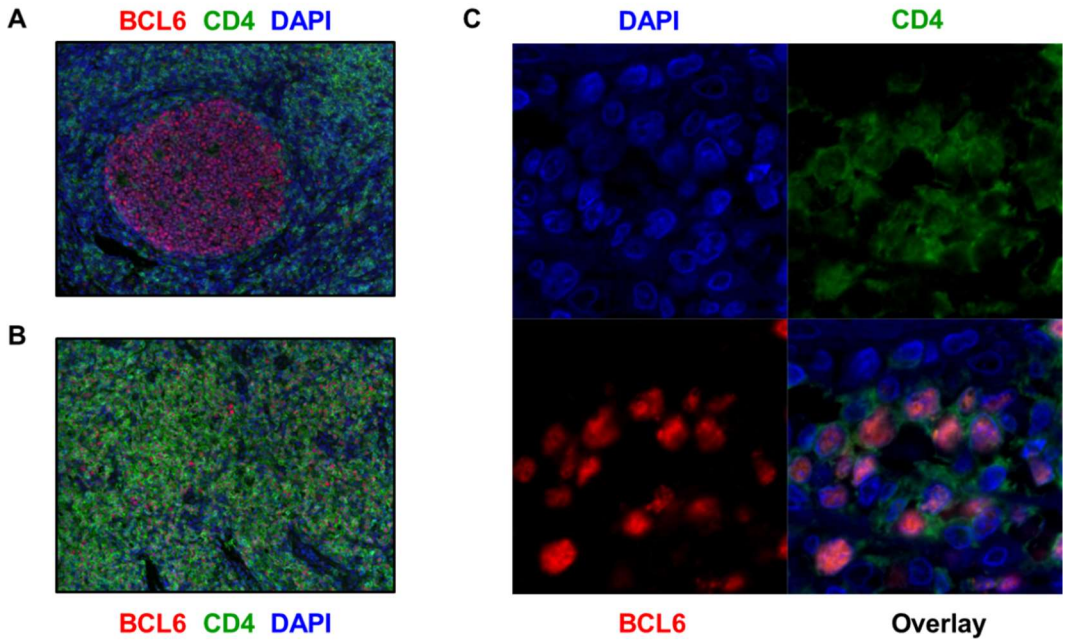

Figure S 2.3 Bcl6 is predominantly expressed in CD4$^+$ cells in human AITL

Immunofluorescence staining of a germinal center within a normal lymphoid follicle (A) and AITL (B). Sections were stained with antibodies against BCL6 (red), CD4 (green) and DAPI (blue). Original magnifications are 100X (A and B) or 400X (C).

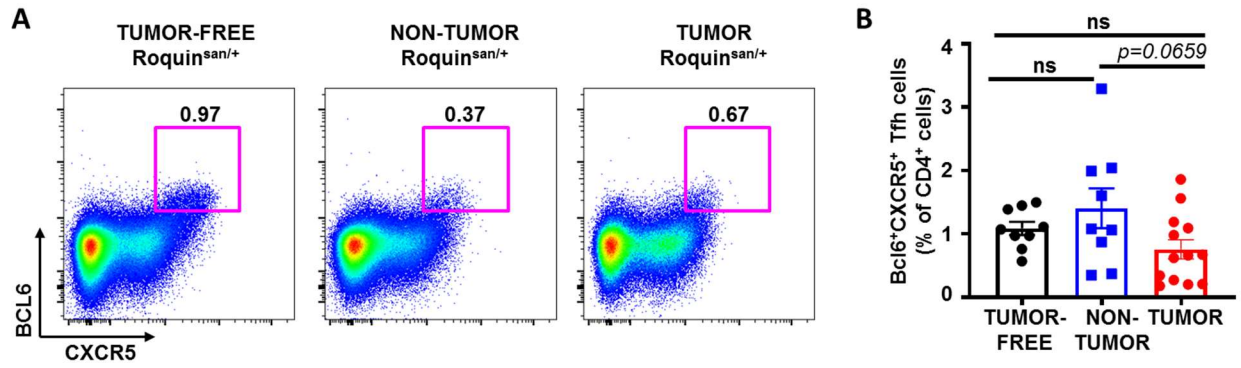

Figure S 2.4 Similar frequencies of Bcl6$^+$CXCR5$^+$ Tfh-like cells regardless of tumor progression

Representative flow cytometric plots for tumor-free, non-tumor and tumor lymph node samples of Bcl6$^+$CXCR5$^+$ CD4 T cell populations (A) and their quantification (B). (n=9 tumor-free; n=9 non-tumor; n=13 tumor samples) Errors bars in B are SEM. Data are pooled from at least 2 independent experiments.

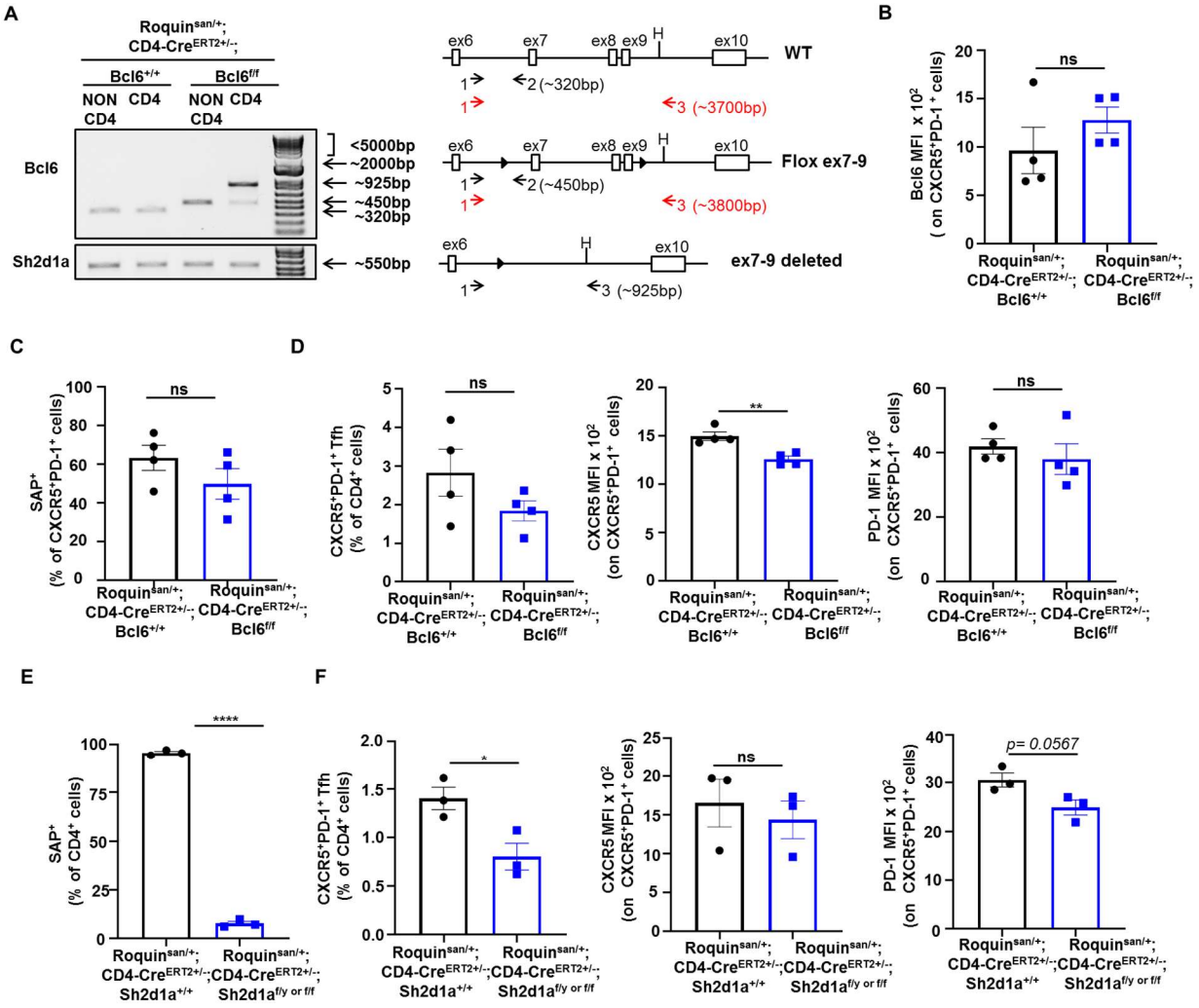

Figure S 2.5 Efficient disruption of conditioned genes in *Cd4-Cre^{ERT2}* system

(A-D) *Roquin$^{san/+}$*; *Cd4-Cre$^{ERT2+/-}$*; *Bcl6$^{f/f}$* or *Roquin$^{san/+}$*; *Cd4-Cre$^{ERT2+/-}$*; *Bcl6$^{+/+}$* mice were treated with tamoxifen for 5 days and lymph nodes were analyzed 24 hours after the last dose of tamoxifen. (A) (Left) Semi-quantitative PCR analysis indicating predominant deletion of *Bcl6* ex7-9 in a CD4-specific manner. (Right) Schematics of wildtype (WT), conditional (Flox ex7-9) and Cre-experienced conditional allele of *Bcl6* (ex7-9 deleted) along with primer sets and expected sizes of PCR products. Note that primer 1 and 3 will amplify PCR products only from the "ex7-9 deleted" allele (in black) but not from the "WT" or "Flox ex7-9" locus (in red) under our PCR condition (60 second elongation) due to size differences. Control primers detect wildtype *Sh2d1a* gene that are equal in all the samples. (B) Median fluorescence intensity (MFI) of Bcl6 on CXCR5^{+}PD-1^{+} Tfh cells. (C) Frequency of SAP-expressing Tfh cells followed by (D) frequency of Tfh cells as well as CXCR5 and PD-1 MFI on CXCR5^{+}PD-1^{+} Tfh cells. For flow cytometry n=4 tumor-free mice per genotype. For PCR n=3 samples per genotype. (E-F) *Roquin$^{san/+}$*; *Cd4-Cre$^{ERT2+/-}$*; *Sh2d1a$^{f/f\ or\ f/y}$* or *Roquin$^{san/+}$*; *Cd4-Cre$^{ERT2+/-}$*; *Sh2d1a$^{+/+}$* tumor-free mice were treated with tamoxifen for 5 days and lymph nodes were analyzed 48 hours after last dose of tamoxifen. (E) Efficient loss of SAP protein in CD4^{+} T cells after tamoxifen treatment. (F) Frequency of CXCR5^{+}PD-1^{+} Tfh cells and MFI of CXCR5 and PD-1 on CXCR5^{+}PD-1^{+} Tfh

cells (n=3 tumor-free mice per genotype). Errors bars in B-F are SEM. Data are pooled from at least 2 independent experiments.

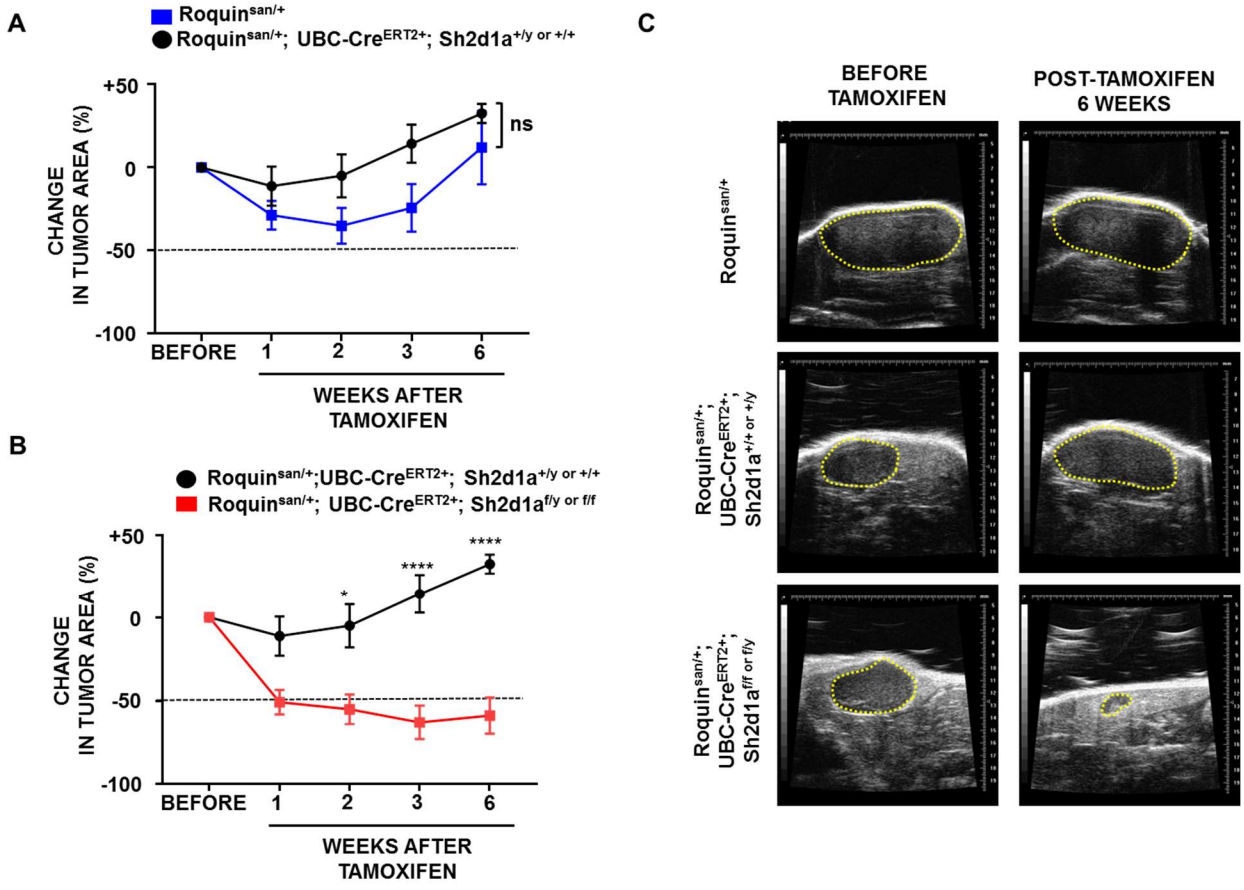

Figure S 2.6 Ubiquitous *Sh2d1a* gene deletion in tumor-bearing mice leads to tumor regression

Changes in tumor area shown over time for tamoxifen versus *UBC-Cre*$^{ERT2+}$ controls (A) and *UBC-Cre*$^{ERT2+}$ controls versus ubiquitous SAP gene deletion (B). The same *UBC-Cre*$^{ERT2+}$ controls are shown in both A and B (n=5 tamoxifen control; n=3 *Roquin*$^{san/+}$; *UBC-Cre*$^{ERT2+}$; *Sh2d1a*$^{+/y\ or\ +/+}$; n=9 Roquin$^{san/+}$; *UBC-Cre*$^{ERT2+}$; *Sh2d1a*$^{f/y\ or\ f/f}$). Representative ultrasound images are shown for each condition (C). Errors bars in A and B are SEM. Data are pooled from at least 2 independent experiments.

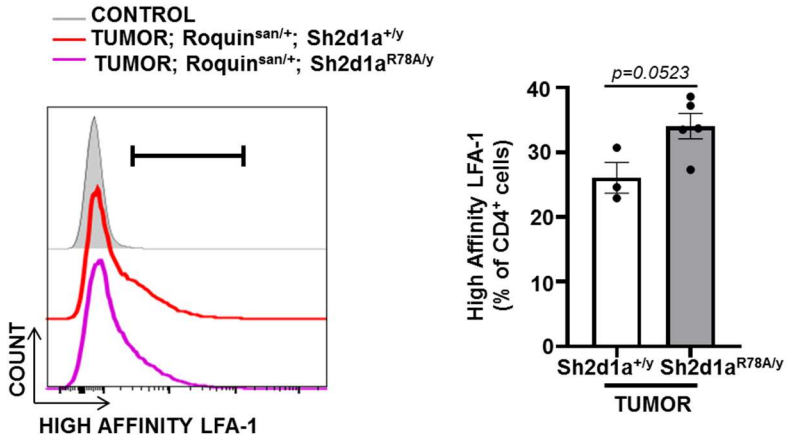

Figure S 2.7 Disruption of SAP-Fyn signaling in AITL-like tumors does not impact affinity of LFA-1

Representative histogram and frequency of high affinity LFA-1 in tumors from wildtype SAP or mutant SAP (n=3 wildtype SAP; n=5 mutant SAP). Errors bars are SEM. Data are pooled from at least 2 independent experiments.

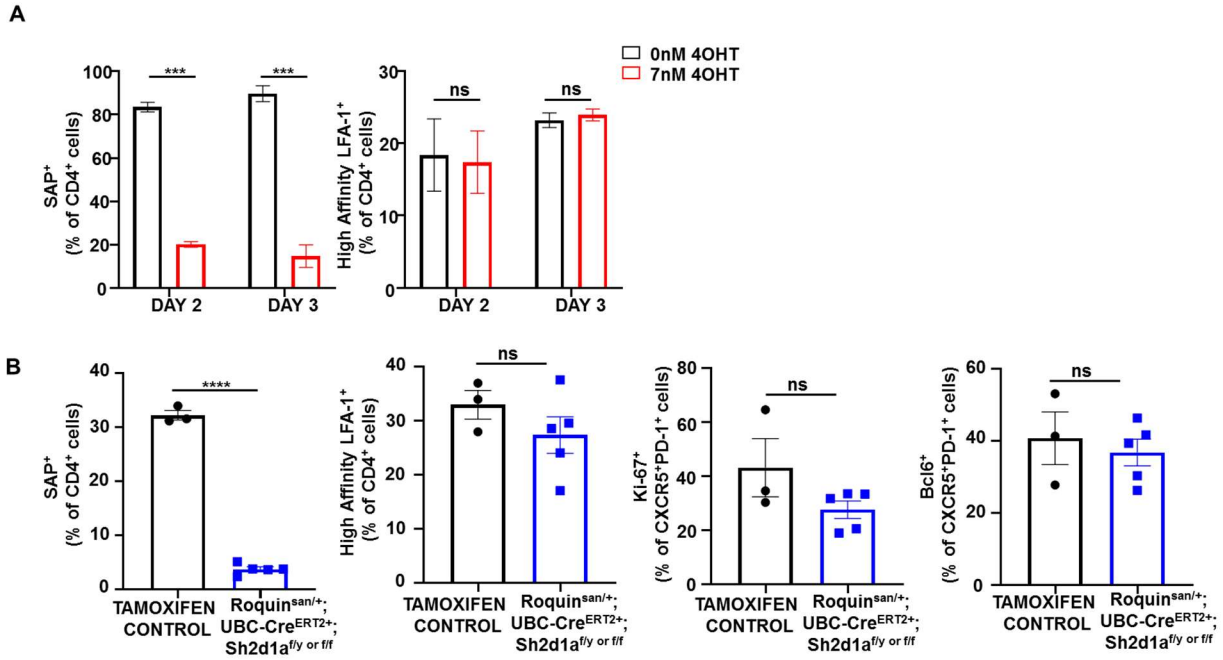

Figure S 2.8 Loss of SAP protein does not impact levels of high affinity LFA-1, Ki-67 and Bcl6

(A) Total lymph node cells from tumor-free *Roquin*$^{san/+}$ mice were incubated with soluble anti-CD3e in the absence or presence of 4-hydroxytamoxifen and analyzed for SAP and high affinity LFA-1 expression on day 2 or 3. (For day 2 n=4 tumor-free mice; for day 3 n=3 tumor-free mice) (B) *Roquin*$^{san/+}$; *UBC-Cre*$^{ERT2+}$; *Sh2d1a*$^{f/y\ or\ f/f}$ tumor-bearing mice were treated with tamoxifen for 3 days and analyzed 3 weeks after finishing tamoxifen regimen. Flow cytometric analysis

confirm low levels of SAP protein after gene deletion but no change in high affinity LFA-1, Ki-67 or Bcl6 expression levels (n=3 tamoxifen control tumors; n=5 *Roquin*$^{san/+}$; *UBC-Cre*$^{ERT2+}$; *Sh2d1a*$^{f/y\ or\ f/f}$ tumors). Errors bars in A and B are SEM. Data are pooled from at least 2 independent experiments.

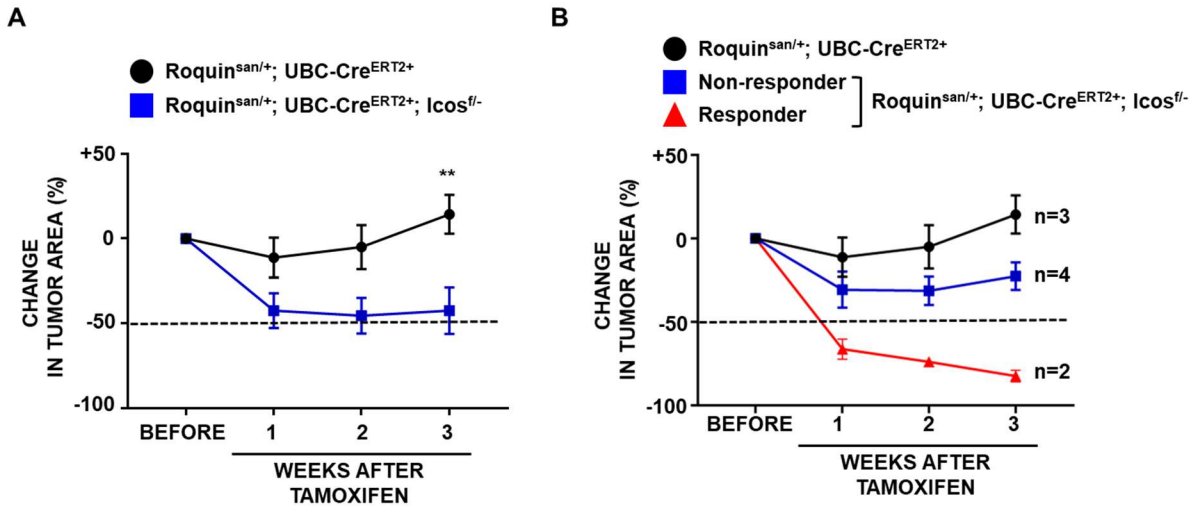

Figure S 2.9 Ubiquitous *Icos* deletion in tumor-bearing mice leads to heterogenous response

(A) Changes in tumor area shown over time for *UBC-Cre*$^{ERT2+}$ controls versus ubiquitous ICOS gene deletion. *UBC-Cre*$^{ERT2+}$ controls are re-used from Figure S2.6 (n=3 *Roquin*$^{san/+}$; *UBC-Cre*$^{ERT2+}$; *Icos*$^{+/+}$; n=6 Roquin$^{san/+}$; *UBC-Cre*$^{ERT2+}$; *Icos*$^{f/-}$). (B) Mice with ICOS gene deletion were further sub-divided according to their response at week 3 post-gene deletion based on the following criteria: non-responder (<50% reduction in area) or responder (>50% reduction in area). Errors bars in A and B are SEM. Data are pooled from at least 2 independent experiments.

Chapter 3 Phagocytic immune surveillance mechanisms in AITL

Investigating the role of phagocytic immune surveillance in AITL-like tumors

Mariko Witalis[1,2], Jiaxin Li[1,2], Vincent Panneton[1,3], Jinsam Chang[1,2], Joanna Li[1,4], André Veillette[1] and Woong-Kyung Suh[1,2,3,4]

[1]Institut de recherches cliniques de Montréal (IRCM), Montréal, QC, Canada
[2]Molecular Biology Department, University of Montréal, Montréal, QC, Canada
[3]Department of Microbiology, Infectious Diseases and Immunology, University of Montréal, Montréal, QC, Canada
[4]Department of Microbiology and Immunology, McGill University, Montréal, QC, Canada

3.1 Summary

Angioimmunoblastic T cell lymphoma (AITL) is an aggressive peripheral T cell lymphoma without effective therapeutic options. Although circulating tumor cells are found in the blood of AITL patients, the rate at which tumors disseminate to nearby lymph nodes can differ between patients, ranging from several months to years. One possibility is that continual immune surveillance may aid in resisting the spread of AITL disease. The phagocytic ability of macrophages is important to control tumor growth and is heavily dependent on positive ("eat me") and negative ("don't eat me") checkpoint signals. Signaling lymphocytic activation molecule F7 (SLAMF7) is expressed in a subset of human AITL patients and is also a positive signal for macrophage activation. This positive SLAMF7 engagement can be counteracted by negative signals provided by the interaction between CD47 (on tumor cells) and SIRPα (on macrophages). It has been reported that inhibiting this CD47-SIRPα signaling pathway can lead to increased phagocytosis of certain B cell lymphomas, which is dependent on SLAMF7 expression on target cells. Using a spontaneous mouse model for AITL-like disease (*Roquin*$^{san/+}$), we confirm expression of SLAMF7 on mouse-derived AITL-like tumor cells and the presence of intratumoral macrophages well-equipped with SLAMF7 and SIRPα. We also demonstrate that *in vitro* blockade of CD47-SIRPα signaling through anti-CD47 antibody increases the ability of macrophages to phagocytose AITL-like tumor cells. Taken together, this suggests that manipulation of the CD47-SIRPα signaling pathway may inhibit AITL tumor cell dissemination and provides a rationale for harnessing macrophages in AITL disease treatment.

3.2 Introduction

AITL is a type of peripheral T cell lymphoma (PTCL), derived from the germinal center (GC) which often presents with symptoms such as generalized lymphadenopathy, B-symptoms, hepatosplenomegaly and hypergammaglobulinemia (1-3, 6, 403). In addition, gross immune dysregulation leaves AITL patients vulnerable to recurrent opportunistic infections, contributing to low survival rates (73, 377, 404). Intriguingly, despite the presence of circulating $CD4^+$ tumor cells in AITL patients, the rate at which tumors spread to distal lymph nodes can vary from a span of several months to years, which may suggest the importance of tumor-specific lymphoid niches or the presence of ongoing immune surveillance (4, 10, 91, 265).

AITL tumor cells originate from a specialized subset of $CD4^+$ T cell, the T follicular helper (Tfh) cell (1, 18, 21, 23, 30, 378). Under physiological conditions, Tfh cells provide support to B cells to drive the generation of high affinity antibodies that ultimately confers protection against foreign pathogens or immunity after vaccination (34, 35, 99, 405). In contrast, pathological hyperactivity of Tfh cells can lead to inappropriate B cell responses, and manifest as autoimmune or AITL disease (35). Despite the Tfh cell origin of AITL, throughout disease evolution, the proportion of tumor cells is maintained at rather low levels, and instead, there is an overabundance of activated B cells which fills the tumor niche (4, 30, 36). Moreover, AITL tumor cells are oligoclonal in nature and propagate inappropriate immune activation as evidenced by intratumoral accumulation of B cells, plasma cells and macrophages (2, 14, 18). While tumor cells in human AITL have been rather well-studied, there has been less investigation on the impact of other immune cell types within the tumor microenvironment and how they may influence the growth and dissemination of these Tfh cell-derived tumor cells.

Macrophage-mediated immune surveillance plays an essential role in controlling cancer growth and spreading (297). Macrophages are important during infection through their ability to clear pathogens, as well as under homeostatic conditions to eliminate cellular debris from aged or dying cells (299, 306, 406). As such, boosting signaling mechanisms to prevent tumor cell evasion while at the same time promoting macrophage-mediated phagocytosis of the same target tumor cells would be a great advantage for antitumor immunity. However, there is a complicated balance between the numerous activating and inhibitory receptors present on the surface of both macrophages and target cells. Signaling lymphocytic activation molecule F7 (SLAMF7) is part of the SLAM family receptors and can interact with SLAM-associated protein (SAP) family of adaptors such as EAT-2. SLAMF7 is found expressed on activated T cells, B cells, natural killer (NK) cells, dendritic cells and macrophages (239). In the framework of hematopoietic cancers, such as B cell lymphomas, prophagocytic SLAMF7 signaling works to support macrophage activation by interacting with integrin Mac-1 (CD11b) rather than binding to SAP family adaptor protein, EAT-2 (241). This positive SLAMF7 signal can be counteracted by negative ("don't eat me") signals provided by the interaction between CD47 (on tumor cells) and SIRPα (on macrophages) (241). CD47 is a transmembrane protein ubiquitously expressed on a wide variety of cell types and is often upregulated on tumor cells (299, 306), while its receptor, SIRPα, is expressed mainly on monocytes, granulocytes, macrophages, dendritic cells and neutrophils

(296, 300). In macrophages, CD47 engagement with SIRPα leads to activation of phosphatases SHP-1 and SHP-2 and a cascade of signaling events that suppresses myosin IIA-mediated phagocytosis of target cells (296, 306).

Numerous B cell-derived lymphomas have higher levels of CD47 and this is predictive of poorer prognosis in B cell non-Hodgkin lymphoma (NHL) (300). In line with this, it has been reported that dual combination therapy of anti-CD47 and anti-CD20 (rituximab) in NHL-PDX models reduced tumor burden and improved survival (318). Additionally, the treatment of patients with diffuse large B-cell lymphoma (DLBCL) or follicular lymphoma with dual anti-CD47 and anti-CD20 therapy demonstrated promising results in patients with aggressive or indolent lymphoma (319). In human AITL, although CD47 expression is variable between patient samples, *in vitro* CD47 blockade led to increased phagocytosis using human AITL tumor cells derived from an AITL-PDX model (323). Thus, understanding how to incorporate CD47 signaling blockade into AITL treatment could be beneficial in improving disease outcomes. SLAMF7 is also expressed in human AITL (321) and has been the focus of studies aimed at utilizing immunostimulatory monoclonal antibodies against SLAMF7 (elotuzumab) in PDX models to assess the therapeutic value of SLAMF7 stimulation in human AITL (336, 337). Considering the critical role of SLAMF7 in the clearance of hematopoietic-derived tumors, further investigation into the functional role of SLAMF7 on both tumor cells and cells involved in immunosurveillance is warranted.

In this study, using the *Roquin*$^{san/+}$ mouse model, which spontaneously develops AITL-like disease at 4-6 months of age (50% penetrance) (270), we observe increased expression of the "don't eat me" signal, CD47 on Tfh-like tumor cells, an indication of potential immune evasion mechanisms. Further, we report a high SLAMF7-expressing CD4$^+$ T cell subset and decreased expression of SLAMF7 on GC B-like cells in AITL-like tumors. Additionally, intratumoral macrophages had increased SLAMF7 levels, which taken together may suggest failed antitumor responses attempting to limit tumor growth. Importantly, we demonstrate that blockade of CD47-SIRPα signaling using an anti-CD47 antibody *in vitro* increased the ability of macrophages to phagocytose AITL-like tumor cells. This work provides evidence that manipulation of CD47 signaling *in vivo* may be promising in designing future AITL therapies.

3.3 Methods

3.3.1 Mice

Roquin$^{san/+}$ mice were provided by Dr. C. Vinuesa (Australia National University, Australia). Mice were maintained within animal facilities at the Institut de recherches cliniques de Montréal (IRCM) in a specific pathogen-free environment and all experiments were performed following animal use protocols approved by the IRCM animal care committee.

3.3.2 Antibodies and chemicals

All antibodies and streptavidin-conjugates and reagents used for flow cytometry were from ThermoFisher unless otherwise stated: B220 (RA3-62), CD4 (GK1.5), CD11b (M1/70, Biolegend), CD16/CD32 (2.4G2, BioXCell), CD47 (miap301), CD95 (Jo2, BD Biosciences), CXCR5 (SPRCL5), F4/80 (BM8), GL7, Ki-67 (SolA15) PD-1 (J43, BD Biosciences), SIRPα (P84), SLAMF7 (4G2, Biolegend), and streptavidin-PE Cy7. Dead cells were stained with 7-AAD (BD Biosciences) or fixable viability dye (ThermoFisher). Fixation/permeabilization kits (ThermoFisher) were used to perform intracellular stainings.

3.3.3 Flow cytometry

Single cell suspensions of lymph nodes were prepared using mechanical dissociation with a 70μM nylon mesh filter (BD Biosciences) in PBS or staining buffer (PBS supplemented with 1% bovine serum albumin (BSA) (Wisent)). To prevent non-specific binding, cells were blocked with anti-CD16/CD32 and then stained with primary antibodies followed by streptavidin-conjugates, if necessary. For intracellular stainings, cells were fixed and permeabilized using eBioscience™ Foxp3/Transcription Factor Staining Buffer set, according to manufacturer's instructions. Samples were acquired using the LSR Fortessa (BD Biosciences) and analyzed on Flowjo Version 10 (Treestar).

3.3.4 Generation of bone marrow-derived macrophages (BMDM)

BMDMs were generated by flushing the femur and tibia bones of wildtype or *Roquin*$^{san/+}$ mice (6-12 weeks old) with macrophage culture media (RPMI supplemented with 10% heat-inactivated FBS, 1% L-glutamine and 1% penicillin/streptomycin). Cells were cultured in

bacterial Petri dishes for ~6 days and media was supplemented with fresh M-CSF (PeproTech), to a final concentration of 10ng/ml.

3.3.5 *In vitro* phagocytosis assay

For phagocytosis assays, 5 x 10^4 BMDMs were seeded overnight in 24-well plates. To isolate $CD4^+$ cells from *Roquin*$^{san/+}$ tumors, EasySEP™ Mouse CD4+ T cell Isolation Kit (STEM Cell) was used, according to manufacturer's instructions. Target cells (2 x 10^5 of total tumor or $CD4^+$ only) were labelled with 2.5μM carboxyfluorescein succinimidyl ester (CFSE, ThermoFisher) and then added to macrophages in the presence of rat IgG2a or anti-CD47 (miap301; 10μg/ml), followed by a 2-hour incubation period at 37°C. After this incubation period, macrophages were washed and imaged using an inverted microscope (Carl Zeiss Axiovert S100 TV). The phagocytosis efficiency was calculated as the number of macrophages containing $CFSE^+$ target cells per 100 macrophages.

3.3.6 Immunohistochemistry

Tumor-free, non-tumor and tumor lymph nodes were fixed in 10% formalin overnight at 4°C and then kept in 70% ethanol until embedded in paraffin. Samples were cut into 6μm sections and stained with F4/80 (clone: C1: A3-1 #MCA497R, AbD Serotec) using an automated Discovery XT (Ventana Medical Systems/Roche). Images were taken using a Leica DM4000B equipped with cellSens digital imaging software Version 1.12 (Olympus).

3.3.7 Statistical Analysis

Data were analyzed using Prism 7.0 (GraphPad Software). When comparing three groups or more, a one-way ANOVA test was used. A p value of <0.05 was considered statistically significant. For all experiments p values are as follows: *$p<0.05$, ** $p<0.01$, ***$p<0.001$, ****$p<0.0001$.

3.4 Results

3.4.1 Alteration in the expression profile of SLAMF7 in CD4$^+$ and B220$^+$ cell subsets within AITL-like tumors

SLAMF7 is expressed in approximately 44% (4/9) of human AITL samples (321) and has recently been identified as an upregulated gene in AITL patients as compared to healthy controls (322). Nevertheless, understanding the implications of these observations have been rather limited. Before initiating experiments to study the role of SLAMF7-mediated phagocytosis in the context of the *Roquin*$^{san/+}$ mouse model, we first performed validation experiments and profiled SLAMF7 expression levels between tumor-free, non-tumor and tumor lymph nodes from *Roquin*$^{san/+}$ mice.

Amongst total CD4$^+$ T cells, there was an increased frequency of SLAMF7-expressing cells in tumor samples as compared to tumor-free or non-tumor lymph nodes (Fig. 3.1A). We also observed an increased SLAMF7^{hi} subpopulation among Tfh-like CXCR5$^+$PD-1$^+$ cells in tumors (Fig. 3.1B). Within AITL-like tumors, these SLAMF7-expressing CD4$^+$ or Tfh-like cells also contained a subpopulation enriched for Ki-67, a marker of cell proliferation (Fig. 3.1C, E). When comparing Ki-67 levels based on SLAMF7 expression, we observed that in CD4$^+$ T cells, regardless of tumor stage, SLAM7^{hi}CD4$^+$ T cells were more proliferative as compared to SLAM7^{lo}CD4$^+$ T cells (Fig. 3.1D). The same observation was not found in Tfh cells, where SLAMF7^{hi} Tfh cells were equally as proliferative as their SLAMF7^{lo} counterpart in tumor-free or non-tumor lymph nodes (Fig. 3.1F). In contrast, we observed that SLAMF7^{hi} Tfh-like cells from tumors were more proliferative than SLAMF7^{lo} Tfh-like cells, a feature unique to AITL-like disease (Fig. 3.1F). It has been reported that activated murine splenic CD4$^+$ T cells stimulated with anti-CD3/CD28 upregulate levels of SLAMF7 in a time-dependent manner (333). While elevated expression of SLAMF7 on CD4$^+$ and Tfh-like cells may increase their probability to be phagocytosed, it remains to be seen whether these CD4$^+$ T cells somehow rely on SLAMF7-mediated signaling pathways for their growth, proliferation and/or survival.

In human AITL and the *Roquin*$^{san/+}$ mouse model, while both share a neoplastic Tfh cell population, the majority of the tumor mass comes from an inappropriate expansion of B cell populations (4, 30, 270). We have previously reported evidence that a subset of B cells found within the tumor environment in *Roquin*$^{san/+}$ tumors had progressed into plasma cell precursors

(402). As such, this may indicate that there is an accumulation of abnormal B cell subsets with atypical expression of proteins involved in macrophage-mediated phagocytosis, such as SLAMF7. While there was no difference in expression of SLAMF7 on total $B220^+$ cells between tumor-free, non-tumor or tumor samples (Fig. 3.1G), within AITL-like tumors, amongst $GL7^{hi}Fas^+$ GC B-like cells, there was a reduction in the expression level of SLAMF7 (Fig. 3.1H). Under non-pathological conditions, activated B cells and plasma cells in mice are reported to highly express SLAMF7 (333), and thus, this small alteration may suggest a survival mechanism to avoid SLAMF7-mediated elimination.

3.4.2 Tfh-like cells within AITL-like tumors have increased expression levels of "don't eat me" signal CD47

SLAMF7 engagement is a crucial activating interaction that is required for efficient phagocytosis when dominating inhibitory CD47-SIRPα interaction is interrupted (241). CD47 is a "don't eat me" signal expressed on target cells, which upon binding to SIRPα prevents phagocytosis (296). We observed no difference in CD47 MFI on both total $CD4^+$ or highly proliferative $SLAMF7^{hi}CD4^+$ cells (Fig. 3.2A-B). However, Tfh-like cells from tumors had slightly increased levels of CD47 as compared to non-tumor or tumor-free samples (Fig. 3.2C). Taken together, this suggests that CD47 upregulation is more specific to Tfh-like cells and likely represents one of the many ways in which AITL-like tumors evade immune-mediated elimination. However, whether this small increase in CD47 MFI amongst Tfh-like tumor cells has any biological significance needs to be tested. When comparing CD47 versus SLAMF7 levels in Tfh cells, we observed that most Tfh cells were single positive for CD47, and in addition to this, we noted a very slight increase in the frequency of this population in AITL-like tumors as compared to non-tumor lymph nodes (Fig. 3.2E). Interestingly, CD47 MFI was generally lower in Tfh cells as opposed to total $CD4^+$ T cells, irrespective of tumor stage (Fig. 3.2A, C). As Tfh cells are reported to be more prone to cell death as compared to naïve or memory T cells (407), lowered levels of inhibitory CD47 on Tfh cells within the $CD4^+$ T cell pool may reflect its preferential clearance during physiological GC responses. Lastly, we did not find a difference in CD47 MFI amongst $GL7^{hi}Fas^+$ GC B-like cells regardless of tumor stage (Fig. 3.2D). In summary, observing these changes in SLAMF7 and CD47 expression in both T

and B cell subsets in AITL-like tumors may reflect the opposing activity of signaling mechanisms which either promote or impede tumor growth.

3.4.3 Macrophages in *Roquin*$^{san/+}$ AITL-like tumors are equipped with necessary molecules to mediate phagocytosis

In order for CD47-SIRPα blockade to be efficient macrophages must be armed with certain proteins such as Mac-1 (CD11b), SLAMF7 and SIRPα (241). Using immunohistochemistry, we identified F4/80 positive macrophages in tumor-free, non-tumor and tumor samples from *Roquin*$^{san/+}$ mice (Fig. 3.3A). We further compared the frequencies of F4/80^{+}Mac-1^{+} macrophages between samples using flow cytometry and observed no differences (Fig. 3.3B). We also found that there was a trend of increased SLAMF7 MFI in F4/80^{+}Mac-1^{+} macrophages within AITL-like tumors (Fig. 3.3C). Interestingly, when comparing the frequency of SLAMF7^{+}SIRPα^{+} amongst F4/80^{+}Mac-1^{+} macrophages between tumor-free, non-tumor and tumor lymph nodes, we observed a gradual continuum of increased frequencies (Fig. 3.3E). Additionally, we also observed a larger percent of F4/80^{-}Mac-1^{+} cells in non-tumor lymph nodes as compared to AITL-like tumors (Fig. 3.3B), which were also enriched for SLAMF7 (Fig. 3.3D). In lymph nodes, both subcapsular and medullary sinus macrophages are reported to express Mac-1, but subcapsular sinus macrophages do not express F4/80, while medullary sinus macrophages are positive for F4/80 (313). However, while F4/80 is commonly accepted as a macrophage marker (408), expression of Mac-1 (CD11b) has also been reported on other immune cell subsets such as CD8^{+} T, NK and B1 cells (409-411). As such, it is challenging to understand the implications of observing an increased proportion of F4/80^{-}Mac-1^{+} cells in non-tumor lymph nodes as opposed to tumors and furthermore, the impact of elevated SLAMF7 levels on this population within AITL-like tumors.

The increased expression of prophagocytic protein SLAMF7 on both macrophages and Tfh-like cells in tumors (Fig. 3.1B) may not be able to overcome the elevated levels of negative signaling protein CD47 on Tfh-like cells in tumors (Fig. 3.2C), as this would strengthen SIRPα-dependent inhibitory pathways in macrophages. Ultimately, this may prevent tumor-associated macrophages from effectively removing newly generated and/or already existing tumor cells. Alternatively, another possibility is that AITL-like tumor cells are continuously being cleared by macrophages and in response to this immune pressure, tumor cells upregulate inhibitory CD47 in

order to escape engulfment and remain within the tumor mass. Furthermore, as GC B-like cells in AITL-like tumors have decreased expression of SLAMF7, this either suggests the development of an evasion mechanism towards CD47-SIRPα controlled phagocytosis or a preferential survival benefit, which allows this lower SLAMF7-expressing GC B-like cell subset to prevail in AITL-like tumors. However, while we confirmed that macrophages in AITL-like tumors express both SLAMF7 and SIRPα, it still needs to be tested whether tumor cells are susceptible to phagocytosis in the context of CD47 signaling blockade.

3.4.4 AITL-like tumor cells can be efficiently phagocytosed upon CD47 blockade

To test whether CD47 signaling inhibition can increase macrophage-mediated phagocytosis of AITL-like tumor cells, we generated bone marrow-derived macrophages (BMDM) *in vitro* and co-cultured them with CFSE-labelled target cells in the presence of control antibody or anti-CD47 blocking antibody (Fig. 3.4A-B). For both wildtype and *Roquin*$^{san/+}$ BMDMs, we observed that blocking CD47 signaling *in vitro* led to an increased phagocytic efficiency of total or CD4$^+$ AITL-like tumor cells (Fig. 3.4C). Generally, we saw an approximate 2-fold increase in the percentage of phagocytosis when macrophages were co-cultured with total or CD4$^+$ tumor cells, suggesting that CD4$^+$ tumor cells as well as other immune cells (mostly B cells) within the tumor are susceptible to increased phagocytosis in a CD47-dependent manner. It has been previously reported that activated CD4$^+$ T cells, which express SLAMF7, are more effectively phagocytosed upon CD47 signaling blockade (241). This is in contrast to naïve CD4$^+$ T cells, which do not express SLAMF7 and are not phagocytosed in the absence or presence of anti-CD47 antibodies (241). Consequently, this suggests that SLAMF7-CD47 dependent phagocytosis actively participates in the phagocytic clearance of activated CD4$^+$ T cells, however, whether CD4$^+$ tumor cells are more or less susceptible to macrophage-mediated engulfment upon CD47 blockade as compared to physiologically activated CD4$^+$ T cells still needs to be determined. Moreover, as we focused only on testing target cells isolated from AITL-like tumors, we were unable to determine whether the small increase of CD47 expression on Tfh-like tumor cells translated to changes in phagocytic efficiency in comparison to Tfh cells from tumor-free or non-tumor lymph nodes.

3.5 Discussion

The data we report here demonstrate that tumor Tfh-like cells have a small relative increase in "don't eat me" signal CD47 as compared to Tfh cells from tumor-free or non-tumor lymph nodes. Moreover, SLAMF7 downregulation on GC B-like cells in AITL-like tumors is suggestive of potential phagocytic evasion. Importantly, F4/80$^+$Mac-1$^+$ macrophages in the tumor microenvironment had an increased proportion of cells double positive for both SIRPα SLAMF7. Nevertheless, despite elevated levels of SLAMF7, AITL-like tumors were present, indicating that CD47 upregulation, and possibly other mechanisms may be sufficient to resist phagocytosis and maintain tumor growth. Finally, we show improved phagocytic efficiency of either total or CD4$^+$ AITL-like tumor cells upon *in vitro* administration of anti-CD47 antibody, demonstrating that this pathway can be manipulated in the context of AITL-like disease.

Among total CD4$^+$ and Tfh-like cells from AITL-like tumors, we observed a subpopulation expressing higher levels of SLAMF7, which may leave these cells more susceptible to SLAMF7-mediated phagocytosis. Moreover, it has been reported that SLAMF7 levels are upregulated in activated CD4$^+$ T cells (333), and thus, our observation in AITL-like tumors could in fact simply be a proxy for T cell activation. In NK cells, the activating impact of SLAMF7 is heavily dependent on SLAM family adaptor protein, EAT-2 (333). CD4$^+$ T cells do not naturally express this adaptor protein, and as a result, SLAMF7 engagement leads to an inhibitory outcome on T cell activation (333). Nonetheless, in both human and mouse AITL, whether tumor Tfh-like cells can abnormally express EAT-2 has yet to be investigated. Future studies should also establish whether SLAMF7 expression on CD4 cell subsets have supportive roles in survival, proliferation and/or activation and determine if increased SLAMF7 expression alters disease progression rates, survival or prognosis in human AITL.

Moreover, it has been described that T cell lymphoma cell lines that express CD47 but lack SLAMF7 are not engulfed after blocking CD47 signaling (241). This may prove to be problematic as only a subset of CD4$^+$ T cells in AITL-like tumors highly express SLAMF7 and, in human AITL, the type of immune cells expressing SLAMF7 is also ill-defined. However, in DLBCL, it has been shown that SLAMF7 expression on tumor cells is not necessary to trigger effective CD47 blockade-induced tumor cell engulfment, nor does *SLAMF7* mRNA levels correlate with DLBCL patient survival (412). As SLAMF7 is not the only signaling molecule that can promote phagocytosis, it is plausible that tumor cells in DLBCL or AITL may also

express other prophagocytic molecules that can augment phagocytosis in the context of CD47 signaling inhibition (296).

While being a Tfh cell-derived lymphoma, inappropriate B cell expansion in AITL tumors influences disease symptoms and pathogenesis (4, 30, 36, 270). Thus, promoting the engulfment of both tumor Tfh-like cells in addition to B cell subsets by macrophages could be most efficient to induce tumor regression. It has been shown that anti-CD47 treatment improved phagocytosis of B cell lymphomas, but not naïve or activated B cells (241). Since B cells within the AITL environment are subject to inappropriate immune activation, they may no longer represent physiological B cells and thus be susceptible to phagocytosis after CD47 blockade. We previously reported that $B220^+$ cells in AITL-like tumors had increased levels of adhesion molecule ICAM-1, which may work to support T cell-B cell crosstalk (402). Moreover, since ICAM-1 is a ligand for Mac-1, this interaction could also function as a positive signal in facilitating target cell engulfment by macrophages (241, 413). Consequently, although we observed that GC B-like cells within tumors had reduced SLAMF7 levels, it is plausible that in addition to homotypic SLAMF7 engagement, Mac-1/ICAM-1 interaction as well as other unidentified signaling pathways may serve as prophagocytic signals. This is further supported by our observation that total AITL-like tumor cells, many of which are $B220^+$ cells, can be phagocytosed *in vitro* upon adding anti-CD47 antibody.

An important consideration regarding CD47 blocking therapies is off-target effects, specifically, anemia (300). As red blood cells age, and prepare to be cleared from the circulation, they downregulate CD47, and start to express various prophagocytic molecules which make them more susceptible to elimination after inhibition of CD47 signaling (300). For AITL patients this may be particularly risky, as autoimmune hemolytic anemia affects approximately 65-70% of patients (6, 414). Future studies focused on the *in vivo* application of CD47 blockade in AITL-like mouse models should consider combination therapies that also inhibit other cell markers which are abundantly expressed in AITL-like tumors such as proteins relating to T cell-B cell crosstalk. Moreover, without boosting prophagocytic signals, simply inhibiting CD47 signaling can be insufficient to promote tumor cell engulfment by macrophages (296), and consequently, using additional therapeutic agents to stimulate these positive signals could further prevent AITL disease progression.

In summary, we have shown evidence of opposing immune evasion and surveillance forces within the context of AITL-like tumors. Importantly, we also report that both total and $CD4^+$ T cells within AITL-like tumors can be efficiently phagocytosed upon *in vitro* CD47 blockade. Experiments in the future should focus on how to translate these findings relating to CD47 and SLAMF7 *in vivo*.

3.6 Acknowledgements

We thank Dr. C. Vinuesa (Australian National University, Australia) for *Roquin*$^{san/+}$ mice. We also thank the IRCM Flow Cytometry Core Facility and IRCM Animal Facilities for their service. This work was supported by operating grants from Cancer Research Society (W.-K. S.) and Canadian Institutes of Health Research (MT-14429, MOP-82906, FDN-143338 to A.V.). A.V. holds the Canada Research Chair on Signaling in the Immune System. M.W. and J.L. received CIHR Master's Awards; M.W. and V.P. received FRQS Doctoral Scholarships.

3.7 Author Contribution

W.-K.S. conceptualized the study; M.W., J.L. (Jiaxin), J.C., Y.B., V.P., J.L. (Joanna), A.V., developed experimental tools; M.W. performed flow cytometry experiments and captured microscopy images of immunohistochemistry samples; phagocytosis assays were performed by J.L. (Jiaxin), and immunohistochemistry completed by the histology core facility at the Institut de recherche en immunologie et en cancérologie (IRIC). M.W. and W.-K.S. analyzed the data; M.W. and W.-K.S. prepared the figures; M.W. and W.-K.S. wrote the manuscript with input from J.L., J.C., Y.B., V.P., J.L., and A.V.

3.8 Figures and figure legends

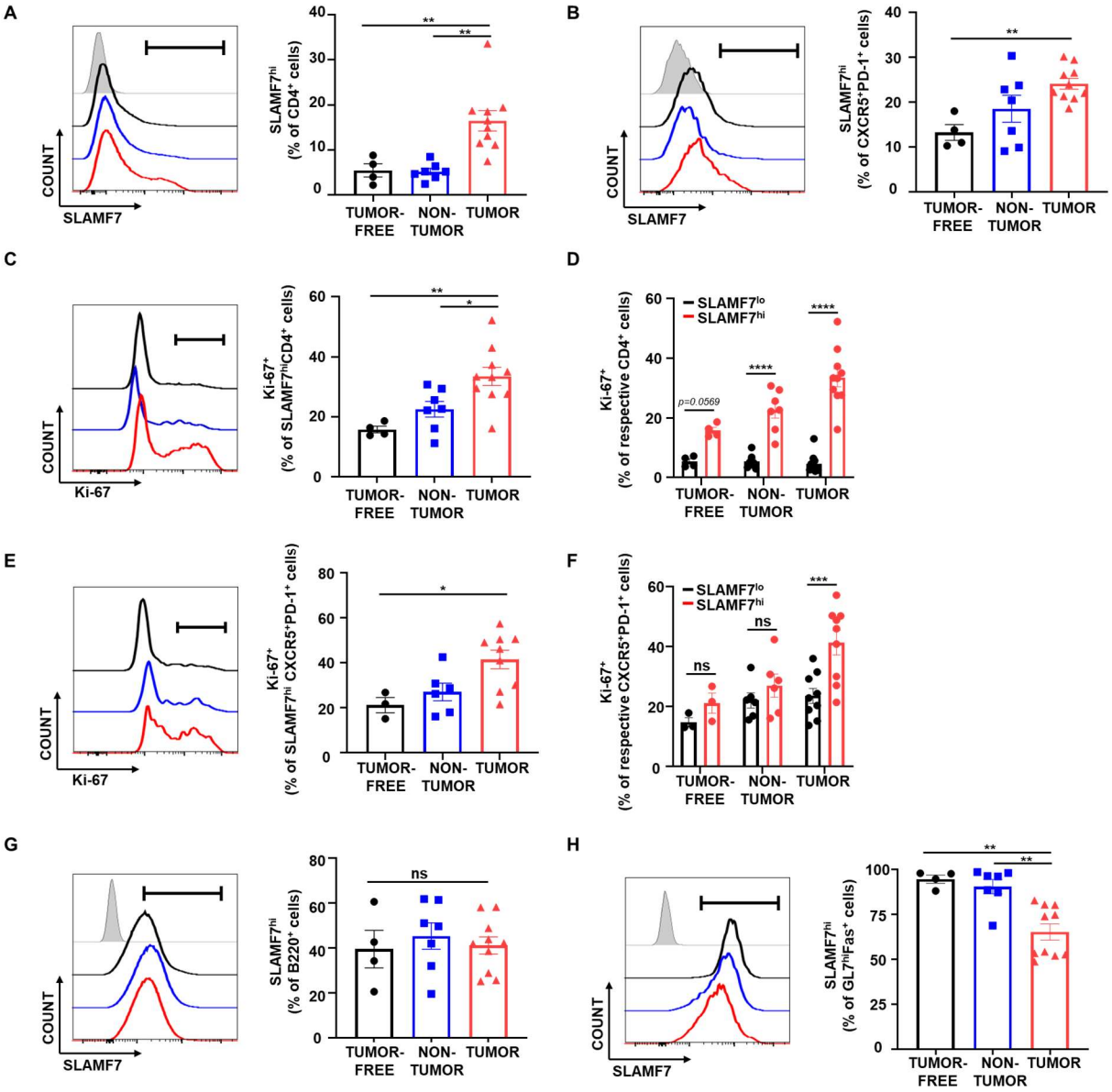

Figure 3.1 Altered SLAMF7 expression profile on CD4$^+$ and B220$^+$ cell subsets within AITL-like tumors

(A-B) Representative flow cytometric analyses and frequency of SLAMF7 expression on CD4$^+$ (A) or Tfh cells (CD4$^+$CXCR5$^+$PD-1$^+$) (B) from tumor-free, non-tumor and tumor samples (n=4 tumor-free; n=7 non-tumor; n=10 tumor). (C-F) Representative graphs and frequencies compare Ki-67 levels between CD4$^+$ or Tfh cells based on SLAMF7 expression and tumor stage. (C) Increased subset of Ki-67-expressing cells amongst SLAMF7^{hi}CD4$^+$ cells from AITL-like tumors. (D) SLAMF7^{hi}CD4$^+$ cells are generally more proliferative than SLAMF7^{lo}CD4$^+$ cells regardless of tumor stage. (E) AITL-like tumors have an increased subset of Ki-67-expressing cells amongst SLAMF7^{hi} Tfh cells (CD4$^+$CXCR5$^+$PD-1$^+$). (F) SLAMF7^{hi} Tfh-like cells from

AITL-like tumors are more proliferative than SLAMF7^{lo} Tfh-like cells, a difference not observed in tumor-free or non-tumor samples. (n=3-4 tumor-free; n=6-7 non-tumor; n=9-10 tumor). (G-H) Representative expression levels and frequency of SLAMF7 expression on B220^{+} (G) or GC B cells (B220^{+}GL7^{hi}Fas^{+}) (H) from tumor-free, non-tumor and tumor samples (n=4 tumor-free; n=7 non-tumor; n=10 tumor). Grey filled histograms in A-C, E, and G-H represent isotype controls. Error bars in A-H represent SEM. Data are pooled from at least 3 independent experiments.

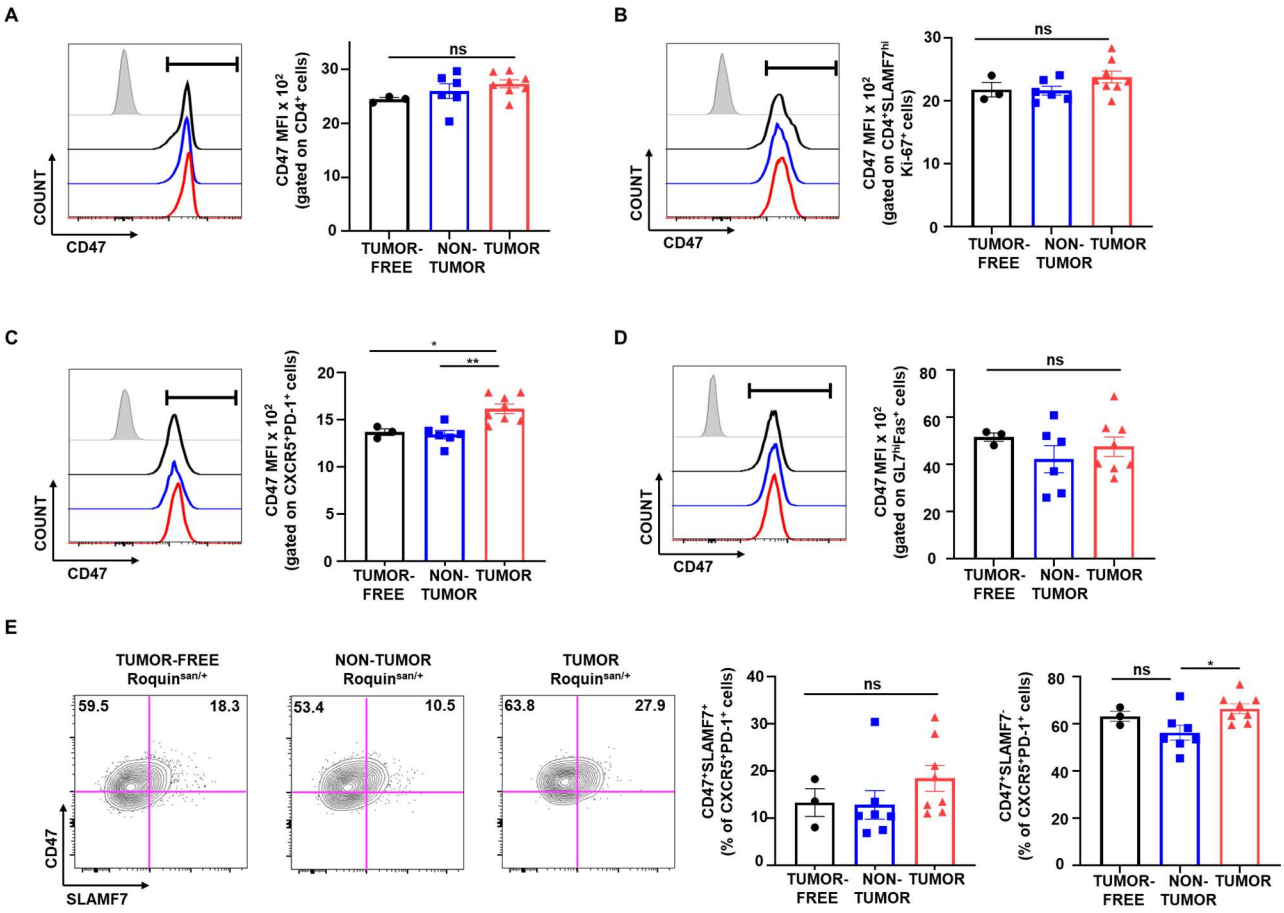

Figure 3.2 Increased levels of inhibitory signal CD47 on tumor Tfh-like cells in *Roquin$^{san/+}$* mice

(A) Representative flow cytometry analyses and CD47 MFI on CD4^{+} cells from tumor-free, non-tumor and tumor samples (n=3 tumor-free; n=6 non-tumor; n=8 tumor). (B) Highly proliferative Ki-67^{+}CD4^{+} cells with increased SLAMF7 levels have similar CD47 MFI between three tumor stages as shown through representative histogram and frequency (n=3 tumor-free; n=6 non-tumor; n=8 tumor). (C-D) Representative expression levels and CD47 MFI on Tfh (C) and GC B (D) cells from tumor-free, non-tumor and tumor samples (n=3 tumor-free; n=6 non-tumor; n=8 tumor). (E) Expression of CD47 versus SLAMF7 levels in Tfh cells from tumor-free, non-tumor and tumor samples (n=3 tumor-free; n=7 non-tumor; n=8 tumor). Grey filled histograms in A-D represent isotype controls. Error bars in A-E represent SEM. Data are pooled from at least 3 independent experiments.

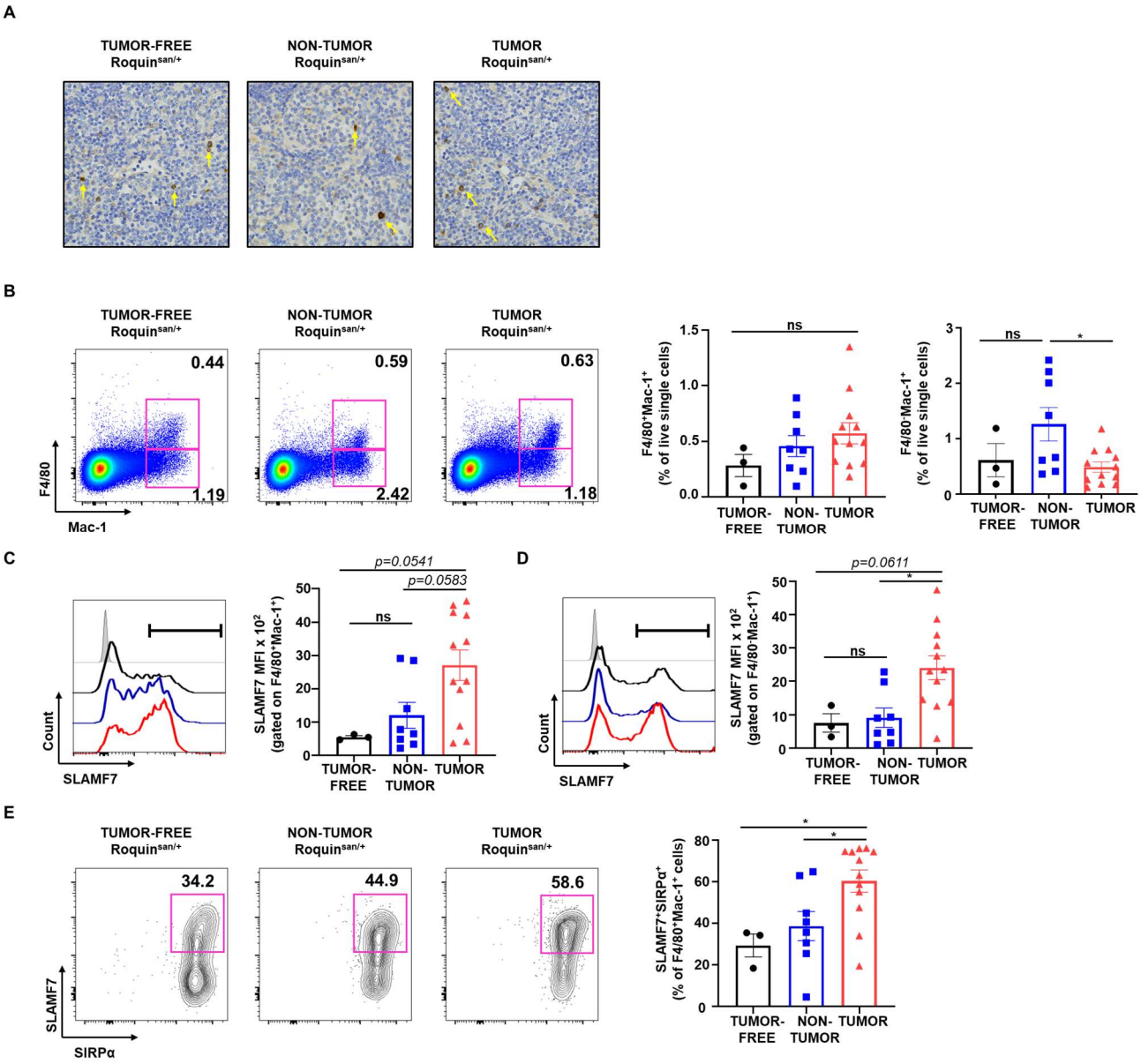

Figure 3.3 Increased frequency of SIRPα$^+$SLAMF7$^+$ expressing subset of F4/80$^+$Mac-1$^+$ macrophages in *Roquin$^{san/+}$* tumors

(A) Exemplary immunohistochemistry staining for F4/80 in tumor-free, non-tumor and tumor samples. Yellow arrows indicate F4/80$^+$ cells. (B) Representative plot and frequency of macrophages based on F4/80 and Mac-1 expression in tumor-free, non-tumor and tumor samples (n=3 tumor-free; n=8 non-tumor; n=12 tumor). (C-D) Trend of increased SLAMF7 MFI on F4/80$^+$Mac-1$^+$ macrophages (C) and F4/80$^-$Mac-1$^+$ cells (D) in AITL-like tumors. (E) Increased frequency of SLAMF7$^+$SIRPα$^+$ amongst F4/80$^+$Mac-1$^+$ macrophages within AITL-like tumors as shown through representative flow cytometric plots and frequencies (n=3 tumor-free; n=8 non-tumor; n=12 tumor). Grey filled histograms in C-D represent isotype controls. Error bars in B-E represent SEM. Data are pooled from at least 3 independent experiments.

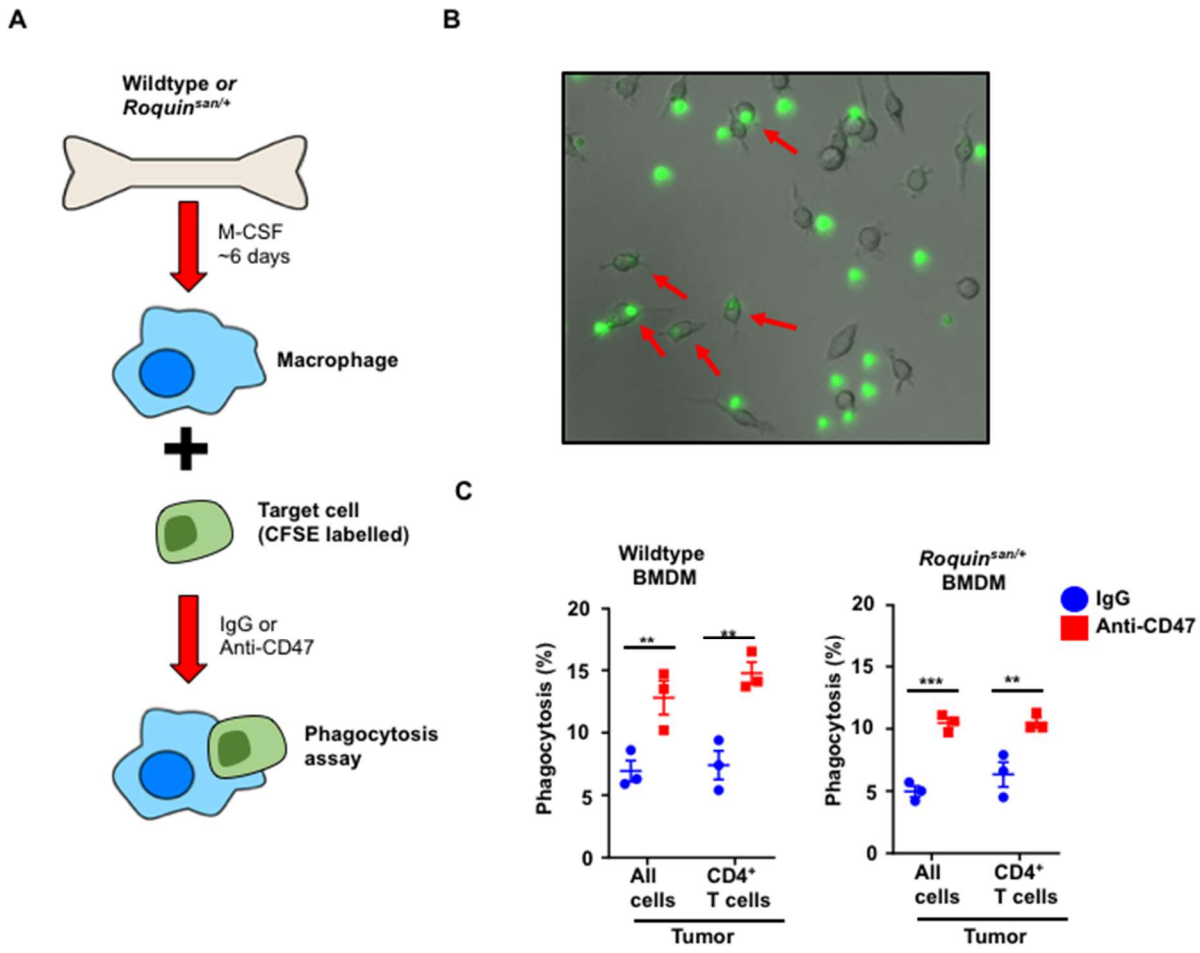

Figure 3.4 *In vitro* CD47 blockade improves phagocytosis efficiency of AITL-like tumor cells

(A) Pictorial schematic of phagocytosis assay. In brief, bone marrow-derived macrophages (BMDM) are generated and then co-cultured with CFSE labelled target cells from AITL-like tumors. After the addition of isotype control or anti-CD47 antibody, phagocytosis efficiency is calculated. (B) Representative image depicting phagocytosis of CFSE labelled target cells (in green) by BMDMs. Red arrows indicate engulfed target cells. (C) Macrophages generated from wildtype or *Roquin*$^{san/+}$ mice have improved phagocytosis efficiency of total cells or CD4^{+} T cells from AITL-like tumors after CD47 blockade (n=3 tumors). Error bars in C represent SEM. Data are pooled from at least 2 independent experiments.

Chapter 4 Discussion

While neoplastic cells from AITL have been well-established to originate from the Tfh cell lineage (3, 20-22, 30, 32, 378), whether AITL tumor cells functionally rely on signaling molecules essential for Tfh cell generation and survival has not been investigated. One of my important findings from Chapter 2 is that not only do Tfh-like cells in AITL-like disease require key Tfh cell molecules Bcl6 and SAP to support tumor maintenance, but they also engage in functional T-B communication. This likely occurs through the generation of high-quality T-B conjugates supported by molecules such as high affinity LFA-1 and SAP, which can promote B cell differentiation into the plasma cell lineage and hypergammaglobulinemia. In Chapter 3, I switched focus onto immune surveillance mechanisms in AITL to specifically determine whether weaker macrophage-mediated phagocytosis might contribute to tumor growth and/or dissemination. I found that Tfh-like tumor cells from AITL-like tumors expressed relatively higher levels of inhibitory "don't eat me" molecule CD47, while intratumoral macrophages also had higher amounts of prophagocytic protein SLAMF7, suggesting the possible presence of opposing evasion versus surveillance mechanisms. Additionally, I demonstrated that a subset of Tfh-like cells in AITL-like tumors highly expressed SLAMF7, potentially leaving these putative tumor cells more vulnerable to macrophage cell engulfment upon CD47 inhibition. The different sections in this discussion aim to contextualize our major observations regarding the implications of T-B crosstalk within AITL and its therapeutic applications, as well as the role of Bcl6 in AITL tumor progression. Additionally, this discussion will also examine the significance of SLAMF7 and macrophage-mediated immunosurveillance in AITL.

4.1 T-B crosstalk: implications and therapeutic applications

Importantly, while AITL is a T cell-derived lymphoma, disease presentation and symptoms are intimately associated with B cells. As such, one natural hypothesis would be that B cell depletion therapies may be effective in promoting AITL tumor regression, especially because B cells represent a majority of the AITL tumor mass, thus making it an easier population to therapeutically target. However, combination therapies of anti-CD20 antibody (rituximab) in combination with traditional CHOP therapies did not demonstrate any clinical benefits beyond that of CHOP usage (91). Patients treated with both regimens had an overall response rate of 80%, a median response duration of only 25 months, and a 2-year progression-free survival rate

of only 42% (91). Thus, while most patients do have a response to rituximab and CHOP therapy, the response is not long-lasting and does not translate into greatly improved survival rates.

One simple explanation is that because AITL tumors are driven by neoplastic Tfh-like cells, without eliminating these tumor cells, only eradicating B cells from the tumor will not lead to tumor regression (91). However, another explanation is that targeting CD20 may not be most effective in AITL, even though it can be found expressed in human tumor biopsies (11, 14). Rituximab is reported to kill target cells directly by mediating cell death or indirectly by initiating antibody-dependent phagocytosis, antibody-dependent cell-mediated cytotoxicity or complement-mediated cytotoxicity (415). Another important consideration is that antibody-dependent phagocytosis is heavily dependent on the balance of antiphagocytic and prophagocytic receptors present on the surface of target cells. Therefore, with regards to AITL, even if B cells are coated with anti-CD20 antibodies, if intratumoral B cells express higher levels of antiphagocytic receptors or insufficient amounts of receptors that can activate phagocytosis, macrophages are left unable to engulf target cells effectively. Furthermore, studies have reported that rituximab does not homogenously deplete all B cell subsets and specifically, GC B cells appear to be particularly resistant to anti-CD20 dependent depletion (416, 417). This may be particularly relevant in AITL, where tumor Tfh-like cells are likely to promote GC-like features in B cell subsets. Moreover, CD40 signaling, which is pivotal to the GC reaction is reported to downregulate CD20 expression levels in human B cells (418), which may also partially explain why GC B cells are more resistant to rituximab-mediated depletion. Therefore, rather than focusing on B cell depletion therapies, redirecting the focus on molecules that continually support communication between Tfh-like cells and B cells within the AITL tumor environment may be more effective. In this way, the end goal still includes the elimination of the bulk B cell mass, but by targeting a continually required signaling axis provided by tumor Tfh-like cells.

In *Roquin*$^{san/+}$ tumors, we demonstrated an accumulation of plasma precursor cells and plasmablasts and proposed that this is related to increased T-B crosstalk facilitated by SAP and adhesion molecules such as LFA-1. In line with this, we also found increases in total IgG1 and IgG2c at steady state in tumor-bearing mice as compared to tumor-free mice from the same *Roquin*$^{san/+}$ background. Based on the autoimmune phenotype observed in mice homozygous for the *sanroque* mutation (182, 373), it is possible that in tumor-bearing mice, a portion of these IgG antibodies are autoantibodies. This would be consistent with human AITL, where it is

common to identify autoantibodies in the serum of patients (11, 14). Moreover, it is unclear whether intrinsic B cell dysfunction as a result of the *sanroque* mutation may also be involved. It has been reported that the *sanroque* mutation contributes to the autoimmune manifestations in *Roquin*$^{san/san}$ mice through T cell intrinsic mechanisms (372, 373). Nonetheless, whether this also holds true in AITL-like disease in *Roquin*$^{san/+}$ mice has yet to be fully investigated.

Removal of CD4-specific SAP from fully developed AITL-like tumors demonstrated long-lasting tumor regression (Fig. 2.3E-G), suggesting that the ability to maintain T-B conjugates is essential for AITL-like tumor growth. Because interactions between SAP and Fyn kinase are well-documented (240, 419, 420), and because Fyn mutations have been implicated in human AITL disease (38, 44, 65), we wanted to test whether this interaction may be important in tumorigenesis. However, AITL-like tumors could still develop when SAP-Fyn signaling was abrogated, and these tumors shared characteristics with those expressing wildtype SAP (Fig. 2.4). While the possibility that SAP-Fyn interactions could still be involved during tumor progression cannot be definitively ruled out, based on what is reported in the scientific literature, namely that loss of SAP-Fyn interactions does not prevent a normal humoral immune response or T-B conjugate formation (421-423), our interpretation is that SAP-Fyn independent mechanisms and SAP-mediated crosstalk are likely to support AITL-like tumor growth.

Thus, one possibility is that SLAM family receptors upstream of SAP but independent of Fyn may be implicated in AITL-like disease. An intriguing pharmacological treatment could be through the manipulation of certain SLAM family receptors, specifically implicated in the humoral immune response, such as SLAMF6. It has been reported that administering anti-SLAMF6 F(ab')$_2$ antibody that stimulates SLAMF6, before protein immunization of wildtype mice reduced the frequency and number of both Tfh and GC B cells (247). This has been attributed to the ability of SLAMF6 to reduce CD3ζ phosphorylation as well as its association with inhibitory phosphatase SHP-1 (423). It has been shown that loss of SAP leads to an increased association between SLAMF6 and SHP-1 (246, 424), however, even in wildtype activated T cells, where SAP is present, SHP-1 binding to SLAMF6 can still be observed to some degree (423), providing an explanation as to why stimulating SLAMF6 inhibited Tfh and GC B cell generation. On this note, we demonstrated that acute loss of SAP from CD4$^+$ T cells led to a decreased frequency in Tfh-like cells after SAP protein loss (Fig. S2.5F). While we found that SLAMF6 was similarly expressed on Tfh cells in *Roquin*$^{san/+}$ mice regardless of tumor

stage (data not shown), we did not quantify SHP-1 levels and its ability to bind SLAMF6. Thus, it is likely that in the absence of CD4-specific SAP, there could be increased SHP-1 association with SLAMF6, which in turn could prevent optimal T-B interactions, leading to AITL-like tumor regression. Accordingly, it is plausible to hypothesize that triggering inhibitory SLAMF6 signaling may be adequate to disturb Tfh-B cell crosstalk within human AITL tumors, even when SAP protein is present. Nevertheless, as we have shown that Tfh-like cells express higher amounts of SAP as compared to total $CD4^+$ T cells (Fig. 2.3A-B), whether the ratio of SAP: SHP-1 proteins would work in favour of inhibitory phosphatase association as opposed to adaptor protein binding is an important consideration in determining whether SLAMF6 stimulation could be effective in impeding T-B crosstalk.

Our observation of increased expression of high affinity LFA-1 on $CD4^+$ T cells along with increased amounts of ICAM-1 on B cells from AITL-like tumors (Fig. 2.5A-B) is consistent with our view that T-B communication underpins AITL-like tumor pathogenesis. Studies have reported that ICAM-1 expression on B cells is important for stable T-B conjugates in an antigen-specific manner that supports B cell selection, proliferation and differentiation into the plasma cell lineage (125, 261). Since *Icam1* expression can be induced downstream of BCR activation (425, 426) and it is reported to be upregulated in activated B cells from human tonsils (427), it is likely that elevated ICAM-1 levels on B cells in AITL-like tumors reflects an activated status, which also increases its probability to engage with tumor cells expressing high affinity LFA-1. The increased high affinity LFA-1 on $CD4^+$ T cells in AITL-like tumors may be due to hyperactive TCR signaling (251), potentially as a response to self and/or innocuous antigens. In turn, binding to ICAM-1 can induce Bcl6 expression and promote Tfh cell identity as well as survival (118). These Tfh cells, which have augmented helper functions compared to non-Tfh cell subsets can then deliver even more specialized help to B cells, and assist in their expansion, differentiation and immunoglobulin hyperproduction. Thus, LFA-1/ICAM-1 binding may represent a mutually beneficial example of T-B crosstalk that supports AITL-like disease.

Additionally, through LFA-1, there may be a converging signaling mechanism between our AITL-like mouse model and human AITL patients with the $RHOA^{G17V}$ mutation. Interactions between RHOA-G17V and VAV1 adaptor protein, which are unique to mutant RHOA have been reported to lead to the phosphorylation and activation of VAV1 which then enhances TCR signaling via SLP76 and PLCγ1 (43). Moreover, VAV1 has also been shown to be required for

TCR-mediated inside-out activation of LFA-1 (428). Accordingly, one possibility is that in human AITL, RHOA-G17V activation of VAV1 and subsequent TCR activation may increase LFA-1 affinity, which in turn reinforces Bcl6 expression and propagates features of Tfh-like cells within tumor cells. For human AITL patients with activating mutations in TCR signaling components, there also remains the possibility that elevated TCR-mediated signaling may also promote the high affinity conformational change of LFA-1 on tumor cells, although, levels of high affinity LFA-1 in human AITL tumors have not been reported.

Our attempt to inhibit the conformational change of LFA-1 using Lovastatin yielded an overall partial and heterogenous response, where 6/13 mice experienced a partial or full regression and 7/13 mice showed no response to treatment (Fig. 2.5E-F). One postulation for the difference between responses may be due to the heterogenous nature of individual tumors. For instance, tumors of similar sizes can have differences in how extensive their vascularization is, which could impact drug accessibility. Additionally, Lovastatin is also a cholesterol-lowering drug (429), and consequently, this may also lower its efficacy in inhibiting the conformational change of LFA-1, especially considering that its metabolized form has a reduced capacity to inhibit LFA-1 (430). It is also important to consider the potential influence of cholesterol reduction on T cell function, as cholesterol can impact the stability of lipid raft domains, and thus, downstream TCR signaling and T cell activation (431). However, even compared to other statins such as Rosuvastatin or Atorvastatin, Lovastatin is less efficient in reducing cholesterol levels and furthermore, Lovastatin has a low bioavailability (5%) and half-life (3 hours), which also may reduce its *in vivo* effect (432). However, derivatives of Lovastatin which are more potent inhibitors of LFA-1 that lack this cholesterol-lowering ability have been produced (387), and if tested in tumor-bearing AITL-like mice could show improved results as compared to Lovastatin.

Within the context of Chapter 2, we primarily focused on the role of Lovastatin in its capacity to inhibit the conformational change of active LFA-1, however, there are several other mechanisms whereby Lovastatin can exert its influence on the immune system (433). In a mouse model of spontaneous mammary tumor development, it was reported that tumor-bearing mice treated with Lovastatin had increased $CD8^+$ T cell infiltration into the tumor site as well as a reduction in pro-tumor M2-like macrophages (434). Accordingly, Lovastatin may promote tumor regression in AITL-like tumors by enhancing tumor immunosurveillance mechanisms. However,

in a model of skin inflammation, it has also been shown that Lovastatin treatment leads to Treg cell recruitment and increased production of immunosuppressive *Il-10* mRNA (435). This may indicate that Lovastatin can also promote protumor Treg cell accumulation in AITL-like tumors, and as such, could partly explain the diverse responses observed when tumor-bearing *Roquin*$^{san/+}$ mice were treated with Lovastatin. One postulation is that in mice that experienced a full regression, Lovastatin treatment tipped the balance in favour of antitumor mechanisms as opposed to protumor immune mechanisms. However, further investigation would be needed in order to fully dissect the specific immune mechanisms by which Lovastatin influences AITL-like tumor progression.

Because of the previously reported role of high affinity LFA-1 in Tfh cells and the germinal center response (118), we primarily focused on addressing the effect of LFA-1 interactions with ICAM-1 in AITL-like tumors. However, since LFA-1 can also bind to numerous other adhesion molecules such as ICAM-2, -3, -4 and -5 and the JAM-1 family (436), these additional adhesion molecules may also help maintain AITL-like disease progression. On this note, gene expression studies from human AITL patients demonstrated an enrichment in genes associated with cell adhesion such as ICAM-1, -2, -3 and -5 (285). At the immunological synapse of T cells, VLA-4 can also be found, although its engagement has been reported to support Th1 cell polarization (437, 438). While Tfh cells mostly express integrin subunits α_L and β_2 which correspond to LFA-1, other integrin subunits such as β_1, β_3, α_4, and α_V can also be found expressed on Tfh cells, albeit at considerably lower levels as compared to LFA-1 (118). Of these other integrins, only α_V has a reported influence in the GC reaction (191). In the absence of α_V in $CD4^+$ T cells, these α_V-deficient Tfh cells can not accumulate in GCs, thereby compromising the production of long-lived plasma cells (191). In human AITL, genes associated with these integrins are not found to be differentially expressed, however, since their biological relevance is linked to their affinity, addressing this aspect of integrin biology in AITL could be informative in predicting patient prognosis.

4.2 Contextualization of SLAMF7, CD47 and macrophage-mediated immune surveillance mechanisms in AITL disease

In Chapter 3, we observed that Tfh-like cells from AITL-like tumors contained a subset with enriched SLAMF7 and Ki-67 expression (Fig. 3.1B, E, F). Based on what has been shown in the scientific literature, we postulated that this could be explained by a natural negative feedback mechanism in highly activated $CD4^+$ T cells (333). Interestingly, the *Slamf7* gene has been shown to be a direct target of Bcl6, leading to *Slamf7* downregulation (199). Consequently, when the DNA-binding activity of Bcl6 is lost from AITL-like tumors, potentially increased SLAMF7 protein levels on Tfh-like cells could also contribute to tumor regression by increasing tumor cell phagocytosis, in addition to the impact of losing Bcl6-driven tumor cell identity. It is curious to observe a highly proliferative subset of Tfh-like cells also expressing increased amounts of SLAMF7 in AITL-like tumors. One possibility is that this subset may represent Tfh-like cells with formerly high levels of Bcl6 activity, now experiencing Bcl6 autoregulation, which in turn may begin to reverse the effects of Bcl6 such as *Slamf7* expression. Additionally, higher SLAMF7 on putative tumor Tfh-like cells may also provide an explanation as to why Tfh-like tumor cells remain a small proportion of the tumor mass in comparison to B cells (270). If the phagocytic rate of $SLAMF7^+$ tumor Tfh-like cells is slower or less efficient than the proliferative rate of neoplastic Tfh-like cells that are superior at quality T-B interactions, AITL-like disease can continue to progress. Nonetheless, it also remains to be tested whether SLAMF7 may play a specialized role unique to Tfh-like cells in the continued maintenance of AITL-like tumors.

To investigate whether SLAMF7 is directly involved in supporting AITL-like tumor growth, a similar method as described with Bcl6 and SAP from Chapter 2 can be used to delete SLAMF7 in a CD4-specific manner once $Roquin^{san/+}$ mice develop tumors. According to my original hypothesis, it can be predicted that loss of prophagocytic SLAMF7 on the surface of $CD4^+$ T cells within fully developed AITL-like tumors would protect tumor cells from being engulfed by intratumoral macrophages. Accordingly, loss of CD4-specific SLAMF7 would be expected to cause tumor-bearing mice to increase the rate of tumor growth and/or spreading to other lymph nodes. However, if SLAMF7 plays a dominant role in promoting the survival or growth of Tfh-like tumor cells, then SLAMF7 deletion can be predicted to cause tumor regression. If this occurs, then understanding SLAMF7 signaling mechanisms through its adaptor

protein EAT-2 may provide more insight into AITL disease progression. Finally, to address the role of SLAMF7 more directly on AITL-like tumor initiation, the *Slamf7* gene could be deleted from $CD4^+$ T cells in young $Roquin^{san/+}$ mice before the age of expected AITL-like tumor development after which the rate of tumor onset can be compared between SLAMF7-sufficient and -deficient mice.

Since SLAMF7 is an activating receptor of macrophage-mediated phagocytosis, increased expression on a subset of Tfh-like cells may also augment its susceptibility to macrophage engulfment (241). While we demonstrated that *in vitro* CD47 blockade increased the frequency of AITL-like tumor cells phagocytosed by macrophages (Fig. 3.4), whether higher SLAMF7 expression levels correlated with this increase was not determined. Furthermore, SLAMF7 is expressed in a subset of AITL patients but not all AITL patients (321, 322), and how it correlates with disease severity or survival has not been studied. Nonetheless, this may not be a limiting factor to enhance macrophage-mediated phagocytosis upon CD47 inhibition, since in DLBCL, lack of SLAMF7 did not impair the ability of CD47 signaling inhibition to increase phagocytosis of tumor cells (412).

Histological identification of $CD47^+$ cells in human AITL demonstrated a wide range of expression profiles, where CD47 levels did not appear to correlate with overall survival (323). However, without co-staining for other Tfh cell markers such as Bcl6, SAP, or PD-1, it is difficult to definitively understand the relation between CD47-expressing tumor cells and patient outcomes. This is also highlighted in our murine AITL-like tumors, where total $CD4^+$ T cells from tumor-free, non-tumor and tumor samples had similar levels of CD47, and increased CD47 MFI could only be appreciated amongst Tfh-like cells from AITL-like tumors (Fig. 3.2A,C). This suggests that either Tfh-like cells are upregulating inhibitory CD47 signals to avoid being engulfed by intratumoral macrophages or Tfh-like cells with lower levels of CD47 are actively being removed, allowing only those with relatively higher levels of CD47 to survive. Although we observed that CD47 MFI was increased by approximately 15% between tumor-free/non-tumor Tfh cells and AITL-like tumor cells, this difference may be sufficient to prevent phagocytosis *in vivo*. Since it has been shown that CD47 clustering patterns influences SIRPα engagement (329), even small differences in total CD47 levels could be meaningful physiologically, depending on how CD47 is organized along the cell membrane. Importantly, it is also the balance between prophagocytic and antiphagocytic signaling in macrophages that

ultimately influences the overall outcome of phagocytosis, such that inhibiting CD47 signaling may be inadequate to induce macrophage-mediated tumor cell engulfment if macrophages do not receive enough positive signaling reinforcements from SLAMF7 and/or Fc receptor signaling.

Chapter 5 Conclusion and Future Directions

5.1 Conclusions

The overarching goal of this thesis was to investigate immune mechanisms in AITL-like disease progression (Fig. 5.1A). In Chapter 2, I presented the results of Aim 1 which sought to determine to what extent tumor Tfh-like cells still retained features of physiological Tfh cells. Within Chapter 3, I examined the influence of macrophage-mediated phagocytosis in AITL-like tumors, focusing on the objectives highlighted in Aim 2. Our findings provide new insight into the importance of signature Tfh cell proteins in AITL-like disease and provide evidence that tumor Tfh cell hyper functionality is vital to support the pathogenic B cell-related activities observed in AITL-like disease. It also increased our understanding of macrophage-related immune surveillance in AITL-like tumors and demonstrated the increased susceptibility of AITL-like tumor cells to macrophage-dependent phagocytosis after CD47 inhibition *in vitro*. Combining the results and interpretations from Chapter 2 and 3 allow us to postulate new pharmacological interventions in AITL that could benefit from the synergy of inhibiting Tfh-B cell crosstalk and boosting macrophage-mediated phagocytic activities against tumor cells.

In Chapter 2, I demonstrated that hyperactive Tfh-like cells in AITL-like tumors can facilitate B cell differentiation into plasma cell precursors and plasmablasts, even in the absence of traditional GCs. Furthermore, expression of Bcl6 was essential in maintaining AITL-like disease, highlighted by the tumor regression observed upon loss of Bcl6 activity. Additionally, within AITL-like tumors, $CD4^+$ T cells with high SAP expression levels were highly proliferative, suggesting that AITL-like tumor cells might somehow utilize SAP for their growth. In line with this, gene deletion of SAP from developed tumors also led to regression. Since loss of SAP-Fyn interactions did not impair AITL-like disease development, we hypothesized that SAP must be promoting AITL-like tumors through T-B conjugation, for instance by using adhesion molecules. By profiling the affinity of integrin LFA-1 and its binding partner ICAM-1, I showed increased expression of these molecules on T and B cells within AITL-like tumors, potentially a reflection of enhanced quality T-B communication. However, inhibition of LFA-1 affinity using Lovastatin showed an overall partial response, and while there is great potential in examining therapies aimed at inhibiting T-B crosstalk, extensive optimization and testing must be done before translating this into the clinic.

In Chapter 3, I presented results suggesting that opposition between immune surveillance and tumor growth exists in AITL-like tumors. I found that within tumors, Tfh-like cells had

elevated levels of inhibitory CD47, potentially signifying a mechanism for evading macrophage-mediated phagocytosis. Conversely, SLAMF7 was highly expressed on both macrophages and a subset of Tfh-like cells from AITL-like tumors, suggesting that even though positive receptors for phagocytosis are present, macrophages are unable to effectively control tumor growth. On GC B-like cells from AITL-like tumors, CD47 levels were similar irrespective of tumor stage, however, SLAMF7 expression was reduced on GC B-like cells in tumors. Nonetheless, we found that co-culturing AITL-like tumor cells with BMDMs in the presence anti-CD47 antibodies could enhance tumor cell engulfment by macrophages.

Taken together, the results of these studies support my hypothesis that Tfh cell identity and function remains pivotal for the neoplastic activities of AITL-like tumor cells, a novel finding which can be important for understanding the mechanisms behind AITL disease pathogenesis as well as clinical applications. Furthermore, these studies also validate that AITL-like tumor cells can be more efficiently phagocytosed after being subject to CD47 signaling inhibition *in vitro*, further demonstrating that this inhibitory "don't eat me" signal can be overcome to promote macrophage-dependent engulfment. As such, manipulating CD47-SIRPα signaling *in vivo* could also be a promising clinical avenue to treat AITL patients.

However, this relatively modest increase in phagocytosis may not translate into tumor regression *in vivo* and may require additional prophagocytic signaling boosts. This could be provided by combining CD47 blockade along with SLAMF7 stimulation or by using antibodies to target Tfh cell-specific surface molecules such as LFA-1 that would also trigger Fc receptor-mediated phagocytosis, the latter being a therapeutic approach with promising results in DLBCL patients with combined anti-CD47 and anti-CD20 antibodies (319, 320). Therefore, combining the direct targeting of Tfh-B cell crosstalk along with indirectly modulating the tumor microenvironment in favour of macrophage-mediated tumor cell clearance may provide the most efficient pharmacologic approach to control AITL disease progression (Fig. 5.1B).

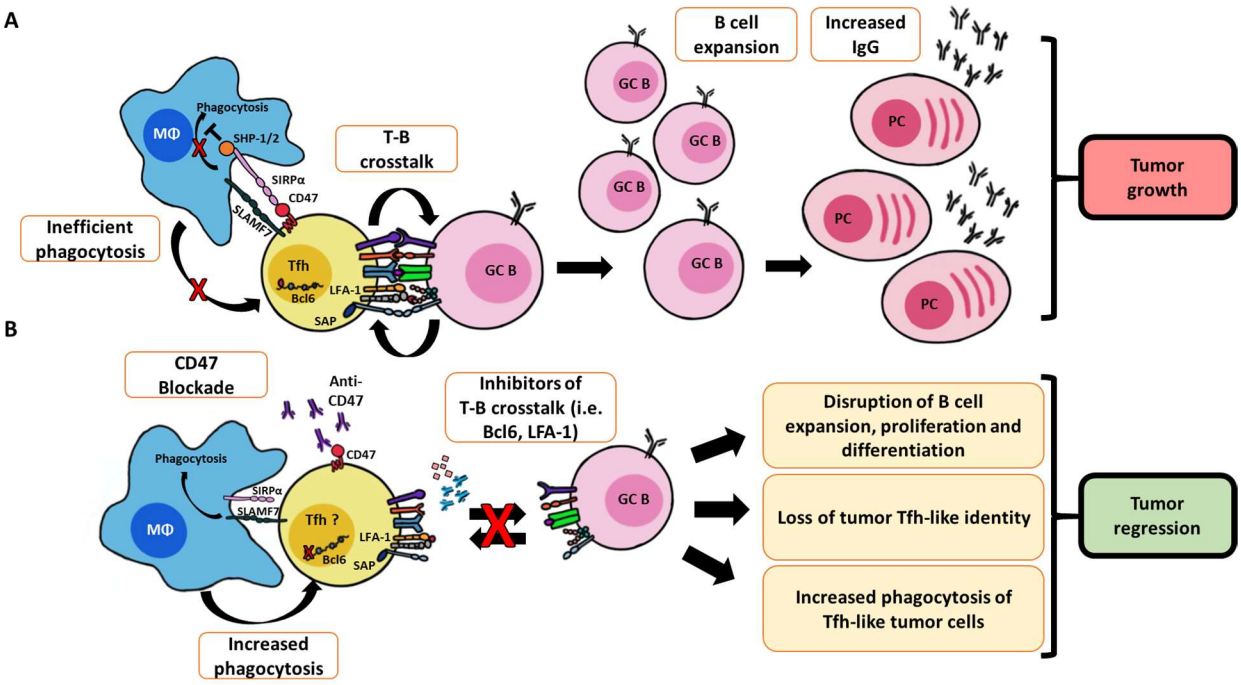

Figure 5.1 Overview of intrinsic and extrinsic mechanisms supporting AITL tumor growth

(A) Intimate T-B interactions between tumor Tfh-like cells and GC B cells in AITL-like tumors facilitated by Tfh cell identity proteins such as Bcl6, SAP and LFA-1 supports B cell expansion, plasma cell differentiation and hypergammaglobulinemia. In parallel, tumor Tfh-like cells can also inhibit immune surveillance mechanisms provided by macrophage-mediated phagocytosis and thus, the overall impact is the promotion of AITL-like tumor progression. (B) Introducing pharmacological inhibition of T-B interactions or Tfh cell identity by using inhibitors of Bcl6 or LFA-1 in addition to removing inhibitory CD47 signaling may synergistically work to encourage tumor regression.

5.2 Future Directions

Although we were able to shed light on our understanding of the Tfh cell nature of AITL-like tumor cells as well as macrophage-related immunosurveillance mechanisms operating in AITL-like disease, we were also unable to address all our inquiries. Thus, certain results left us with several important questions for which future extension studies are warranted.

5.2.1 Bcl6-dependent mechanisms in AITL disease initiation and progression

Our finding that Bcl6 activity is continually utilized in developed AITL-like tumors is altogether not surprising considering the Tfh cell origin of this disease and the well-established

role of Bcl6 in B cell lymphomagenesis (207). Additionally, several studies have established the essential role of Bcl6 in Tfh cell identity and development (111-113, 197, 215), however, beyond its function as a master regulator transcription factor for Tfh cells, does Bcl6 acquire AITL-specific gene targets to facilitate tumor growth? One series of questions relates to how Bcl6 drives and supports AITL tumor growth as there remains numerous possibilities for how Bcl6 impacts AITL tumorigenesis. One easy explanation is that loss of Bcl6 activity immediately causes Tfh-like tumor cells to lose their identity and successive signaling pathways which support their tumorous activities. An additional possibility is that dysregulated Bcl6 expression is necessary to transform pre-tumor cells into their fully neoplastic form.

In DLBCL, certain patients have point mutations in the first non-coding exon of *BCL6*, which is associated with loss of Bcl6-mediated auto-inhibition (213, 214). In AITL, such *BCL6* mutations have been not identified, however, understanding whether Bcl6 autoregulatory feedback is active or inactive in tumor Tfh-like cells would be informative in understanding Bcl6 within the context of AITL disease. In human AITL patients with *TET2* mutations as well as mice with reduced TET2 function, hypermethylation of Bcl6 at intron 1 occurs more frequently and correlates with increased protein expression (54, 55). However, even in AITL patients without *TET2* mutations, it is still possible that these negative regulatory regions could become inaccessible to Bcl6 binding and self-regulation, thereby promoting AITL disease through sustained overexpression of Bcl6. This can be determined using experimental techniques such as bisulfite sequencing to identify potential hypermethylation of regions associated with Bcl6 negative autoregulation. Alternatively, there could also be other mechanisms driving AITL tumorigenesis which do not require Bcl6 overexpression.

Bcl6 regulation can also exist at the post-translational level to control its localization and stability. For instance, in Tfh cells, Bcl6 phosphorylation by Prkd2 has been reported to cause a reduction in its nuclear localization (226). In another situation, B cell-specific FBXO11 was shown to regulate Bcl6 ubiquitylation and degradation (222). In human AITL, it has not yet been described whether Bcl6 may become deregulated through increased production, nuclear localization and/or increased stability. Additionally, because our experimental design specifically focused on the DNA-binding portion of Bcl6, it remains possible that interactions between Bcl6 and corepressors or other protein complexes may also contribute to AITL tumor progression.

Profiling levels of SAP, PD-1 or CXCR5 shortly after loss of Bcl6 DNA-binding activity demonstrated very minimal changes, primarily in the reduction of CXCR5 MFI amongst Tfh-like cells (Fig. S2.5C-D). It has been reported that Bcl6 is involved in a "repressor-of-repressors" regulatory gene network where Bcl6 is central to Tfh cell identity by inhibiting transcription factors such as Runx2, Runx3 and Klf2, negative regulators of Tfh cell genes such as *Pdcd1*, *Icos*, *Il6ra*, *Il21* and *Il4* (215). Consequently, studying the acute impact of *Bcl6* deletion shortly after tamoxifen administration was likely insufficient to visualize changes in downstream Tfh cell proteins such as SAP, PD-1 or CXCR5 which are regulated through a cascade of transcription factors. Nonetheless, paired with the knowledge that Bcl6 is essential for Tfh cell generation and that in the long-term, loss of Bcl6 activity causes AITL-like tumor regression, Bcl6 can be expected to be involved in Tfh cell and AITL tumor cell-specific gene expression changes.

In our mouse model, we observed similar levels of Bcl6 MFI amongst Tfh or Tfh-like $CD4^+CXCR5^+PD\text{-}1^+$ cells when comparing tumor-free, non-tumor and tumor samples (Fig. 2.2F), suggesting that neoplastic transformation can occur without Bcl6 overexpression. This may better reflect the situation in human AITL patients without *TET2* mutations. However, it is highly probable that AITL-like tumor cells develop a tumor-specific gene signature, distinct from what is found in non-neoplastic Tfh cells coming from tumor-free lymph nodes. Moreover, since we observed that loss of Bcl6 activity leads to AITL-like tumor regression, these tumor-specific gene signatures presumably still rely on Bcl6-dependent pathways, whether directly or indirectly. Thus, on the one hand, it is conceivable to hypothesize that $CD4^+CXCR5^+PD\text{-}1^+$ Tfh-like cells in tumors could be a homogenous population of tumor Tfh-like cells that have acquired an "oncogenic" gene signature. On the other hand, a second possibility is that within AITL-like tumors, there might be heterogeneity amongst $CD4^+CXCR5^+PD\text{-}1^+$ Tfh-like cells, where only a subpopulation has this tumor-specific gene signature. Based on data presented in Chapter 2 and 3, where we observe diverse protein expression levels of Ki-67, SAP or SLAMF7, it is more likely that there exists heterogeneity amongst Tfh-like cells within AITL-like tumors. Nonetheless, these important questions can be addressed using genomic approaches such as Bcl6 ChIP-Seq, single-cell ATAC-Seq or single-cell RNA-Seq and will offer important insights into understanding AITL disease progression.

After Tfh cell development, during the natural course of the GC reaction, Tfh cells are reported to downregulate Bcl6 levels and acquire memory-like features, such as IL7Rα expression (99, 149, 151). Moreover, since memory Tfh cells are generally considered to express CXCR5 but can have high or low levels of PD-1 (34, 152, 439-442), our observation of reduced PD-1 MFI (Fig. 2.2D) in Tfh-like cells from AITL-like tumors may suggest the presence of memory-like characteristics. Thus, within our mouse model and possibly human patients without *TET2* mutations, one postulation is that neoplastic transformation of tumor Tfh-like cells occurs after a Bcl6-mediated negative autoregulation loop and acquisition of memory-like features. Although memory Tfh cell-derived lymphomas are not reported, recent studies demonstrate that aggressive B cell lymphomas can arise from B cells with epigenetic and transcriptomic features of memory B cells (427, 443), and consequently, an in-depth genomic analysis could help address whether tumor-Tfh like cells express additional markers typically associated with a memory phenotype.

Since Bcl6 is reported to associate with histone methyltransferase EZH2 and the non-canonical PRC1-BCOR-CBX8 complex to promote hyperactive GCs and DLBCL onset (219), in AITL, whether Bcl6 may also be involved in disease maintenance by cooperating with proteins involved in epigenetic modifications is an important line of future investigation. Moreover, both BCOR and EZH2 have also been demonstrated to support Tfh cell generation (220, 221), and thus, it is useful to study whether a similar mechanism involving Bcl6, BCOR and EZH2 could also operate in Tfh cells and further, this may explain how Bcl6 supports AITL disease. On this note, in one cohort of AITL patients studied, approximately 60% of patients highly expressed EZH2 and in the same study, PTCL patients with high EZH2 expression were also observed to experience poorer overall survival rates (82), suggesting that higher EZH2 expression could be associated with more aggressive disease characteristics. In line with this, I found that Tfh-like cells from AITL-like tumors expressed the highest amounts of EZH2 as compared to Tfh cells from tumor-free or non-tumor lymph nodes (data not shown). Additionally, the 3'UTR of *Bcor* has been recently identified as a Roquin-1 target (444), and thus, it would be interesting to study whether there are also elevated levels of BCOR protein in AITL-like tumors and if this also translates to increased Bcl6-BCOR interactions. To address whether AITL-like disease initiation requires Bcl6-BCOR interactions, *Roquin*$^{san/+}$ mice can be bred with Bcl6 mutant mice without the ability to interact with BCOR and monitored for tumor development (204, 208). Moreover,

since another Bcl6 corepressor, NCOR1 has been implicated in the negative autoregulation of Bcl6 within Tfh cells (215), addressing whether NCOR1 might also play a role in AITL-like disease growth is important. To understand whether BCOR, NCOR1 or EZH2 are required to sustain AITL-like tumor progression, genes encoding these proteins can be acutely deleted from fully developed AITL-like tumors using an experimental method similar to SAP or Bcl6 gene deletion from Chapter 2.

Finally, although our gene deletion approach allowed us to reveal the importance of Bcl6 in AITL-like tumors from *Roquin*$^{san/+}$ mice, we did not extend this to demonstrate whether the same results could be achieved using Bcl6 inhibitors, a method more applicable in the clinical setting. Within the B cell lymphoma field, at least two Bcl6 inhibitors, 79-6 and FX-1 have been reported with promising results (95, 445). These inhibitors bind to the BTB domain of Bcl6 and prevent corepressor binding to Bcl6, thus disrupting the ability of Bcl6 to bind its target genes (95, 445). In DLBCL xenografted mice, treatment with FX-1 suppressed tumor growth and importantly, FX-1 appeared to be well-tolerated in treated mice (95). Additionally, there is another type of Bcl6 inhibitor that has been developed, which also targets the BTB domain, but instead of preventing corepressor binding, it targets the BTB domain by inducing ubiquitylation and proteasome-mediated degradation of Bcl6 (446). In AITL, it can be predicted that Bcl6 may be an excellent therapeutic candidate that targets not only the identity of Tfh cells but also the overall GC response. An important consideration is the potential negative impact from the long-term use of Bcl6 inhibitors, which has not been fully validated. In mouse models, mice were treated for approximately 10 days, and no signs of toxicity, inflammation or infection were observed (95), but in a clinical setting, patients would likely need routine treatment that would extend beyond 10 days, which could leave them more vulnerable to infection.

5.2.2 Impact of macrophage-mediated immune surveillance in AITL tumor growth and spreading

In AITL-like tumors, we identified an increased proportion of F4/80^{+}Mac-1^{+} macrophages that expressed both SIRPα and prophagocytic molecule SLAMF7 in comparison to tumor-free or non-tumor lymph nodes (Fig. 3.3C). It appears that macrophages within AITL-like tumors are well-equipped to phagocytose AITL-like tumor cells, and yet, have failed to control tumor initiation and progression. Although we did observe that BMDMs from the *Roquin*$^{san/+}$

background were able to increase phagocytic efficiency of total or $CD4^+$ T cells from AITL-like tumors after treatment with anti-CD47 antibody (Fig. 3.4C), this may not be easily recapitulated in a more complex *in vivo* environment. Firstly, since neoplastic Tfh-like cells represent a minority of the tumor mass in both humans and mice (30, 270), macrophages could have difficulty directly accessing and engulfing tumor cells. Secondly, tumor cells may not only express inhibitory CD47, but other unidentified proteins that have a negative effect on macrophage-mediated phagocytosis. Nevertheless, with certain types of stimulation, regardless of CD47 expression, the phagocytic capacity of macrophages within AITL could still be enhanced. This was been demonstrated using a mouse model of pancreatic ductal adenocarcinoma, where it was reported that CpG administration was able to metabolically reprogram macrophages to more effectively phagocytose tumor cells even when CD47 was expressed on tumor cells (447). Thus, if therapies aimed at targeting *in vivo* inhibition of CD47 signaling does not reduce tumor growth, testing therapies such as CpG to promote macrophage activation could be applied to AITL-like tumor-bearing mice.

It will be important to understand the features of macrophages within the AITL tumor microenvironment beyond the simple M1 and M2 macrophage subsets (78, 81), especially because lymph nodes contain many macrophage subsets, such as tingible body, subcapsular sinus, medullary sinus and medullary cord macrophages (308, 309). Understanding what other proteins are expressed by intratumoral macrophages and to what degree they contribute to tumor growth and spreading is also important to determine their impact in immunosurveillance. If macrophage-mediated phagocytosis is indeed directly controlling AITL tumor growth and spreading, then eliminating macrophages in tumor-bearing mice can be hypothesized to increase the rate of AITL tumor growth and appearance in secondary locations. This idea can be tested by depleting macrophages from tumor-bearing mice using clodronate liposomes (448) or through genetic models such as CD11b-diptheria toxin receptor (DTR) mice (449), although, the caveat with both methods is that they can also eliminate other cell populations such as dendritic cells and they only provide temporary depletion (448, 449).

In addition to macrophage depletion, future experiments should also focus on assessing the *in vivo* phagocytic ability of intratumoral macrophages in AITL-like tumors. One way this can be addressed is by performing multi-colour confocal imaging to visualize macrophages engulfing Tfh or Tfh-like cells (450). In order to see whether the minor increase in CD47

expression on Tfh-like cells within AITL-like tumors corresponds to any *in vivo* resistance to phagocytosis, experiments to characterize the baseline level of phagocytosis in tumor-free, non-tumor and tumor samples could be performed. Moreover, using the same methodology, comparing the rate of phagocytosis in *Roquin*$^{san/+}$ tumor-bearing mice treated with or without anti-CD47 antibodies could also help validate our *in vitro* observations. Another way to test the *in vivo* functionality of intratumoral macrophages could be to inject pHrodo dye labelled AITL-like tumor cells into tumor-bearing mice with or without CD47 inhibition. This type of dye only emits fluorescence at low pH levels, which occurs within phagocytic cells during lysosomal fusion (451). The rate of tumor cell engulfment could then be quantified using flow cytometry or immunofluorescence imaging. This method may help demonstrate whether intratumoral macrophages can still function as phagocytes and whether they are more or less effective than macrophages found within non-tumor lymph nodes of the same mouse. There is however the possibility that the injected tumor cells may not survive this type of experimental manipulation, especially if they are heavily reliant on signals from the tumor microenvironment.

In human AITL, an increased ratio of M2 macrophages is associated with poor survival, largely due to their immunosuppressive nature (78, 81). Although this feature has not been directly associated with any specific AITL mutation, it has been reported that AITL and PTCL-NOS patients with *TET2* mutations are associated with advanced disease stage, which is also a reflection of the number of lymph nodes impacted and extranodal involvement (50). One possible explanation for this could be that *TET2* mutations may cause dysregulated Bcl6 expression in T cells, B cells and macrophages, where in T and B cells, this promotes their GC phenotype. However, in macrophages, this may reduce their responsiveness and ability to mount an effective antitumor response against tumor cells, since Bcl6 has been reported to prevent macrophages from entering a hyperinflammatory and proliferative state by inhibiting IL-6/STAT3 signaling (200, 452). Thus, AITL patients with *TET2* mutations may experience poorer clinical presentation because they not only have a propensity towards developing hyperactive Tfh and B cells but also macrophage populations that may not be apt for phagocytosis.

Chapter 6 References

1. Federico M, Rudiger T, Bellei M, Nathwani BN, Luminari S, Coiffier B, et al. Clinicopathologic characteristics of angioimmunoblastic T-cell lymphoma: analysis of the international peripheral T-cell lymphoma project. Journal of clinical oncology : official journal of the American Society of Clinical Oncology. 2013;31(2):240-6.
2. Lunning MA, Vose JM. Angioimmunoblastic T-cell lymphoma: the many-faced lymphoma. Blood. 2017;129(9):1095-102.
3. Yabe M, Dogan A, Horwitz SM, Moskowitz AJ. Angioimmunoblastic T-Cell Lymphoma. In: Querfeld C, Zain J, Rosen ST, editors. T-Cell and NK-Cell Lymphomas: From Biology to Novel Therapies. Cham: Springer International Publishing; 2019. p. 99-126.
4. Attygalle AD, Kyriakou C, Dupuis J, Grogg KL, Diss TC, Wotherspoon AC, et al. Histologic Evolution of Angioimmunoblastic T-cell Lymphoma in Consecutive Biopsies: Clinical Correlation and Insights Into Natural History and Disease Progression. The American Journal of Surgical Pathology. 2007;31(7):1077-88.
5. Moskowitz AJ. Practical Treatment Approach for Angioimmunoblastic T-Cell Lymphoma. Journal of oncology practice. 2019;15(3):137-43.
6. Mourad N, Mounier N, Briere J, Raffoux E, Delmer A, Feller A, et al. Clinical, biologic, and pathologic features in 157 patients with angioimmunoblastic T-cell lymphoma treated within the Groupe d'Etude des Lymphomes de l'Adulte (GELA) trials. Blood. 2008;111(9):4463-70.
7. Kang HY, Hwang JH, Park YS, Bang SM, Lee JS, Chung JH, et al. Angioimmunoblastic T-cell lymphoma mimicking Crohn's disease. Dig Dis Sci. 2007;52(10):2743-7.
8. Chams S, Hajj Hussein I, El Sayegh S, Chams N, Zakaria K. Hypercalcemia as a rare presentation of angioimmunoblastic T cell lymphoma: a case report. J Med Case Rep. 2018;12(1):101.
9. Cortes JR, Palomero T. The curious origins of angioimmunoblastic T-cell lymphoma. Current opinion in hematology. 2016;23(4):434-43.
10. Cho YU, Chi HS, Park CJ, Jang S, Seo EJ, Huh J. Distinct features of angioimmunoblastic T-cell lymphoma with bone marrow involvement. American journal of clinical pathology. 2009;131(5):640-6.
11. de Leval L, Gisselbrecht C, Gaulard P. Advances in the understanding and management of angioimmunoblastic T-cell lymphoma. Br J Haematol. 2010;148(5):673-89.
12. Dunleavy K, Wilson WH, Jaffe ES. Angioimmunoblastic T cell lymphoma: pathobiological insights and clinical implications. Current opinion in hematology. 2007;14(4):348-53.
13. Frizzera G, Moran EM, Rappaport H. Angio-immunoblastic lymphadenopathy. Diagnosis and clinical course. Am J Med. 1975;59(6):803-18.
14. Dogan A. Angioimmunoblastic T cell Lymphoma
British Journal of Haematology. 2003;121:681 - 91.
15. Willenbrock K, Brauninger A, Hansmann ML. Frequent occurrence of B-cell lymphomas in angioimmunoblastic T-cell lymphoma and proliferation of Epstein-Barr virus-infected cells in early cases. Br J Haematol. 2007;138(6):733-9.

16. Eladl AE, Shimada K, Suzuki Y, Takahara T, Kato S, Kohno K, et al. EBV status has prognostic implication among young patients with angioimmunoblastic T-cell lymphoma. Cancer Med. 2020;9(2):678-88.
17. Zhou Y, Attygalle AD, Chuang SS, Diss T, Ye H, Liu H, et al. Angioimmunoblastic T-cell lymphoma: histological progression associates with EBV and HHV6B viral load. Br J Haematol. 2007;138(1):44-53.
18. Attygalle A, Al-Jehani R, Diss TC, Munson P, Liu H, Du MQ, et al. Neoplastic T cells in angioimmunoblastic T-cell lymphoma express CD10. Blood. 2002;99(2):627-33.
19. Ree HJ, Kadin ME, Kikuchi M, Ko YH, Suzumiya J, Go JH. Bcl-6 expression in reactive follicular hyperplasia, follicular lymphoma, and angioimmunoblastic T-cell lymphoma with hyperplastic germinal centers: heterogeneity of intrafollicular T-cells and their altered distribution in the pathogenesis of angioimmunoblastic T-cell lymphoma. Human pathology. 1999;30(4):403-11.
20. Baseggio L, Traverse-Glehen A, Berger F, Ffrench M, Jallades L, Morel D, et al. CD10 and ICOS expression by multiparametric flow cytometry in angioimmunoblastic T-cell lymphoma. Modern pathology : an official journal of the United States and Canadian Academy of Pathology, Inc. 2011;24(7):993-1003.
21. Roncador G, Verdes-Montenegro J-FG, Tedoldi S, Paterson JC, Klapper W, Ballabio E, et al. Expression of two markers of germinal center T cells (SAP and PD-1) in angioimmunoblastic T-cell lymphoma. Haematologica. 2007;92(8):1059-66.
22. Dorfman DM, Brown JA, Shahsafaei A, Freeman GJ. Programmed death-1 (PD-1) is a marker of germinal center-associated T cells and angioimmunoblastic T-cell lymphoma. The American journal of surgical pathology. 2006;30(7):802-10.
23. Yu H, Shahsafaei A, Dorfman DM. Germinal-center T-helper-cell markers PD-1 and CXCL13 are both expressed by neoplastic cells in angioimmunoblastic T-cell lymphoma. American journal of clinical pathology. 2009;131(1):33-41.
24. Yuan CM, Vergilio JA, Zhao XF, Smith TK, Harris NL, Bagg A. CD10 and BCL6 expression in the diagnosis of angioimmunoblastic T-cell lymphoma: utility of detecting CD10+ T cells by flow cytometry. Human pathology. 2005;36(7):784-91.
25. Stacchini A, Demurtas A, Aliberti S, Francia di Celle P, Godio L, Palestro G, et al. The usefulness of flow cytometric CD10 detection in the differential diagnosis of peripheral T-cell lymphomas. American journal of clinical pathology. 2007;128(5):854-64.
26. Horwitz S, O'Connor OA, Pro B, Illidge T, Fanale M, Advani R, et al. Brentuximab vedotin with chemotherapy for CD30-positive peripheral T-cell lymphoma (ECHELON-2): a global, double-blind, randomised, phase 3 trial. Lancet. 2019;393(10168):229-40.
27. Piccaluga PP, Agostinelli C, Califano A, Carbone A, Fantoni L, Ferrari S, et al. Gene expression analysis of angioimmunoblastic lymphoma indicates derivation from T follicular helper cells and vascular endothelial growth factor deregulation. Cancer research. 2007;67(22):10703-10.
28. Zhao WL, Mourah S, Mounier N, Leboeuf C, Daneshpouy ME, Legres L, et al. Vascular endothelial growth factor-A is expressed both on lymphoma cells and endothelial cells in angioimmunoblastic T-cell lymphoma and related to lymphoma progression. Lab Invest. 2004;84(11):1512-9.
29. de Leval L, Foss F, Gaulard P. Molecular and Clinical Aspects of Angioimmunoblastic T-Cell Lymphoma. 2013:57-69.

30. de Leval L, Rickman DS, Thielen C, Reynies A, Huang YL, Delsol G, et al. The gene expression profile of nodal peripheral T-cell lymphoma demonstrates a molecular link between angioimmunoblastic T-cell lymphoma (AITL) and follicular helper T (TFH) cells. Blood. 2007;109(11):4952-63.
31. Zhan HQ, Li XQ, Zhu XZ, Lu HF, Zhou XY, Chen Y. Expression of follicular helper T cell markers in nodal peripheral T cell lymphomas: a tissue microarray analysis of 162 cases. Journal of clinical pathology. 2011;64(4):319-24.
32. Sato F, Ishida T, Ito A, Mori F, Masaki A, Takino H, et al. Angioimmunoblastic T-cell lymphoma mice model. Leuk Res. 2013;37(1):21-7.
33. Li X, Liu Z, Mi M, Zhang C, Xiao Y, Liu X, et al. Identification of hub genes and key pathways associated with angioimmunoblastic T-cell lymphoma using weighted gene co-expression network analysis. Cancer management and research. 2019;11:5209-20.
34. Crotty S. T follicular helper cell differentiation, function, and roles in disease. Immunity. 2014;41(4):529-42.
35. Vinuesa CG, Linterman MA, Yu D, MacLennan ICM. Follicular Helper T Cells. Annual Review of Immunology. 2016;34(1):335-68.
36. Sakata-Yanagimoto M, Enami T, Yoshida K, Shiraishi Y, Ishii R, Miyake Y, et al. Somatic RHOA mutation in angioimmunoblastic T cell lymphoma. Nature genetics. 2014;46(2):171-5.
37. Yoo HY, Sung MK, Lee SH, Kim S, Lee H, Park S, et al. A recurrent inactivating mutation in RHOA GTPase in angioimmunoblastic T cell lymphoma. Nature genetics. 2014;46(4):371-5.
38. Palomero T, Couronné L, Khiabanian H, Kim M-Y, Ambesi-Impiombato A, Perez-Garcia A, et al. Recurrent mutations in epigenetic regulators, RHOA and FYN kinase in peripheral T cell lymphomas. Nature genetics. 2014;46(2):166-70.
39. Miyoshi H, Sakata-Yanagimoto M, Shimono J, Yoshida N, Hattori K, Arakawa F, et al. RHOA mutation in follicular T-cell lymphoma: Clinicopathological analysis of 16 cases. Pathol Int. 2020.
40. Dobay MP, Lemonnier F, Missiaglia E, Bastard C, Vallois D, Jais JP, et al. Integrative clinicopathological and molecular analyses of angioimmunoblastic T-cell lymphoma and other nodal lymphomas of follicular helper T-cell origin. Haematologica. 2017;102(4):e148-e51.
41. Nagata Y, Kontani K, Enami T, Kataoka K, Ishii R, Totoki Y, et al. Variegated RHOA mutations in adult T-cell leukemia/lymphoma. Blood. 2016;127(5):596-604.
42. Schwartz FH, Cai Q, Fellmann E, Hartmann S, Mayranpaa MI, Karjalainen-Lindsberg ML, et al. TET2 mutations in B cells of patients affected by angioimmunoblastic T-cell lymphoma. The Journal of pathology. 2017;242(2):129-33.
43. Fujisawa M, Sakata-Yanagimoto M, Nishizawa S, Komori D, Gershon P, Kiryu M, et al. Activation of RHOA-VAV1 signaling in angioimmunoblastic T-cell lymphoma. Leukemia. 2018;32(3):694-702.
44. Vallois D, Dobay MPD, Morin RD, Lemonnier F, Missiaglia E, Juilland M, et al. Activating mutations in genes related to TCR signaling in angioimmunoblastic and other follicular helper T-cell–derived lymphomas. Blood. 2016;128(11):1490-502.
45. Cortes JR, Ambesi-Impiombato A, Couronne L, Quinn SA, Kim CS, da Silva Almeida AC, et al. RHOA G17V Induces T Follicular Helper Cell Specification and Promotes Lymphomagenesis. Cancer cell. 2018;33(2):259-73.e7.

46. Ng SY, Brown L, Stevenson K, deSouza T, Aster JC, Louissaint A, Jr., et al. RhoA G17V is sufficient to induce autoimmunity and promotes T-cell lymphomagenesis in mice. Blood. 2018;132(9):935-47.
47. Zang S, Li J, Yang H, Zeng H, Han W, Zhang J, et al. Mutations in 5-methylcytosine oxidase TET2 and RhoA cooperatively disrupt T cell homeostasis. The Journal of clinical investigation. 2017;127(8):2998-3012.
48. Jogdand GM, Mohanty S, Devadas S. Regulators of Tfh Cell Differentiation. Front Immunol. 2016;7:520.
49. Cairns RA, Iqbal J, Lemonnier F, Kucuk C, de Leval L, Jais JP, et al. IDH2 mutations are frequent in angioimmunoblastic T-cell lymphoma. Blood. 2012;119(8):1901-3.
50. Lemonnier F, Couronne L, Parrens M, Jais JP, Travert M, Lamant L, et al. Recurrent TET2 mutations in peripheral T-cell lymphomas correlate with TFH-like features and adverse clinical parameters. Blood. 2012;120(7):1466-9.
51. Ito S, Shen L, Dai Q, Wu SC, Collins LB, Swenberg JA, et al. Tet proteins can convert 5-methylcytosine to 5-formylcytosine and 5-carboxylcytosine. Science. 2011;333(6047):1300-3.
52. Ko M, An J, Rao A. DNA methylation and hydroxymethylation in hematologic differentiation and transformation. Curr Opin Cell Biol. 2015;37:91-101.
53. Yao WQ, Wu F, Zhang W, Chuang SS, Thompson JS, Chen Z, et al. Angioimmunoblastic T-cell lymphoma contains multiple clonal T-cell populations derived from a common TET2 mutant progenitor cell. The Journal of pathology. 2020;250(3):346-57.
54. Nishizawa S, Sakata-Yanagimoto M, Hattori K, Muto H, Nguyen T, Izutsu K, et al. BCL6 locus is hypermethylated in angioimmunoblastic T-cell lymphoma. International journal of hematology. 2017;105(4):465-9.
55. Muto H, Sakata-Yanagimoto M, Nagae G, Shiozawa Y, Miyake Y, Yoshida K, et al. Reduced TET2 function leads to T-cell lymphoma with follicular helper T-cell-like features in mice. Blood cancer journal. 2014;4:e264.
56. Delhommeau F, Dupont S, Della Valle V, James C, Trannoy S, Masse A, et al. Mutation in TET2 in myeloid cancers. N Engl J Med. 2009;360(22):2289-301.
57. Ko M, Huang Y, Jankowska AM, Pape UJ, Tahiliani M, Bandukwala HS, et al. Impaired hydroxylation of 5-methylcytosine in myeloid cancers with mutant TET2. Nature. 2010;468(7325):839-43.
58. Dominguez PM, Ghamlouch H, Rosikiewicz W, Kumar P, Beguelin W, Fontan L, et al. TET2 Deficiency Causes Germinal Center Hyperplasia, Impairs Plasma Cell Differentiation, and Promotes B-cell Lymphomagenesis. Cancer Discov. 2018;8(12):1632-53.
59. Yang L, Rau R, Goodell MA. DNMT3A in haematological malignancies. Nat Rev Cancer. 2015;15(3):152-65.
60. Couronne L, Bastard C, Bernard OA. TET2 and DNMT3A mutations in human T-cell lymphoma. N Engl J Med. 2012;366(1):95-6.
61. Steinhilber J, Mederake M, Bonzheim I, Serinsoz-Linke E, Muller I, Fallier-Becker P, et al. The pathological features of angioimmunoblastic T-cell lymphomas with IDH2(R172) mutations. Modern pathology : an official journal of the United States and Canadian Academy of Pathology, Inc. 2019.
62. Scourzic L, Couronne L, Pedersen MT, Della Valle V, Diop M, Mylonas E, et al. DNMT3A(R882H) mutant and Tet2 inactivation cooperate in the deregulation of DNA methylation control to induce lymphoid malignancies in mice. Leukemia. 2016;30(6):1388-98.

63. Wang C, McKeithan TW, Gong Q, Zhang W, Bouska A, Rosenwald A, et al. IDH2R172 mutations define a unique subgroup of patients with angioimmunoblastic T-cell lymphoma. Blood. 2015;126(15):1741-52.
64. Figueroa ME, Abdel-Wahab O, Lu C, Ward PS, Patel J, Shih A, et al. Leukemic IDH1 and IDH2 mutations result in a hypermethylation phenotype, disrupt TET2 function, and impair hematopoietic differentiation. Cancer cell. 2010;18(6):553-67.
65. Willemsen M, Abdul Hamid M, Winkens B, Zur Hausen A. Mutational heterogeneity of angioimmunoblastic T-cell lymphoma indicates distinct lymphomagenic pathways. Blood cancer journal. 2018;8(1):6.
66. Odejide O, Weigert O, Lane AA, Toscano D, Lunning MA, Kopp N, et al. A targeted mutational landscape of angioimmunoblastic T-cell lymphoma. Blood. 2014;123(9):1293-6.
67. Lemonnier F, Cairns RA, Inoue S, Li WY, Dupuy A, Broutin S, et al. The IDH2 R172K mutation associated with angioimmunoblastic T-cell lymphoma produces 2HG in T cells and impacts lymphoid development. Proceedings of the National Academy of Sciences of the United States of America. 2016;113(52):15084-9.
68. Nguyen TB, Sakata-Yanagimoto M, Asabe Y, Matsubara D, Kano J, Yoshida K, et al. Identification of cell-type-specific mutations in nodal T-cell lymphomas. Blood cancer journal. 2017;7(1):e516.
69. Rohr J, Guo S, Huo J, Bouska A, Lachel C, Li Y, et al. Recurrent activating mutations of CD28 in peripheral T-cell lymphomas. Leukemia. 2016;30(5):1062-70.
70. Lee SH, Kim JS, Kim J, Kim SJ, Kim WS, Lee S, et al. A highly recurrent novel missense mutation in CD28 among angioimmunoblastic T-cell lymphoma patients. Haematologica. 2015;100(12):e505-e7.
71. Yoo HY, Kim P, Kim WS, Lee SH, Kim S, Kang SY, et al. Frequent CTLA4-CD28 gene fusion in diverse types of T-cell lymphoma. Haematologica. 2016;101(6):757-63.
72. Fujisawa M, Chiba S, Sakata-Yanagimoto M. Recent Progress in the Understanding of Angioimmunoblastic T-cell Lymphoma. J Clin Exp Hematop. 2017;57(3):109-19.
73. Xu B, Liu P. No survival improvement for patients with angioimmunoblastic T-cell lymphoma over the past two decades: a population-based study of 1207 cases. PloS one. 2014;9(3):e92585.
74. Ondrejka SL, Grzywacz B, Bodo J, Makishima H, Polprasert C, Said JW, et al. Angioimmunoblastic T-cell Lymphomas With the RHOA p.Gly17Val Mutation Have Classic Clinical and Pathologic Features. The American journal of surgical pathology. 2016;40(3):335-41.
75. Hsu YT, Wang YC, Chen RY, Hung LY, Li SS, Yen CC, et al. Angioimmunoblastic T-cell lymphoma in Taiwan reveals worse progression-free survival for RHOA G17V mutated subtype. Leuk Lymphoma. 2020;61(5):1108-18.
76. Nagao R, Kikuti YY, Carreras J, Kikuchi T, Miyaoka M, Matsushita H, et al. Clinicopathologic Analysis of Angioimmunoblastic T-cell Lymphoma With or Without RHOA G17V Mutation Using Formalin-fixed Paraffin-embedded Sections. The American journal of surgical pathology. 2016;40(8):1041-50.
77. Shiratori S, Kosugi-Kanaya M, Shigematsu A, Kobayashi H, Yamamoto S, Kobayashi N, et al. Ultra-high level of serum soluble interleukin-2 receptor at diagnosis predicts poor outcome for angioimmunoblastic T-cell lymphoma. Leuk Lymphoma. 2015;56(9):2592-7.

78. Ham JS, Park HY, Ryu KJ, Ko YH, Kim WS, Kim SJ. Elevated serum interleukin-10 level and M2 macrophage infiltration are associated with poor survival in angioimmunoblastic T-cell lymphoma. Oncotarget. 2017;8(44):76231-40.
79. Shang Y, Fu X, Chang Y, Li Y, Zhang M. B2 microglobulin is a novel prognostic marker of Angioimmunoblastic T-cell lymphoma. Sci Rep. 2018;8(1):12907.
80. Qian J, Meng H, Lv B, Wang J, Lu Y, Su L, et al. High expression levels of TLR9 and PD-L1 indicates a poor prognosis in patients with angioimmunoblastic T-cell lymphoma: a retrospective study of 88 cases in a single center. J Cancer. 2020;11(1):57-68.
81. Niino D, Komohara Y, Murayama T, Aoki R, Kimura Y, Hashikawa K, et al. Ratio of M2 macrophage expression is closely associated with poor prognosis for Angioimmunoblastic T-cell lymphoma (AITL). Pathol Int. 2010;60(4):278-83.
82. Zhang H, Lv H, Jia X, Hu G, Kong L, Zhang T, et al. Clinical significance of enhancer of zeste homolog 2 and histone deacetylases 1 and 2 expression in peripheral T-cell lymphoma. Oncol Lett. 2019;18(2):1415-23.
83. Xu M, Wang F, Chen H, Liu L, Liu W, Yang Y, et al. Inactivation of FOXO1 induces T follicular cell polarization and involves angioimmunoblastic T cell lymphoma. Cancer Biol Med. 2019;16(4):743-55.
84. Stone EL, Pepper M, Katayama CD, Kerdiles YM, Lai CY, Emslie E, et al. ICOS coreceptor signaling inactivates the transcription factor FOXO1 to promote Tfh cell differentiation. Immunity. 2015;42(2):239-51.
85. Kim YA, Byun JM, Park K, Bae GH, Lee D, Kim DS, et al. Redefining the role of etoposide in first-line treatment of peripheral T-cell lymphoma. Blood Adv. 2017;1(24):2138-46.
86. Schmitz N, Trumper L, Ziepert M, Nickelsen M, Ho AD, Metzner B, et al. Treatment and prognosis of mature T-cell and NK-cell lymphoma: an analysis of patients with T-cell lymphoma treated in studies of the German High-Grade Non-Hodgkin Lymphoma Study Group. Blood. 2010;116(18):3418-25.
87. Ellin F, Landstrom J, Jerkeman M, Relander T. Real-world data on prognostic factors and treatment in peripheral T-cell lymphomas: a study from the Swedish Lymphoma Registry. Blood. 2014;124(10):1570-7.
88. Vose J, Armitage J, Weisenburger D, International TCLP. International peripheral T-cell and natural killer/T-cell lymphoma study: pathology findings and clinical outcomes. Journal of clinical oncology : official journal of the American Society of Clinical Oncology. 2008;26(25):4124-30.
89. Savage KJ, Chhanabhai M, Gascoyne RD, Connors JM. Characterization of peripheral T-cell lymphomas in a single North American institution by the WHO classification. Ann Oncol. 2004;15(10):1467-75.
90. Le Gouill S, Milpied N, Buzyn A, De Latour RP, Vernant JP, Mohty M, et al. Graft-versus-lymphoma effect for aggressive T-cell lymphomas in adults: a study by the Societe Francaise de Greffe de Moelle et de Therapie Cellulaire. Journal of clinical oncology : official journal of the American Society of Clinical Oncology. 2008;26(14):2264-71.
91. Delfau-Larue MH, de Leval L, Joly B, Plonquet A, Challine D, Parrens M, et al. Targeting intratumoral B cells with rituximab in addition to CHOP in angioimmunoblastic T-cell lymphoma. A clinicobiological study of the GELA. Haematologica. 2012;97(10):1594-602.
92. Nguyen TB, Sakata-Yanagimoto M, Fujisawa M, Nuhat ST, Miyoshi H, Nannya Y, et al. Dasatinib Is an Effective Treatment for Angioimmunoblastic T-cell Lymphoma. Cancer research. 2020;80(9):1875-84.

93. Preite S, Huang B, Cannons JL, McGavern DB, Schwartzberg PL. PI3K Orchestrates T Follicular Helper Cell Differentiation in a Context Dependent Manner: Implications for Autoimmunity. Front Immunol. 2018;9:3079.
94. Horwitz SM, Koch R, Porcu P, Oki Y, Moskowitz A, Perez M, et al. Activity of the PI3K-delta,gamma inhibitor duvelisib in a phase 1 trial and preclinical models of T-cell lymphoma. Blood. 2018;131(8):888-98.
95. Cardenas MG, Yu W, Beguelin W, Teater MR, Geng H, Goldstein RL, et al. Rationally designed BCL6 inhibitors target activated B cell diffuse large B cell lymphoma. The Journal of clinical investigation. 2016;126(9):3351-62.
96. Itzykson R, Kosmider O, Cluzeau T, Mansat-De Mas V, Dreyfus F, Beyne-Rauzy O, et al. Impact of TET2 mutations on response rate to azacitidine in myelodysplastic syndromes and low blast count acute myeloid leukemias. Leukemia. 2011;25(7):1147-52.
97. Bejar R, Lord A, Stevenson K, Bar-Natan M, Perez-Ladaga A, Zaneveld J, et al. TET2 mutations predict response to hypomethylating agents in myelodysplastic syndrome patients. Blood. 2014;124(17):2705-12.
98. Delarue R, Dupuis J, Sujobert P, Barbieux S, Marçais A, Tournilhac O, et al. Treatment with Hypomethylating Agent 5-Azacytidine Induces Sustained Response in Angioimmunoblastic T Cell Lymphomas. Blood. 2016;128(22):4164-.
99. Crotty S. Follicular helper CD4 T cells (TFH). Annual review of immunology. 2011;29:621-63.
100. Mintz MA, Cyster JG. T follicular helper cells in germinal center B cell selection and lymphomagenesis. Immunol Rev. 2020.
101. Stebegg M, Kumar SD, Silva-Cayetano A, Fonseca VR, Linterman MA, Graca L. Regulation of the Germinal Center Response. Front Immunol. 2018;9:2469.
102. Victora GD, Nussenzweig MC. Germinal centers. Annual review of immunology. 2012;30:429-57.
103. Reboldi A, Cyster JG. Peyer's patches: organizing B-cell responses at the intestinal frontier. Immunological reviews. 2016;271(1):230-45.
104. Mesin L, Ersching J, Victora GD. Germinal Center B Cell Dynamics. Immunity. 2016;45(3):471-82.
105. Heesters BA, Myers RC, Carroll MC. Follicular dendritic cells: dynamic antigen libraries. Nat Rev Immunol. 2014;14(7):495-504.
106. Allen CD, Okada T, Cyster JG. Germinal-center organization and cellular dynamics. Immunity. 2007;27(2):190-202.
107. Crotty S. T Follicular Helper Cell Biology: A Decade of Discovery and Diseases. Immunity. 2019;50(5):1132-48.
108. Song W, Craft J. T follicular helper cell heterogeneity: Time, space, and function. Immunol Rev. 2019;288(1):85-96.
109. Fazilleau N, McHeyzer-Williams LJ, Rosen H, McHeyzer-Williams MG. The function of follicular helper T cells is regulated by the strength of T cell antigen receptor binding. Nat Immunol. 2009;10(4):375-84.
110. Baumjohann D, Okada T, Ansel KM. Cutting Edge: Distinct waves of BCL6 expression during T follicular helper cell development. J Immunol. 2011;187(5):2089-92.
111. Johnston RJ, Poholek AC, DiToro D, Yusuf I, Eto D, Barnett B, et al. Bcl6 and Blimp-1 are reciprocal and antagonistic regulators of T follicular helper cell differentiation. Science. 2009;325(5943):1006-10.

112. Nurieva RI, Chung Y, Martinez GJ, Yang XO, Tanaka S, Matskevitch TD, et al. Bcl6 mediates the development of T follicular helper cells. Science. 2009;325(5943):1001-5.
113. Yu D, Rao S, Tsai LM, Lee SK, He Y, Sutcliffe EL, et al. The transcriptional repressor Bcl-6 directs T follicular helper cell lineage commitment. Immunity. 2009;31(3):457-68.
114. Haynes NM, Allen CD, Lesley R, Ansel KM, Killeen N, Cyster JG. Role of CXCR5 and CCR7 in follicular Th cell positioning and appearance of a programmed cell death gene-1high germinal center-associated subpopulation. J Immunol. 2007;179(8):5099-108.
115. Xu H, Li X, Liu D, Li J, Zhang X, Chen X, et al. Follicular T-helper cell recruitment governed by bystander B cells and ICOS-driven motility. Nature. 2013;496(7446):523-7.
116. Shi J, Hou S, Fang Q, Liu X, Liu X, Qi H. PD-1 Controls Follicular T Helper Cell Positioning and Function. Immunity. 2018;49(2):264-74 e4.
117. Mizuno R, Sugiura D, Shimizu K, Maruhashi T, Watada M, Okazaki IM, et al. PD-1 Primarily Targets TCR Signal in the Inhibition of Functional T Cell Activation. Front Immunol. 2019;10:630.
118. Meli AP, Fontes G, Avery DT, Leddon SA, Tam M, Elliot M, et al. The Integrin LFA-1 Controls T Follicular Helper Cell Generation and Maintenance. Immunity. 2016;45(4):831-46.
119. Qi H, Cannons JL, Klauschen F, Schwartzberg PL, Germain RN. SAP-controlled T-B cell interactions underlie germinal centre formation. Nature. 2008;455(7214):764-9.
120. Cannons JL, Qi H, Lu KT, Dutta M, Gomez-Rodriguez J, Cheng J, et al. Optimal Germinal Center Responses Require a Multistage T Cell:B Cell Adhesion Process Involving Integrins, SLAM-Associated Protein, and CD84. Immunity. 2010;32(2):253-65.
121. Webb LMC, Linterman MA. Signals that drive T follicular helper cell formation. Immunology. 2017;152(2):185-94.
122. Zhang Y, Garcia-Ibanez L, Toellner KM. Regulation of germinal center B-cell differentiation. Immunol Rev. 2016;270(1):8-19.
123. Chevrier S, Kratina T, Emslie D, Tarlinton DM, Corcoran LM. IL4 and IL21 cooperate to induce the high Bcl6 protein level required for germinal center formation. Immunol Cell Biol. 2017;95(10):925-32.
124. Liu D, Xu H, Shih C, Wan Z, Ma X, Ma W, et al. T-B-cell entanglement and ICOSL-driven feed-forward regulation of germinal centre reaction. Nature. 2015;517(7533):214-8.
125. Ise W, Fujii K, Shiroguchi K, Ito A, Kometani K, Takeda K, et al. T Follicular Helper Cell-Germinal Center B Cell Interaction Strength Regulates Entry into Plasma Cell or Recycling Germinal Center Cell Fate. Immunity. 2018;48(4):702-15.e4.
126. Shulman Z, Gitlin AD, Weinstein JS, Lainez B, Esplugues E, Flavell RA, et al. Dynamic signaling by T follicular helper cells during germinal center B cell selection. Science. 2014;345(6200):1058-62.
127. Allen CD, Okada T, Tang HL, Cyster JG. Imaging of germinal center selection events during affinity maturation. Science. 2007;315(5811):528-31.
128. Veillette A, Zhang S, Shi X, Dong Z, Davidson D, Zhong M-C. SAP expression in T cells, not in B cells, is required for humoral immunity. Proceedings of the National Academy of Sciences. 2008;105(4):1273-8.
129. Nutt SL, Hodgkin PD, Tarlinton DM, Corcoran LM. The generation of antibody-secreting plasma cells. Nat Rev Immunol. 2015;15(3):160-71.
130. Zhang Y, Tech L, George LA, Acs A, Durrett RE, Hess H, et al. Plasma cell output from germinal centers is regulated by signals from Tfh and stromal cells. J Exp Med. 2018;215(4):1227-43.

131. Alinikula J, Nera KP, Junttila S, Lassila O. Alternate pathways for Bcl6-mediated regulation of B cell to plasma cell differentiation. Eur J Immunol. 2011;41(8):2404-13.
132. Shi W, Liao Y, Willis SN, Taubenheim N, Inouye M, Tarlinton DM, et al. Transcriptional profiling of mouse B cell terminal differentiation defines a signature for antibody-secreting plasma cells. Nat Immunol. 2015;16(6):663-73.
133. Laidlaw BJ, Schmidt TH, Green JA, Allen CD, Okada T, Cyster JG. The Eph-related tyrosine kinase ligand Ephrin-B1 marks germinal center and memory precursor B cells. J Exp Med. 2017;214(3):639-49.
134. Wang Y, Shi J, Yan J, Xiao Z, Hou X, Lu P, et al. Germinal-center development of memory B cells driven by IL-9 from follicular helper T cells. Nat Immunol. 2017;18(8):921-30.
135. Kwon H, Thierry-Mieg D, Thierry-Mieg J, Kim HP, Oh J, Tunyaplin C, et al. Analysis of interleukin-21-induced Prdm1 gene regulation reveals functional cooperation of STAT3 and IRF4 transcription factors. Immunity. 2009;31(6):941-52.
136. Minnich M, Tagoh H, Bonelt P, Axelsson E, Fischer M, Cebolla B, et al. Multifunctional role of the transcription factor Blimp-1 in coordinating plasma cell differentiation. Nat Immunol. 2016;17(3):331-43.
137. Kallies A, Hasbold J, Fairfax K, Pridans C, Emslie D, McKenzie BS, et al. Initiation of plasma-cell differentiation is independent of the transcription factor Blimp-1. Immunity. 2007;26(5):555-66.
138. Sciammas R, Shaffer AL, Schatz JH, Zhao H, Staudt LM, Singh H. Graded expression of interferon regulatory factor-4 coordinates isotype switching with plasma cell differentiation. Immunity. 2006;25(2):225-36.
139. Ochiai K, Maienschein-Cline M, Simonetti G, Chen J, Rosenthal R, Brink R, et al. Transcriptional regulation of germinal center B and plasma cell fates by dynamical control of IRF4. Immunity. 2013;38(5):918-29.
140. Klein U, Casola S, Cattoretti G, Shen Q, Lia M, Mo T, et al. Transcription factor IRF4 controls plasma cell differentiation and class-switch recombination. Nat Immunol. 2006;7(7):773-82.
141. Tellier J, Shi W, Minnich M, Liao Y, Crawford S, Smyth GK, et al. Blimp-1 controls plasma cell function through the regulation of immunoglobulin secretion and the unfolded protein response. Nat Immunol. 2016;17(3):323-30.
142. Tangye SG. Staying alive: regulation of plasma cell survival. Trends Immunol. 2011;32(12):595-602.
143. Lindquist RL, Niesner RA, Hauser AE. In the Right Place, at the Right Time: Spatiotemporal Conditions Determining Plasma Cell Survival and Function. Front Immunol. 2019;10:788.
144. Kurosaki T, Kometani K, Ise W. Memory B cells. Nat Rev Immunol. 2015;15(3):149-59.
145. Phan TG, Paus D, Chan TD, Turner ML, Nutt SL, Basten A, et al. High affinity germinal center B cells are actively selected into the plasma cell compartment. J Exp Med. 2006;203(11):2419-24.
146. Suan D, Sundling C, Brink R. Plasma cell and memory B cell differentiation from the germinal center. Curr Opin Immunol. 2017;45:97-102.
147. Suan D, Krautler NJ, Maag JLV, Butt D, Bourne K, Hermes JR, et al. CCR6 Defines Memory B Cell Precursors in Mouse and Human Germinal Centers, Revealing Light-Zone Location and Predominant Low Antigen Affinity. Immunity. 2017;47(6):1142-53 e4.

148. Shinnakasu R, Inoue T, Kometani K, Moriyama S, Adachi Y, Nakayama M, et al. Regulated selection of germinal-center cells into the memory B cell compartment. Nat Immunol. 2016;17(7):861-9.
149. Kitano M, Moriyama S, Ando Y, Hikida M, Mori Y, Kurosaki T, et al. Bcl6 Protein Expression Shapes Pre-Germinal Center B Cell Dynamics and Follicular Helper T Cell Heterogeneity. Immunity. 2011;34(6):961-72.
150. Shulman Z, Gitlin AD, Targ S, Jankovic M, Pasqual G, Nussenzweig MC, et al. T follicular helper cell dynamics in germinal centers. Science. 2013;341(6146):673-7.
151. Choi YS, Yang JA, Yusuf I, Johnston RJ, Greenbaum J, Peters B, et al. Bcl6 expressing follicular helper CD4 T cells are fate committed early and have the capacity to form memory. J Immunol. 2013;190(8):4014-26.
152. Hale JS, Ahmed R. Memory T follicular helper CD4 T cells. Front Immunol. 2015;6:16.
153. Ise W, Inoue T, McLachlan JB, Kometani K, Kubo M, Okada T, et al. Memory B cells contribute to rapid Bcl6 expression by memory follicular helper T cells. Proceedings of the National Academy of Sciences of the United States of America. 2014;111(32):11792-7.
154. Choi YS, Eto D, Yang JA, Lao C, Crotty S. Cutting edge: STAT1 is required for IL-6-mediated Bcl6 induction for early follicular helper cell differentiation. J Immunol. 2013;190(7):3049-53.
155. Nish SA, Schenten D, Wunderlich FT, Pope SD, Gao Y, Hoshi N, et al. T cell-intrinsic role of IL-6 signaling in primary and memory responses. Elife. 2014;3:e01949.
156. Karnowski A, Chevrier S, Belz GT, Mount A, Emslie D, D'Costa K, et al. B and T cells collaborate in antiviral responses via IL-6, IL-21, and transcriptional activator and coactivator, Oct2 and OBF-1. J Exp Med. 2012;209(11):2049-64.
157. Eto D, Lao C, DiToro D, Barnett B, Escobar TC, Kageyama R, et al. IL-21 and IL-6 are critical for different aspects of B cell immunity and redundantly induce optimal follicular helper CD4 T cell (Tfh) differentiation. PloS one. 2011;6(3):e17739.
158. Eddahri F, Denanglaire S, Bureau F, Spolski R, Leonard WJ, Leo O, et al. Interleukin-6/STAT3 signaling regulates the ability of naive T cells to acquire B-cell help capacities. Blood. 2009;113(11):2426-33.
159. Nurieva R, Yang XO, Martinez G, Zhang Y, Panopoulos AD, Ma L, et al. Essential autocrine regulation by IL-21 in the generation of inflammatory T cells. Nature. 2007;448(7152):480-3.
160. Hiramatsu Y, Suto A, Kashiwakuma D, Kanari H, Kagami S, Ikeda K, et al. c-Maf activates the promoter and enhancer of the IL-21 gene, and TGF-beta inhibits c-Maf-induced IL-21 production in CD4+ T cells. J Leukoc Biol. 2010;87(4):703-12.
161. Zotos D, Coquet JM, Zhang Y, Light A, D'Costa K, Kallies A, et al. IL-21 regulates germinal center B cell differentiation and proliferation through a B cell-intrinsic mechanism. J Exp Med. 2010;207(2):365-78.
162. Poholek AC, Hansen K, Hernandez SG, Eto D, Chandele A, Weinstein JS, et al. In vivo regulation of Bcl6 and T follicular helper cell development. J Immunol. 2010;185(1):313-26.
163. Vogelzang A, McGuire HM, Yu D, Sprent J, Mackay CR, King C. A fundamental role for interleukin-21 in the generation of T follicular helper cells. Immunity. 2008;29(1):127-37.
164. Nurieva RI, Chung Y, Hwang D, Yang XO, Kang HS, Ma L, et al. Generation of T follicular helper cells is mediated by interleukin-21 but independent of T helper 1, 2, or 17 cell lineages. Immunity. 2008;29(1):138-49.

165. Linterman MA, Beaton L, Yu D, Ramiscal RR, Srivastava M, Hogan JJ, et al. IL-21 acts directly on B cells to regulate Bcl-6 expression and germinal center responses. J Exp Med. 2010;207(2):353-63.
166. Weinstein JS, Herman EI, Lainez B, Licona-Limon P, Esplugues E, Flavell R, et al. TFH cells progressively differentiate to regulate the germinal center response. Nat Immunol. 2016;17(10):1197-205.
167. Bolduc A, Long E, Stapler D, Cascalho M, Tsubata T, Koni PA, et al. Constitutive CD40L expression on B cells prematurely terminates germinal center response and leads to augmented plasma cell production in T cell areas. J Immunol. 2010;185(1):220-30.
168. Dedeoglu F, Horwitz B, Chaudhuri J, Alt FW, Geha RS. Induction of activation-induced cytidine deaminase gene expression by IL-4 and CD40 ligation is dependent on STAT6 and NFkappaB. Int Immunol. 2004;16(3):395-404.
169. Ozaki K, Spolski R, Feng CG, Qi CF, Cheng J, Sher A, et al. A critical role for IL-21 in regulating immunoglobulin production. Science. 2002;298(5598):1630-4.
170. Reinhardt RL, Liang HE, Locksley RM. Cytokine-secreting follicular T cells shape the antibody repertoire. Nat Immunol. 2009;10(4):385-93.
171. McGuire HM, Vogelzang A, Warren J, Loetsch C, Natividad KD, Chan TD, et al. IL-21 and IL-4 Collaborate To Shape T-Dependent Antibody Responses. J Immunol. 2015;195(11):5123-35.
172. Liao W, Lin JX, Leonard WJ. IL-2 family cytokines: new insights into the complex roles of IL-2 as a broad regulator of T helper cell differentiation. Curr Opin Immunol. 2011;23(5):598-604.
173. Johnston RJ, Choi YS, Diamond JA, Yang JA, Crotty S. STAT5 is a potent negative regulator of TFH cell differentiation. J Exp Med. 2012;209(2):243-50.
174. Ballesteros-Tato A, Leon B, Graf BA, Moquin A, Adams PS, Lund FE, et al. Interleukin-2 inhibits germinal center formation by limiting T follicular helper cell differentiation. Immunity. 2012;36(5):847-56.
175. DiToro D, Winstead CJ, Pham D, Witte S, Andargachew R, Singer JR, et al. Differential IL-2 expression defines developmental fates of follicular versus nonfollicular helper T cells. Science. 2018;361(6407).
176. Papillion A, Powell MD, Chisolm DA, Bachus H, Fuller MJ, Weinmann AS, et al. Inhibition of IL-2 responsiveness by IL-6 is required for the generation of GC-TFH cells. Sci Immunol. 2019;4(39).
177. Rudd CE, Schneider H. Unifying concepts in CD28, ICOS and CTLA4 co-receptor signalling. Nat Rev Immunol. 2003;3(7):544-56.
178. Schildberg FA, Klein SR, Freeman GJ, Sharpe AH. Coinhibitory Pathways in the B7-CD28 Ligand-Receptor Family. Immunity. 2016;44(5):955-72.
179. Suh WK, Tafuri A, Berg-Brown NN, Shahinian A, Plyte S, Duncan GS, et al. The inducible costimulator plays the major costimulatory role in humoral immune responses in the absence of CD28. J Immunol. 2004;172(10):5917-23.
180. Gigoux M, Shang J, Pak Y, Xu M, Choe J, Mak TW, et al. Inducible costimulator promotes helper T-cell differentiation through phosphoinositide 3-kinase. Proceedings of the National Academy of Sciences of the United States of America. 2009;106(48):20371-6.
181. Wikenheiser DJ, Stumhofer JS. ICOS Co-Stimulation: Friend or Foe? Front Immunol. 2016;7:304.

182. Vinuesa CG, Cook MC, Angelucci C, Athanasopoulos V, Rui L, Hill KM, et al. A RING-type ubiquitin ligase family member required to repress follicular helper T cells and autoimmunity. Nature. 2005;435(7041):452-8.
183. Walker LS, Wiggett HE, Gaspal FM, Raykundalia CR, Goodall MD, Toellner KM, et al. Established T cell-driven germinal center B cell proliferation is independent of CD28 signaling but is tightly regulated through CTLA-4. J Immunol. 2003;170(1):91-8.
184. Linterman MA, Denton AE, Divekar DP, Zvetkova I, Kane L, Ferreira C, et al. CD28 expression is required after T cell priming for helper T cell responses and protective immunity to infection. Elife. 2014;3.
185. Choi YS, Kageyama R, Eto D, Escobar TC, Johnston RJ, Monticelli L, et al. ICOS receptor instructs T follicular helper cell versus effector cell differentiation via induction of the transcriptional repressor Bcl6. Immunity. 2011;34(6):932-46.
186. Sage PT, Paterson AM, Lovitch SB, Sharpe AH. The coinhibitory receptor CTLA-4 controls B cell responses by modulating T follicular helper, T follicular regulatory, and T regulatory cells. Immunity. 2014;41(6):1026-39.
187. Wang CJ, Heuts F, Ovcinnikovs V, Wardzinski L, Bowers C, Schmidt EM, et al. CTLA-4 controls follicular helper T-cell differentiation by regulating the strength of CD28 engagement. Proceedings of the National Academy of Sciences of the United States of America. 2015;112(2):524-9.
188. Weber JP, Fuhrmann F, Feist RK, Lahmann A, Al Baz MS, Gentz LJ, et al. ICOS maintains the T follicular helper cell phenotype by down-regulating Kruppel-like factor 2. J Exp Med. 2015;212(2):217-33.
189. Leavenworth JW, Verbinnen B, Yin J, Huang H, Cantor H. A p85alpha-osteopontin axis couples the receptor ICOS to sustained Bcl-6 expression by follicular helper and regulatory T cells. Nat Immunol. 2015;16(1):96-106.
190. Papa I, Vinuesa CG. Synaptic Interactions in Germinal Centers. Front Immunol. 2018;9:1858.
191. Schrock DC, Leddon SA, Hughson A, Miller J, Lacy-Hulbert A, Fowell DJ. Pivotal role for alphaV integrins in sustained Tfh support of the germinal center response for long-lived plasma cell generation. Proceedings of the National Academy of Sciences of the United States of America. 2019;116(10):4462-70.
192. Yan H, Wu L, Shih C, Hou S, Shi J, Mao T, et al. Plexin B2 and Semaphorin 4C Guide T Cell Recruitment and Function in the Germinal Center. Cell reports. 2017;19(5):995-1007.
193. Lu P, Shih C, Qi H. Ephrin B1-mediated repulsion and signaling control germinal center T cell territoriality and function. Science. 2017;356(6339).
194. Ye BH, Lista F, Lo Coco F, Knowles DM, Offit K, Chaganti RS, et al. Alterations of a zinc finger-encoding gene, BCL-6, in diffuse large-cell lymphoma. Science. 1993;262(5134):747-50.
195. Basso K, Dalla-Favera R. BCL6: master regulator of the germinal center reaction and key oncogene in B cell lymphomagenesis. Adv Immunol. 2010;105:193-210.
196. Liu X, Yan X, Zhong B, Nurieva RI, Wang A, Wang X, et al. Bcl6 expression specifies the T follicular helper cell program in vivo. J Exp Med. 2012;209(10):1841-52, S1-24.
197. Hollister K, Kusam S, Wu H, Clegg N, Mondal A, Sawant DV, et al. Insights into the Role of Bcl6 in Follicular Th Cells Using a New Conditional Mutant Mouse Model. The Journal of Immunology. 2013;191(7):3705-11.

198. Hatzi K, Nance JP, Kroenke MA, Bothwell M, Haddad EK, Melnick A, et al. BCL6 orchestrates Tfh cell differentiation via multiple distinct mechanisms. J Exp Med. 2015;212(4):539-53.
199. Liu X, Lu H, Chen T, Nallaparaju KC, Yan X, Tanaka S, et al. Genome-wide Analysis Identifies Bcl6-Controlled Regulatory Networks during T Follicular Helper Cell Differentiation. Cell reports. 2016;14(7):1735-47.
200. Barish GD, Yu RT, Karunasiri M, Ocampo CB, Dixon J, Benner C, et al. Bcl-6 and NF-kappaB cistromes mediate opposing regulation of the innate immune response. Genes Dev. 2010;24(24):2760-5.
201. Dent AL, Shaffer AL, Yu X, Allman D, Staudt LM. Control of inflammation, cytokine expression, and germinal center formation by BCL-6. Science. 1997;276(5312):589-92.
202. Ye BH, Cattoretti G, Shen Q, Zhang J, Hawe N, de Waard R, et al. The BCL-6 proto-oncogene controls germinal-centre formation and Th2-type inflammation. Nature genetics. 1997;16(2):161-70.
203. Toney LM, Cattoretti G, Graf JA, Merghoub T, Pandolfi P-P, Dalla-Favera R, et al. BCL-6 regulates chemokine gene transcription in macrophages. Nat Immunol. 2000;1(3):214-20.
204. Huang C, Hatzi K, Melnick A. Lineage-specific functions of Bcl-6 in immunity and inflammation are mediated by distinct biochemical mechanisms. Nat Immunol. 2013;14(4):380-8.
205. Huang C, Gonzalez DG, Cote CM, Jiang Y, Hatzi K, Teater M, et al. The BCL6 RD2 domain governs commitment of activated B cells to form germinal centers. Cell reports. 2014;8(5):1497-508.
206. Yang H, Green MR. Epigenetic Programing of B-Cell Lymphoma by BCL6 and Its Genetic Deregulation. Front Cell Dev Biol. 2019;7:272.
207. Cardenas MG, Oswald E, Yu W, Xue F, MacKerell AD, Jr., Melnick AM. The Expanding Role of the BCL6 Oncoprotein as a Cancer Therapeutic Target. Clin Cancer Res. 2017;23(4):885-93.
208. Nance JP, Belanger S, Johnston RJ, Takemori T, Crotty S. Cutting edge: T follicular helper cell differentiation is defective in the absence of Bcl6 BTB repressor domain function. J Immunol. 2015;194(12):5599-603.
209. Fujita N, Jaye DL, Geigerman C, Akyildiz A, Mooney MR, Boss JM, et al. MTA3 and the Mi-2/NuRD complex regulate cell fate during B lymphocyte differentiation. Cell. 2004;119(1):75-86.
210. Nance JP, Belanger S, Johnston RJ, Hu JK, Takemori T, Crotty S. Bcl6 middle domain repressor function is required for T follicular helper cell differentiation and utilizes the corepressor MTA3. Proceedings of the National Academy of Sciences of the United States of America. 2015;112(43):13324-9.
211. Niu H, Ye BH, Dalla-Favera R. Antigen receptor signaling induces MAP kinase-mediated phosphorylation and degradation of the BCL-6 transcription factor. Genes Dev. 1998;12(13):1953-61.
212. Mendez LM, Polo JM, Yu JJ, Krupski M, Ding BB, Melnick A, et al. CtBP is an essential corepressor for BCL6 autoregulation. Molecular and cellular biology. 2008;28(7):2175-86.
213. Pasqualucci L, Migliazza A, Basso K, Houldsworth J, Chaganti RS, Dalla-Favera R. Mutations of the BCL6 proto-oncogene disrupt its negative autoregulation in diffuse large B-cell lymphoma. Blood. 2003;101(8):2914-23.

214. Wang X, Li Z, Naganuma A, Ye BH. Negative autoregulation of BCL-6 is bypassed by genetic alterations in diffuse large B cell lymphomas. Proceedings of the National Academy of Sciences of the United States of America. 2002;99(23):15018-23.
215. Choi J, Diao H, Faliti CE, Truong J, Rossi M, Belanger S, et al. Bcl-6 is the nexus transcription factor of T follicular helper cells via repressor-of-repressor circuits. Nat Immunol. 2020;21(7):777-89.
216. Mascle X, Albagli O, Lemercier C. Point mutations in BCL6 DNA-binding domain reveal distinct roles for the six zinc fingers. Biochem Biophys Res Commun. 2003;300(2):391-6.
217. Kaji T, Ishige A, Hikida M, Taka J, Hijikata A, Kubo M, et al. Distinct cellular pathways select germline-encoded and somatically mutated antibodies into immunological memory. J Exp Med. 2012;209(11):2079-97.
218. Hatzi K, Jiang Y, Huang C, Garrett-Bakelman F, Gearhart MD, Giannopoulou EG, et al. A hybrid mechanism of action for BCL6 in B cells defined by formation of functionally distinct complexes at enhancers and promoters. Cell reports. 2013;4(3):578-88.
219. Beguelin W, Teater M, Gearhart MD, Calvo Fernandez MT, Goldstein RL, Cardenas MG, et al. EZH2 and BCL6 Cooperate to Assemble CBX8-BCOR Complex to Repress Bivalent Promoters, Mediate Germinal Center Formation and Lymphomagenesis. Cancer cell. 2016;30(2):197-213.
220. Yang JA, Tubo NJ, Gearhart MD, Bardwell VJ, Jenkins MK. Cutting edge: Bcl6-interacting corepressor contributes to germinal center T follicular helper cell formation and B cell helper function. J Immunol. 2015;194(12):5604-8.
221. Li F, Zeng Z, Xing S, Gullicksrud JA, Shan Q, Choi J, et al. Ezh2 programs TFH differentiation by integrating phosphorylation-dependent activation of Bcl6 and polycomb-dependent repression of p19Arf. Nat Commun. 2018;9(1):5452.
222. Duan S, Cermak L, Pagan JK, Rossi M, Martinengo C, di Celle PF, et al. FBXO11 targets BCL6 for degradation and is inactivated in diffuse large B-cell lymphomas. Nature. 2012;481(7379):90-3.
223. Schneider C, Kon N, Amadori L, Shen Q, Schwartz FH, Tischler B, et al. FBXO11 inactivation leads to abnormal germinal-center formation and lymphoproliferative disease. Blood. 2016;128(5):660-6.
224. Bereshchenko OR, Gu W, Dalla-Favera R. Acetylation inactivates the transcriptional repressor BCL6. Nature genetics. 2002;32(4):606-13.
225. Lu X, Fernando TM, Lossos C, Yusufova N, Liu F, Fontan L, et al. PRMT5 interacts with the BCL6 oncoprotein and is required for germinal center formation and lymphoma cell survival. Blood. 2018;132(19):2026-39.
226. Misawa T, SoRelle JA, Choi JH, Yue T, Wang KW, McAlpine W, et al. Mutual inhibition between Prkd2 and Bcl6 controls T follicular helper cell differentiation. Sci Immunol. 2020;5(43).
227. Tunyaplin C, Shaffer AL, Angelin-Duclos CD, Yu X, Staudt LM, Calame KL. Direct repression of prdm1 by Bcl-6 inhibits plasmacytic differentiation. J Immunol. 2004;173(2):1158-65.
228. Basso K, Saito M, Sumazin P, Margolin AA, Wang K, Lim WK, et al. Integrated biochemical and computational approach identifies BCL6 direct target genes controlling multiple pathways in normal germinal center B cells. Blood. 2010;115(5):975-84.

229. Saito M, Gao J, Basso K, Kitagawa Y, Smith PM, Bhagat G, et al. A signaling pathway mediating downregulation of BCL6 in germinal center B cells is blocked by BCL6 gene alterations in B cell lymphoma. Cancer cell. 2007;12(3):280-92.
230. Klein U, Dalla-Favera R. Germinal centres: role in B-cell physiology and malignancy. Nat Rev Immunol. 2008;8(1):22-33.
231. Phan RT, Dalla-Favera R. The BCL6 proto-oncogene suppresses p53 expression in germinal-centre B cells. Nature. 2004;432(7017):635-9.
232. Phan RT, Saito M, Basso K, Niu H, Dalla-Favera R. BCL6 interacts with the transcription factor Miz-1 to suppress the cyclin-dependent kinase inhibitor p21 and cell cycle arrest in germinal center B cells. Nat Immunol. 2005;6(10):1054-60.
233. Nakayamada S, Poholek AC, Lu KT, Takahashi H, Kato M, Iwata S, et al. Type I IFN induces binding of STAT1 to Bcl6: divergent roles of STAT family transcription factors in the T follicular helper cell genetic program. J Immunol. 2014;192(5):2156-66.
234. Lee SK, Silva DG, Martin JL, Pratama A, Hu X, Chang PP, et al. Interferon-gamma excess leads to pathogenic accumulation of follicular helper T cells and germinal centers. Immunity. 2012;37(5):880-92.
235. Choi YS, Gullicksrud JA, Xing S, Zeng Z, Shan Q, Li F, et al. LEF-1 and TCF-1 orchestrate T(FH) differentiation by regulating differentiation circuits upstream of the transcriptional repressor Bcl6. Nat Immunol. 2015;16(9):980-90.
236. Kusam S, Toney LM, Sato H, Dent AL. Inhibition of Th2 differentiation and GATA-3 expression by BCL-6. J Immunol. 2003;170(5):2435-41.
237. Kroenke MA, Eto D, Locci M, Cho M, Davidson T, Haddad EK, et al. Bcl6 and Maf cooperate to instruct human follicular helper CD4 T cell differentiation. J Immunol. 2012;188(8):3734-44.
238. Liu X, Chen X, Zhong B, Wang A, Wang X, Chu F, et al. Transcription factor achaete-scute homologue 2 initiates follicular T-helper-cell development. Nature. 2014;507(7493):513-8.
239. Veillette A. SLAM-family receptors: immune regulators with or without SAP-family adaptors. Cold Spring Harbor perspectives in biology. 2010;2(3):a002469-a.
240. Wu N, Veillette A. SLAM family receptors in normal immunity and immune pathologies. Curr Opin Immunol. 2016;38:45-51.
241. Chen J, Zhong MC, Guo H, Davidson D, Mishel S, Lu Y, et al. SLAMF7 is critical for phagocytosis of haematopoietic tumour cells via Mac-1 integrin. Nature. 2017;544(7651):493-7.
242. Yusuf I, Kageyama R, Monticelli L, Johnston RJ, Ditoro D, Hansen K, et al. Germinal center T follicular helper cell IL-4 production is dependent on signaling lymphocytic activation molecule receptor (CD150). J Immunol. 2010;185(1):190-202.
243. Cannons JL, Tangye SG, Schwartzberg PL. SLAM family receptors and SAP adaptors in immunity. Annual review of immunology. 2011;29:665-705.
244. Zhong M-C, Veillette A. Critical role of SAP in progression and reactivation but not maintenance of T cell-dependent humoral immunity. Molecular and cellular biology. 2013;33(6):1223-32.
245. Zhong MC, Veillette A. The adaptor molecule signaling lymphocytic activation molecule (SLAM)-associated protein (SAP) is essential in mechanisms involving the Fyn tyrosine kinase for induction and progression of collagen-induced arthritis. The Journal of biological chemistry. 2013;288(44):31423-36.

246. Kageyama R, Cannons Jennifer L, Zhao F, Yusuf I, Lao C, Locci M, et al. The Receptor Ly108 Functions as a SAP Adaptor-Dependent On-Off Switch for T Cell Help to B Cells and NKT Cell Development. Immunity. 2012;36(6):986-1002.
247. Wang N, Halibozek PJ, Yigit B, Zhao H, O'Keeffe MS, Sage P, et al. Negative Regulation of Humoral Immunity Due to Interplay between the SLAMF1, SLAMF5, and SLAMF6 Receptors. Front Immunol. 2015;6:158.
248. Hu JK, Crampton JC, Locci M, Crotty S. CRISPR-Mediated Slamf1Delta/Delta Slamf5Delta/Delta Slamf6Delta/Delta Triple Gene Disruption Reveals NKT Cell Defects but Not T Follicular Helper Cell Defects. PloS one. 2016;11(5):e0156074.
249. Chen S, Cai C, Li Z, Liu G, Wang Y, Blonska M, et al. Dissection of SAP-dependent and SAP-independent SLAM family signaling in NKT cell development and humoral immunity. The Journal of Experimental Medicine. 2017.
250. Veillette A. Immune regulation by SLAM family receptors and SAP-related adaptors. Nat Rev Immunol. 2006;6(1):56-66.
251. Walling BL, Kim M. LFA-1 in T Cell Migration and Differentiation. Frontiers in immunology. 2018;9:952-.
252. Evans R, Patzak I, Svensson L, De Filippo K, Jones K, McDowall A, et al. Integrins in immunity. J Cell Sci. 2009;122(Pt 2):215-25.
253. Biram A, Davidzohn N, Shulman Z. T cell interactions with B cells during germinal center formation, a three-step model. Immunol Rev. 2019;288(1):37-48.
254. Sebzda E, Bracke M, Tugal T, Hogg N, Cantrell DA. Rap1A positively regulates T cells via integrin activation rather than inhibiting lymphocyte signaling. Nat Immunol. 2002;3(3):251-8.
255. Katagiri K, Maeda A, Shimonaka M, Kinashi T. RAPL, a Rap1-binding molecule that mediates Rap1-induced adhesion through spatial regulation of LFA-1. Nat Immunol. 2003;4(8):741-8.
256. Verma NK, Kelleher D. Not Just an Adhesion Molecule: LFA-1 Contact Tunes the T Lymphocyte Program. J Immunol. 2017;199(4):1213-21.
257. Calderwood DA, Campbell ID, Critchley DR. Talins and kindlins: partners in integrin-mediated adhesion. Nat Rev Mol Cell Biol. 2013;14(8):503-17.
258. Evans R, Lellouch AC, Svensson L, McDowall A, Hogg N. The integrin LFA-1 signals through ZAP-70 to regulate expression of high-affinity LFA-1 on T lymphocytes. Blood. 2011;117(12):3331-42.
259. Wang Y, Shibuya K, Yamashita Y, Shirakawa J, Shibata K, Kai H, et al. LFA-1 decreases the antigen dose for T cell activation in vivo. Int Immunol. 2008;20(9):1119-27.
260. Kandula S, Abraham C. LFA-1 on CD4+ T cells is required for optimal antigen-dependent activation in vivo. J Immunol. 2004;173(7):4443-51.
261. Zaretsky I, Atrakchi O, Mazor RD, Stoler-Barak L, Biram A, Feigelson SW, et al. ICAMs support B cell interactions with T follicular helper cells and promote clonal selection. J Exp Med. 2017;214(11):3435-48.
262. Dunn GP, Old LJ, Schreiber RD. The three Es of cancer immunoediting. Annual review of immunology. 2004;22:329-60.
263. Bruchard M, Ghiringhelli F. Deciphering the Roles of Innate Lymphoid Cells in Cancer. Front Immunol. 2019;10:656.
264. de Charette M, Houot R. Hide or defend, the two strategies of lymphoma immune evasion: potential implications for immunotherapy. Haematologica. 2018;103(8):1256-68.

265. Yabe M, Gao Q, Ozkaya N, Huet S, Lewis N, Pichardo JD, et al. Bright PD-1 expression by flow cytometry is a powerful tool for diagnosis and monitoring of angioimmunoblastic T-cell lymphoma. Blood cancer journal. 2020;10(3):32.
266. Voron T, Colussi O, Marcheteau E, Pernot S, Nizard M, Pointet AL, et al. VEGF-A modulates expression of inhibitory checkpoints on CD8+ T cells in tumors. J Exp Med. 2015;212(2):139-48.
267. Yang J, Yan J, Liu B. Targeting VEGF/VEGFR to Modulate Antitumor Immunity. Front Immunol. 2018;9:978.
268. Mouly E, Ghamlouch H, Della-Valle V, Scourzic L, Quivoron C, Roos-Weil D, et al. B-cell tumor development in Tet2-deficient mice. Blood Adv. 2018;2(6):703-14.
269. Gaulard P, de Leval L. Follicular helper T cells: implications in neoplastic hematopathology. Semin Diagn Pathol. 2011;28(3):202-13.
270. Ellyard JI, Chia T, Rodriguez-Pinilla SM, Martin JL, Hu X, Navarro-Gonzalez M, et al. Heterozygosity for Roquinsan leads to angioimmunoblastic T-cell lymphoma-like tumors in mice. Blood. 2012;120(4):812-21.
271. Lindhout E, Lakeman A, Mevissen ML, de Groot C. Functionally active Epstein-Barr virus-transformed follicular dendritic cell-like cell lines. J Exp Med. 1994;179(4):1173-84.
272. Iqbal J, Wright G, Wang C, Rosenwald A, Gascoyne RD, Weisenburger DD, et al. Gene expression signatures delineate biological and prognostic subgroups in peripheral T-cell lymphoma. Blood. 2014;123(19):2915-23.
273. Lundberg J, Berglund D, Molin D, Kinch A. Intratumoral expression of FoxP3-positive regulatory T-cells in T-cell lymphoma: no correlation with survival. Ups J Med Sci. 2019;124(2):105-10.
274. Bruneau J, Canioni D, Renand A, Marafioti T, Paterson JC, Martin-Garcia N, et al. Regulatory T-cell depletion in angioimmunoblastic T-cell lymphoma. Am J Pathol. 2010;177(2):570-4.
275. Tanaka A, Sakaguchi S. Regulatory T cells in cancer immunotherapy. Cell Res. 2017;27(1):109-18.
276. Badalamenti G, Fanale D, Incorvaia L, Barraco N, Listi A, Maragliano R, et al. Role of tumor-infiltrating lymphocytes in patients with solid tumors: Can a drop dig a stone? Cell Immunol. 2019;343:103753.
277. Schreiber RD, Old LJ, Smyth MJ. Cancer immunoediting: integrating immunity's roles in cancer suppression and promotion. Science. 2011;331(6024):1565-70.
278. Schumacher TN, Scheper W, Kvistborg P. Cancer Neoantigens. Annual review of immunology. 2019;37:173-200.
279. Martinez-Lostao L, Anel A, Pardo J. How Do Cytotoxic Lymphocytes Kill Cancer Cells? Clin Cancer Res. 2015;21(22):5047-56.
280. Garrido F, Aptsiauri N, Doorduijn EM, Garcia Lora AM, van Hall T. The urgent need to recover MHC class I in cancers for effective immunotherapy. Curr Opin Immunol. 2016;39:44-51.
281. Hu B, Jacobs R, Ghosh N. Checkpoint Inhibitors Hodgkin Lymphoma and Non-Hodgkin Lymphoma. Curr Hematol Malig Rep. 2018;13(6):543-54.
282. Kim HJ, Cantor H. CD4 T-cell subsets and tumor immunity: the helpful and the not-so-helpful. Cancer Immunol Res. 2014;2(2):91-8.

283. Ali HR, Provenzano E, Dawson SJ, Blows FM, Liu B, Shah M, et al. Association between CD8+ T-cell infiltration and breast cancer survival in 12,439 patients. Ann Oncol. 2014;25(8):1536-43.
284. Muris JJ, Meijer CJ, Cillessen SA, Vos W, Kummer JA, Bladergroen BA, et al. Prognostic significance of activated cytotoxic T-lymphocytes in primary nodal diffuse large B-cell lymphomas. Leukemia. 2004;18(3):589-96.
285. Iqbal J, Weisenburger DD, Greiner TC, Vose JM, McKeithan T, Kucuk C, et al. Molecular signatures to improve diagnosis in peripheral T-cell lymphoma and prognostication in angioimmunoblastic T-cell lymphoma. Blood. 2010;115(5):1026-36.
286. Alexandrov LB, Nik-Zainal S, Wedge DC, Aparicio SA, Behjati S, Biankin AV, et al. Signatures of mutational processes in human cancer. Nature. 2013;500(7463):415-21.
287. Morley S, He J, Intlekofer AM, Bailey M, Nahas M, Heilmann A, et al. Comprehensive Genomic Profiling (CGP) Informs Molecular Diagnosis, Prognosis, and Therapeutic Decision-Making for Patients with Angioimmunoblastic T-Cell Lymphoma (AITL). Blood. 2017;130(Supplement 1):5134-.
288. Bennani NN, Pederson LD, Atherton P, Micallef I, Colgan JP, Thanarajasingam G, et al. A Phase II Study of Nivolumab in Patients with Relapsed or Refractory Peripheral T-Cell Lymphoma. Blood. 2019;134(Supplement_1):467-.
289. Ratner L, Waldmann TA, Janakiram M, Brammer JE. Rapid Progression of Adult T-Cell Leukemia-Lymphoma after PD-1 Inhibitor Therapy. N Engl J Med. 2018;378(20):1947-8.
290. Vivier E, Tomasello E, Baratin M, Walzer T, Ugolini S. Functions of natural killer cells. Nat Immunol. 2008;9(5):503-10.
291. Ben-Shmuel A, Biber G, Barda-Saad M. Unleashing Natural Killer Cells in the Tumor Microenvironment-The Next Generation of Immunotherapy? Front Immunol. 2020;11:275.
292. Waldhauer I, Steinle A. NK cells and cancer immunosurveillance. Oncogene. 2008;27(45):5932-43.
293. Ercolano G, Falquet M, Vanoni G, Trabanelli S, Jandus C. ILC2s: New Actors in Tumor Immunity. Front Immunol. 2019;10:2801.
294. Dhar P, Wu JD. NKG2D and its ligands in cancer. Curr Opin Immunol. 2018;51:55-61.
295. Dubois S, Feigenbaum L, Waldmann TA, Muller JR. NK cells prevent T cell lymphoma development in T cell receptor-transgenic mice. Cell Immunol. 2020;352:104081.
296. Veillette A, Chen J. SIRPalpha-CD47 Immune Checkpoint Blockade in Anticancer Therapy. Trends Immunol. 2018;39(3):173-84.
297. Jaiswal S, Chao MP, Majeti R, Weissman IL. Macrophages as mediators of tumor immunosurveillance. Trends Immunol. 2010;31(6):212-9.
298. Mosser DM, Edwards JP. Exploring the full spectrum of macrophage activation. Nat Rev Immunol. 2008;8(12):958-69.
299. Zhou J, Tang Z, Gao S, Li C, Feng Y, Zhou X. Tumor-Associated Macrophages: Recent Insights and Therapies. Frontiers in oncology. 2020;10:188.
300. Zhang W, Huang Q, Xiao W, Zhao Y, Pi J, Xu H, et al. Advances in Anti-Tumor Treatments Targeting the CD47/SIRPalpha Axis. Front Immunol. 2020;11:18.
301. Murray PJ, Wynn TA. Protective and pathogenic functions of macrophage subsets. Nat Rev Immunol. 2011;11(11):723-37.
302. Shapouri-Moghaddam A, Mohammadian S, Vazini H, Taghadosi M, Esmaeili SA, Mardani F, et al. Macrophage plasticity, polarization, and function in health and disease. J Cell Physiol. 2018;233(9):6425-40.

303. Mantovani A, Sica A, Sozzani S, Allavena P, Vecchi A, Locati M. The chemokine system in diverse forms of macrophage activation and polarization. Trends Immunol. 2004;25(12):677-86.
304. Genard G, Lucas S, Michiels C. Reprogramming of Tumor-Associated Macrophages with Anticancer Therapies: Radiotherapy versus Chemo- and Immunotherapies. Front Immunol. 2017;8:828.
305. Roszer T. Understanding the Mysterious M2 Macrophage through Activation Markers and Effector Mechanisms. Mediators Inflamm. 2015;2015:816460.
306. Mantovani A, Marchesi F, Malesci A, Laghi L, Allavena P. Tumour-associated macrophages as treatment targets in oncology. Nature Reviews Clinical Oncology. 2017;14(7):399-416.
307. Brown JM, Recht L, Strober S. The Promise of Targeting Macrophages in Cancer Therapy. Clin Cancer Res. 2017;23(13):3241-50.
308. Gray EE, Cyster JG. Lymph node macrophages. J Innate Immun. 2012;4(5-6):424-36.
309. Smith JP, Burton GF, Tew JG, Szakal AK. Tingible body macrophages in regulation of germinal center reactions. Dev Immunol. 1998;6(3-4):285-94.
310. Li SN, Wang W, Fu SP, Wang JF, Liu HM, Xie SS, et al. IL-21 modulates release of proinflammatory cytokines in LPS-stimulated macrophages through distinct signaling pathways. Mediators Inflamm. 2013;2013:548073.
311. Xu M, Liu M, Du X, Li S, Li H, Li X, et al. Intratumoral Delivery of IL-21 Overcomes Anti-Her2/Neu Resistance through Shifting Tumor-Associated Macrophages from M2 to M1 Phenotype. J Immunol. 2015;194(10):4997-5006.
312. Siveen KS, Kuttan G. Role of macrophages in tumour progression. Immunol Lett. 2009;123(2):97-102.
313. Louie DAP, Liao S. Lymph Node Subcapsular Sinus Macrophages as the Frontline of Lymphatic Immune Defense. Front Immunol. 2019;10:347.
314. Aderem A, Underhill DM. Mechanisms of phagocytosis in macrophages. Annual review of immunology. 1999;17:593-623.
315. Gordon S. Phagocytosis: An Immunobiologic Process. Immunity. 2016;44(3):463-75.
316. Barclay AN, Van den Berg TK. The interaction between signal regulatory protein alpha (SIRPalpha) and CD47: structure, function, and therapeutic target. Annual review of immunology. 2014;32:25-50.
317. Majeti R, Chao MP, Alizadeh AA, Pang WW, Jaiswal S, Gibbs KD, Jr., et al. CD47 is an adverse prognostic factor and therapeutic antibody target on human acute myeloid leukemia stem cells. Cell. 2009;138(2):286-99.
318. Chao MP, Alizadeh AA, Tang C, Myklebust JH, Varghese B, Gill S, et al. Anti-CD47 antibody synergizes with rituximab to promote phagocytosis and eradicate non-Hodgkin lymphoma. Cell. 2010;142(5):699-713.
319. Advani R, Flinn I, Popplewell L, Forero A, Bartlett NL, Ghosh N, et al. CD47 Blockade by Hu5F9-G4 and Rituximab in Non-Hodgkin's Lymphoma. N Engl J Med. 2018;379(18):1711-21.
320. Advani R, Volkmer JP, Chao MP. CD47 Blockade and Rituximab in Non-Hodgkin's Lymphoma. N Engl J Med. 2019;380(5):497-8.
321. Hsi ED, Steinle R, Balasa B, Rice A, Ko Y-H, Afar DEH. CS-1 Is Expressed in Nasal Type NK/T Cell Lymphomas and Angioimmunoblastic T-Cell Lymphomas: Implications for Targeted Therapy with Elotuzumab (HuLuc63). Blood. 2008;112(11):1779-.

322. Shin W, Mun S, Choi S, Han K. Application of NanoString technologies in angioimmunoblastic T cell lymphoma. Genes Genomics. 2020.
323. Jain S, Van Scoyk A, Morgan EA, Matthews A, Stevenson K, Newton G, et al. Targeted inhibition of CD47-SIRPα requires Fc-FcγR interactions to maximize activity in T-cell lymphomas. Blood. 2019;134(17):1430-40.
324. Tsai RK, Discher DE. Inhibition of "self" engulfment through deactivation of myosin-II at the phagocytic synapse between human cells. J Cell Biol. 2008;180(5):989-1003.
325. Van VQ, Raymond M, Baba N, Rubio M, Wakahara K, Susin SA, et al. CD47(high) expression on CD4 effectors identifies functional long-lived memory T cell progenitors. J Immunol. 2012;188(9):4249-55.
326. Khandelwal S, van Rooijen N, Saxena RK. Reduced expression of CD47 during murine red blood cell (RBC) senescence and its role in RBC clearance from the circulation. Transfusion. 2007;47(9):1725-32.
327. Yanagita T, Murata Y, Tanaka D, Motegi SI, Arai E, Daniwijaya EW, et al. Anti-SIRPalpha antibodies as a potential new tool for cancer immunotherapy. JCI Insight. 2017;2(1):e89140.
328. Zhang M, Hutter G, Kahn SA, Azad TD, Gholamin S, Xu CY, et al. Anti-CD47 Treatment Stimulates Phagocytosis of Glioblastoma by M1 and M2 Polarized Macrophages and Promotes M1 Polarized Macrophages In Vivo. PloS one. 2016;11(4):e0153550.
329. Lv Z, Bian Z, Shi L, Niu S, Ha B, Tremblay A, et al. Loss of Cell Surface CD47 Clustering Formation and Binding Avidity to SIRPalpha Facilitate Apoptotic Cell Clearance by Macrophages. J Immunol. 2015;195(2):661-71.
330. Azcutia V, Routledge M, Williams MR, Newton G, Frazier WA, Manica A, et al. CD47 plays a critical role in T-cell recruitment by regulation of LFA-1 and VLA-4 integrin adhesive functions. Mol Biol Cell. 2013;24(21):3358-68.
331. Azcutia V, Bassil R, Herter JM, Engelbertsen D, Newton G, Autio A, et al. Defects in CD4+ T cell LFA-1 integrin-dependent adhesion and proliferation protect Cd47-/- mice from EAE. J Leukoc Biol. 2017;101(2):493-505.
332. Shi L, Bian Z, Chen CX, Guo YN, Lv Z, Zeng C, et al. CD47 deficiency ameliorates autoimmune nephritis in Fas(lpr) mice by suppressing IgG autoantibody production. The Journal of pathology. 2015;237(3):285-95.
333. Cruz-Munoz M-E, Dong Z, Shi X, Zhang S, Veillette A. Influence of CRACC, a SLAM family receptor coupled to the adaptor EAT-2, on natural killer cell function. Nat Immunol. 2009;10(3):297-305.
334. Roncagalli R, Taylor JE, Zhang S, Shi X, Chen R, Cruz-Munoz ME, et al. Negative regulation of natural killer cell function by EAT-2, a SAP-related adaptor. Nat Immunol. 2005;6(10):1002-10.
335. Ng SY, Yoshida N, Christie AL, Ghandi M, Dharia NV, Dempster J, et al. Targetable vulnerabilities in T- and NK-cell lymphomas identified through preclinical models. Nat Commun. 2018;9(1):2024.
336. Parameswaran N, Zhao X, Bodo J, Durkin L, Parker Y, Lindner D, et al. Hypomethylating Agent 5-Azacytidine Sensitizes Peripheral T-Cell Lymphoma to SLAMF7-Targeting Therapeutic Antibody, Elotuzumab. Blood. 2019;134(Supplement_1):1515-.
337. Zhao X, Przychodzen B, Bodo J, Durkin L, Lindner D, Parameswaran N, et al. Angioimmunoblastic T-Cell Lymphoma: Molecular Characterization of Clonal T and B-Cells

and a Patient Derived Xenograft Model of Coexisting T and B-Cell Proliferations. Blood. 2019;134(Supplement_1):1572-.
338. Choi Y, Lee S, Kim K, Kim S-H, Chung Y-J, Lee C. Studying cancer immunotherapy using patient-derived xenografts (PDXs) in humanized mice. Experimental & Molecular Medicine. 2018;50(8):99.
339. Nagatani M, Kodera T, Suzuki D, Igura S, Fukunaga Y, Kanemitsu H, et al. Comparison of biological features between severely immuno-deficient NOD/Shi-scid Il2rg(null) and NOD/LtSz-scid Il2rg(null) mice. Exp Anim. 2019;68(4):471-82.
340. Shultz LD, Brehm MA, Garcia-Martinez JV, Greiner DL. Humanized mice for immune system investigation: progress, promise and challenges. Nat Rev Immunol. 2012;12(11):786-98.
341. Chappaz S, Finke D. The IL-7 signaling pathway regulates lymph node development independent of peripheral lymphocytes. J Immunol. 2010;184(7):3562-9.
342. Economopoulos V, Noad JC, Krishnamoorthy S, Rutt BK, Foster PJ. Comparing the MRI appearance of the lymph nodes and spleen in wild-type and immuno-deficient mouse strains. PloS one. 2011;6(11):e27508.
343. Takenaka K, Prasolava TK, Wang JC, Mortin-Toth SM, Khalouei S, Gan OI, et al. Polymorphism in Sirpa modulates engraftment of human hematopoietic stem cells. Nat Immunol. 2007;8(12):1313-23.
344. Yamauchi T, Takenaka K, Urata S, Shima T, Kikushige Y, Tokuyama T, et al. Polymorphic Sirpa is the genetic determinant for NOD-based mouse lines to achieve efficient human cell engraftment. Blood. 2013;121(8):1316-25.
345. Hu Z, Van Rooijen N, Yang YG. Macrophages prevent human red blood cell reconstitution in immunodeficient mice. Blood. 2011;118(22):5938-46.
346. Li Z, Cai X, Cai CL, Wang J, Zhang W, Petersen BE, et al. Deletion of Tet2 in mice leads to dysregulated hematopoietic stem cells and subsequent development of myeloid malignancies. Blood. 2011;118(17):4509-18.
347. Asmar F, Punj V, Christensen J, Pedersen MT, Pedersen A, Nielsen AB, et al. Genome-wide profiling identifies a DNA methylation signature that associates with TET2 mutations in diffuse large B-cell lymphoma. Haematologica. 2013;98(12):1912-20.
348. Quivoron C, Couronne L, Della Valle V, Lopez CK, Plo I, Wagner-Ballon O, et al. TET2 inactivation results in pleiotropic hematopoietic abnormalities in mouse and is a recurrent event during human lymphomagenesis. Cancer cell. 2011;20(1):25-38.
349. Lewis NE, Petrova-Drus K, Huet S, Epstein-Peterson ZD, Gao Q, Sigler AE, et al. Clonal hematopoiesis in angioimmunoblastic T-cell lymphoma with divergent evolution to myeloid neoplasms. Blood Adv. 2020;4(10):2261-71.
350. Pan F, Wingo TS, Zhao Z, Gao R, Makishima H, Qu G, et al. Tet2 loss leads to hypermutagenicity in haematopoietic stem/progenitor cells. Nat Commun. 2017;8:15102.
351. Moran-Crusio K, Reavie L, Shih A, Abdel-Wahab O, Ndiaye-Lobry D, Lobry C, et al. Tet2 loss leads to increased hematopoietic stem cell self-renewal and myeloid transformation. Cancer cell. 2011;20(1):11-24.
352. Russler-Germain DA, Spencer DH, Young MA, Lamprecht TL, Miller CA, Fulton R, et al. The R882H DNMT3A mutation associated with AML dominantly inhibits wild-type DNMT3A by blocking its ability to form active tetramers. Cancer cell. 2014;25(4):442-54.
353. Jain S, Chen J, Nicolae A, Wang H, Shin DM, Adkins EB, et al. IL-21-driven neoplasms in SJL mice mimic some key features of human angioimmunoblastic T-cell lymphoma. Am J Pathol. 2015;185(11):3102-14.

354. Ponzio NM, Thorbecke GJ. Requirement for reverse immune surveillance for the growth of germinal center-derived murine lymphomas. Semin Cancer Biol. 2000;10(5):331-40.
355. Zhang DJ, Tsiagbe VK, Huang C, Thorbecke GJ. Control of endogenous mouse mammary tumor virus superantigen expression in SJL lymphomas by a promoter within the env region. J Immunol. 1996;157(8):3510-7.
356. Herek TA, Cutucache CE. Using Murine Models to Investigate Tumor-Lymphoid Interactions: Spotlight on Chronic Lymphocytic Leukemia and Angioimmunoblastic T-Cell Lymphoma. Frontiers in oncology. 2017;7:86.
357. Mondragon L, Mhaidly R, De Donatis GM, Tosolini M, Dao P, Martin AR, et al. GAPDH Overexpression in the T Cell Lineage Promotes Angioimmunoblastic T Cell Lymphoma through an NF-kappaB-Dependent Mechanism. Cancer cell. 2019;36(3):268-87 e10.
358. Heissmeyer V, Vogel KU. Molecular control of Tfh-cell differentiation by Roquin family proteins. Immunol Rev. 2013;253(1):273-89.
359. Schaefer JS, Klein JR. Roquin--a multifunctional regulator of immune homeostasis. Genes Immun. 2016;17(2):79-84.
360. Athanasopoulos V, Ramiscal RR, Vinuesa CG. ROQUIN signalling pathways in innate and adaptive immunity. Eur J Immunol. 2016;46(5):1082-90.
361. Vogel KU, Edelmann SL, Jeltsch KM, Bertossi A, Heger K, Heinz GA, et al. Roquin paralogs 1 and 2 redundantly repress the Icos and Ox40 costimulator mRNAs and control follicular helper T cell differentiation. Immunity. 2013;38(4):655-68.
362. Athanasopoulos V, Barker A, Yu D, Tan AH, Srivastava M, Contreras N, et al. The ROQUIN family of proteins localizes to stress granules via the ROQ domain and binds target mRNAs. FEBS J. 2010;277(9):2109-27.
363. Glasmacher E, Hoefig KP, Vogel KU, Rath N, Du L, Wolf C, et al. Roquin binds inducible costimulator mRNA and effectors of mRNA decay to induce microRNA-independent post-transcriptional repression. Nat Immunol. 2010;11(8):725-33.
364. Leppek K, Schott J, Reitter S, Poetz F, Hammond MC, Stoecklin G. Roquin promotes constitutive mRNA decay via a conserved class of stem-loop recognition motifs. Cell. 2013;153(4):869-81.
365. Jeltsch KM, Hu D, Brenner S, Zoller J, Heinz GA, Nagel D, et al. Cleavage of roquin and regnase-1 by the paracaspase MALT1 releases their cooperatively repressed targets to promote T(H)17 differentiation. Nat Immunol. 2014;15(11):1079-89.
366. Pratama A, Ramiscal RR, Silva DG, Das SK, Athanasopoulos V, Fitch J, et al. Roquin-2 shares functions with its paralog Roquin-1 in the repression of mRNAs controlling T follicular helper cells and systemic inflammation. Immunity. 2013;38(4):669-80.
367. Essig K, Kronbeck N, Guimaraes JC, Lohs C, Schlundt A, Hoffmann A, et al. Roquin targets mRNAs in a 3'-UTR-specific manner by different modes of regulation. Nat Commun. 2018;9(1):3810.
368. Srivastava M, Duan G, Kershaw NJ, Athanasopoulos V, Yeo JH, Ose T, et al. Roquin binds microRNA-146a and Argonaute2 to regulate microRNA homeostasis. Nat Commun. 2015;6:6253.
369. Essig K, Hu D, Guimaraes JC, Alterauge D, Edelmann S, Raj T, et al. Roquin Suppresses the PI3K-mTOR Signaling Pathway to Inhibit T Helper Cell Differentiation and Conversion of Treg to Tfr Cells. Immunity. 2017;47(6):1067-82 e12.
370. Schaefer JS, Montufar-Solis D, Klein JR. A role for IL-10 in the transcriptional regulation of Roquin-1. Gene. 2014;549(1):134-40.

371. Bertossi A, Aichinger M, Sansonetti P, Lech M, Neff F, Pal M, et al. Loss of Roquin induces early death and immune deregulation but not autoimmunity. The Journal of Experimental Medicine. 2011;208(9):1749-56.
372. Linterman MA, Rigby RJ, Wong R, Silva D, Withers D, Anderson G, et al. Roquin differentiates the specialized functions of duplicated T cell costimulatory receptor genes CD28 and ICOS. Immunity. 2009;30(2):228-41.
373. Linterman MA, Rigby RJ, Wong RK, Yu D, Brink R, Cannons JL, et al. Follicular helper T cells are required for systemic autoimmunity. J Exp Med. 2009;206(3):561-76.
374. Yu D, Tan AH, Hu X, Athanasopoulos V, Simpson N, Silva DG, et al. Roquin represses autoimmunity by limiting inducible T-cell co-stimulator messenger RNA. Nature. 2007;450(7167):299-303.
375. Zhang Z, Procissi D, Li W, Kim DH, Li K, Han G, et al. High resolution MRI for non-invasive mouse lymph node mapping. J Immunol Methods. 2013;400-401:23-9.
376. Auguste T, Travert M, Tarte K, Ame-Thomas P, Artchounin C, Martin-Garcia N, et al. ROQUIN/RC3H1 alterations are not found in angioimmunoblastic T-cell lymphoma. PloS one. 2013;8(6):e64536.
377. Chihara D, Fanale MA, Miranda RN, Noorani M, Westin JR, Nastoupil LJ, et al. The survival outcome of patients with relapsed/refractory peripheral T-cell lymphoma-not otherwise specified and angioimmunoblastic T-cell lymphoma. Br J Haematol. 2017;176(5):750-8.
378. Dupuis J, Boye K, Martin N, Copie-Bergman C, Plonquet A, Fabiani B, et al. Expression of CXCL13 by Neoplastic Cells in Angioimmunoblastic T-Cell Lymphoma (AITL): A New Diagnostic Marker Providing Evidence That AITL Derives From Follicular Helper T Cells. The American Journal of Surgical Pathology. 2006;30(4):490-4.
379. Dogan A, Ngu LS, Ng SH, Cervi PL. Pathology and clinical features of angioimmunoblastic T-cell lymphoma after successful treatment with thalidomide. Leukemia. 2005;19(5):873-5.
380. Li X, Gadzinsky A, Gong L, Tong H, Calderon V, Li Y, et al. Cbl Ubiquitin Ligases Control B Cell Exit from the Germinal-Center Reaction. Immunity. 2018;48(3):530-41.e6.
381. Ruzankina Y, Pinzon-Guzman C, Asare A, Ong T, Pontano L, Cotsarelis G, et al. Deletion of the developmentally essential gene ATR in adult mice leads to age-related phenotypes and stem cell loss. Cell stem cell. 2007;1(1):113-26.
382. Sledzinska A, Hemmers S, Mair F, Gorka O, Ruland J, Fairbairn L, et al. TGF-beta signalling is required for CD4(+) T cell homeostasis but dispensable for regulatory T cell function. PLoS biology. 2013;11(10):e1001674.
383. Davidson D, Shi X, Zhang S, Wang H, Nemer M, Ono N, et al. Genetic Evidence Linking SAP, the X-Linked Lymphoproliferative Gene Product, to Src-Related Kinase FynT in TH2 Cytokine Regulation. Immunity. 2004;21(5):707-17.
384. Meli AP, Fontes G, Leung Soo C, King IL. T Follicular Helper Cell-Derived IL-4 Is Required for IgE Production during Intestinal Helminth Infection. J Immunol. 2017;199(1):244-52.
385. Bogush T, Dudko E, Bogush E, Polotsky B, Tjulandin S, Davydov M. Tamoxifen non-estrogen receptor mediated molecular targets. Oncol Rev. 2012;6(2):e15-e.
386. Wang Y, Li D, Jones D, Bassett R, Sale GE, Khalili J, et al. Blocking LFA-1 activation with lovastatin prevents graft-versus-host disease in mouse bone marrow transplantation. Biology of blood and marrow transplantation : journal of the American Society for Blood and Marrow Transplantation. 2009;15(12):1513-22.

387. Weitz-Schmidt G, Welzenbach K, Dawson J, Kallen J. Improved Lymphocyte Function-associated Antigen-1 (LFA-1) Inhibition by Statin Derivatives: MOLECULAR BASIS DETERMINED BY X-RAY ANALYSIS AND MONITORING OF LFA-1 CONFORMATIONAL CHANGES IN VITRO AND EX VIVO. Journal of Biological Chemistry. 2004;279(45):46764-71.
388. Dong Z, Davidson D, Pérez-Quintero Luis A, Kurosaki T, Swat W, Veillette A. The Adaptor SAP Controls NK Cell Activation by Regulating the Enzymes Vav-1 and SHIP-1 and by Enhancing Conjugates with Target Cells. Immunity. 2012;36(6):974-85.
389. Panneton V, Chang J, Witalis M, Li J, Suh WK. Inducible T-cell co-stimulator: Signaling mechanisms in T follicular helper cells and beyond. Immunol Rev. 2019;291(1):91-103.
390. Basso K, Dalla-Favera R. Germinal centres and B cell lymphomagenesis. Nat Rev Immunol. 2015;15(3):172-84.
391. Ma CS, Suryani S, Avery DT, Chan A, Nanan R, Santner-Nanan B, et al. Early commitment of naive human CD4(+) T cells to the T follicular helper (T(FH)) cell lineage is induced by IL-12. Immunol Cell Biol. 2009;87(8):590-600.
392. Li DY, Xiong XZ. ICOS(+) Tregs: A Functional Subset of Tregs in Immune Diseases. Front Immunol. 2020;11:2104.
393. Linterman MA, Pierson W, Lee SK, Kallies A, Kawamoto S, Rayner TF, et al. Foxp3+ follicular regulatory T cells control the germinal center response. Nat Med. 2011;17(8):975-82.
394. Wu H, Chen Y, Liu H, Xu LL, Teuscher P, Wang S, et al. Follicular regulatory T cells repress cytokine production by follicular helper T cells and optimize IgG responses in mice. Eur J Immunol. 2016;46(5):1152-61.
395. Fu W, Liu X, Lin X, Feng H, Sun L, Li S, et al. Deficiency in T follicular regulatory cells promotes autoimmunity. J Exp Med. 2018;215(3):815-25.
396. Togashi Y, Shitara K, Nishikawa H. Regulatory T cells in cancer immunosuppression - implications for anticancer therapy. Nat Rev Clin Oncol. 2019;16(6):356-71.
397. Wing JB, Tekguc M, Sakaguchi S. Control of Germinal Center Responses by T-Follicular Regulatory Cells. Front Immunol. 2018;9:1910.
398. Xie MM, Chen Q, Liu H, Yang K, Koh B, Wu H, et al. T follicular regulatory cells and IL-10 promote food antigen-specific IgE. The Journal of clinical investigation. 2020;130(7):3820-32.
399. Clement RL, Daccache J, Mohammed MT, Diallo A, Blazar BR, Kuchroo VK, et al. Follicular regulatory T cells control humoral and allergic immunity by restraining early B cell responses. Nat Immunol. 2019;20(10):1360-71.
400. Yue X, Lio CJ, Samaniego-Castruita D, Li X, Rao A. Loss of TET2 and TET3 in regulatory T cells unleashes effector function. Nat Commun. 2019;10(1):2011.
401. Warner K, Weit N, Crispatzu G, Admirand J, Jones D, Herling M. T-cell receptor signaling in peripheral T-cell lymphoma - a review of patterns of alterations in a central growth regulatory pathway. Curr Hematol Malig Rep. 2013;8(3):163-72.
402. Witalis M, Chang J, Zhong MC, Bouklouch Y, Panneton V, Li J, et al. Progression of AITL-like tumors in mice is driven by Tfh signature proteins and T-B cross talk. Blood Adv. 2020;4(5):868-79.
403. Lachenal F, Berger F, Ghesquières H, Biron P, Hot A, Callet-Bauchu E, et al. Angioimmunoblastic T-Cell Lymphoma: Clinical and Laboratory Features at Diagnosis in 77 Patients. Medicine. 2007;86(5):282-92.

404. Jaffe ES, Pittaluga S, Anastasi J. Chapter 73 - The Pathologic Basis for the Classification of Non-Hodgkin and Hodgkin Lymphomas. In: Hoffman R, Benz EJ, Silberstein LE, Heslop HE, Weitz JI, Anastasi J, et al., editors. Hematology (Seventh Edition): Elsevier; 2018. p. 1187-203.
405. Suh W-K. Life of T Follicular Helper Cells. Molecules and Cells. 2015;38(3):195-201.
406. Bercovici N, Guerin MV, Trautmann A, Donnadieu E. The Remarkable Plasticity of Macrophages: A Chance to Fight Cancer. Front Immunol. 2019;10:1563.
407. Yu D, Vinuesa CG. Multiple checkpoints keep follicular helper T cells under control to prevent autoimmunity. Cellular & molecular immunology. 2010;7(3):198-203.
408. Dos Anjos Cassado A. F4/80 as a Major Macrophage Marker: The Case of the Peritoneum and Spleen. Results Probl Cell Differ. 2017;62:161-79.
409. Christensen JE, Andreasen SO, Christensen JP, Thomsen AR. CD11b expression as a marker to distinguish between recently activated effector CD8(+) T cells and memory cells. Int Immunol. 2001;13(4):593-600.
410. Ghosn EE, Yang Y, Tung J, Herzenberg LA, Herzenberg LA. CD11b expression distinguishes sequential stages of peritoneal B-1 development. Proceedings of the National Academy of Sciences of the United States of America. 2008;105(13):5195-200.
411. Goh W, Huntington ND. Regulation of Murine Natural Killer Cell Development. Front Immunol. 2017;8:130.
412. He Y, Bouwstra R, Wiersma VR, de Jong M, Jan Lourens H, Fehrmann R, et al. Cancer cell-expressed SLAMF7 is not required for CD47-mediated phagocytosis. Nat Commun. 2019;10(1):533.
413. Abram CL, Lowell CA. The ins and outs of leukocyte integrin signaling. Annual review of immunology. 2009;27:339-62.
414. Li Y, Yang C, Mao L, Wang J, Li C, Qian W. Clinical characteristics of angioimmunoblastic T-cell lymphoma in China and C-reactive protein as an independent prognostic factor. Medicine (Baltimore). 2017;96(39):e8091.
415. Pierpont TM, Limper CB, Richards KL. Past, Present, and Future of Rituximab-The World's First Oncology Monoclonal Antibody Therapy. Frontiers in oncology. 2018;8:163.
416. Leandro MJ. B-cell subpopulations in humans and their differential susceptibility to depletion with anti-CD20 monoclonal antibodies. Arthritis Res Ther. 2013;15 Suppl 1:S3.
417. Gong Q, Ou Q, Ye S, Lee WP, Cornelius J, Diehl L, et al. Importance of cellular microenvironment and circulatory dynamics in B cell immunotherapy. J Immunol. 2005;174(2):817-26.
418. Anolik J, Looney RJ, Bottaro A, Sanz I, Young F. Down-regulation of CD20 on B cells upon CD40 activation. Eur J Immunol. 2003;33(9):2398-409.
419. Latour S, Gish G, Helgason CD, Humphries RK, Pawson T, Veillette A. Regulation of SLAM-mediated signal transduction by SAP, the X-linked lymphoproliferative gene product. Nat Immunol. 2001;2(8):681-90.
420. Chan B, Lanyi A, Song HK, Griesbach J, Simarro-Grande M, Poy F, et al. SAP couples Fyn to SLAM immune receptors. Nat Cell Biol. 2003;5(2):155-60.
421. Cannons JL, Yu LJ, Jankovic D, Crotty S, Horai R, Kirby M, et al. SAP regulates T cell-mediated help for humoral immunity by a mechanism distinct from cytokine regulation. J Exp Med. 2006;203(6):1551-65.
422. McCausland MM, Yusuf I, Tran H, Ono N, Yanagi Y, Crotty S. SAP regulation of follicular helper CD4 T cell development and humoral immunity is independent of SLAM and Fyn kinase. J Immunol. 2007;178(2):817-28.

423. Chu C, Wang Y, Zhang X, Ni X, Cao J, Xu W, et al. SAP-Regulated T Cell–APC Adhesion and Ligation-Dependent and -Independent Ly108–CD3ζ Interactions. The Journal of Immunology. 2014;193(8):3860-71.
424. Zhao F, Cannons JL, Dutta M, Griffiths GM, Schwartzberg PL. Positive and negative signaling through SLAM receptors regulate synapse organization and thresholds of cytolysis. Immunity. 2012;36(6):1003-16.
425. Gururajan M, Simmons A, Dasu T, Spear BT, Calulot C, Robertson DA, et al. Early growth response genes regulate B cell development, proliferation, and immune response. J Immunol. 2008;181(7):4590-602.
426. Maltzman JS, Carmen JA, Monroe JG. Transcriptional regulation of the Icam-1 gene in antigen receptor- and phorbol ester-stimulated B lymphocytes: role for transcription factor EGR1. J Exp Med. 1996;183(4):1747-59.
427. Holmes AB, Corinaldesi C, Shen Q, Kumar R, Compagno N, Wang Z, et al. Single-cell analysis of germinal-center B cells informs on lymphoma cell of origin and outcome. J Exp Med. 2020;217(10).
428. Ardouin L, Bracke M, Mathiot A, Pagakis SN, Norton T, Hogg N, et al. Vav1 transduces TCR signals required for LFA-1 function and cell polarization at the immunological synapse. Eur J Immunol. 2003;33(3):790-7.
429. Zeiser R. Immune modulatory effects of statins. Immunology. 2018;154(1):69-75.
430. Kallen J, Welzenbach K, Ramage P, Geyl D, Kriwacki R, Legge G, et al. Structural basis for LFA-1 inhibition upon lovastatin binding to the CD11a I-domain. J Mol Biol. 1999;292(1):1-9.
431. Jury EC, Flores-Borja F, Kabouridis PS. Lipid rafts in T cell signalling and disease. Semin Cell Dev Biol. 2007;18(5):608-15.
432. Schachter M. Chemical, pharmacokinetic and pharmacodynamic properties of statins: an update. Fundam Clin Pharmacol. 2005;19(1):117-25.
433. Weitz-Schmidt G. Statins as anti-inflammatory agents. Trends in Pharmacological Sciences. 2002;23(10):482-7.
434. Mira E, Carmona-Rodriguez L, Tardaguila M, Azcoitia I, Gonzalez-Martin A, Almonacid L, et al. A lovastatin-elicited genetic program inhibits M2 macrophage polarization and enhances T cell infiltration into spontaneous mouse mammary tumors. Oncotarget. 2013;4(12):2288-301.
435. Mira E, Leon B, Barber DF, Jimenez-Baranda S, Goya I, Almonacid L, et al. Statins induce regulatory T cell recruitment via a CCL1 dependent pathway. J Immunol. 2008;181(5):3524-34.
436. Harjunpaa H, Llort Asens M, Guenther C, Fagerholm SC. Cell Adhesion Molecules and Their Roles and Regulation in the Immune and Tumor Microenvironment. Front Immunol. 2019;10:1078.
437. Mittelbrunn M, Molina A, Escribese MM, Yanez-Mo M, Escudero E, Ursa A, et al. VLA-4 integrin concentrates at the peripheral supramolecular activation complex of the immune synapse and drives T helper 1 responses. Proceedings of the National Academy of Sciences of the United States of America. 2004;101(30):11058-63.
438. Bertoni A, Alabiso O, Galetto AS, Baldanzi G. Integrins in T Cell Physiology. Int J Mol Sci. 2018;19(2).
439. Schmitt N, Ueno H. Blood Tfh cells come with colors. Immunity. 2013;39(4):629-30.

440. Asrir A, Aloulou M, Gador M, Perals C, Fazilleau N. Interconnected subsets of memory follicular helper T cells have different effector functions. Nat Commun. 2017;8(1):847.
441. Locci M, Havenar-Daughton C, Landais E, Wu J, Kroenke MA, Arlehamn CL, et al. Human circulating PD-1+CXCR3-CXCR5+ memory Tfh cells are highly functional and correlate with broadly neutralizing HIV antibody responses. Immunity. 2013;39(4):758-69.
442. Pepper M, Jenkins MK. Origins of CD4(+) effector and central memory T cells. Nat Immunol. 2011;12(6):467-71.
443. Venturutti L, Teater M, Zhai A, Chadburn A, Babiker L, Kim D, et al. TBL1XR1 Mutations Drive Extranodal Lymphoma by Inducing a Pro-tumorigenic Memory Fate. Cell. 2020;182(2):297-316 e27.
444. Miladi M, Sokhoyan E, Houwaart T, Heyne S, Costa F, Gruning B, et al. GraphClust2: Annotation and discovery of structured RNAs with scalable and accessible integrative clustering. Gigascience. 2019;8(12).
445. Cerchietti LC, Ghetu AF, Zhu X, Da Silva GF, Zhong S, Matthews M, et al. A small-molecule inhibitor of BCL6 kills DLBCL cells in vitro and in vivo. Cancer cell. 2010;17(4):400-11.
446. Kerres N, Steurer S, Schlager S, Bader G, Berger H, Caligiuri M, et al. Chemically Induced Degradation of the Oncogenic Transcription Factor BCL6. Cell reports. 2017;20(12):2860-75.
447. Liu M, O'Connor RS, Trefely S, Graham K, Snyder NW, Beatty GL. Metabolic rewiring of macrophages by CpG potentiates clearance of cancer cells and overcomes tumor-expressed CD47-mediated 'don't-eat-me' signal. Nat Immunol. 2019;20(3):265-75.
448. Moreno SG. Depleting Macrophages In Vivo with Clodronate-Liposomes. Methods Mol Biol. 2018;1784:259-62.
449. Hua L, Shi J, Shultz LD, Ren G. Genetic Models of Macrophage Depletion. Methods Mol Biol. 2018;1784:243-58.
450. Fumagalli S, Fiordaliso F, Perego C, Corbelli A, Mariani A, De Paola M, et al. The phagocytic state of brain myeloid cells after ischemia revealed by superresolution structured illumination microscopy. J Neuroinflammation. 2019;16(1):9.
451. Miksa M, Komura H, Wu R, Shah KG, Wang P. A novel method to determine the engulfment of apoptotic cells by macrophages using pHrodo succinimidyl ester. J Immunol Methods. 2009;342(1-2):71-7.
452. Yu RY, Wang X, Pixley FJ, Yu JJ, Dent AL, Broxmeyer HE, et al. BCL-6 negatively regulates macrophage proliferation by suppressing autocrine IL-6 production. Blood. 2005;105(4):1777-84.